Reduction of Residual Stress and Distortion in HY100 and HY130 High Strength Steels During Welding

by

RICHARD ALLEN BASS
B.S. Electrical Engineering, Purdue University
1977, Lafayette, Indiana

MBA, Savannah State College
1985, Savannah, Georgia

SUBMITTED IN PARTIAL FULFILLMENT OF THE REQUIREMENT FOR THE DEGREE OF

Master of Science in Naval Architecture and Marine Engineering
at the
Massachusetts Institute of Technology
JUNE, 1989

Signature of Author Richard A. Bass
Richard A. Bass, Dept. of Ocean Engineering
May 15, 1989

Certified by Koichi Masubuchi
Dr. Koichi Masubuchi
Professor, Department of Ocean Engineering
Thesis Supervisor

Accepted by ______________________
Professor A. Douglas Carmichael
Chairman, Ocean Engineering Graduate Committee

89 10 10 133

Reduction of Residual Stress and Distortion in HY100 and HY130 High Strength Steels During Welding

RICHARD ALLEN BASS

ubmitted to the Department of Ocean Engineering on May 15, 1989 in artial fulfillment of the requirement for the degree of Master of Science Naval Architecture and Marine Engineering.

BSTRACT

An experimental study was carried out with the specific intention of ducing the undesirable effects of both high residual stresses and stortion in HY100 and HY130 high strength steels during welding. Tests ere also conducted on Mild Steel for comparison. The goal of these tests as to first ascertain the distortion and residual stresses during and after elding of test pieces of the three different steels. Test specimens were: 5" wide by 18" long and 0.5" thick. A nominal 20 KJ/inch heat input was ed in all experiments. Bead on edge was utilized as representative of a itt weld. An automated GMA process was utilized for welding with 98 % gon and 2% oxygen as shielding gas.

The first phase of this experimental investigation established excellent nperature, strain, distortion profiles, and a baseline residual stress. XY dimensional) surface mounted strain gages, K type thermocouples, and ree dial gages were used on the test pieces. A personal computer and a ta acquisition machine was utilized with the capability to track and cord temperature and strain data every 1 to 2 seconds.

The second phase involved the introduction of a secondary heat source, an oxy-acetylene side heat torch. Several experiments were conducted to get an effective flame and optimum positioning of the torch in relation to the weld arc. The optimal placement of the torch was determined to be longitudinally matched to the arc and 4" transverse. The flame from the torch was adjusted to raise the temperature of the plate roughly 200°C. The purpose of the secondary heat source traveling along with the welding arc is to use its thermal effects to directly oppose those of the welding arc and to arrest as much of the distortion and residual stress as possible during welding.

The final series of experiments yielded superb results. Side heating during welding does reduce the distortion by roughly one-half. Using a stress relaxation technique to obtain the residual stress affirmed that a significant reduction in the residual stress was also achieved on all three types of steels tested: Mild Steel, HY100, and HY130 ranging from 17 - 39%. This provides a basis for establishing a method to reduce the distortion and residual stress during the welding process for inclusion in a system that can ultimately control them in process.

Thesis Supervisor: Prof. K. Masubuchi

Title: Professor of Ocean Engineering and Material Science

Acknowledgements

I wish to extend my sincere appreciation to my "lab partner" and friend, Chirdpan Vitoorapom ("CP"), without whose assistance and tenacity have bought these experiments to fruition. CP and I did much of the work on these experiments with little regard for the time of day or day of the week to get them completed to produce this document.

I would also like to extend my appreciation to Mr. Tony Zona for his helpful advice, suggestions in running experiments, and quickly responding to any equipment need in the laboratory.

To Professor Masubuchi, who patiently guided the focus of this study and for imparting the knowledge to help me understand what we are doing, I remain deeply appreciative. I personally enjoyed taking classes from Professor Masubuchi and found his office to be the best place to find definitive works on the subject of Welding. Thank you for giving me the run of your office and for being the best advisor a student could have.

To the Laboratory for Nuclear Science in Building 20 for cutting our test pieces on short notice and fabricating the adjustable torch holder used in the experiments. I wish to thank Mr. Mike Aliosi, Remo and the rest of the LNS gang who were very helpful and informative in teaching us about milling, cutting, and fabricating metal.

A special thanks to Commander Paul Sullivan, the 13A academic advisor and to Captain Barrick Tibbitts, the Officer in Charge, for their encouragement and advice throughout my stay at MIT

To Mr. Paul Holtzberg, Ernie Cyzrika, and Gene Franke at the David Taylor Naval Research Center in Annapolis, MD for providing the test plate, reference material, and technical assistance during the experiments, thank you very much.

To my wife, Kyoko, whose devotion and love stayed above the hardships and strain of my stay at MIT, I thank you. For remaining steadfast despite the abnormal hours I kept, housing and financial woes we experienced, managing to work two jobs, keeping my family on an even keel, and still providing unflinching support; I am forever grateful.

Table of Contents

List of Figures

List of Tables

Data Table	Title	Readings
12	Strain (x) MS #4 w/o Tcomp	Longitudinal strain on MS EXPERIMENT #4
13	Strain (y) HY100 #5 w/o Tcomp	Transverse strain on HY100 EXPERIMENT #5
14	Strain (x) HY100 #5 w/o Tcomp	Longitudinal strain on HY100 EXPERIMENT #5
15	Strain (y) HY130 #6 w/o Tcomp	Transverse strain on HY130 EXPERIMENT #6
16	Strain (x) HY130 #6 w/o Tcomp	Longitudinal strain on HY130 EXPERIMENT #6
17	Residual (3 pages)	(Longitudinal and transverse of Mild Steel. HY100, then HY130). The last six columns with side heat same sequence.
18	Residual (2 pages)	Before cutting and after cutting microstrain used to compute residual stress without side heat (#4 through #6).

Data Table 19	Distortion Data	Strain Readings
	without side heating	HY130 column 1 - 4 HY100 column 5 - 8 Mild Steel column 9 - 12

Data Table 19	Distortion Data	Strain Readings
	side heating longitudinally matched to arc	MS column 13 - 16 HY100 column 17 - 20 HY130 column 21 - 24

side heating positioned 9" ahead of arc: MS column 25 - 28; HY100 column 29 - 32; HY130 column 33 - 36

side heating positioned 9" longitudinally behind arc: MS column 36 - 40; HY100 column 41 - 44; HY130 column 45 - 58

strain data taken during the final series of experiments with side heat matched longitudinally to arc: MS column 49 - 52; HY100 column 53 - 56; HY130 column 57 - 60

Data Table 20	Strain Readings
SIDE HEAT ONLY	Mild Steel columns 1 - 4 HY100 columns 5 - 8 HY130 columns 9 - 12

Data Table 21	Residual Stress
For the final series of test (experiment #26 - #28) with side heat temperature	Temperature & Strain Measurements

Data Table	Steel Type
22	MS Temperature
23	HY100 Temperature
24	HY130 Temperature

Strain	Steel Type
25	MS Transverse (y) w/Tcomp
26	Ms Longitudinal (x) w/Tcomp
27	HY100 Transverse (y) w/Tcomp
28	HY100 Longitudinal (x) w/Tcomp
29	HY130 Transverse (y) w/Tcomp
30	MS (y) Transverse w/o Tcomp
31	MS (x) Longitudinal w/o Tcomp
32	HY100 (y) Transverse w/o Tcomp
33	HY100 (x) Transverse w/o Tcomp
34	HY130 (y) Longitudinal w/o Tcomp
35	HY130 (x) Longitudinal w/o Tcomp

List of Photographs*

1. EXPERIMENT #1: Splash plate buckled and arc blew holes in it.
2. EXPERIMENT #2: Good bead, no spillover.
3. Prepared Specimens ready for welding (4) XY Strain Gages mounted with shielded cable.
4. LAB SET-UP: (from left to right), Test Bench with EXPERIMENT #2 on it; Millermatic GMA weld machine; table with shield cables; terminal block on table; HP3852A Data Acquisition and Control System; and PC, AT&T 6300.
5. EXPERIMENT #3: Bead on Edge.
6. EXPERIMENT #4: Full test piece after welding with (4) XY Strain Gages, (4) Thermocouples, and (3) Dial Gages at the bottom of a piece of Mild Steel.
7. "Tempo-Lac" in EXPERMENT #4: Mild Steel.
8. "Tempo-Lac" in EXPERMENT #5: HY100.
9. Terminal Block: Cable connections from the test piece to the equipment.
10. EXPERMENT #4 - #6: Stress Relieved pieces.
11. Close up of Stress Relieved Mild Steel piece from EXPERMENT #4: Mild Steel.
12. Stress Relieved piece from EXPERMENT #5: HY100.
13. Close up Stress Relieved piece from EXPERIMENT #6: HY130.
14. Side Heat set-up (9" ahead).
15. Final test piece after weld, EXPERIMENT #28: HY130: (4) XY Strain Gages; (4) Thermocouples; and (3) Dial Gages with Side Heat.

* This list of photographs can be deleted without loss of continuity.

16. Stress Relieved pieces form EXPERIMENT #26, #27, and #28.

CHAPTER 1

1.0: Introduction

1.0.1: Basic Information on Mechanical Properties:

1.0.1.1: Stress

Stress is usually expressed in terms of load force per unit area:

$$\sigma = \frac{F}{A}$$

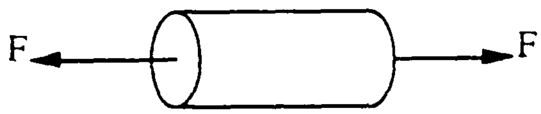

Tension
Figure 1

Compression
Figure 2

F = load force (+ tensile, - compressive)

A = cross - sectional area

Generally, the stress field is not uniformly distributed and for a two dimensional analysis plane stress requires $\sigma_z = \tau_{xz} = \tau_{yz} = 0$. Therefore, a force N applied in plane BC yields stress components, these are displayed in figure 3[1] .

$$\sigma_z = \sigma_x \cos^2 \varnothing + \sigma_y \sin^2 \varnothing + 2\tau_{xy} \sin \varnothing \cos \varnothing$$
$$\tau = \tau_{xy} (\cos^2 \varnothing - \sin^2 \varnothing) + \sigma_y - \sigma_x) \sin \varnothing \cos \varnothing$$

[1] Masubuchi, K., "Analysis of Welded Structures", Permagnon Press, p. 89.

where:

σ_n is the normal stress on plane BC

τ is the shear stress on plane BC

$\varnothing$ the angle between the normal to the plane BC, N, and the x-axis

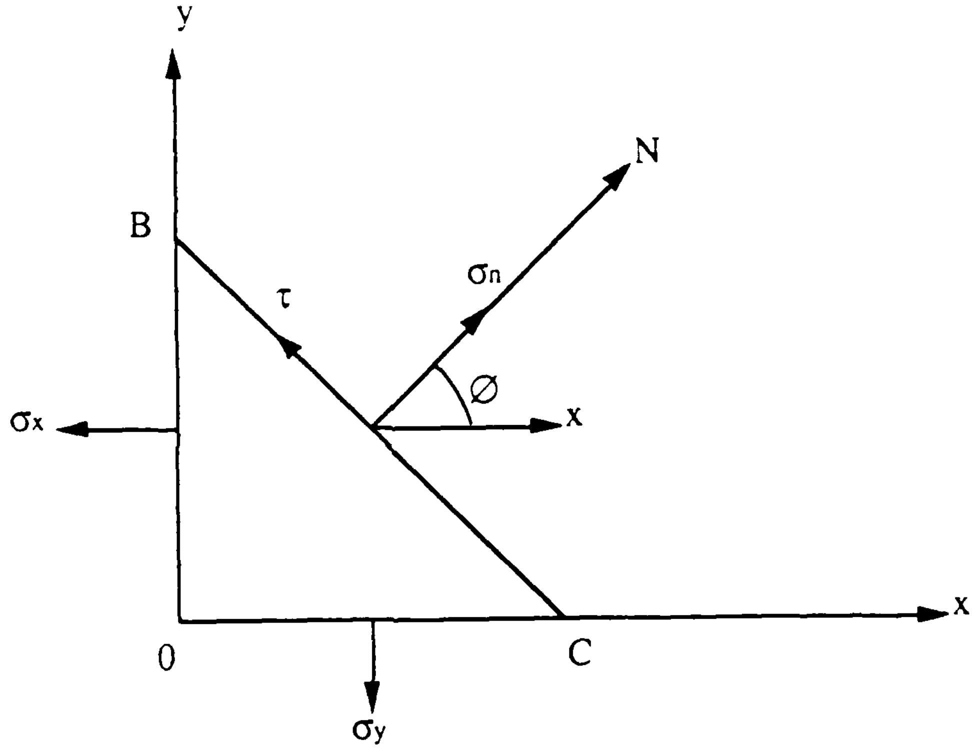

Figure 3

1.0.1.2: Strain

The slight deformation a body undergoes with the application of an applied force (F). With most solids; this is not usually visible unless the strain is excessive, or the material goes in the plastic region and deforms permanently, figure 4:

$$\varepsilon = \frac{\Delta L}{L}$$

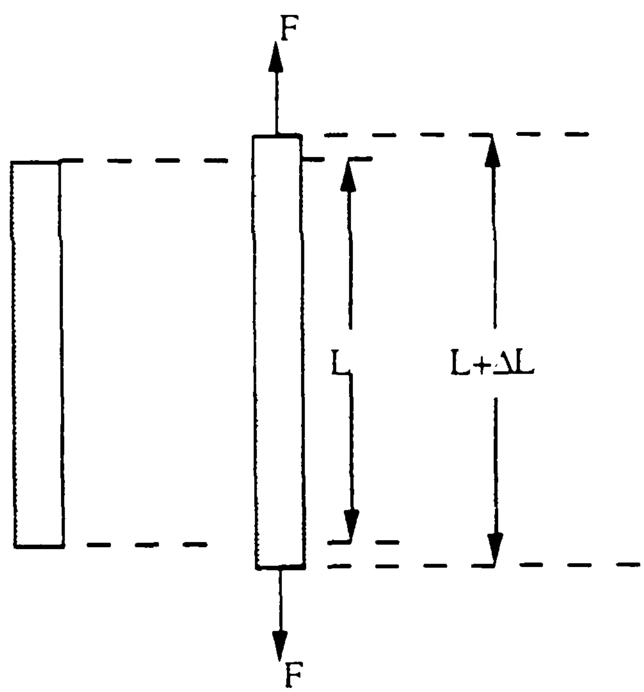

Figure 4

1.0.1.3: **Stress - Strain Relation** (Hooke's Law):

The relationship between stress and strain is usually expressed assuming the material is isotopic, homogeneous, and purely elastic[2] .

$$\varepsilon_x = \frac{1}{E}[\sigma_x - \nu(\sigma_y + \sigma_z)] + \alpha\Delta T$$
$$\varepsilon_y = \frac{1}{E}[\sigma_y - \nu(\sigma_x + \sigma_z)] + \alpha\Delta T$$
$$\varepsilon_z = \frac{1}{E}[\sigma_z - \nu(\sigma_x + \sigma_y)] + \alpha\Delta T$$
$$\gamma_{xy} = \frac{1}{G}\tau_{xy}$$
$$\gamma_{yz} = \frac{1}{G}\tau_{yz}$$
$$\gamma_{xz} = \frac{1}{G}\tau_{xz}$$

ε = Strain

σ = Stress

E = Modulus of Elasticity (tensile)

ν = Poisson's Ratio

G = Modulus of Rigidity or Shear Modulus $G = \frac{E}{2(1+\nu)}$

α = Thermal Expansion Coefficient

Δ = Temperature Change

T = Temperature

The stress field associated with rigid bodies in a three dimensional as displayed on the following page, figure 5:

---

[2] Cook, Nathan H., "Mechanics and Materials for Design", McGraw-Hill, 1984, p. 197.

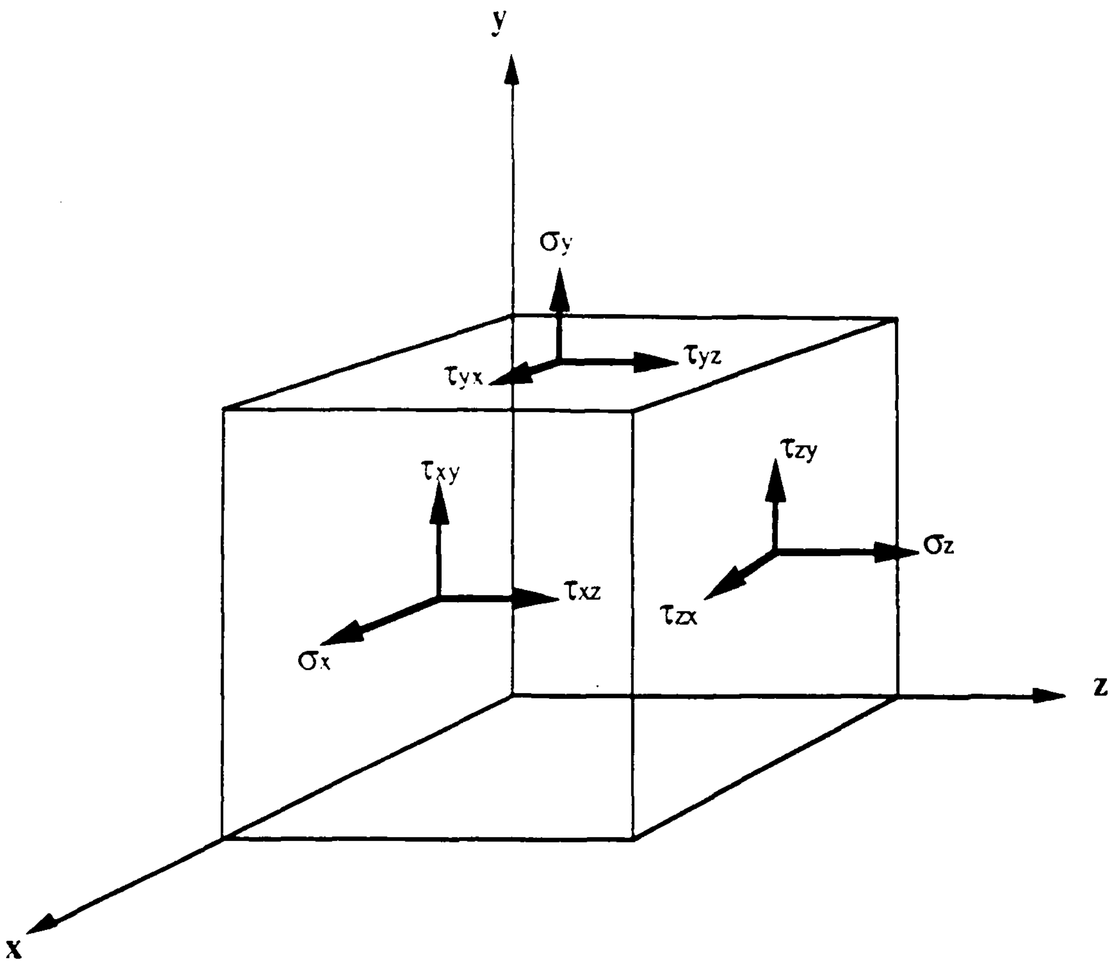

Three Dimensional Stress Field

Figure 5

Six independent quantities exist when the rigid body is in equilibrium:

$$\sigma_x,\ \sigma_y,\ \sigma_z,\ \tau_{xy} = \tau_{yx},\ \tau_{xz} = \tau_{zx},\ \tau_{yz} = \tau_{zy}$$

$$\sigma = \text{stress},\quad \tau = \text{shear stress}$$

1.1: Typical Stress - Strain Curve for Metals:

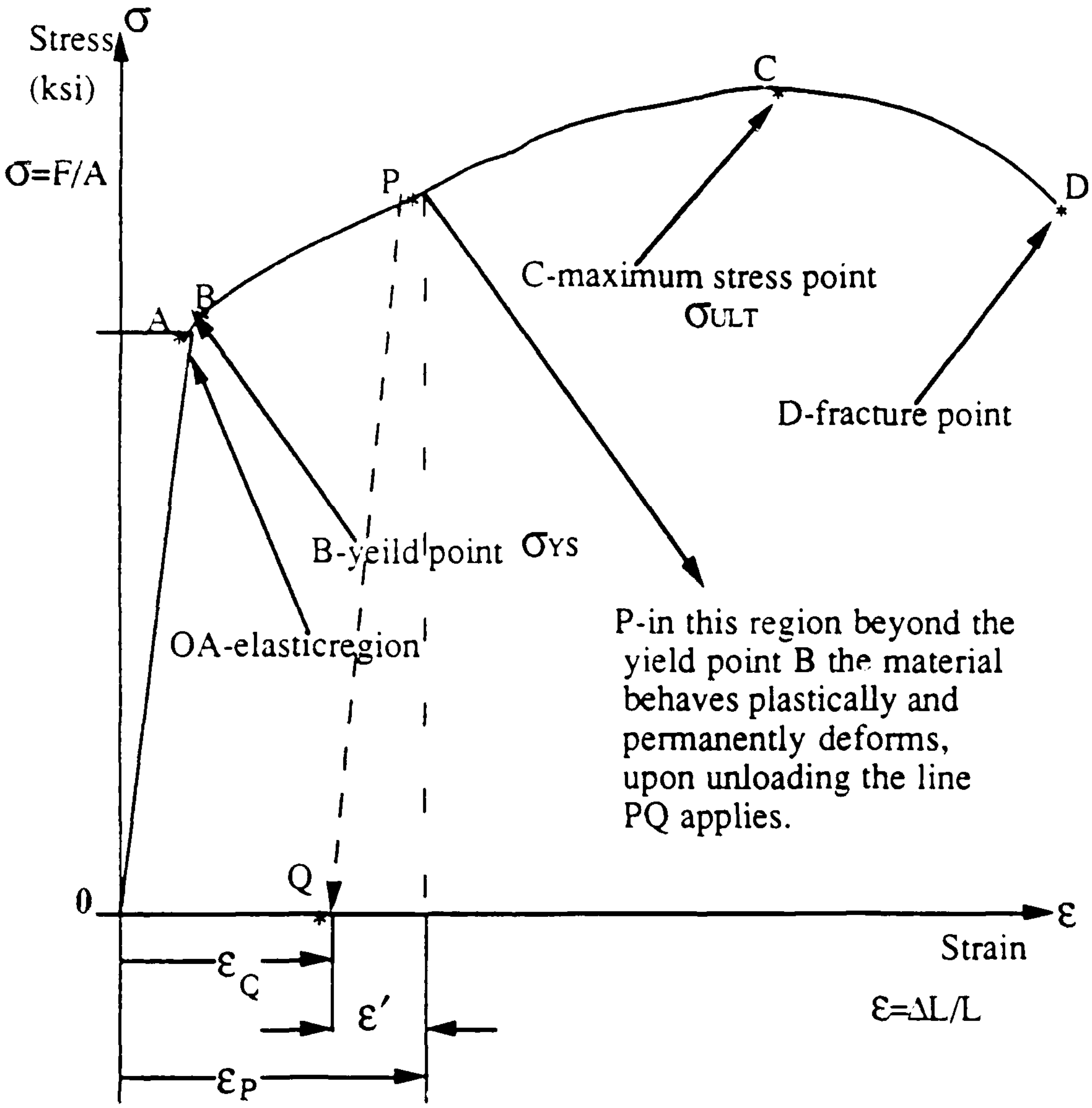

Stress-Strain Relationship

Figure 6

Figure 6 graphically displays a typical stress strain curve for metals. As the load is increased, the material changes in stress and strain can be described by curve O, A, B, C, and D[3].

OA - Elastic Region, the material does not undergo any permanent change in length under loading or unloading, and the relationship between stress and strain is typically linear. Small strain changes are common.

B - Point B usually describes the yield point, or the point where the material begins to deform plastically and permanent changes in length result. For aluminum, this point is reached at 2% elongation, and for most metals, including steels, points A and B coincide. No recovery point exists when the material deforms plastically. For the HY(high yield) series steels, the rating number is the yield stress point σ_{YS}.

C - Maximum stress point; usually referred to as ultimate stress point, or tensile stress σ_{ULT}.

D - The point where the material fractures under loading.

When a material is loaded beyond the yield point B, then plastic deformation occurs. When unloaded from an arbitrary point P beyond the yield point, the path of recovery is to point Q. What is happening is that,

---

[3] Ibid., p. 63.

yield point, the path of recovery is to point Q. What is happening is that, upon unloading, most metals recover elasticity. It is this elastic recovery that allows for stress relaxation techniques to measure residual strain, ε': ε_p is the strain measured after yield is exceeded, ε_Q is the strain measured after stress relieved and recovery, the difference is the residual strain ε' in figure 6.

$$\text{Residual Strain} \quad \varepsilon' = \varepsilon_p - \varepsilon_a$$

For Mild Steel, the yield point is 35 to 55 Ksi. For the high strength steels, HY100 and HY130 the minimum yield stress is 100 Ksi and 130 Ksi, respectively.

The heat generated by the welding arc is computed as follows:

$$h(\text{heat input}) = \left(\frac{60\ \text{sec}}{\text{min}}\right) \frac{V\ (\text{volts})\ \ I\ (\text{amps})}{v\ (\text{weld speed}\ \frac{\text{in}}{\text{min}})(1000)} = \frac{KJ}{\text{in}}$$

The heat generated by the arc include the heat input of the electric arc, and chemical reactions, which take place by the interaction of the atmosphere, shielding gases, coatings and impurities, and the heat of transformation of the metal to a liquid state which forms the weld pool.

The largest contributor to this process is the heat provided by the electric arc. If v = travel speed is expressed in in/sec, then heat input h is:

$$h(\text{heat input}) = \frac{V(\text{volts})\ I(\text{amps})}{v(\text{weld speed}\frac{in}{sec})\ (1000)} = \frac{KJ}{in}$$

Q, the heat supplied to the weld piece is usually expressed as a portion of the heat input depending on arc efficiency. For a GMA process, arc efficiency is typically 66-70%[4] for deposition on Mild Steel.

$$Q = N_a VI$$

where: N_a = arc efficiency

In our experiments on Mild Steel and High Strength Steels, HY100 and HY130, the temperature distribution compared well with the predicted values using a quasi-stationary heat flow technique with a finite breadth of one-half inch for all experiments. The arc efficiency, however, seems to range about 90% or better throughout this investigation. The first series of the experiments used 25V, and the average current was approximately 200 amps. With a speed of .385" per second yielded a heat input of:

$$\frac{(25V)(200A)}{\left(.385\ \frac{in}{sec}\right)} = 12{,}987\ \frac{J}{in}$$

Therefore, a weld heat input of roughly 13 $\frac{KJ}{in}$ was recorded. By lowering the speed to .3" per second the anticipated heat input was:

$$\frac{(25V)\ (200A)}{\left(.3\ \frac{in}{sec}\right)} = 16{,}666\ \frac{J}{in}$$

[4]Ed.: Phillips, A.L., "Current Welding Process", American Welding Society, 1964.

But the amperage on most experiments conducted at speed of .3" per second allowed for the welding current to increase to 230A; therefore, the actual heat input was[5]:

$$\frac{(25V)\ (230A)}{.3\ \frac{in}{sec}} = 19{,}167\ \frac{J}{in}$$

There is correlation between weld speed and arc current, as travel speed is decreased the average current increased with the GMA process. To obtain predicted values for the temperature distribution, a two dimensional model with a finite breadth of 5 1/2" was utilized.

[5]See Appendix 1, experiment #3.

Masubuchi, K., "Analysis of Welded Structure", Pergamon Press, 1980, p. 65.

1.1.1: Symbols for Heat Flow Analysis[6]

Symbol	Designation	Units CGS	English Units
θ	Temperature	°C	$°F = \frac{5}{9}(F - 32)$
θ_0	Initial Temperature	°C	$°F = \frac{5}{9}(F - 32)$
λ	Thermal Conductivity	$\frac{Cal}{cm\ sec\ °C}$	$\frac{.56 \times 10^{-2}\ Btu}{in\ sec\ °F}$
K	Thermal Diffusivity	$K = \frac{\lambda}{C\rho}\ \frac{cm^2}{sec}$	$\frac{.155\ in^2}{sec}$
C	Specific Heat	$\frac{cal}{g\ °C}$	$\frac{.9999\ Btu}{lb\ °F}$
ρ	Density	$\frac{g}{cm^2}$	$\frac{.03613\ lb}{in^3}$
t	Time	sec	sec
t_0	Time of Arc Welding	sec	sec
t_1	Time of Extinguishment	sec	sec
x_0	Fixed Start Point of Weld	cm	.3937 in
x, y, z	Fixed coordinate of a Point	cm	.3937 in
x_1	Fixed Finish Point of Weld $x_1 = x_0 - vt_0$	cm	.39137 in
w	Moving Coordinate $w = x - vt$	cm	.3937 in
v	Travel Speed of Weld Arc	$\frac{cm}{sec}$	$\frac{23.6\ in}{min}$
Q	Effective Thermal Power of Weld Arc	$\frac{cal}{sec}$	$\frac{.238\ Btu}{min}$
q	Intensity of Heat Source	$q = \frac{Q}{T}$	$\frac{cal}{cm\ sec}$
T	Plate Thickness	cm	.3937 in
V	Arc Voltage	volts	volt
I	Welding Current	ampere	ampere
η_a	Arc Efficiency		

1.2: Thermal Analysis of the Welding Process[7]

Many studies have been completed relating to heat flow in welding. Some of the most common utilize the concept of heat flow in a quasi-stationary state by Boulton and Lance-Martin[8], Rosenthal[9], Rykalin[10], and many others[11]. This technique proposes using a cartesian coordinate system (w, y, z) which moves in the x direction at the speed of the welding arc where: $w = x - vt$

w = moving x coordinate hence quasi-stationary

v = speed of welding arc

t = time

The temperature is assumed to undergo no change with the moving coordinate system, therefore:

$$\frac{dw}{dx} = 1, \quad \frac{dw}{dt} = -v$$

$$\frac{\partial \theta}{\partial x} = \frac{\partial \theta}{\partial w} \bullet \frac{\partial w}{\partial x} = \frac{\partial \theta}{\partial w} \quad \text{and} \quad \frac{\partial^2 \theta}{\partial x^2} = \frac{\partial^2 w}{\partial w^2}$$

---

[7] The solution to this Bessel function can be found in Advanced Calculus for Application., 2nd Ed., by FB.Hiddebrand. Prentice-Hall, Inc. Section 4.8, 4.9, and 4.10 and other books on Advanced Calculus.

[8] Boulton, N.S. and H.E. Lance-Martin, "Residual Stresses in Arc Welded Plates", Proceedings of the Institution of Mechanical Engineering, 1936, p. 295 - 339.

[9] Rosenthal, D. and R. Schmerber, "Thermal Study of Arc Welding", Welding Journal 17 (4) Supplement 208, 1938.

[10] Rykalin, N.N., "Calculation of the Heat Process in Welding", printed in USSR, 1960.

[11] Masubuchi, K., "Analysis of Welded Structure - Residual Stresses, Distortion and Their Consequences", Pergamon Press, 1980.

The relationship $\left(\frac{\partial\theta}{\partial t}\right)$ for the fixed coordinate $\left(\frac{\partial\theta}{\partial t}\right)_{FC}$ and the moving coordinate: $\left(\frac{\partial\theta}{\partial t}\right)_{MC}$ is: $\left(\frac{\partial\theta}{\partial E}\right)_{FC} = \left(\frac{\partial\theta}{\partial t}\right)_{MC} + \frac{\partial\theta}{\partial w} \bullet \frac{\partial\theta}{\partial t} = \left(\frac{\partial\theta}{\partial t}\right)_{MC} - v\left(\frac{\partial\theta}{\partial w}\right)$, and it follows that:

$$\frac{\partial^2\theta}{\partial w^2} + \frac{\partial^2\theta}{\partial y^2} + \frac{\partial^2\theta}{\partial z^2} = -\frac{v}{k}\left(\frac{\partial\theta}{\partial w}\right)$$

Now, θ is a function of position only and the solution to the above equation:

$$\theta = \theta_0 + e^{-(v/2k)\,w}\ \phi(w, y, z)$$

where θ_0 = initial temperature of the plate ϕ (w, y, z) = function to be determined.

For a three dimensional, semi-infinite plate which applies to a single bead deposited on a surface where the thickness T is assumed to be infinite ($T \rightarrow \infty$), the solution satisfies the following conditions:

(a)
$$\lim_{R = \sqrt{w^2 + y^2 + z^2}} -2\Pi R^2 \lambda \frac{\partial\theta}{\partial R} = Q_\rho$$

Q_ρ = total heat delivered to the plate

(b) Assuming heat loss through the surface negligible, no heat loss to the atmosphere: $\frac{\partial\theta}{\partial z} = \theta$ for $z = 0$ and $R \neq 0$

(c) For large distances from the source, the temperature remains unchanged, therefore: $\theta = \theta_0$, for $R = \infty$

Thus, the above equation satisfies:

$$\theta - \theta_0 = \frac{Q}{2\pi\lambda}\left[\frac{e^{-(v/2\kappa)R_n}}{R_n} + \frac{e^{-(v/2\kappa)R_n'}}{R_n'}\right]$$

For finite thicknesses neglecting radiant heat loss from the surface:

$$\frac{\partial\theta}{\partial z} = 0, \quad \text{for} \quad z = 0 \quad \text{and} \quad z = T$$

The solution can be obtained by adding an infinite series so that:

$$\theta - \theta_0 = \frac{Q}{2\pi\lambda} e^{-(v/2\kappa)w}\left[\frac{e^{-(v/2\kappa)R}}{R} + \sum_{n-1}^{\infty}\left(\frac{e^{-(v/2\kappa)R_n}}{R_n} + \frac{e^{-(v/2\kappa)R_n'}}{R_n'}\right)\right]$$

$$\text{where} \quad R_n' = \sqrt{w^2 + y^2 + (2nT - z)^2}$$

$$R_n = \sqrt{w^2 + y^2 + (2nT + z)^2}$$

$$T = \text{plate thickness}$$

For the two dimensional case, the equation for heat flow is best described by:

$$\theta - \theta_0 = \frac{q}{2\pi\lambda} e^{(v/2\kappa)w} \quad K_0\left(\frac{v}{2\kappa} r\right)$$

where: $r = (w^2 + y^2)$ and $K_0(z)$ is a modified Bessel function of second kind and order zero: $K_0(z) = \int_{-1}^{\infty} \frac{e^{-st}}{\sqrt{t^2 - 1}} dt$ and when the argument z is large, the Bessel function reduces to approximately: $K_0(z) \cong \sqrt{\frac{\pi}{2z}} e^{-z}$; therefore, if a finite breadth is considered:

$$\theta - \theta_0 = \frac{q}{2\pi\lambda} e^{(v/2\kappa)w} \left[K_0\left(\frac{v}{2\kappa}\right) r + \sum_{n=1}^{\infty} \left(K_0\left(\frac{v}{2\kappa}\right) B - K_0\left(\frac{v}{2\kappa}\right) B \right) \right]$$

The thermal distribution in this case is best described by a Bessel function, $K_0(z)$, this modified Bessel function of the second kind order zero[12], and its shape is displayed in the following figure (please see the following page for the diagram):

[12] The solution to the Bessel function can be found in Advanced Calculus for Applications, 2nd Ed. by F.B. Hidderbrand, Prentice-Hall, Inc., Section 4.8, 4.9, 4.10, and other books on Advanced Calculus.

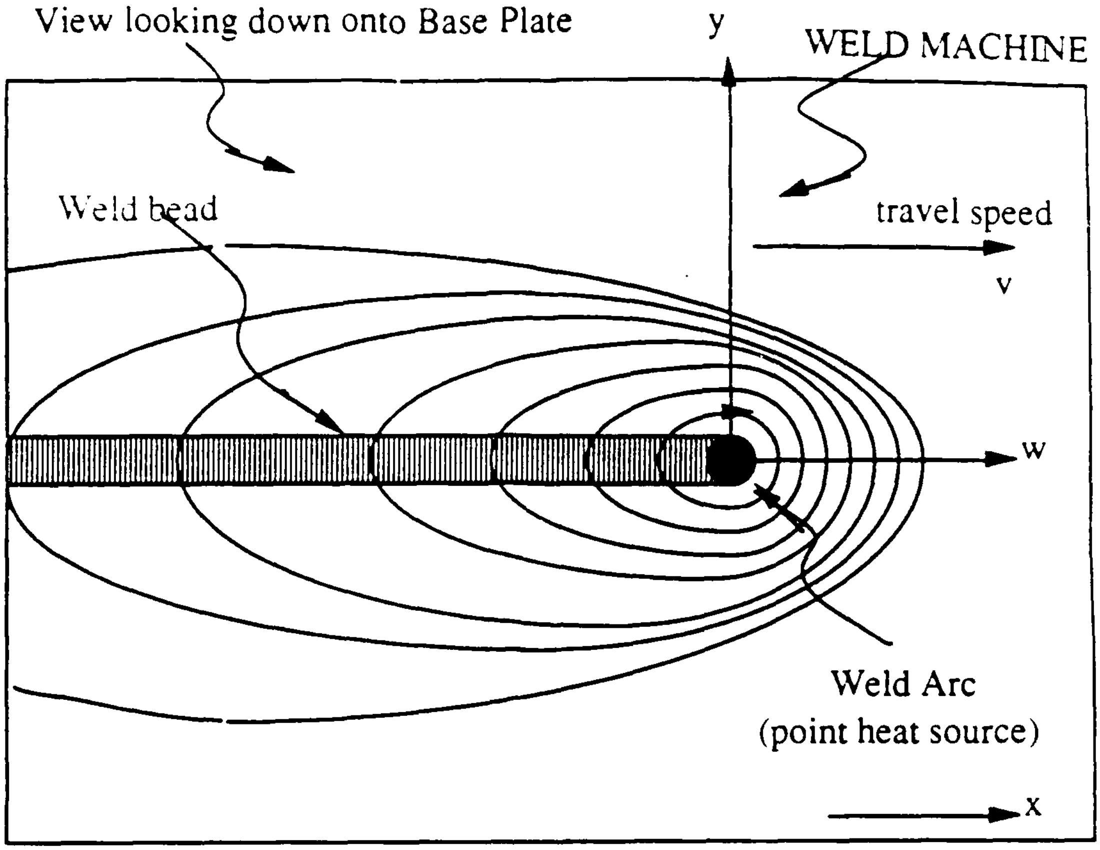

Isotherms generated as a result of welding

Figure 7

1.3: Background Discussion:

Currently, there is an increase in interest in utilizing high strength steels in a wide variety of applications. An examination of the US Navy's interest in high strength steels provides a good understanding as to why this is occurring. During WWII, US Navy ships were built with steel commonly referred to as "Mild Steel" today. The performance of those all steel ships is legendary. Many of those ships, although designed ostensibly to last the length of the war or five years, were still afloat and operating thirty years later with the US fleet, and a few, like the New Jersey class Battleships are still operating despite their forty five years of age. During the 1950 - 1980's, the US Navy began building aluminum superstructures on steel hulls in an effort to reduce weight topside and allow for more weapons, engineering, and other equipment to be aboard.

For submarines, the US Navy stuck with steel and developed the HY (High Yields) Steels for pressure hulls and special applications like flight decks where aluminum is impractical to use. HY80 is the most famous and most widely used of the HYQ & T steels developed. Interest waned in widely using the steels with strengths above HY80 because of cracking problems associated with the higher strength steels and from a combination of problems in internal residual stress, thermal residual stress from welding, and applied stresses[13]. More recently, a better understanding of the weld process and advances in material development have led to a new high strength standard for the US Navy; HY100 which is now certified for

[13] Carlsberg, J., "Review and Assessment of Linear Elastic Analysis Techniques for Surface Cracks in Structural Details With Residual Stresses", DTNRDC - 84/1070, March 1985.

flight decks. If HY100 can be used on a submarine, it could provide for a deeper operating depth. Although the US Navy has not been involved in a war at sea since WWII, close examination of the Middle - Eastern Wars in 1967 and 1973, the Falklands in 1983, and more recently, the damaged frigates in the Persian Gulf in 1986(USS Stark and USS Morrison): one by missiles and one by a mine, have prompted a new interest in going back to all steel for US Navy ships. The newest class of destroyer being built is a return to all steel ships(USS Arleigh Burke DDG-51 Class). The primary reason for using the aluminum was to reduce weight without losing strength. Aluminum alloys are commonly three times higher in strength to weight ratio over steel. But this advantage is eliminated with the high strength steels. For example, HY130 has a strength to weight ratio similar to aluminum alloys.

There are numerous studies completed that address cracking problems in steel and general agreement exists with how it occurs. The basic mechanism of cracking is similar for all steel types when carbide solutionizing in the heat affected zone causes subsequent precipitation of alloy carbides. This also occurs during post weld heat treatment or use during elevated service temperatures[14]. The precipitation that occurs reduces creep ductility in the heat affected zone to a level which the strains necessary for stress relaxation cannot be tolerated and intergranular cracking occurs[15]. Preheat and post weld heat treatment cause this same

[14] Meitzner, C.F., "Stress Relief Cracking in Steel Weldments", WRC Bulletin 211, p. 6 - 12.

[15] Boulton, N.S. and H.E. Lance-Martin, "Residual Stress in Arc Welded Plates", Proceedings of the Institution of Mechanical Engineering (London), p. 133, 295 - 347, 1936.

type of cracking to occur but are generally helpful in mitigating stress relief cracking.

Residual stresses are the thermal stresses associated with the welding process. When the welded material cools, it is commonplace for high residual stresses to exist particularly in the heat affected zone. Thermal stresses have been widely investigated; Boulton and Lance-Martin in 1936 first presented analytical and experimental results and displayed that welding induced plastic deformation of the material and that high residual stresses resulted upon cooling[16].

After a number of research programs have been carried out on residual stresses and distortion in weldments, several reviews and books have been written relating to residual stresses and distortion[17, 12, 13]. Transient thermal stresses for the most part are extremely complex and only limited studies have been completed on them. Masubuchi and Martin[18] investigated residual stresses in butt welds on SAE 4340 high strength steel oil quenched and tempered and low carbon steel through hydrogen induced cracking. Residual stresses were tensile near the weld and compressive away from the weld, and despite considerable difference in their yield strength and the different weld metal used, the residual stresses were similar. Experimental results by Kihara, et al. established the ratio of the maximum residual stress to the yield strength of the material[19].

---

[16] Masubuchi, K., "Control of Distortion and Shrinkage During Welding", Welding Research Council Bulletin 149, April 1970.

[17] Boulton, N.S. and H.E. Lance-Martin, "Residual Stresses in Arc Welded Plates", Proceedings of the Institution of Mechanical Engineering, Vol. 133, p. 295 - 336, 1936.

[18] Masubuchi, K. and D.C. Martin, "Investigation of Residual Stresses by Use of Hydrogen Cracking", Welding Journal, Vol. 40, No. 12, Research Supplement, p. 401 - 418s.

[19] Iketa, Y. and H. Kihara, "Brittle Fracture Strength of Welded Joints", Welding Research Supplement, Welding Journal, Vol. 49, p. 106s, 1970.

The maximum residual stress is no more than one-half the yield strength. As yield strength increases, the maximum residual stress tends to decrease by experiment. Our experiments showed this same phenomena, the HY130 piece generally showed the lower readings in distortion and residual stress when compared to HY100 or Mild Steel.

The purpose of this study is, once again, to examine residual stresses and distortion using simple weldments with the specific purpose of seeking a method to control the distortion during welding.

CHAPTER 2

2.0: Material Characteristics

2.0.1: Selected Test Material:

The selected materials for this study was HY100 and HY130. Mild Steel was included as a control and for comparative purposes to verify the results obtained on the high strength steels. The HY100 and HY130 were obtained from the David Taylor Naval Research Center (DTNRC) in Annapolis, Maryland to support this research. The test pieces utilized had dimensions 5.5 inches (140 mm) wide, 18 inches (457 mm) long, and .5 inches (12.7 mm). Care was taken to ensure that all test pieces were cut such that the length corresponded to the rolling direction of the plate. Figure 18 displays the specimen size and the relation between length and rolling direction when the steel was produced. Slightly different characteristics is experienced if the material is not cut with the length in the rolled direction from the fabrication process. When the experimental plates were picked up at DTNRC, all the plates were clearly marked with the rolling direction on them. The following diagram shows clearly how the length of the test pieces matched the rolling direction of the steel from when the steel was fabricated.

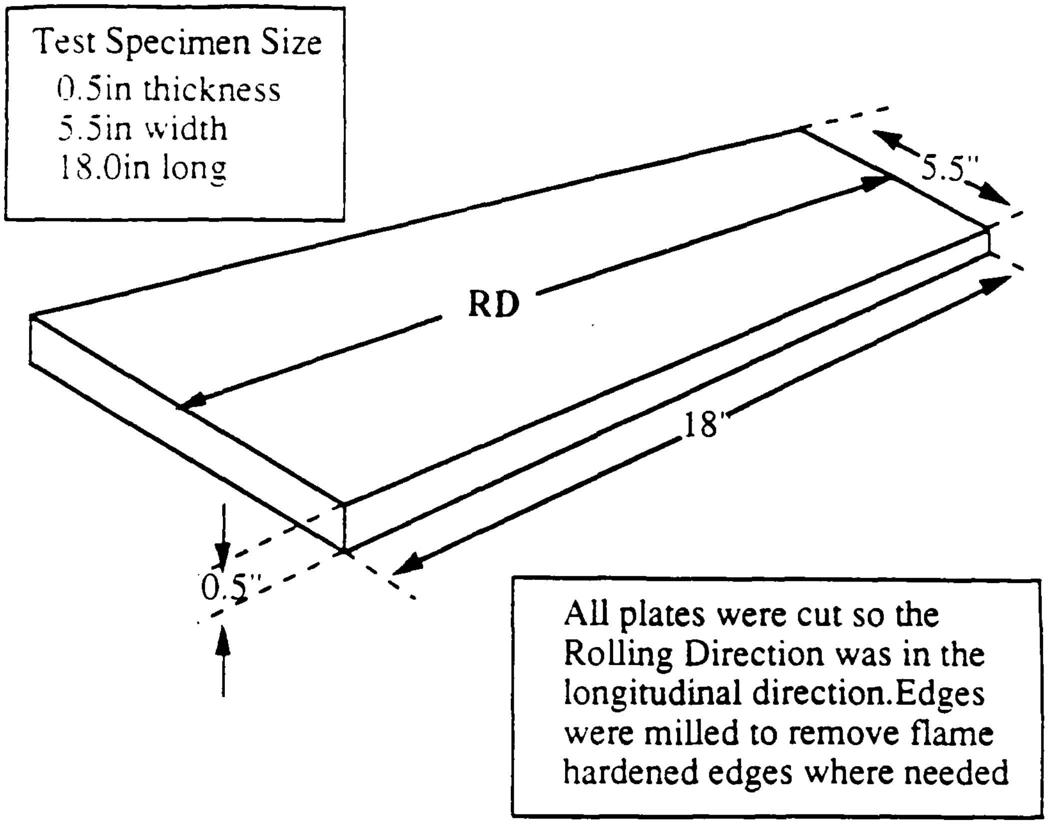

Specimen Size with Rolling Direction

Figure 8

This was done to eliminate any difference in experimental results due to the orientation of the rolling direction (RD) of the plate from the production process. Steel plate utilized with the RD matched to the length provides the best characteristics. The selection of a length of 18 inches is a results of using information of De Garmo, et al.[20] who examined residual stresses and their relations to test specimen length. In examining both longitudinal and transverse stresses, 18 inches in length is needed to achieve

[20] De Garmo, E.P., et.al., "The Effect of Weld Length Upon Residual Stresses of Unrestrained Butt Welds", Welding Journal 25 (8), Research supplement, p. 4855 - 4865, 1946.

the maximum residual stress for a nominal welding condition. In other words, if longer than 18", the residual stresses, both longitudinal and transverse, are level. If a test piece is shorter than 18", then the values of residual stress, both longitudinally and transverse, decrease with length. We experienced with a few test pieces that were only 12 inches long, the values of distortion read were considerably lower than an 18 inch piece with identical welding conditions.

2.1: Bead on Edge

Bead on edge weld is a simple weldment representative of a butt weld. The simple weld type was selected for simplicity and economy in conducting these tests. The following diagram shows how a bead on edge is accomplished:

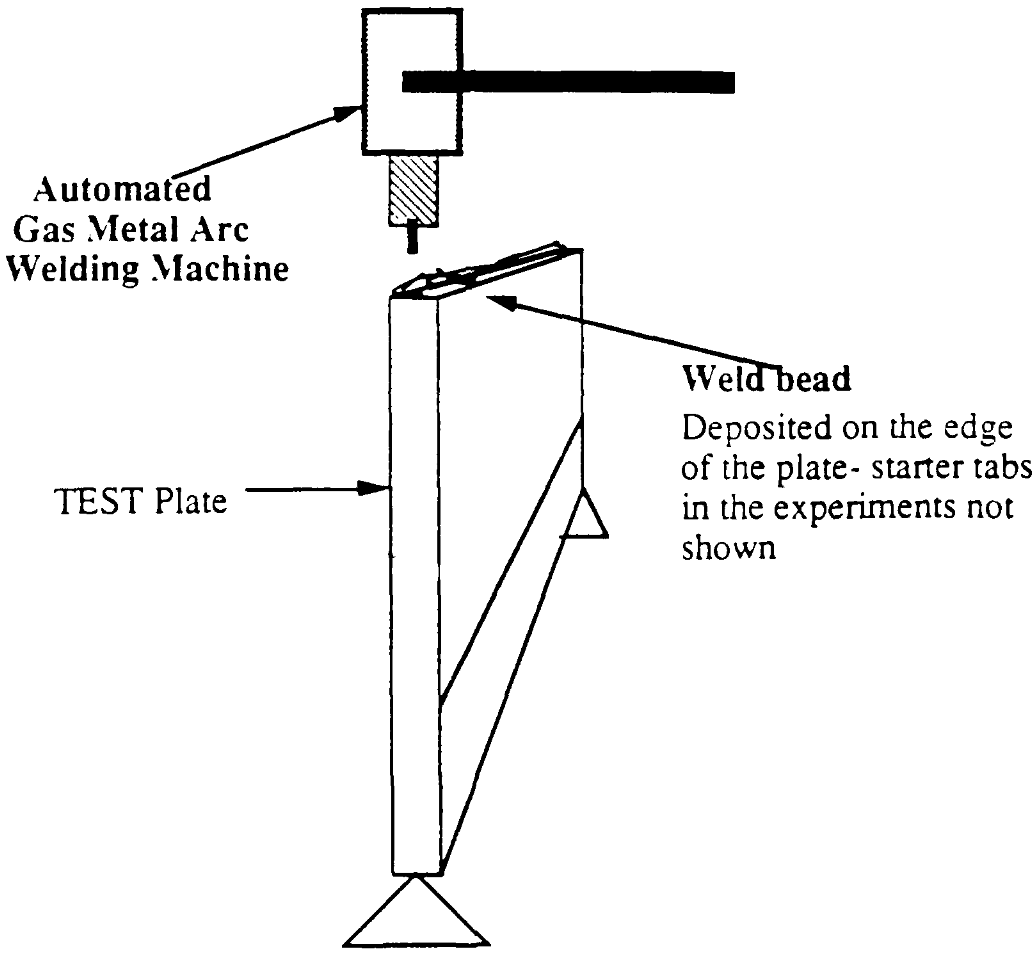

Weld Bead on Edge

Figure 9

2.2: Types of Simple Weldments

The following diagram graphically displays simple types of weldments:

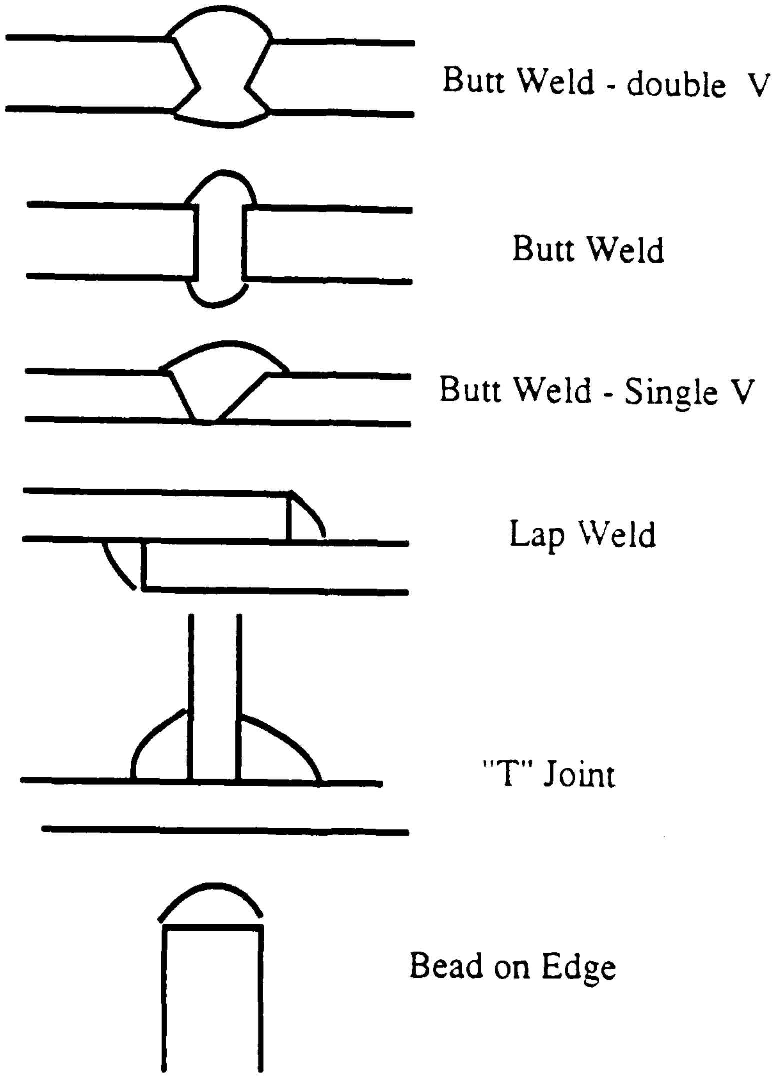

Simple Types Weldments

Figure 11

Butt Welding is the most common for welding plates together, so this type of weld (one side of it) is essentially the type of weldment being used in this investigation.

2.2.1: The Butt Weld:

For HY100 and HY130, butt welding using Shielded Metal Arc Welding (SMAW), Gas Tungsten Arc Welding (GTAW), Gas Metal Arc Welding (GMAW), Submerged Arc Welding (SAW), and Stud Welding (SW) the recommended joint preparation is as follows[21] :

Cleaning: the joint and area where welding should be thoroughly cleaned with acetone or trichloroethane.

Preheat: No cyclic or large temperature differences. for 1/2" - 1/8" preheat and interpass temperatures should be between 125°F and 300°F.

Heat input:	MAX
1/2" and less	45,000 KJ/in
1/2" and above	55,000 KJ/in

$$h = \frac{(\text{Arc Voltage})(\text{Welding Amps}) \times 60}{\text{Rate of Travel (inches/min)}}$$

The following diagram shows what a butt weld looks like. In the experiments conducted the Heat Affected Zone (HAZ) was visible and extended about a half inch from the weld line.

[21] General Dynamics Corporation Handbook for Welding HY80, HY100, and HY130, 1975.

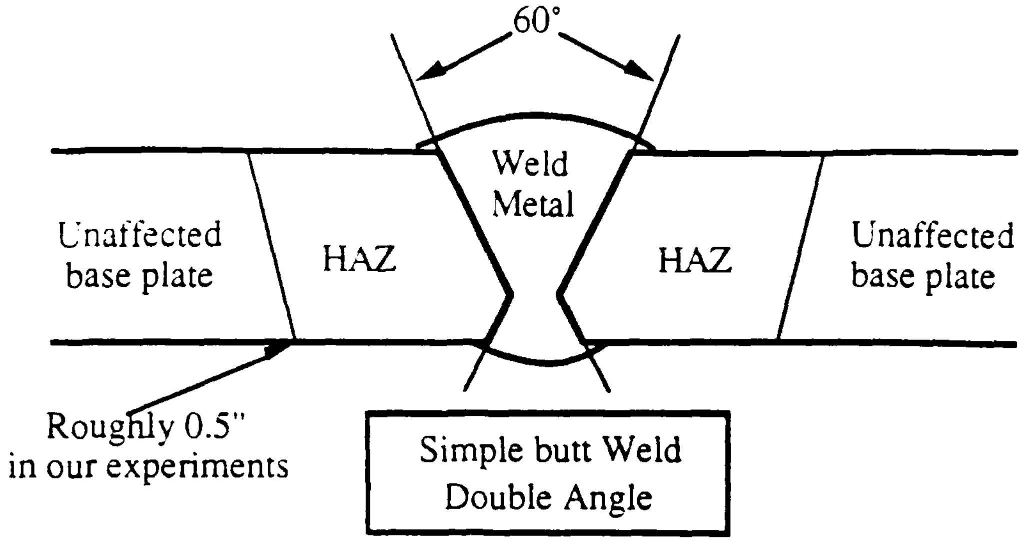

Figure 10

A Bead on Edge is representative of a butt weld but only one side of the plate is used, and the Welder's Handbook from General Dynamics Corporation was helpful in setting up the Millermatic GMA Weld Machine with the proper settings. The Weld Machine also has a reference guide to select the proper settings.

2.3: Material Properties:

CHEMICAL COMPOSITION OF TEST PIECES

		Mild Steel	HY100	HY130
C	Carbon	.21	.20	.09
M_n	Manganese	1.0	.1 - .4	.71
P	Phosphorous	.05	.025	.008
S	Sulphur	.05	.025	.003
C_u	Copper	-	-	.15
S_i	Silicon	-(3)	.25	.28
N_i	Nickel	-(3)	3.2	4.83
C_r	Chromium	-(3)	1.5	.55
M_o	Molybdium	-(3)	.40	.40
V	Vanadium	-(3)	-	.08
T_i	Titanium	-(3)	-	.005

Identifier	ABS Class B	USX TAG328	Lukens Steel TAG323
Min. Yield	30	100	130(1)
Actual Yield			139(1)
Min. Tensile Strength	56	110(2)	142(2)
Process	As rolled	Q&T(4)	Q&T(4)
Elongation (in 2")%	28	18	24
Approx NDT Range:			
	°F -20 to +40	-130 or lower	-100 or lower
Density (lb/in^3)	.29	.30	.30

% Reduction in Area:			
		55 Longitudinal 50 Transverse	55 longitudinal 53 Transverse
Cost	1	3.5(5)	5.0(5)

Notes:

(1) - Actually measured value from production run.

(2) - Usually 10 - 15Ksi above minimum yield.

(3) - Actual values of these vary with supplier and can range from .09 - 1.4%.

(4) - Q&T = quenched and tempered. For the HY130 the plate test heated 16251 - 1675°F held 1 hour per inch min., and water quenched, then tempered at 1180°F held 1 hour per in min. and again water quenched, from the original sheet.

(5) - Approximate cost relative to ABS Class B Mild Steel.

	Mild Steel	HY100	HY130
Modulus of Elasticity ($x10^6$)	29	29	29
Strength to Weight Ratio = $\frac{\text{Ultimate Strength}}{(\text{density})(x1000)}$	193	367	473

HY100 is covered under the same MIL-SPEC specification as HY80 with slight differences in composition and production process. Most conditions that apply to HY80 are also true of HY100. HY130 has a little more chemical difference and with the increase in strength approaches a strength to weight ratio similar to aluminum. This is interesting to point out for using high strength steel in place of aluminum where the weight is critical and light weight with high strength are desired. The HY130 compares favorably with the 5083 - H113 which has a strength to weight ratio of 480, 5086 - H34, 490, and 6061 - T6 which has a ratio of 460. The aluminum alloys mentioned above are all used for structural purposes and are commonly welded.

2.4: Measurement of Residual Stresses by Stress Relaxation

The principle of stress relaxation is based on the idea that strains created during unloading are elastic even when the material itself has undergone a plastic deformation as that occurs in welding. Therefore, it is the possible to measure residual stress in the material with no fore hand knowledge of the material's history.

The method of measuring residual stresses employed in this investigation was to measure the strain in the plate after it cooled down form welding. The plate was then cut and the measured strain data was taken to be the strain associated with the residual stress.ε'_x, ε'_y, γ'_{xy} represent the elastic strain components of residual stress. The strain changes $\overline{\varepsilon_x}$, $\overline{\varepsilon_y}$, and $\overline{\gamma_{xy}}$. If accurately measured, no residual stress exists when: $\overline{\varepsilon_x} = -\varepsilon'_x$, $\overline{\varepsilon_y} = -\varepsilon'_y$, $\overline{\gamma_{xy}} = -\gamma'_{xy}$. The minus sign indicates tensile residual stress exists and shrinkage takes place after relaxation (cutting the plate) as opposed to elongation. The residual stress can then be computed by the relation: $\sigma_x = \frac{E}{1 - \nu^2}(\overline{\varepsilon_x} + \nu\overline{\varepsilon_y})$, $\sigma_y = \frac{E}{1 - \nu^2}(\overline{\varepsilon_y} + \overline{\varepsilon_x})$, $\sigma_{xy} = -G\overline{\nu_{xy}}$.

where:	σ = Stress	E = Young's Modulus of Elasticity
	ε = Strain	G = Shear Modulus
	γ = Shear Strain	ν = Poisson's Ration

This technique yields the average strain only and does not show highly localized concentrated strains. However, this technique is simple, reliable, and is independent of type of material used. This technique is destructive since you have to cut the metal and can be expensive and time consuming.

In our investigation, we discovered that cutting the high strength steels was not only time consuming but expensive as well. The carbide cutting saw blades would only survive cutting two pieces of HY130, in particular, and then had to be replaced due to dullness or broken teeth. The same occurred when milling HY130 and HY100 to a lesser extent. We were advised that cutters for the milling machine cost $400.00, and after milling several pieces of HY130, the milling cutter had to be replaced.

Residual stress due to welding are typically tensile near the weld and compressive away from the weld. The following diagrams displays this:

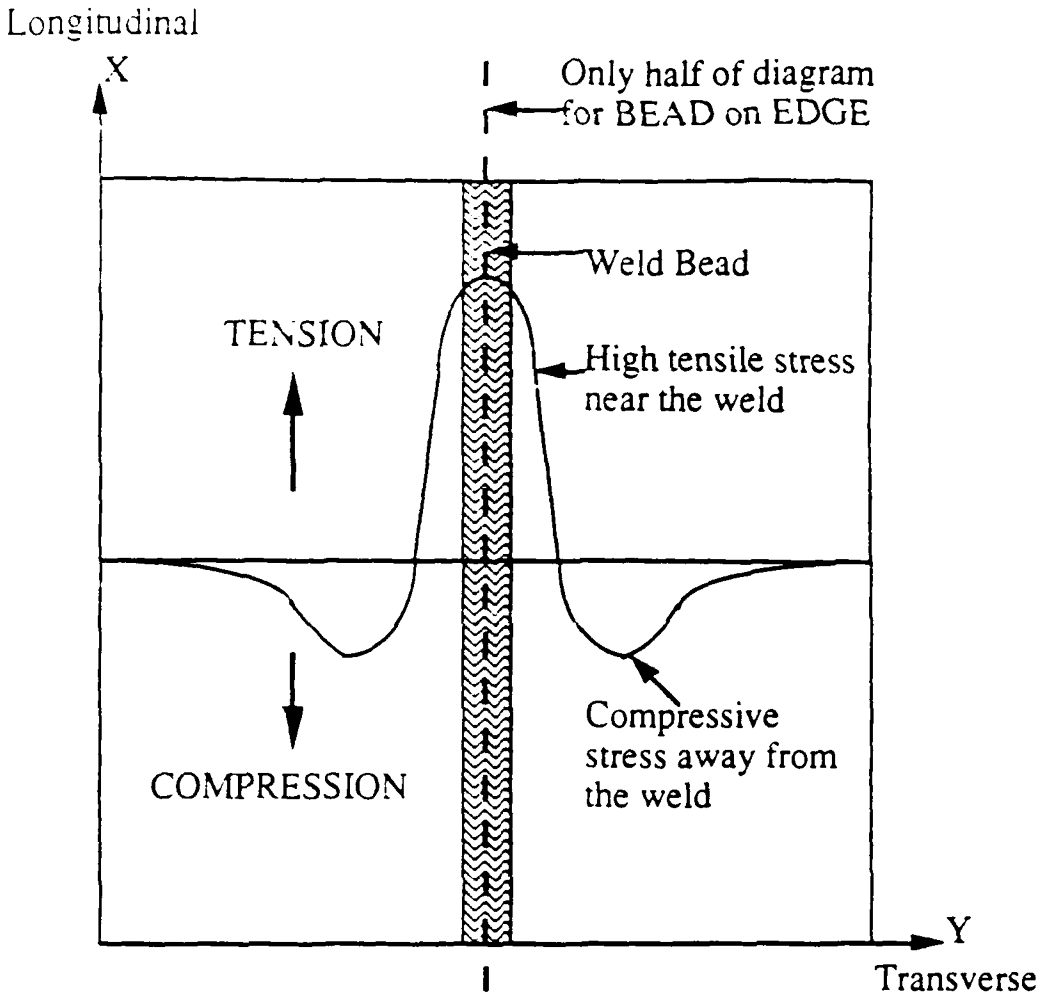

Residual Stress Distribution After Welding

Figure 12

Our results generally agreed favorably with predicted results. The following four diagrams display predicted residual stress from previous experiments and calculated values.

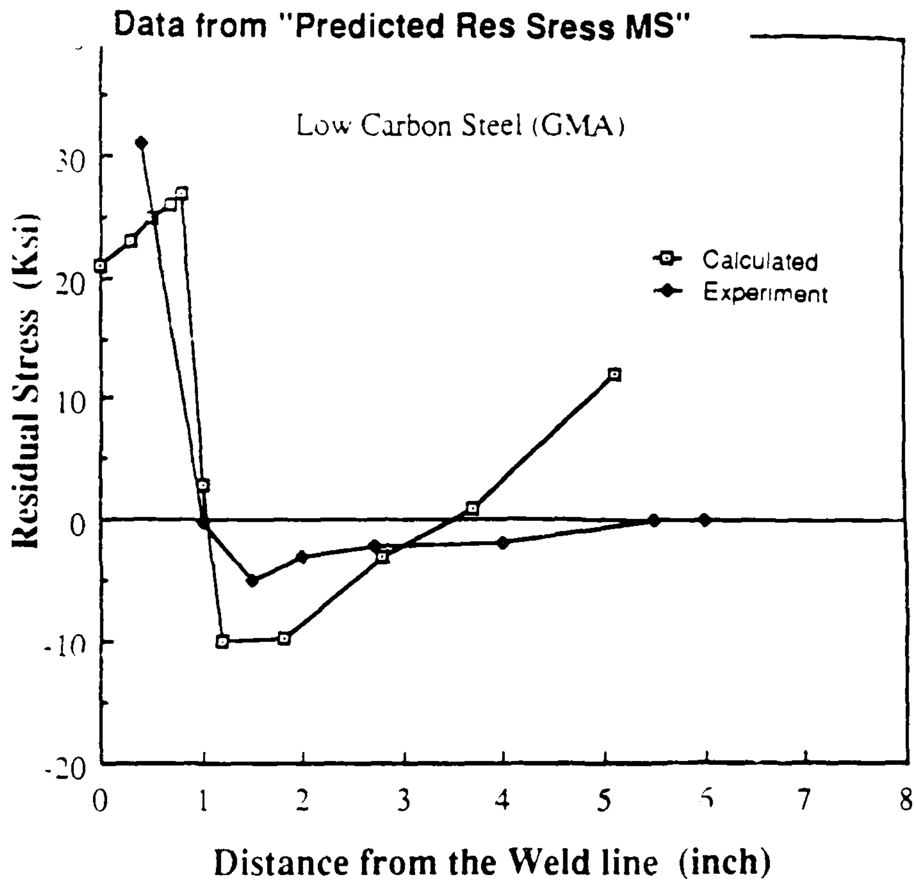
Data from "Predicted Res Sress MS"
Low Carbon Steel (GMA)
Calculated
Experiment
Residual Stress (Ksi)
30
20
10
0
-10
-20
0
1
2
3
4
5
6
7
8
Distance from the Weld line (inch)

Figure 13

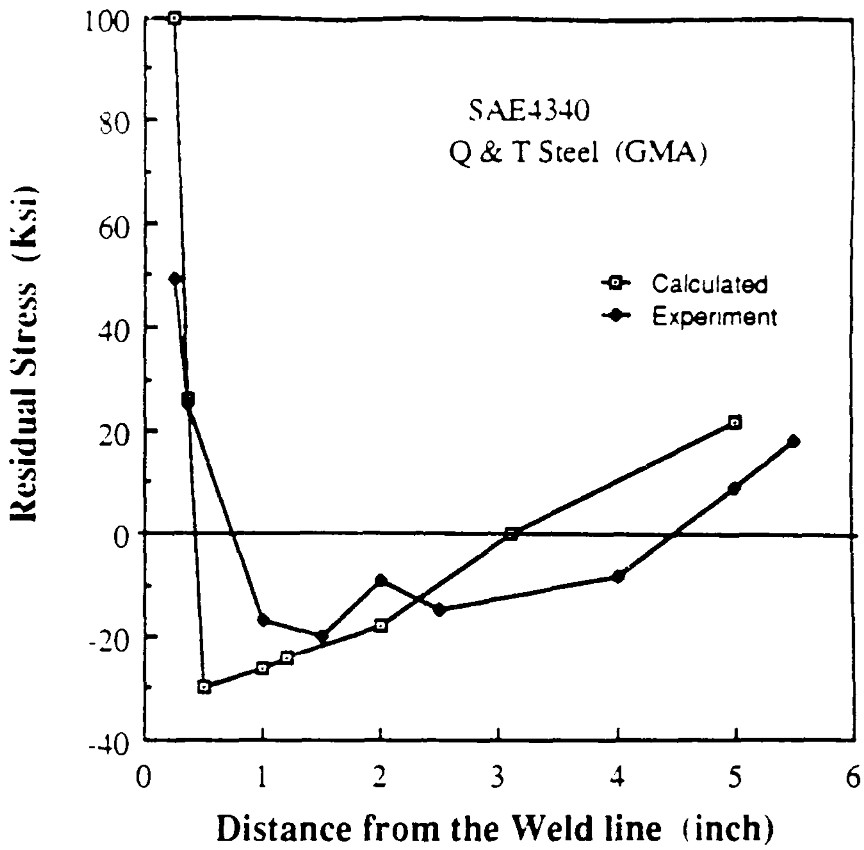

SAE4340
Q & T Steel (GMA)
Calculated
Experiment
Residual Stress (Ksi)
100
80
60
40
20
0
-20
-40
0
1
2
3
4
5
6
Distance from the Weld line (inch)

Figure 14

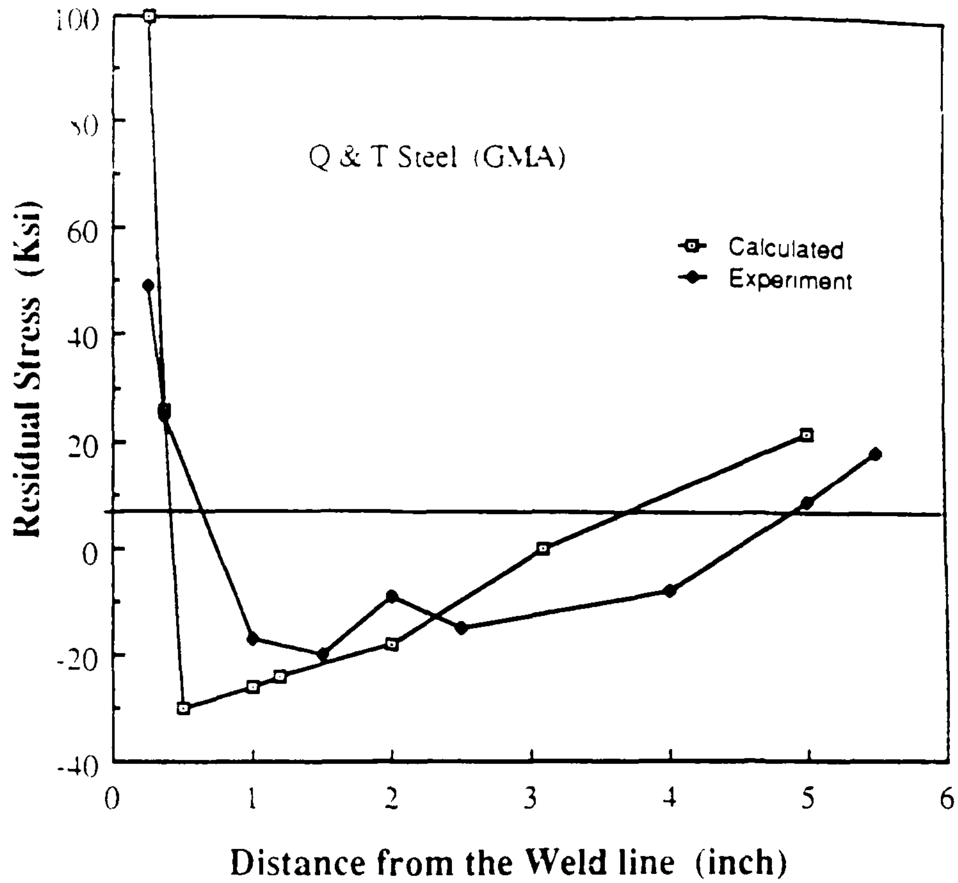
Q & T Steel (GMA)
Calculated
Experiment
Residual Stress (Ksi)
100
80
60
40
20
0
-20
-40
0
1
2
3
4
5
6
Distance from the Weld line (inch)

Figure 15

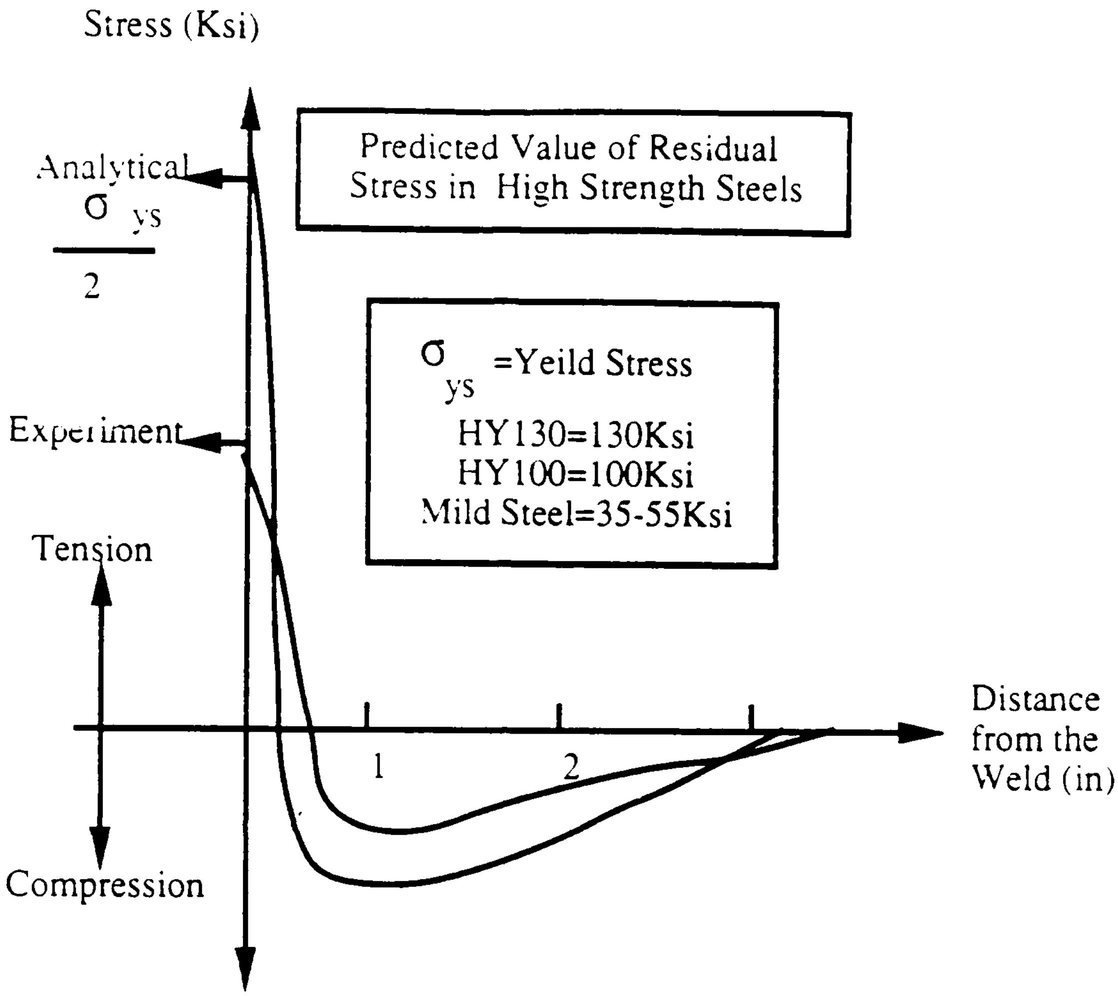

Figure 16

The residual stress examined in the experiments is expected to be like the foregoing.

CHAPTER 3

3.0: Problem - Why High Strength Steels Crack

The problems associated with high strength steels have been widely investigated. At MIT, K.M. Klein sponsored by the Navy wrote his thesis on the subject as well as J.S. Hwang in 1976. Several studies over the years have been completed by Professor K. Masubuchi at MIT as well. In discussions with Prof. Masubuchi and reviewing numerous previous studies on residual stresses and problems associated with using high strength steels reveal some similarities.

Apparently when high strength steels are welded, the weld pool solution forms and the portion of the base metal which is affected by the high temperature that undergos changes is called the Heat Affected Zone (HAZ).

In the HAZ, carbide solutionizing precipitation occurs. The grain boundary becomes coarse and after cooling the metal become brittle. It is this precipitation that occurs at elevated temperatures that cause the steel to become brittle. The high residual stress that exists exceeds the yield stress of the metal and causes microfractures along the grain boundaries. when a sufficient number of these cracks along the grain boundaries align, intergranular cracking occurs and the material fractures. This same phenomena can occur during post weld heat treatment temperatures. What is clear is that cracking problems associated with HY130 in particular is a combination of normal residual stress internal to the material with all of its alloying elements, thermal residual stress caused by the welding process, and lastly the applied stresses. The thermal residual stress induced the welding process are the largest of the components listed above. This investigation is intended to focus on the thermal residual stress and the distortion (metal movement) associated with the welding process.

3.2: Purpose of Experimental Investigation

3.2.1: Objective:

The objective of this experimental investigation was to obtain a series of data which accurately display thermal and residual stresses and the distortion in navy specified high strength steels HY100 and HY130. Mild steel specimens were included as a control and to verify the results obtained. This study required accurate measurement of temperature, strain and distortion for the test specimens both during welding and for some time afterward to allow the material to completely cool down. The specific goal of this entire investigation is to reduce both the residual stress after welding and the distortion associated with welding in these high strength steels. The target or desired reduction of residual stress and distortion was fifty percent. Simple weldments were to be utilized to accomplish this goal. Weld bead on edge was selected as the test weld of choice. This minimized the use of material, reduced cost, and yielded excellent results. Bead on edge is representative of butt welding (equivalent to one half a butt weld). This also simplified analysis with only one transverse side from the weld and eliminated the need to mill angles on the edge for butt welding.

A common problem which frequently arises from discussion and literature in the use of high strength steels is cracking. The cracking of the steel frequently arises from high residual stress associated with the welding process where the metal is joined. The separation as a result of distortion when making long welds is another attendant problem when using high strength steel. both of these problems are addressed in the experimental investigation and a novel side heating technique was utilized to reduce the magnitude of both residual stresses and distortion. The secondary heat source used was an oxy-acetylene torch traveling with the welding arc. The welding process used is Gas Metal Arc (GMA). This process was formerly known as Metal Inert Gas (MIG). The experiments were conducted using an automated GMA machine to ensure consistency between welds. From the set-up with side heat shown in figure 17, the hypothesis set forth is that a secondary point source introduced with the intention of opposing the thermal effects of the weld arc can effectively reduce both residual stress and distortion and hence diminish these attendant problems associated with the use of High Yield Steels. Specifically, a side heat torch can reduce significantly both residual stress and distortion in the High Strength Steel.

The experimental investigation is set-up in three phases:

Phase 1 - Establish temperature, strain and distortion profiles for all three steels and to provide a baseline residual stress for Mild Steel, HY100, and HY130 without Side Heat.

Phase 2 - To determine what and where the secondary heat source should be placed and confirm the hypothesis.

Phase 3 - Again, replicate temperature, strain and distortion profiles and to measure residual stress using stress relaxation to determine how much average residual stress is reduced.

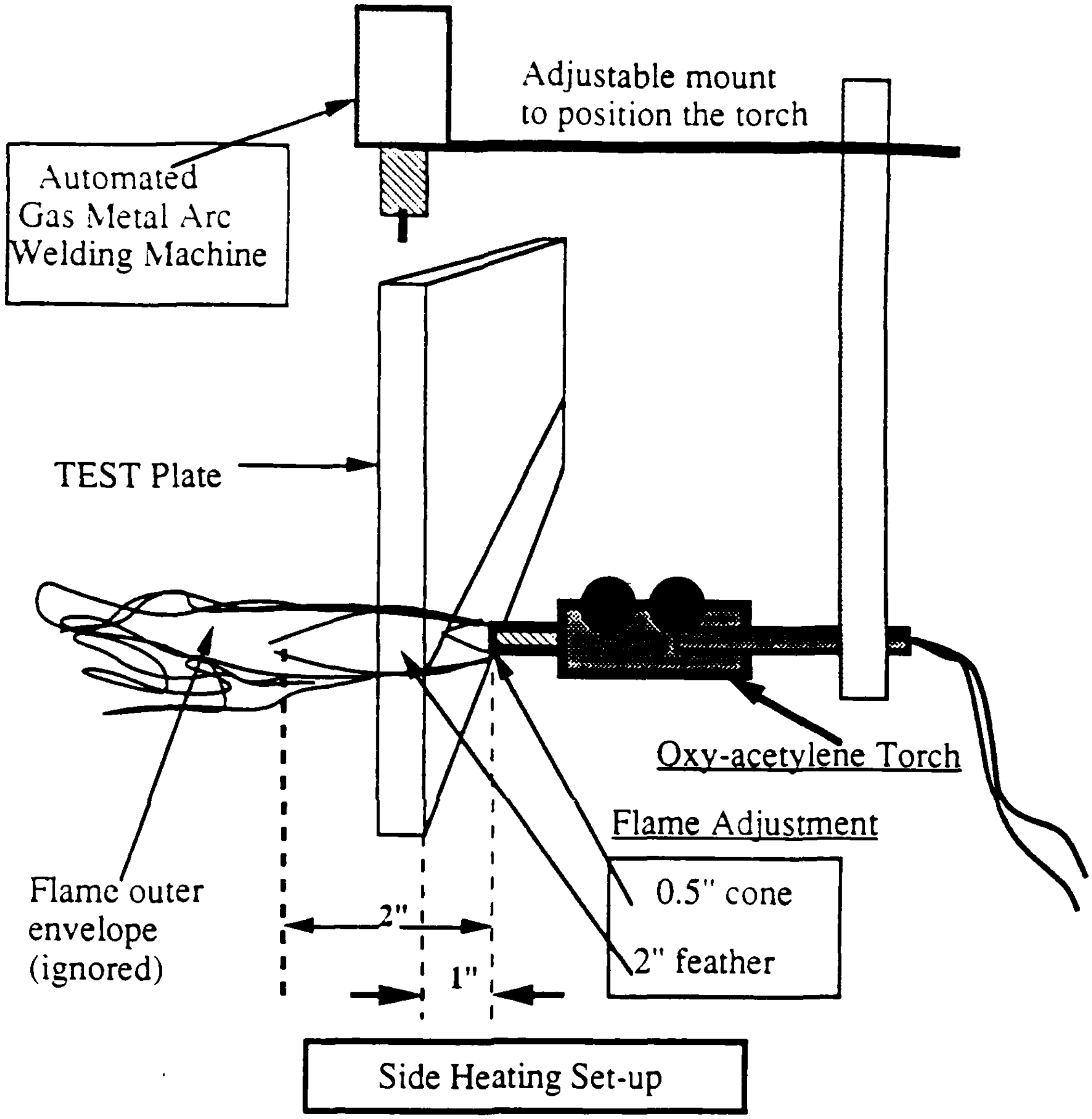
Adjustable mount
to position the torch
Automated
Gas Metal Arc
Welding Machine
TEST Plate
Oxy-acetylene Torch
Flame Adjustment
0.5" cone
2" feather
Flame outer
envelope
(ignored)
2"
1"
Side Heating Set-up

Figure 17

3.3: Experimental Investigation

3.3.1: Prepai ation:

During the months of February and March, equipment for this experimental investigation was gathered and set-up. The test plate steel was obtained form David Taylor Naval Research Center in Annapolis, MD. To manage the data, an HP3852A Data Acquisition machine was purchased with modules to handle up to 20 strain gages and then thermocouples simultaneously. The personal computer used was an AT&T 6300 type, and IBM XT compatible with a 640K RAM. We had to purchase a Hard Disk and install a board to put in this computer to be able to run the data managing software associated with the HP3852A. Nearly a month was spent in getting the personal computer and HP3852A running together. In addition, the HP3852A that we purchased had a bad memory board which had to be replaced. Several trips to the Hewlett Packard facility in Burlington, MA were required to finally straighten this out.

The strain gages for this experiment were acquired from the Hottinger Baldwin Measurement Co., Inc. which has a facility in nearby Framingham, MA. XY11, two dimensional 350Ω strain gages were selected (see appendix 3 for details on strain gages).

The thermocouples utilized in the experiments were obtained form Omega Engineering Co., K-type Cromel-Alumel thermocouples were selected for use due to their wide temperature range and ruggedness (see appendix 4 for more details on thermocouples).

3.3.2: Experimental Procedure

Appendix 1 - Experimental Synopses gives a detailed account of what occurred in each experiment.

Phase I - the objective of the first phase was to establish temperature and strain profiles for the material being used: Mild Steel, HY100, and HY130. The Mild Steel was the control piece, while the vouch of the investigation was the high strength steel HY100 and HY130.

Plate Preparation - the specimens used in this study was 1/2" thick Mild Steel, Navy specified high strength steels HY100 and HY180, the standard specimen size for this investigation was 5.5" wide and 18" long. During the full series experiments (#4 - #6) 4 thermocouples and 4 XY strain gages were mounted, 3 dial gages were fitted at the bottom of the plate to record distortion in .0001" increments.

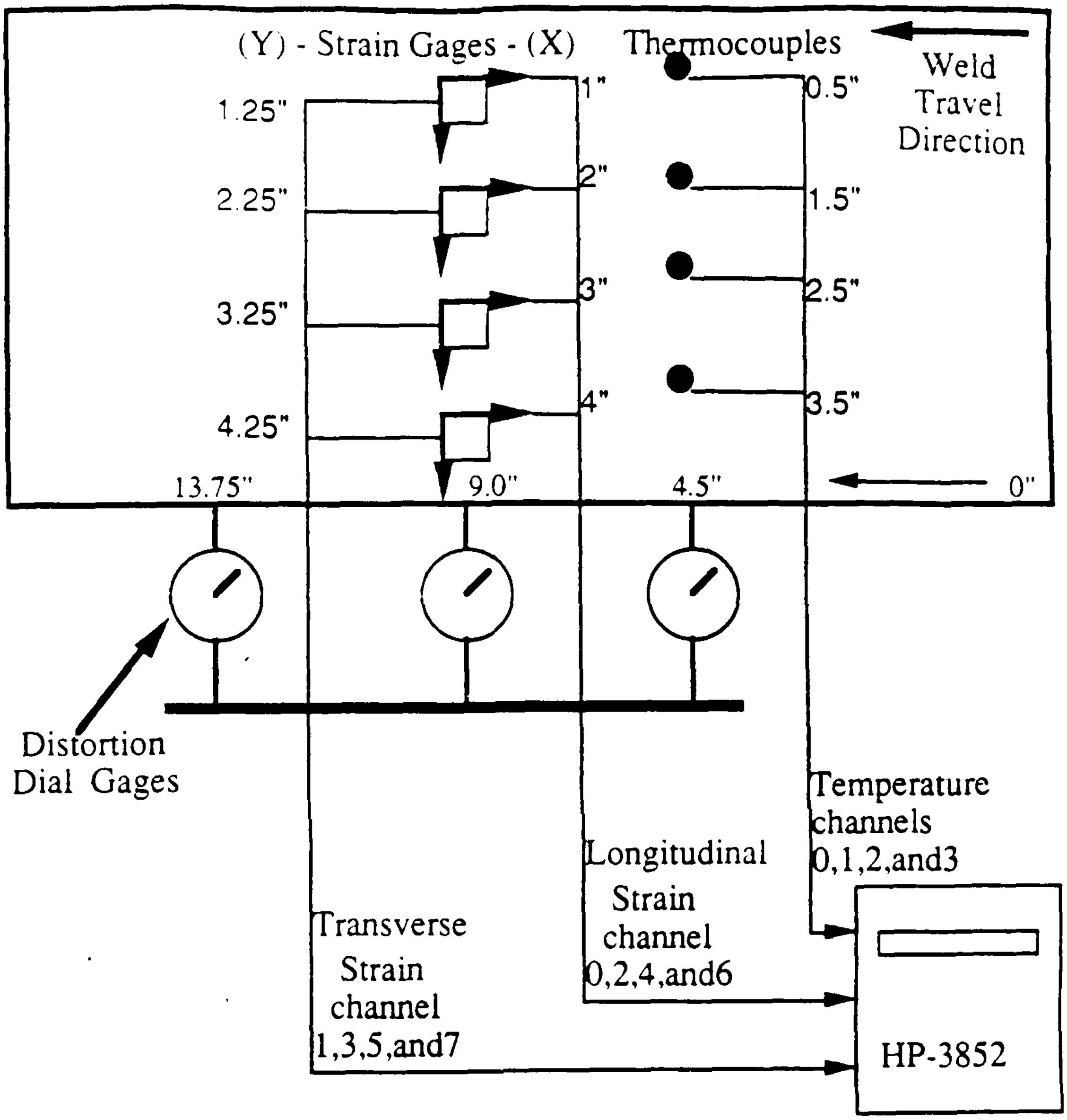

Specimen Experimental Set-up

Front View

Figure 18

Surface Preparation - the specimens were prepared as follows:

- The surface was cleaned using a disc sanding wheel to remove paint, oxides, oil, and all foreign matter.

- The surface, once smooth, was cleaned with acetone.
- The strain gages were mounted at 1" intervals from the top of the plate using the Z70 quick dry adhesive. The strain gage were pain stakingly handled with tweezers during mounting, never touched by hand, and only removed from their package just to mount them.
- Single conductor shielded cable was soldered to the strain gages.
- Clear RTV compound was placed over the entire strain gage and a portion of the wire to cover from foreign matter and help hold the wires in place.
- Thermocouples were then positioned on the plates at 1" apart. A thermally conductive adhesive was placed at the junction to hold the tip in place. Glass tape was placed under the remaining pat of the thermocouple wire to insulate it form the plate.
- After the thermocouples were fitted, more RTV was used to cover the instruments mounted, and after the RTV dried, the entire area was covered with glass tape for protection.
- Starter tabs were then tack welded onto the plates, using a Helliarc manual welding machine.
- The plate was then mounted so that the temperature profiles obtained in experiments #4 - #6 agreed well with predicted values. Graphs displaying the temperature profile for the Mild Steel, HY100, HY130, and a comparison of temperatures at 0.5" from the weld line confirmed this.

The following temperature profiles were obtained in the first full series of experiments from Phase 1:

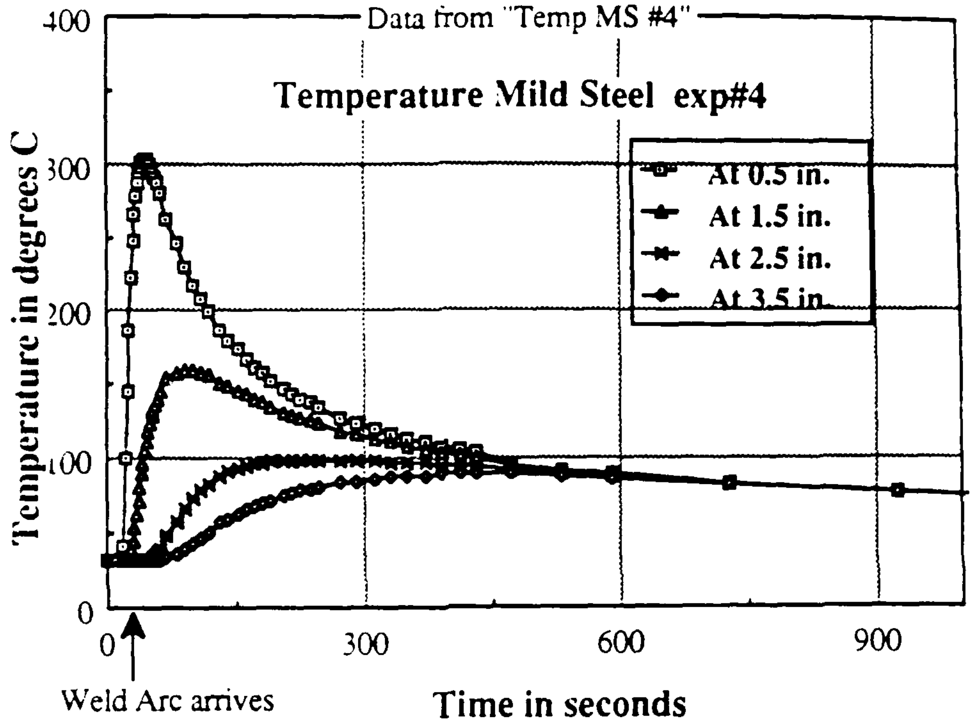

Figure 19

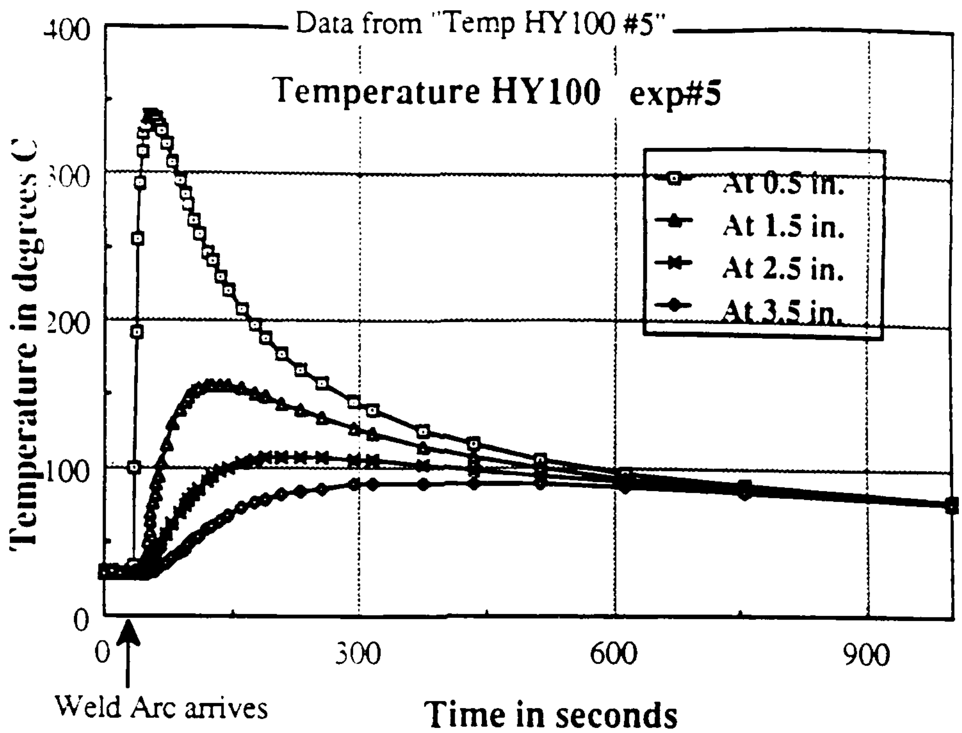
Data from "Temp HY100 #5"
Temperature HY100 exp#5
At 0.5 in.
At 1.5 in.
At 2.5 in.
At 3.5 in.
Temperature in degrees C
400
300
200
100
0
0
300
600
900
Weld Arc arrives
Time in seconds

Figure 20

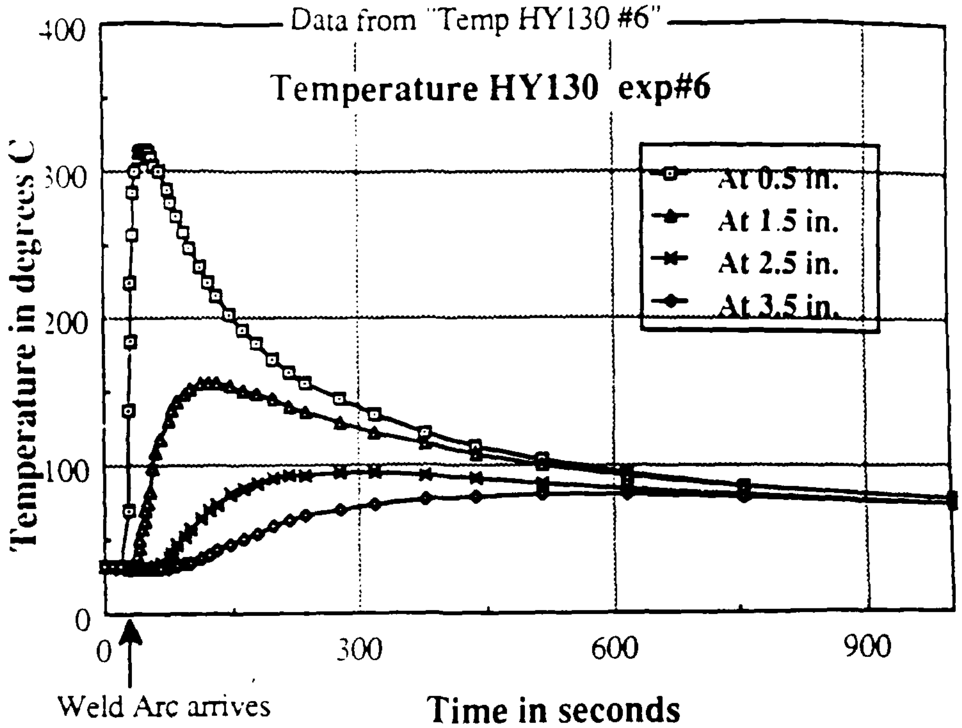
Data from "Temp HY130 #6"
Temperature HY130 exp#6
At 0.5 in.
At 1.5 in.
At 2.5 in.
At 3.5 in.
Temperature in degrees C
400
300
200
100
0
0
300
600
900
Weld Arc arrives
Time in seconds

Figure 21

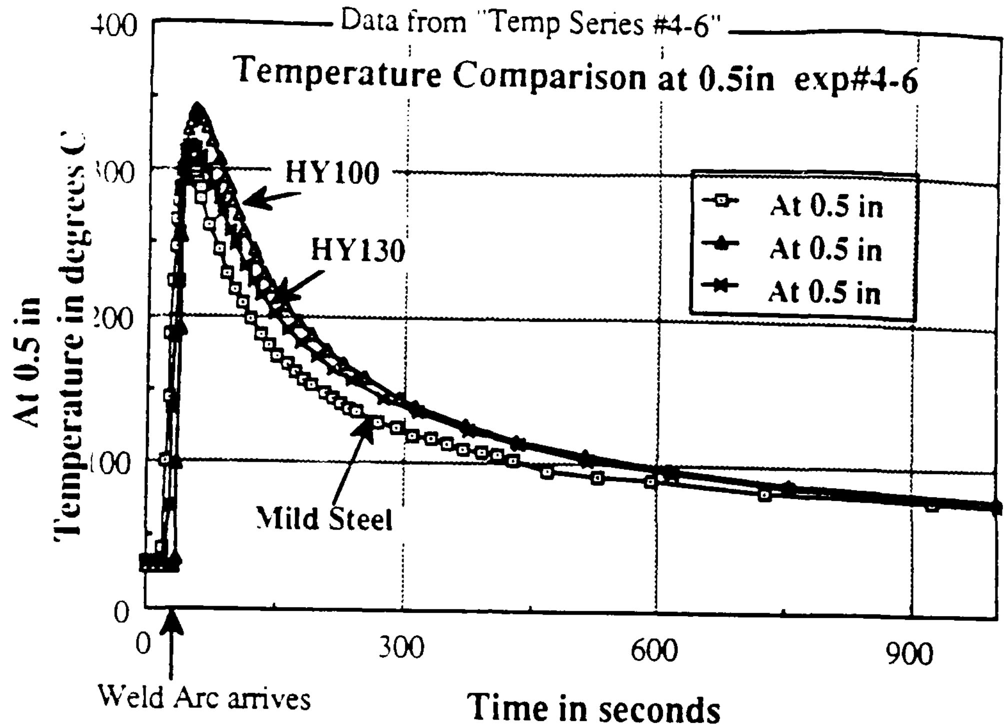

Data from "Temp Series #4-6"
Temperature Comparison at 0.5in exp#4-6
400
300
200
100
0
At 0.5 in
Temperature in degrees C
HY100
HY130
Mild Steel
At 0.5 in
At 0.5 in
At 0.5 in
0
300
600
900
Weld Arc arrives
Time in seconds

Figure 22

• The strain was also examined both longitudinally and transverse on each type of steel.

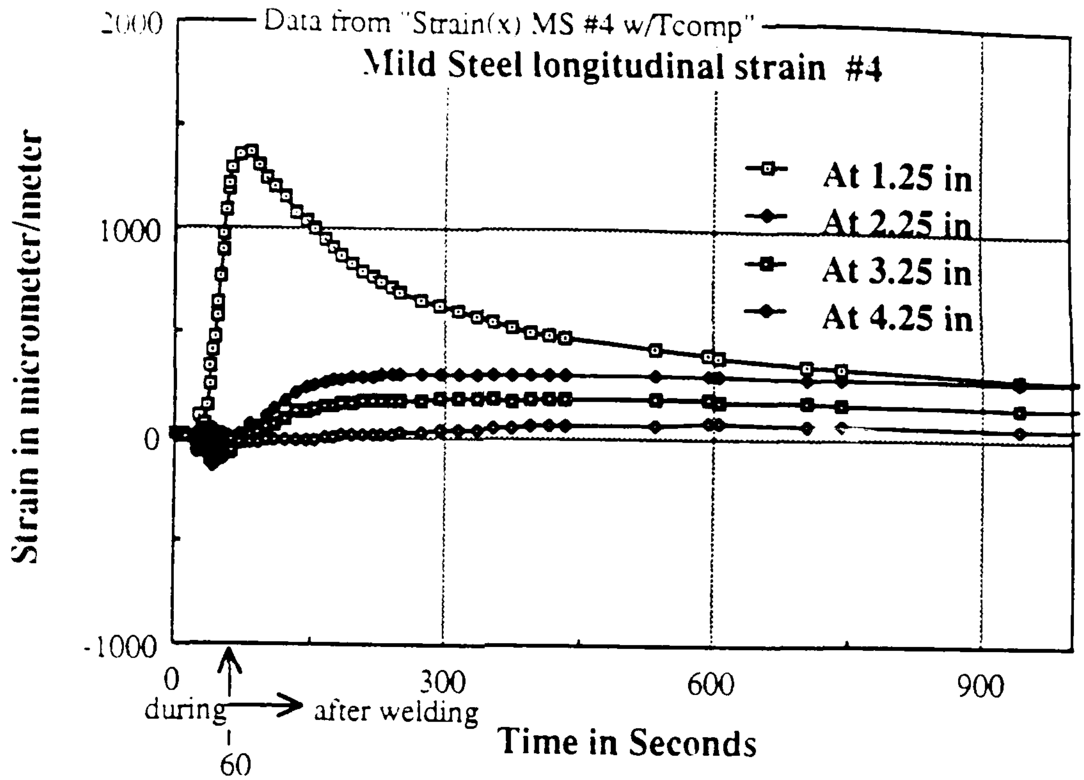

Figure 23

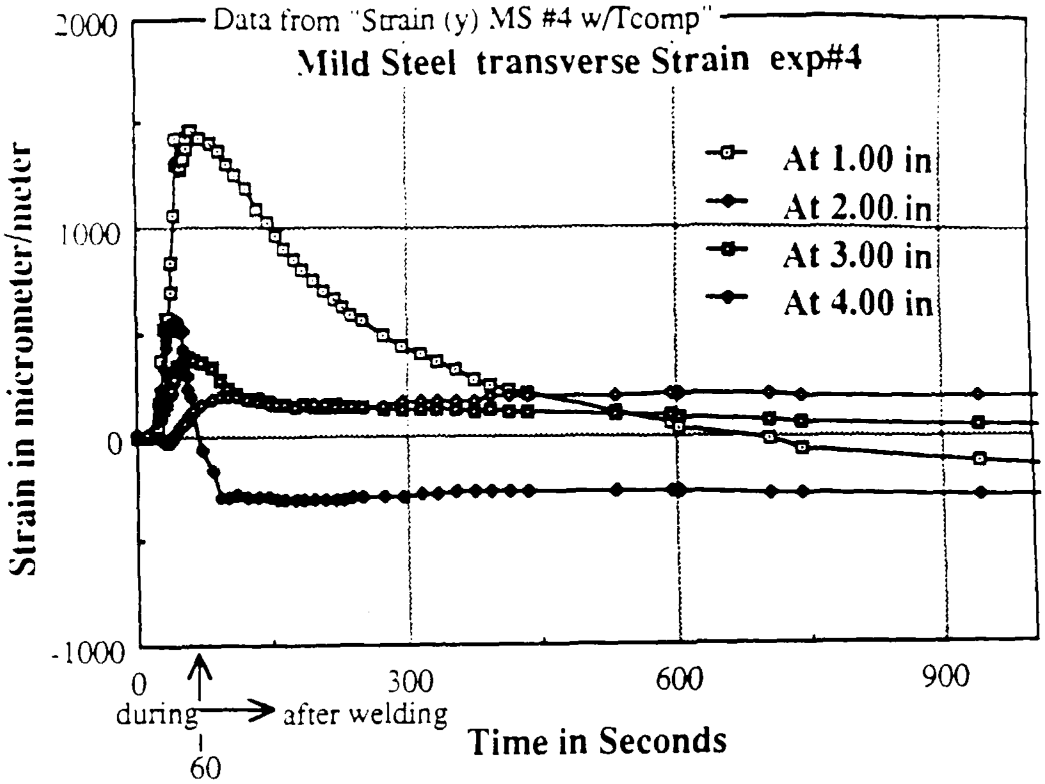

Data from "Strain (y) MS #4 w/Tcomp"
Mild Steel transverse Strain exp#4
At 1.00 in
At 2.00 in
At 3.00 in
At 4.00 in
2000
1000
0
-1000
Strain in micrometer/meter
0
300
600
900
during
after welding
60
Time in Seconds

Figure 24

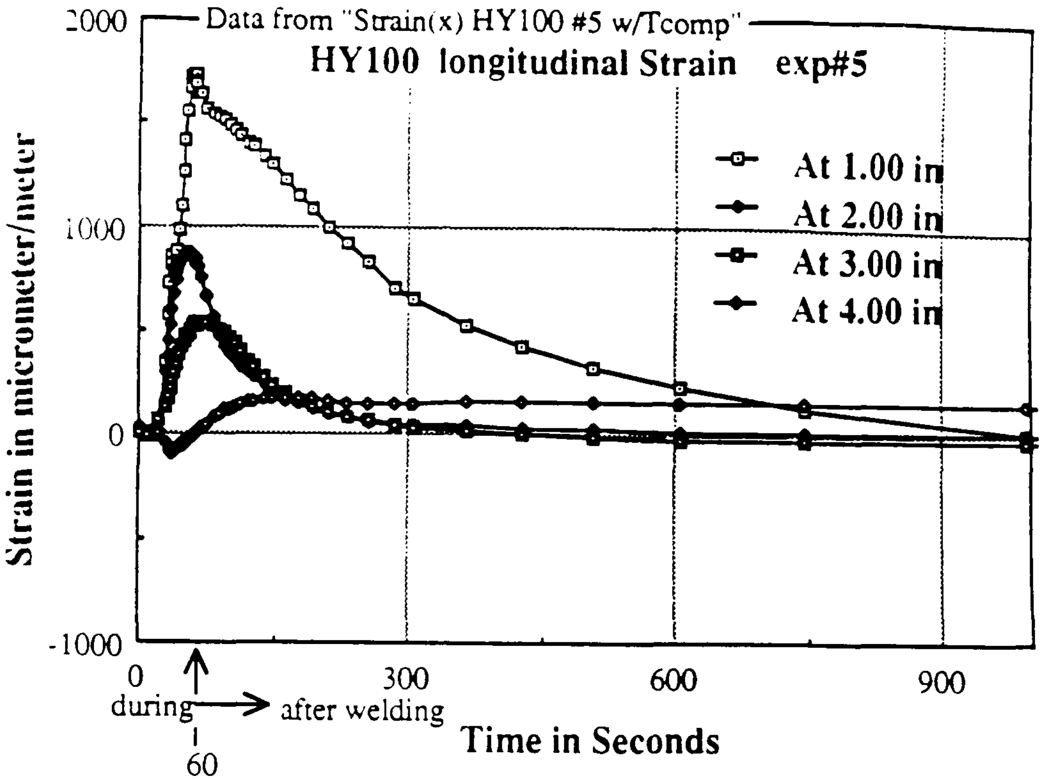
Data from "Strain(x) HY100 #5 w/Tcomp"
HY100 longitudinal Strain exp#5
At 1.00 in
At 2.00 in
At 3.00 in
At 4.00 in
Strain in micrometer/meter
2000
1000
0
-1000
0
300
600
900
during
after welding
60
Time in Seconds

Figure 25

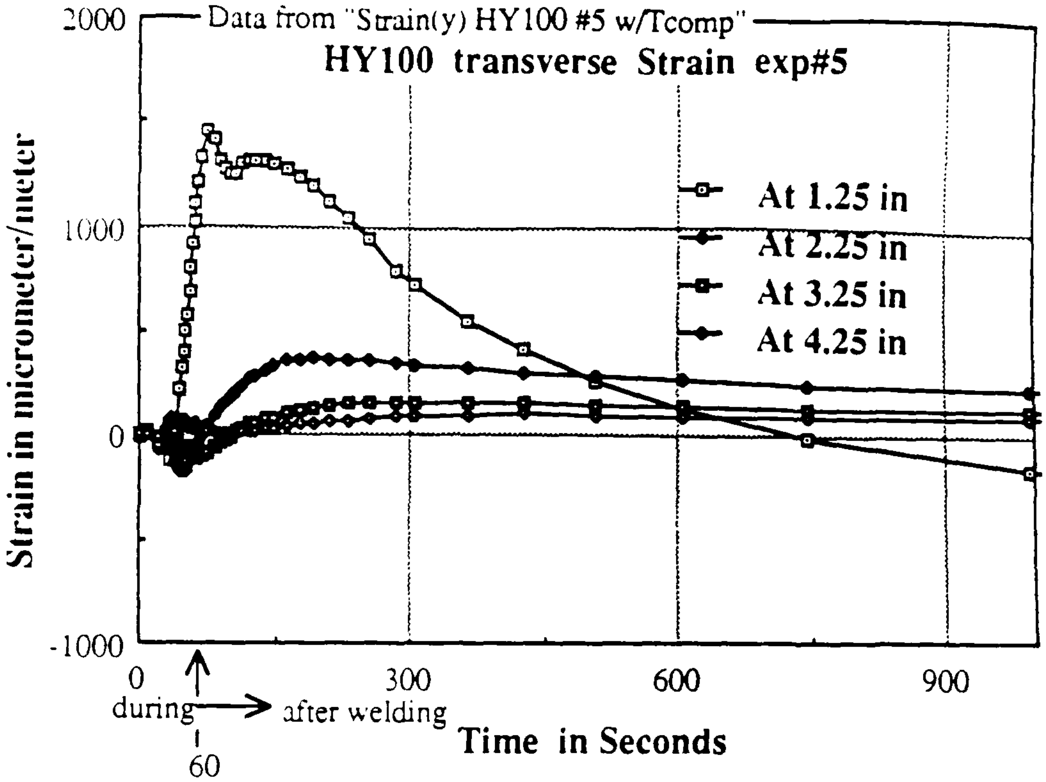

Data from "Strain(y) HY100 #5 w/Tcomp"
HY100 transverse Strain exp#5
Strain in micrometer/meter
2000
1000
0
-1000
At 1.25 in
At 2.25 in
At 3.25 in
At 4.25 in
0
300
600
900
during
after welding
60
Time in Seconds

Figure 26

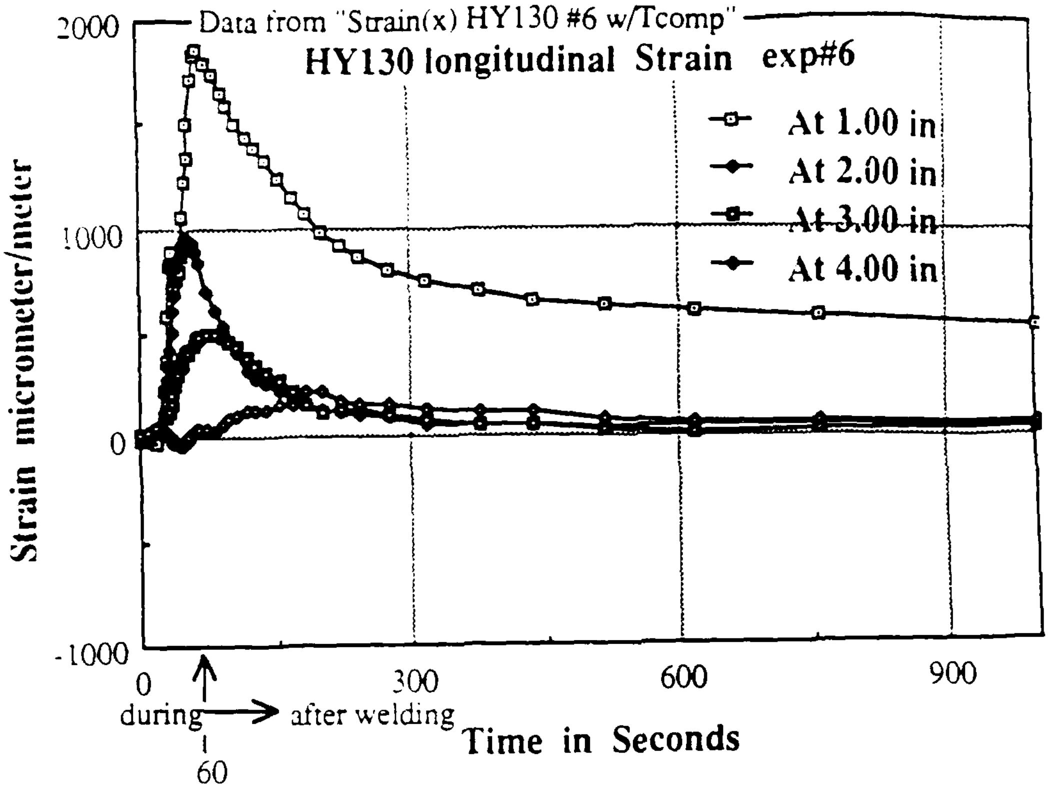

Data from "Strain(x) HY130 #6 w/Tcomp"
HY130 longitudinal Strain exp#6
At 1.00 in
At 2.00 in
At 3.00 in
At 4.00 in
2000
1000
0
-1000
Strain micrometer/meter
0
300
600
900
during
after welding
60
Time in Seconds

Figure 27

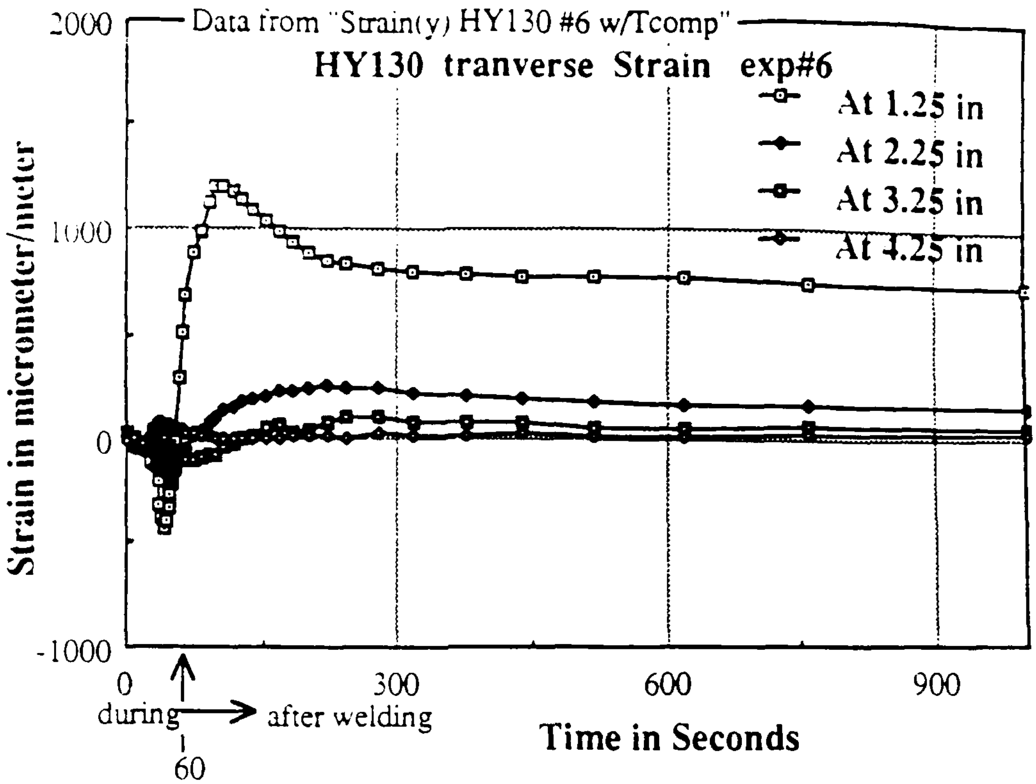
Data from "Strain(y) HY130 #6 w/Tcomp"
HY130 tranverse Strain exp#6
At 1.25 in
At 2.25 in
At 3.25 in
At 4.25 in
2000
1000
0
-1000
Strain in micrometer/meter
0
300
600
900
during
after welding
60
Time in Seconds

Figure 28

• The longitudinal and transverse strain was also examined at 1.0 inch from the weld line on a single plot:

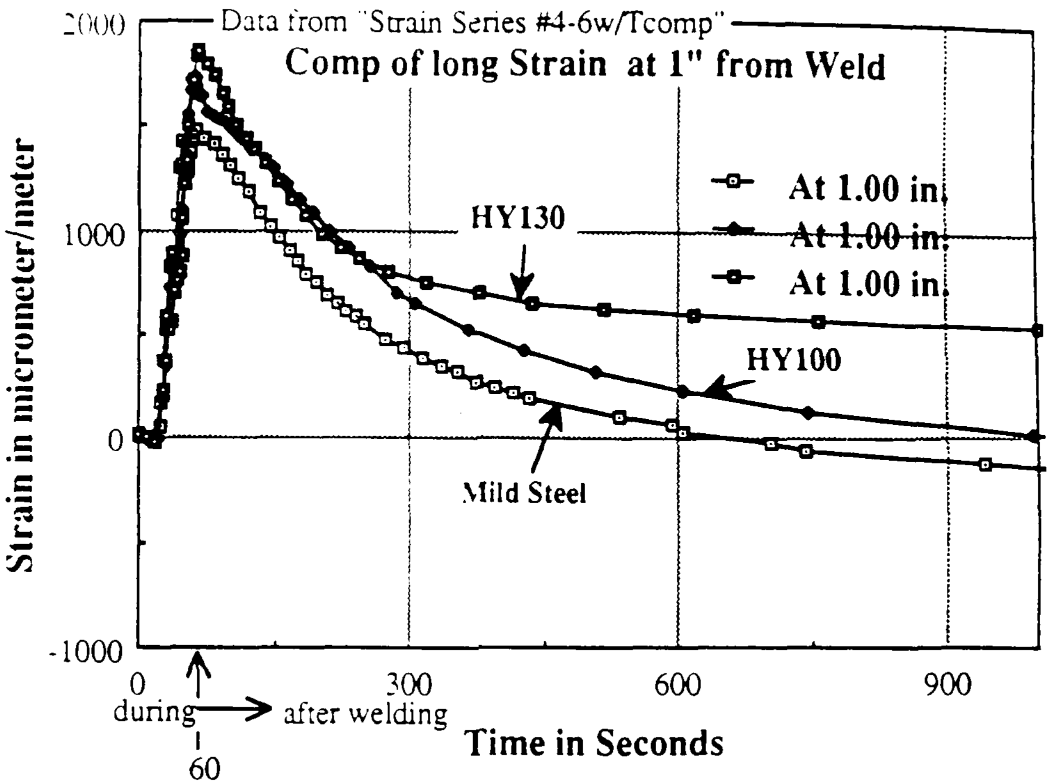

Figure 29

The HY100 rose to the highest temperature. These profiles looked excellent when compared to predicted values.

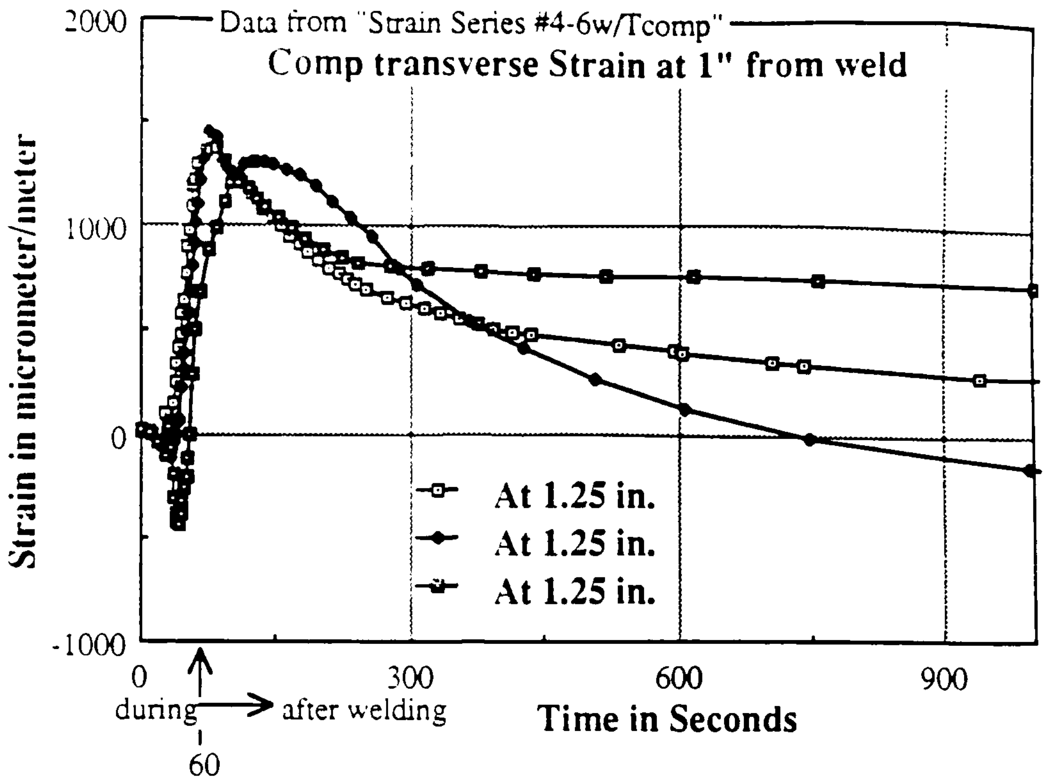

Figure 30

This completed the Phase I of this project and established baseline residual stress data (contained in appendix 2). The data table 18 shows the strain readings before and after cutting.

Phase II - the second phase of this investigation involved several series of experiments examining the distortion on these three steels. First to measure the distortion without side heating, then to measure the distortion with side heating. A set of experiments was also conducted using side heat only to isolate the effects of the side heat. This involved experiments #8 through #25. All the distortion data is compiled in data tables 19, "Distortion" and data table 20 "Side Heat Only" in appendix 2.

The distortion experiments were interesting and revealing. Initially, a distortion profile was established for each type of steel, and the distortion at the midpoint (9") examined for all pieces for ease of comparison and scales were matched. The distortion measured on the deal gages is opposite to hat is occurring at the weld line.

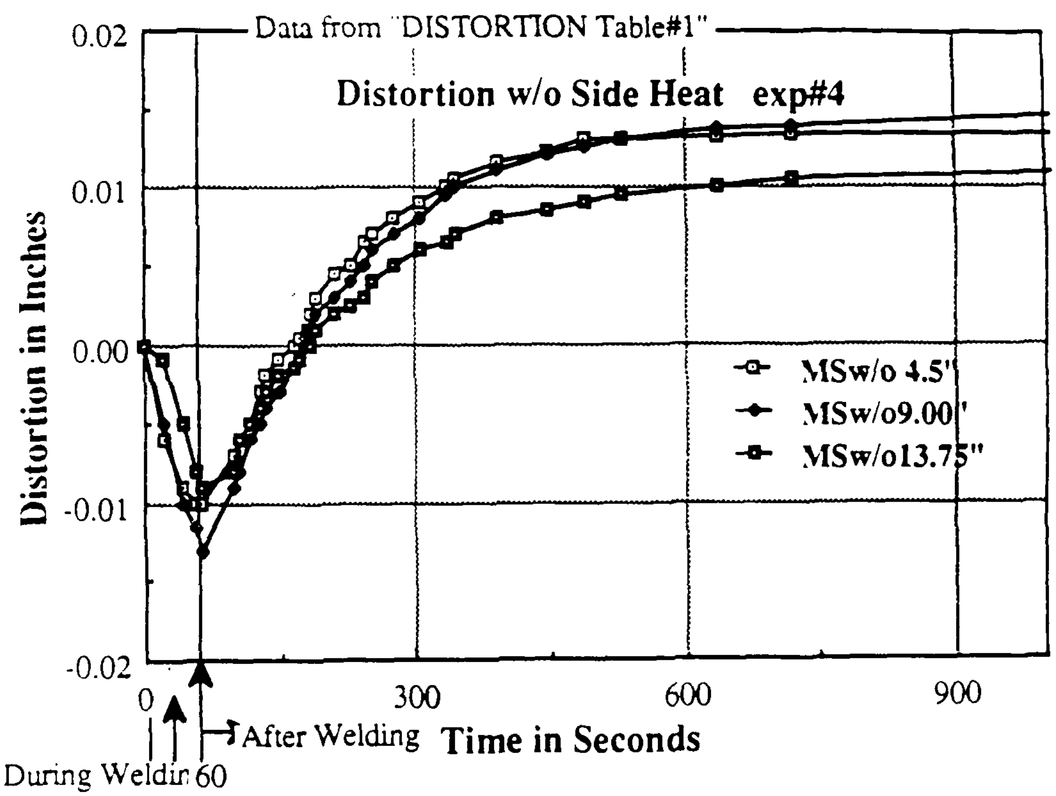

Figure 31

In figure 31, the distortion is initially negative (compressive) which means the top of the plate where the welding occurs is above the plate's neutral axis and therefore must be in tension.

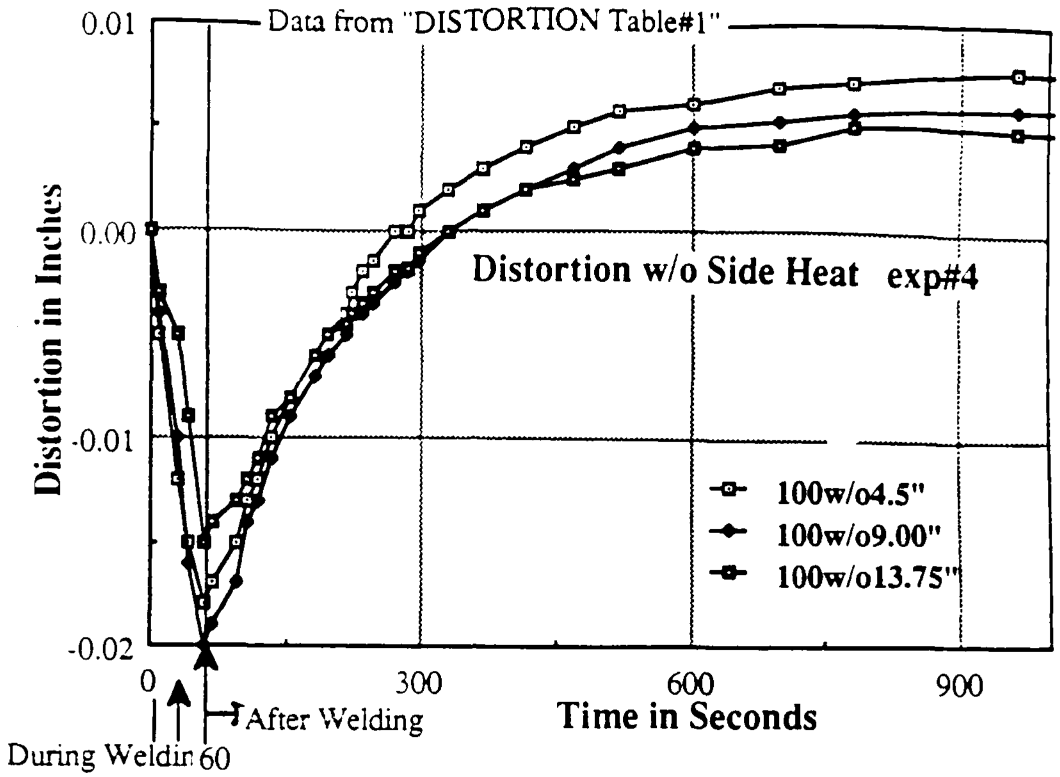
0.01
Data from "DISTORTION Table#1"
0.00
-0.01
-0.02
Distortion in Inches
Distortion w/o Side Heat exp#4
100w/o4.5"
100w/o9.00"
100w/o13.75"
0
300
600
900
After Welding
Time in Seconds
During Weldin
60

Figure 32

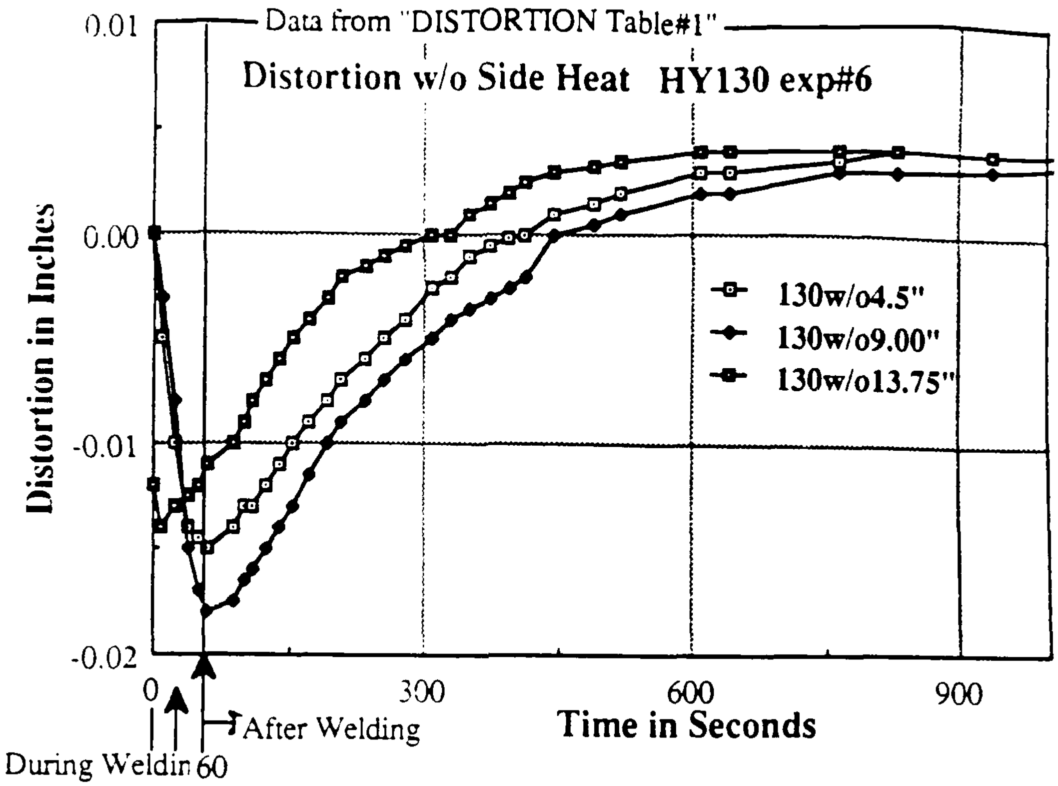

Figure 33

The highest distortion readings in tension were attained on HY100 then HY130 and Mild Steel, but the swing from tension to compression was widest for the Mild Steel, then HY100 followed by HY130. After cooling down the final distortion readings were lowest on HY130 (see figure 34) which shows this at the midpoint.

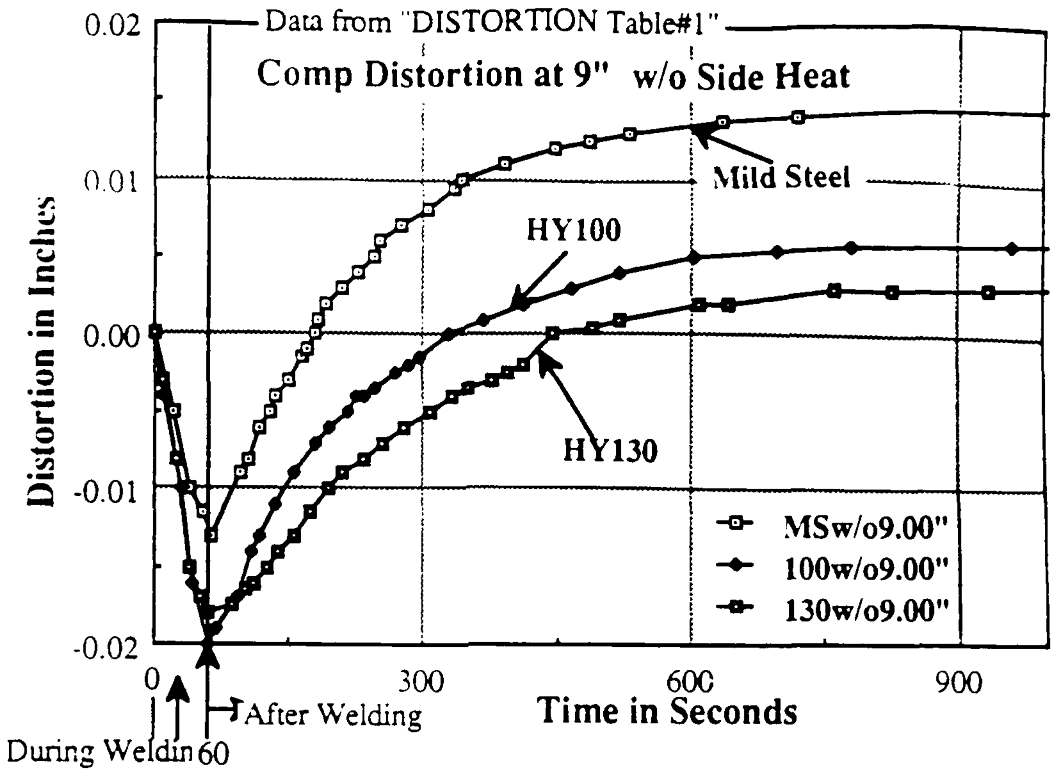

Data from "DISTORTION Table#1"
Comp Distortion at 9" w/o Side Heat
0.02
0.01
0.00
-0.01
-0.02
Distortion in Inches
Mild Steel
HY100
HY130
MSw/o9.00"
100w/o9.00"
130w/o9.00"
0
300
600
900
Time in Seconds
After Welding
During Weldin
60

Figure 34

• Next the distortion with side heating was examined. A considerable reduction in all distortion readings were observed again compared at the midpoint.

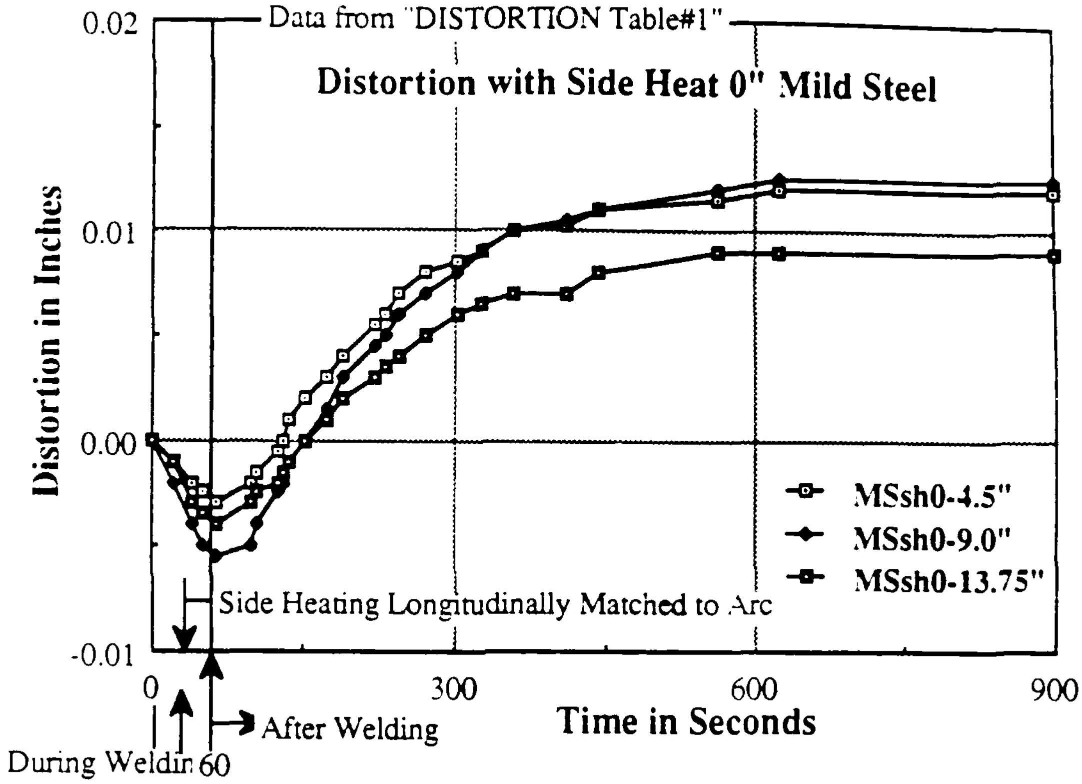

Figure 35

Notice the dramatic reduction in distortion during welding comparing figure 31 and 35 for the Mild Steel (roughly 50%).

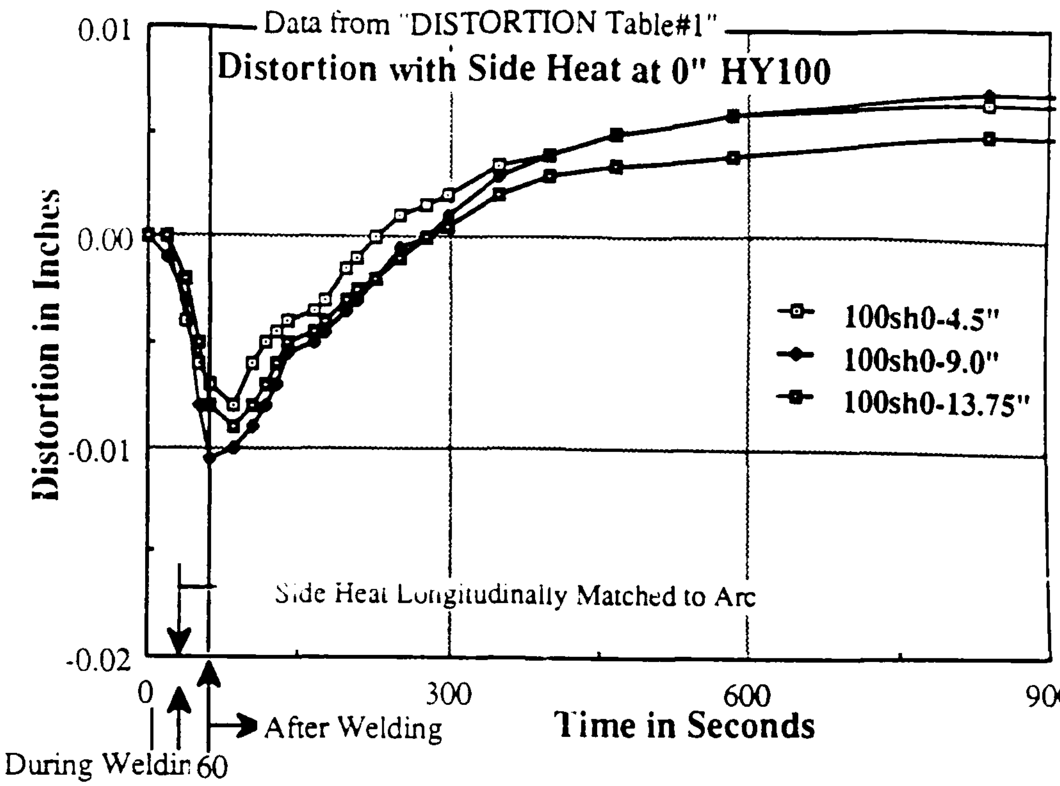

Figure 36

Again, look back at figure 32 and notice the reduction which is about 50%.

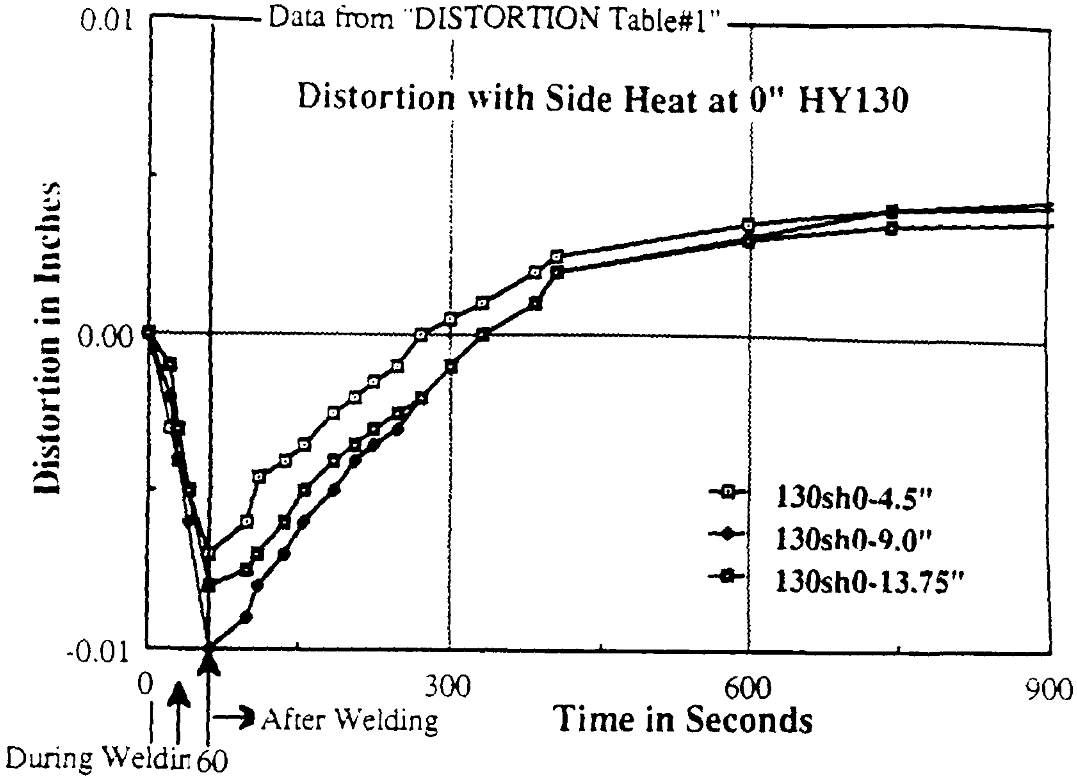

Figure 37

Compare with figure 33, again about 50% reduction during welding.

• The next series of graphs display the results of positioning the side heating torch 9" ahead of the arc longitudinally (30 sec.).

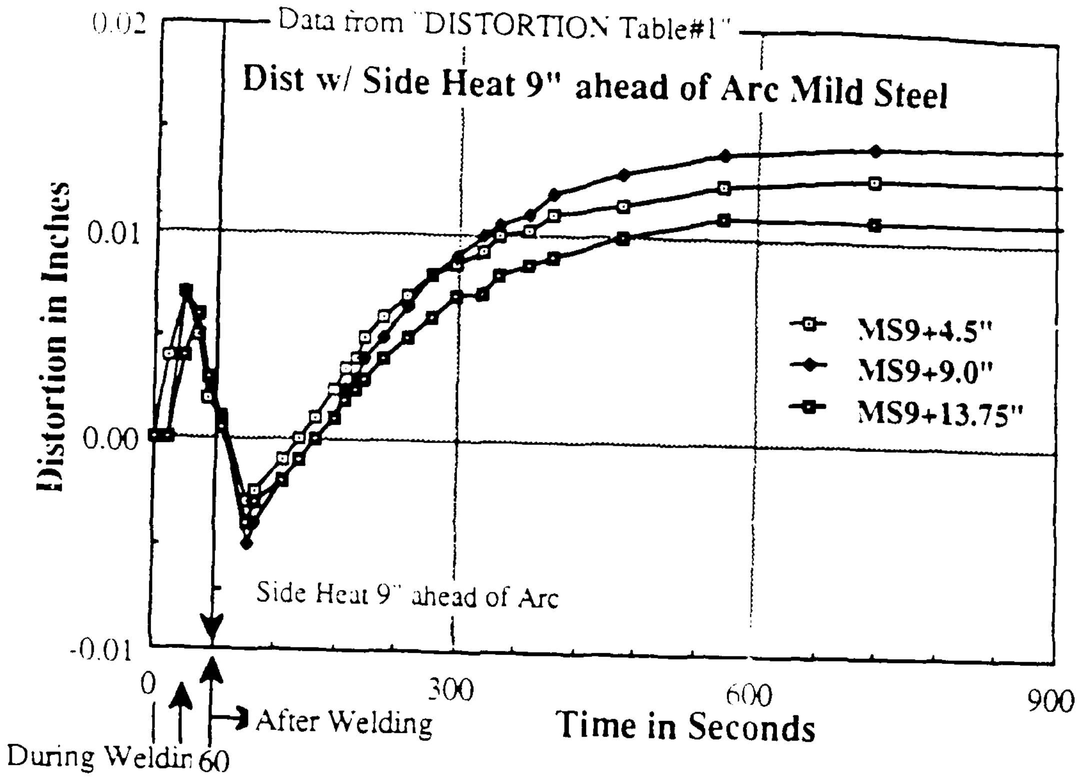

Figure 38

The side heating ahead causes the distortion to be nearly zero during welding, but shortly afterward the metal continues to move in tension form the effects of the arc.

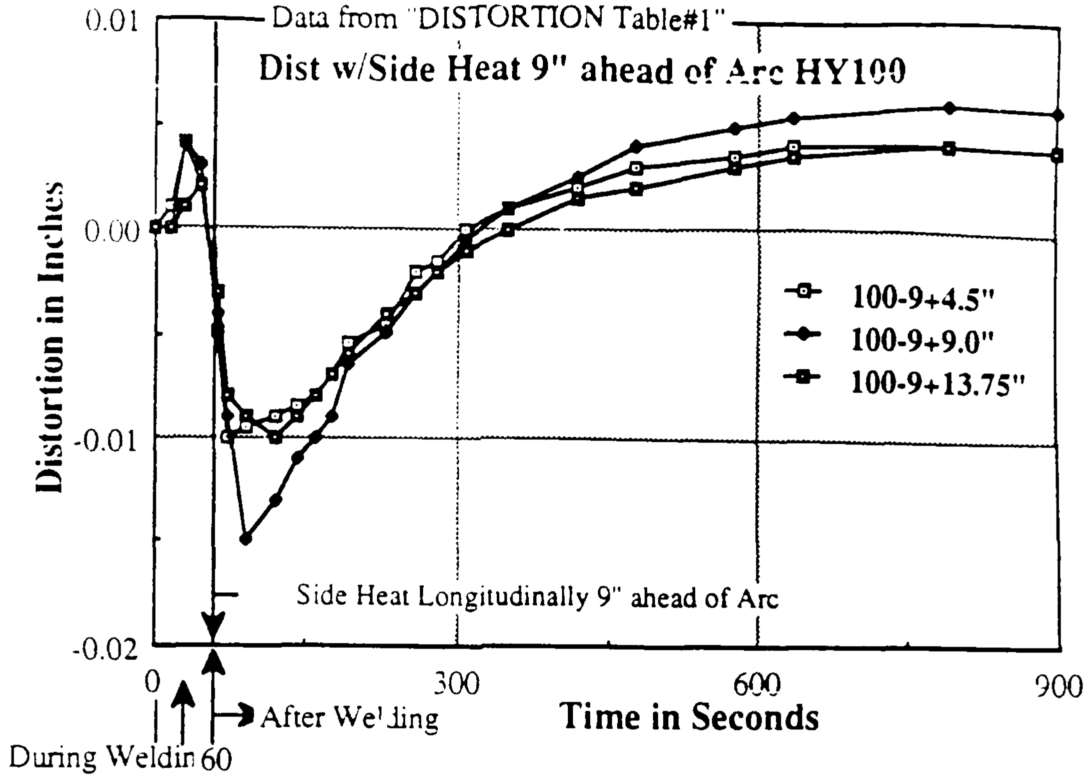

Figure 39

Again, the metal movement opposes the effect of the arc and distortion is near zero at the completion of the weld.

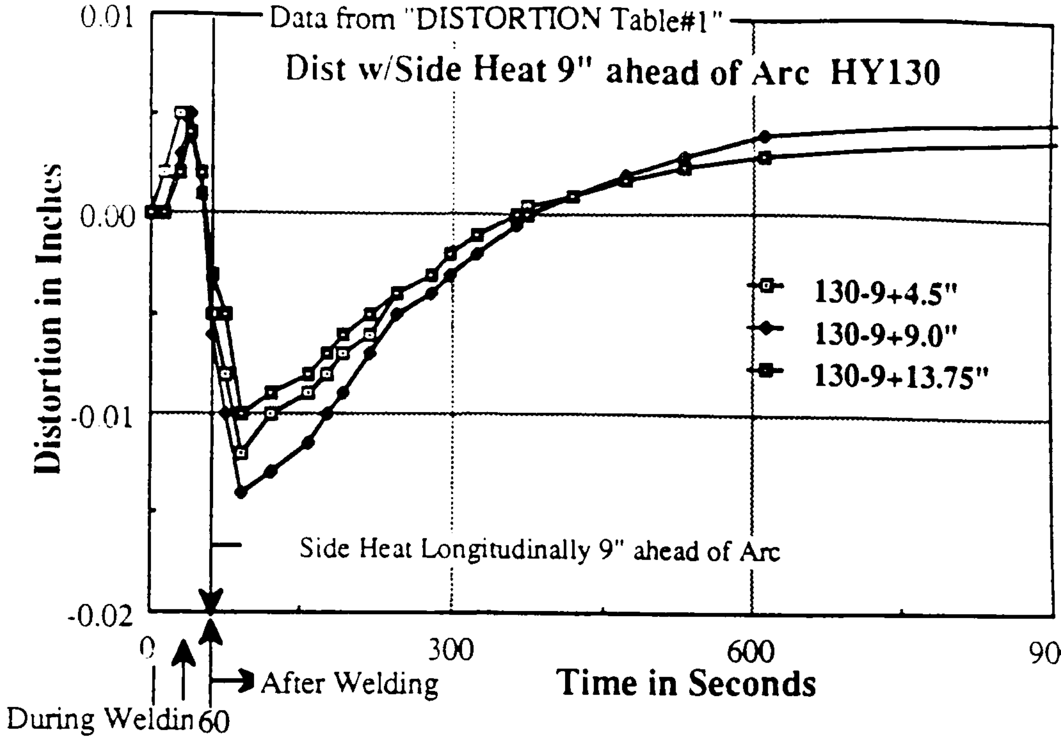

Figure 40

The distortion rate with HY130 is fastest, but it is smaller in magnitude compared to HY100 or Mild Steel.

• The next series of graphs display the results of positioning the side heating torch 9" behind and matched on Mild Steel of the arc longitudinally (30 sec.).

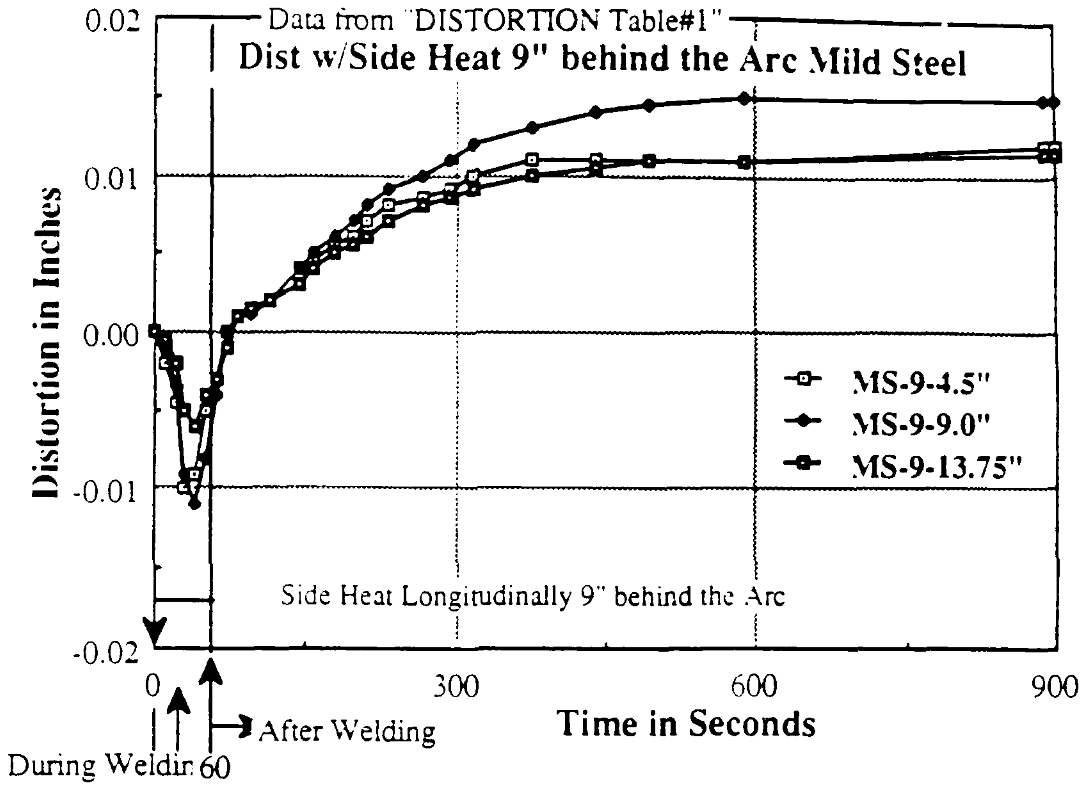

Figure 41

Placing side heat behind the arc causes the plate to accelerate into compression and has little effect on the magnitude of distortion. Compare this figure 41 with figure 31 to see this.

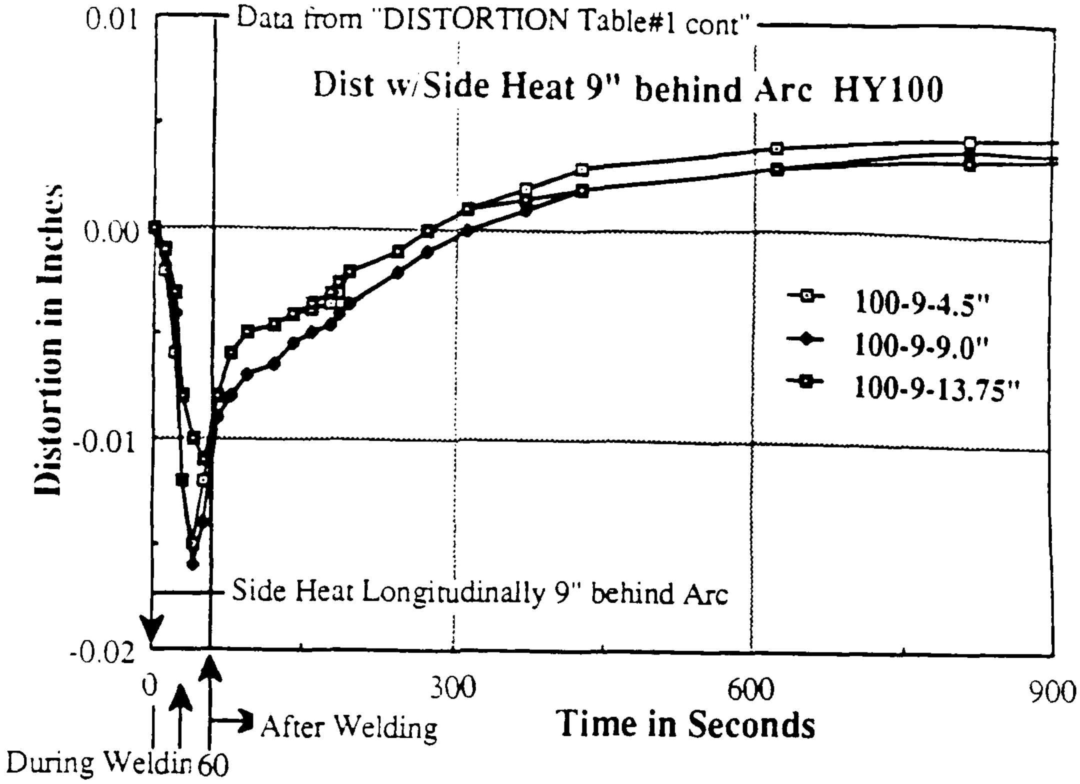

Figure 42

Again the plate is accelerated into compression with little effect on final distortion. However, distortion during welding was slightly reduced with HY100.

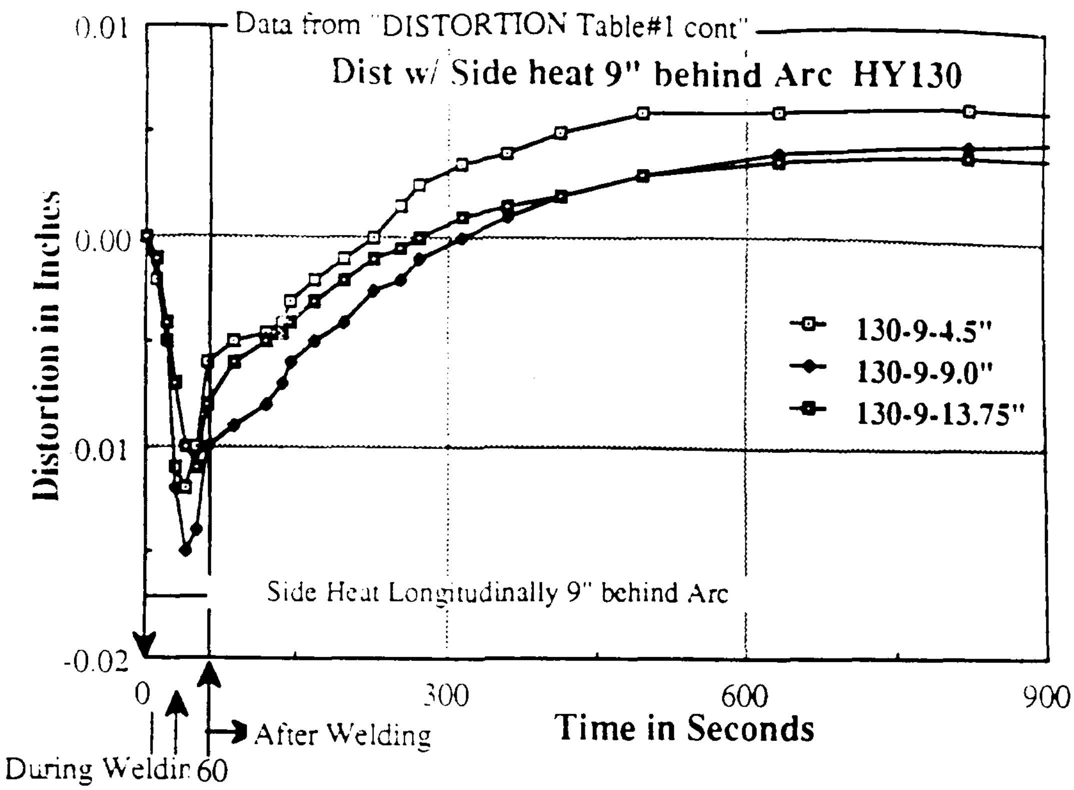

Figure 43

Again, as with the HY100, the HY130 plate was accelerated into compression and the distortion during welding was slightly reduced (10% - 20%).

• The effects of the side heating alone were examined on a separate series of tests with side heat only (table 20).

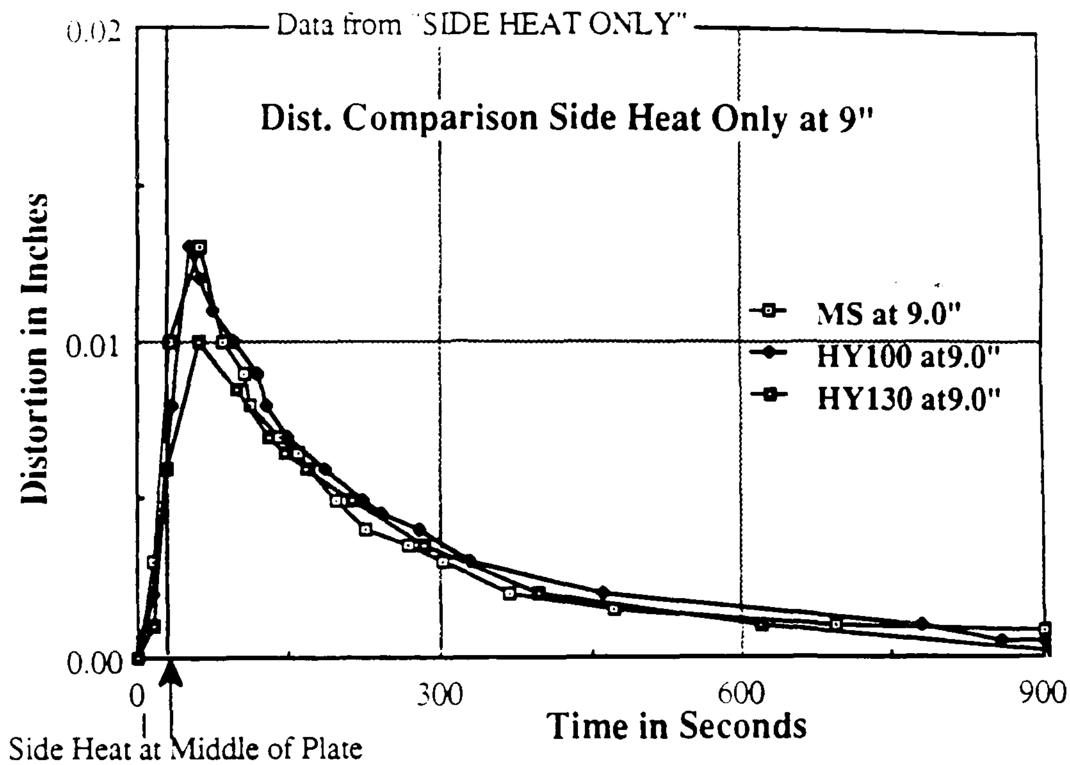

Figure 44

The effect of the Side Heat alone shows that the Side Heat causes metal movement that does directly oppose the movement caused by the arc.

• For close scrutiny a set a graphs depicting each steel with and without side heating and with side heat only reveals just how much of a desirable effect the side heat has.

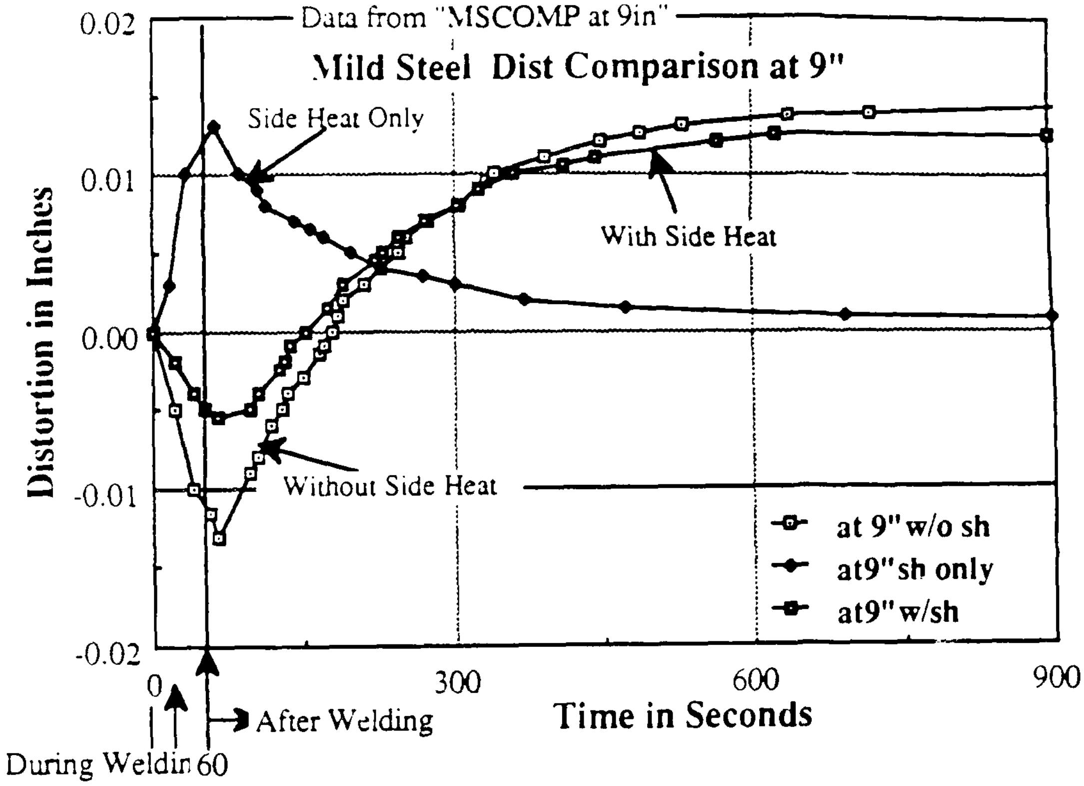

Figure 45

The above figure shows clearly how the distortion is being reduced by the side heat (notice the "With Side Heat" Curve Above).

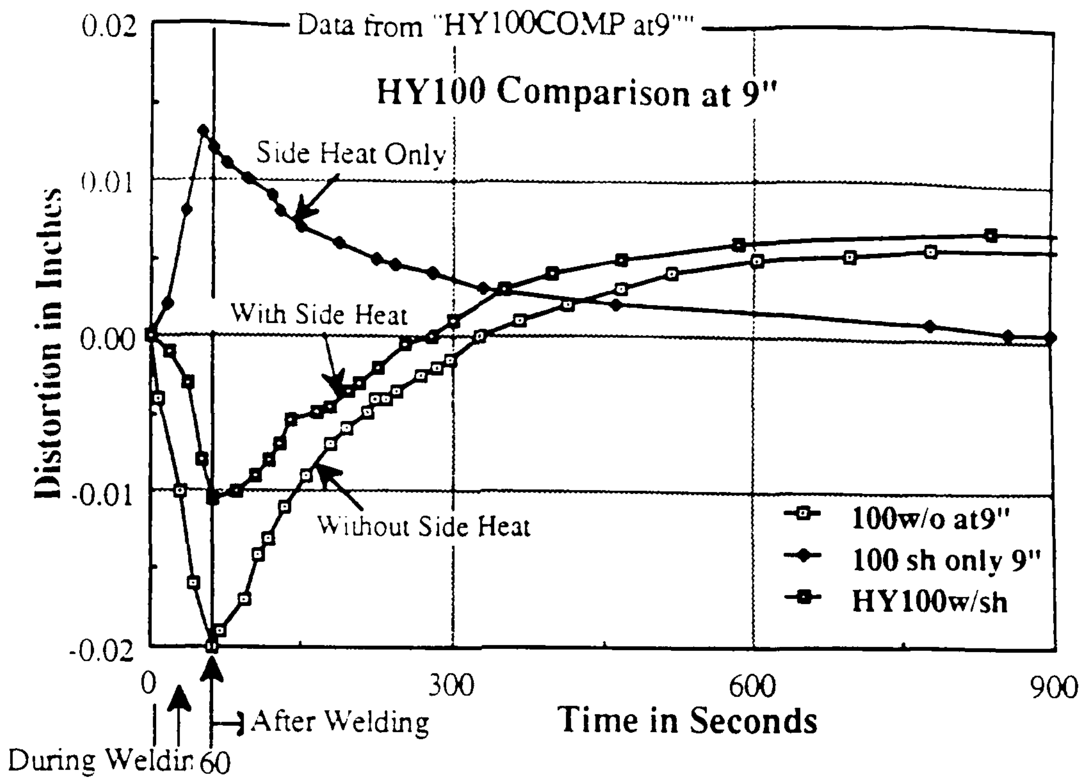

Figure 46

Again, notice the "With Side Heat" curve on the HY100 piece above in figure 46. The following curve showing HY130 again shows both the reductions in distortion during welding and the slowed rate of distortion both of which are beneficial.

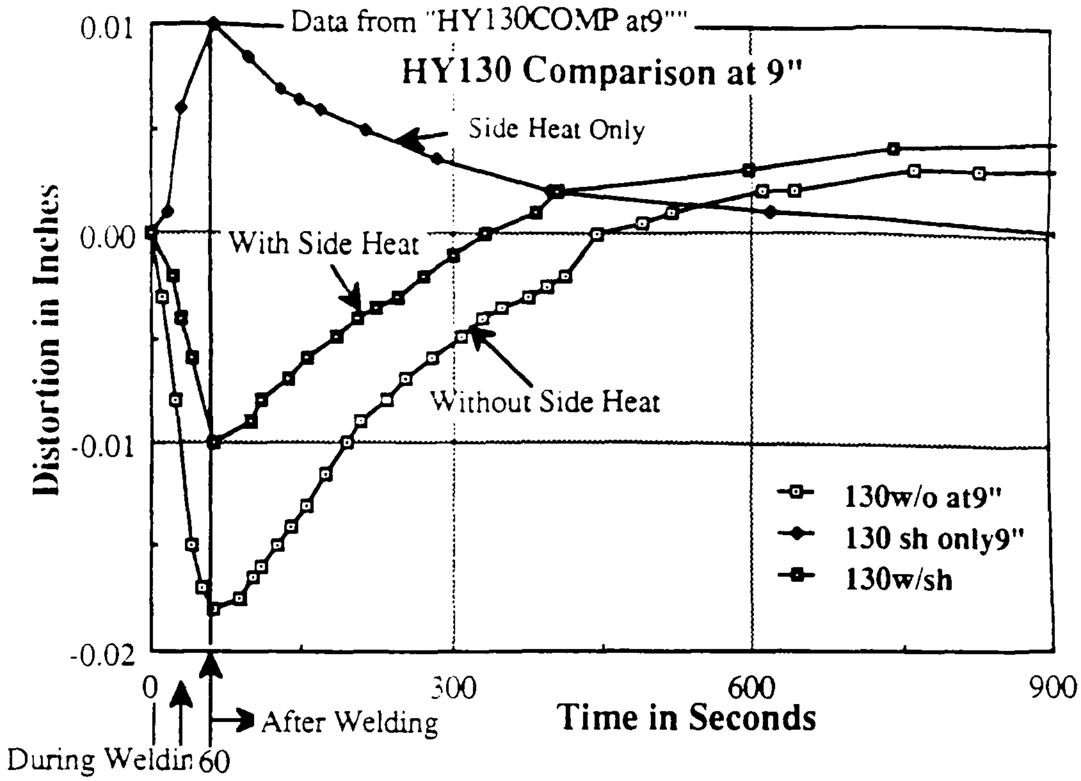

Figure 47

What was determined from shifting the side heat around is that it has the best effect if it is roughly positioned same as the arc or slightly ahead (by eyeball). This conclusion is so significant in that the side heating will work well so long as it is close to the arc longitudinally and preferably slightly ahead, it does not have to be precise. Little difference was noted when the side heat was 2 1/4" ahead (7 sec.), and when it was matched longitudinally. Therefore, this could also be used manually as long as the secondary heat source is moved roughly along with the weld arc and approximately 3" - 5" transverse.

What is most noteworthy is the effect on distortion during welding. This value is reduced significantly in every situation which confirms the hypothesis that introduction of a secondary heat source away form the weld can be effectively utilized to counter the thermal effects from the weld arc. While the side heat input is not a great as the weld arc, the side heat is spread over a wider area (since the flame represents a poor point source) and moves metal over a wide area to oppose the movement from the weld arc. These diagrams confirm that the distortion during welding can be cut in half in using this technique.

3.3.3: Residual Stress:

This final series of data collected from experiments #26 - #28 and again the temperature, strain, and distortion data with the side heat now matched to the arc longitudinally and 4" transverse was taken. An additional two experiments were run because during the stress relieving cutting process to get the residual stress on HY100 and HY130, the strain gages closest to the weld were damaged. These tests were run to verify the strain data previously collected in experiments #27 and #28 at 1".

The temperature, strain, and distortion data collected was similar to experiments #4 - #6 with the exception of the raised temperature readings far way from the weld so the graphs were excluded, but the data is included in appendix 2. In this section, the residual stress is the salient quantity examined. The experimental set-up was as follow:

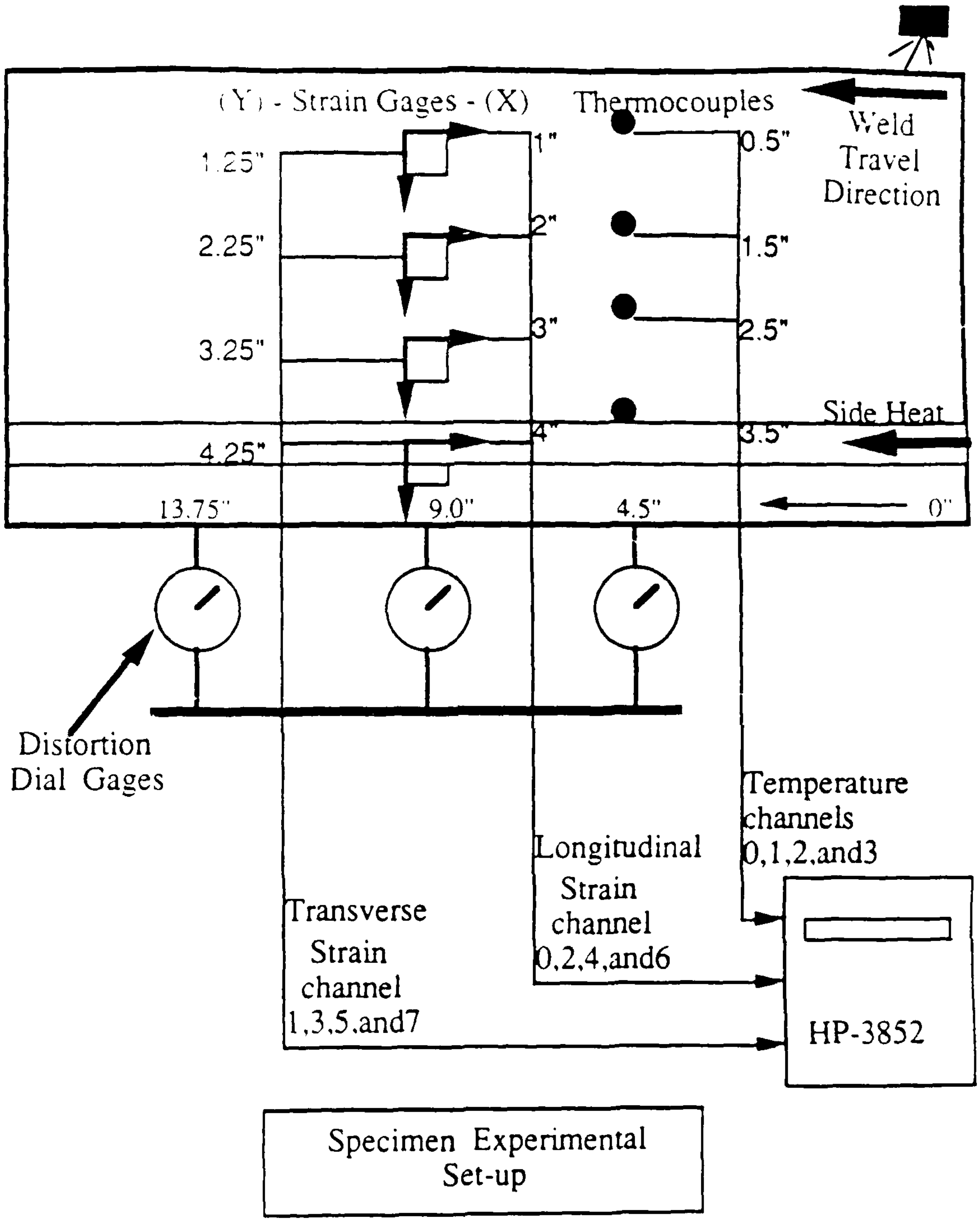

Front View

Figure 48

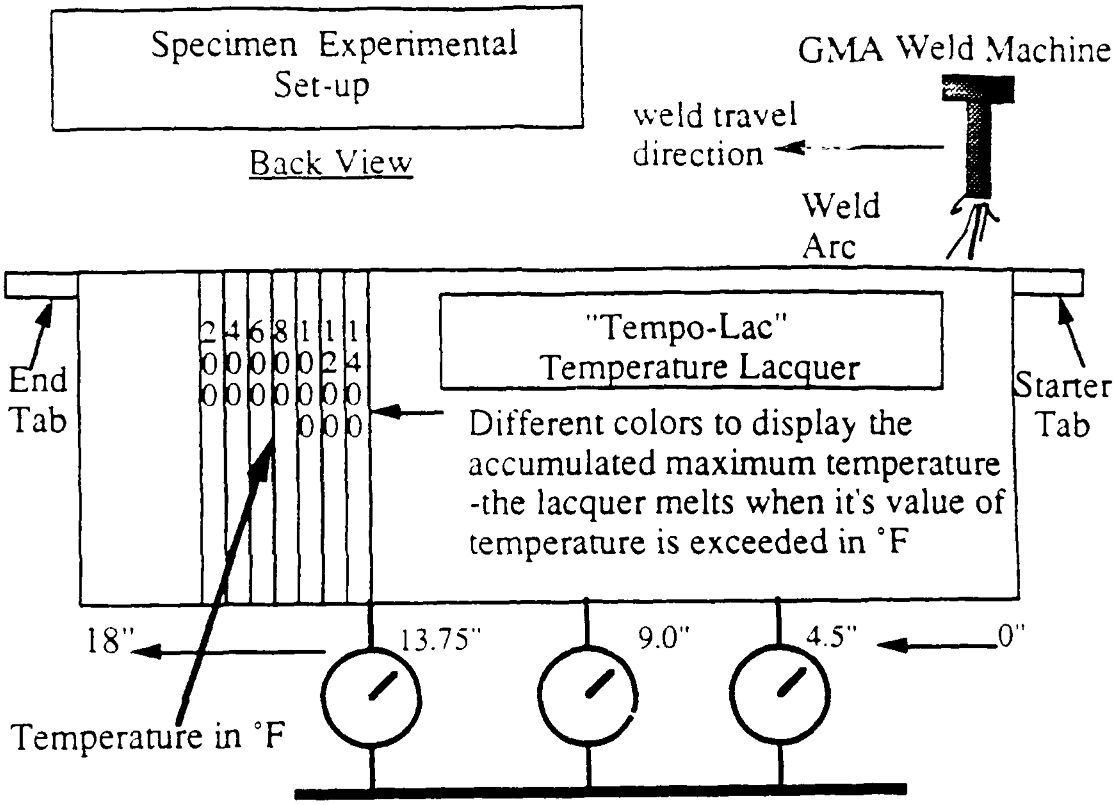

Figure 49

Of course, automated welding processes are best because the optimum side heat position can be determined and set for a particular material being welded. Again, the temperature, strain, and distortion data was tabulated and examined to see if any significant differences occurred from the first series of data (experiments #4 - #6). Other than elevated temperatures at 3 at 3" and 4" away from the weld, the profiles were similar to those previously shown. However, a close examination of the residual stress is in order!

Residual Stresses Data Compared w/o Side Heat and w/Side Heat

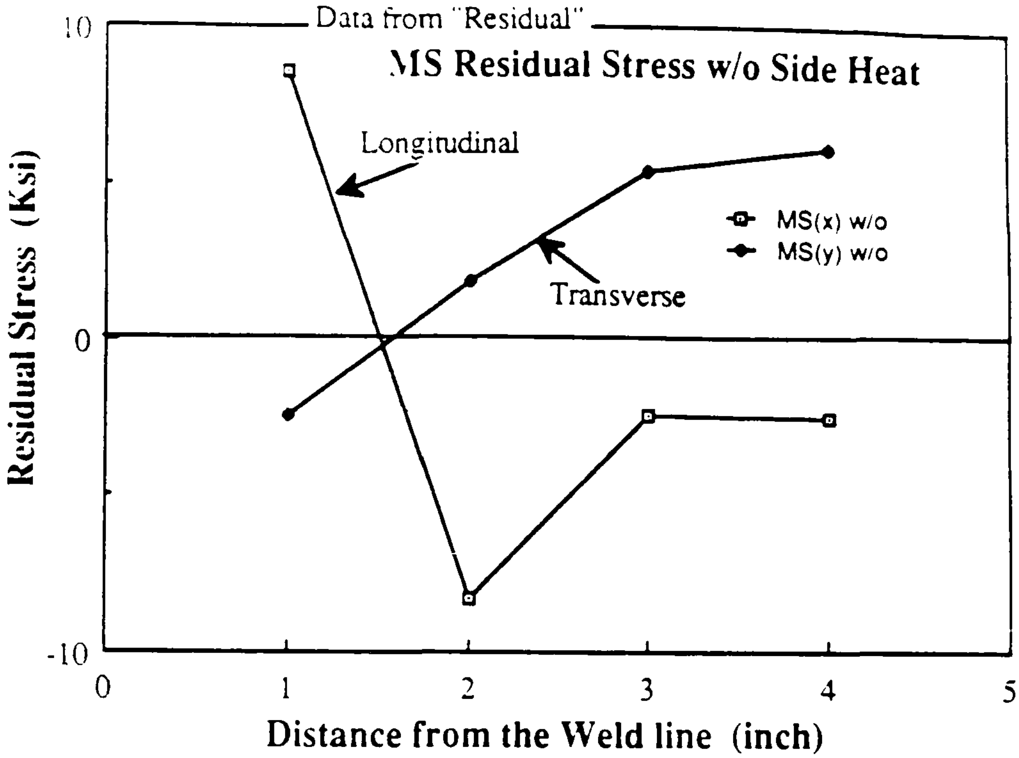

Figure 50

As expected, the residual stress is tensile close to the weld and goes compressive at about 1.5" from the weld line. This is a little further away form the weld than anticipated, but he results on all these tests were similar. Previous experiments show the crossover form tension to compression much closer to the weld line. But this is a function of heat input and the size of the plate. Our plates are as small as possible and still get valid residual stress readings (see figures 13 though 16).

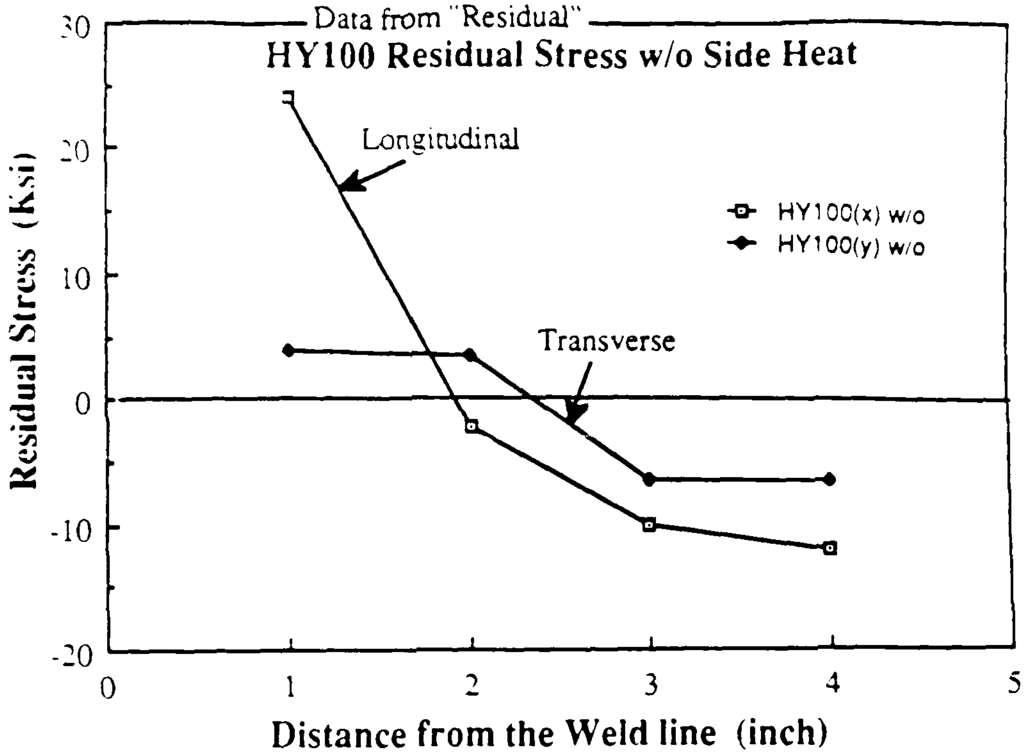

Figure 51

On HY100, the crossover form tension to compression is closer to 2" away from the weld and our test pieces stayed compressive away from the weld line.

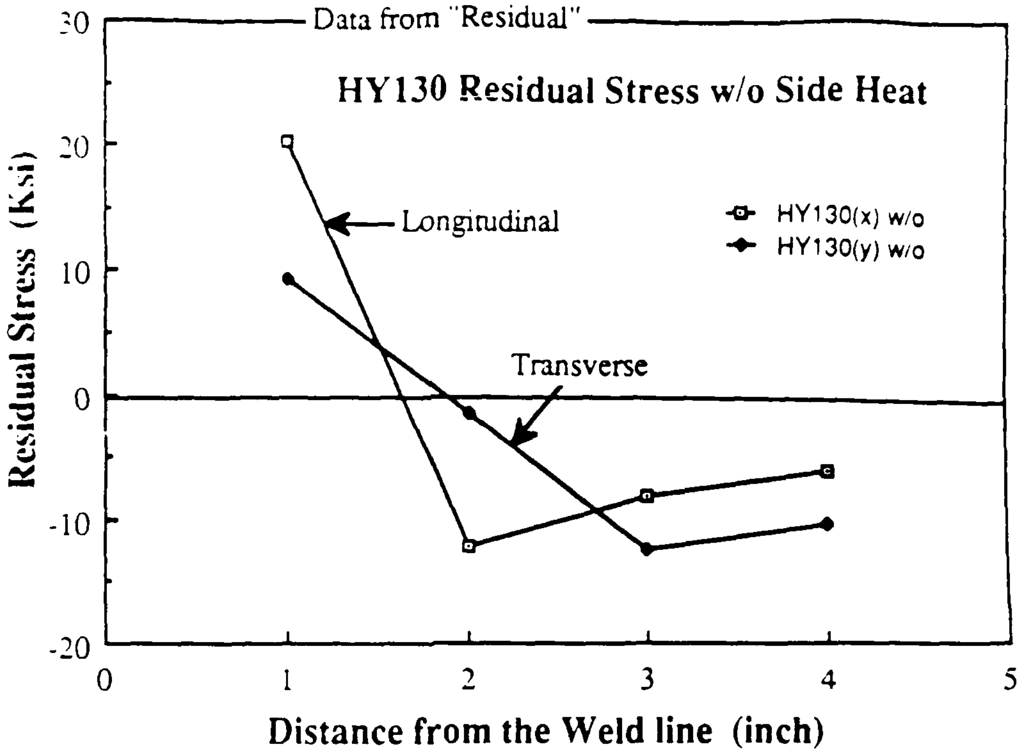

Figure 52

Again, the crossover is closer to 2" from the weld. AT least the HY130 pieces did begin to turn toward tension as in figure 16.

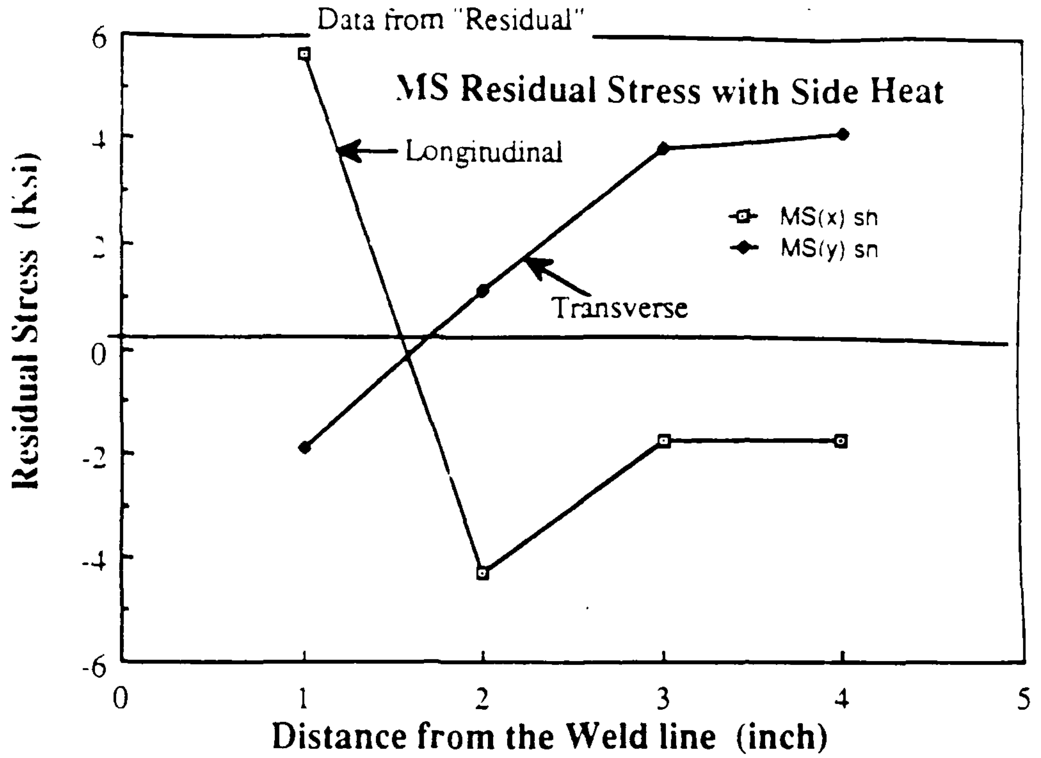

Figure 53

Compare the above with figure 50, but notice the scale of the residual stress value, it looks similar but is reduced significantly.

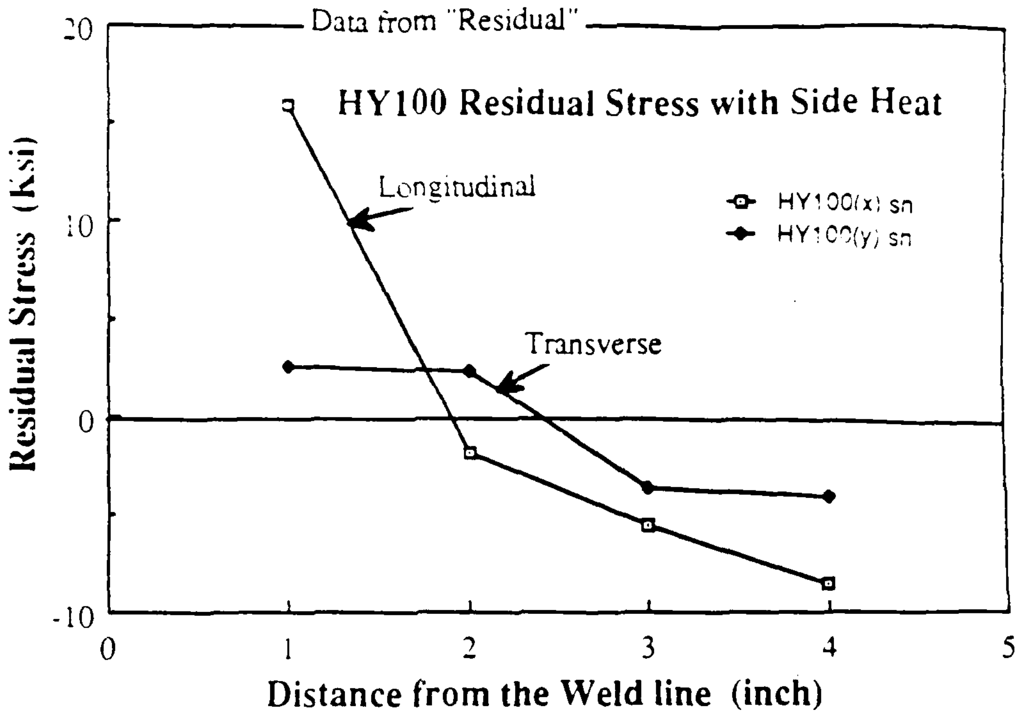

Figure 54

Again, with HY100 compare figure 54 above with figure 51 to see the reduction.

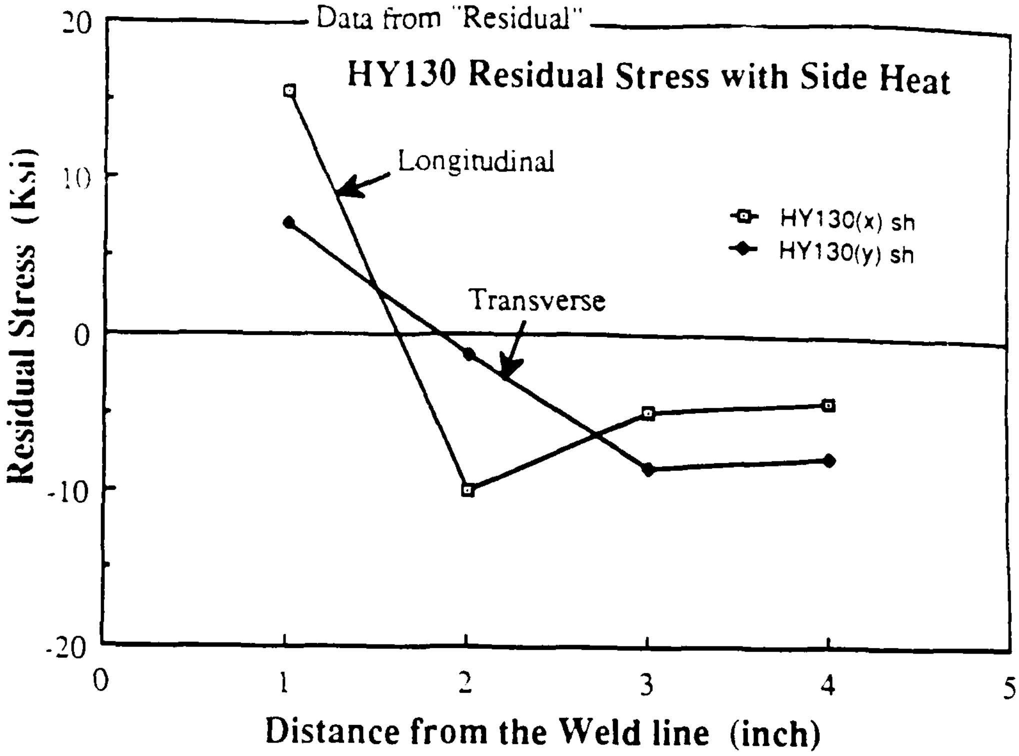

Figure 55

Again, both longitude and transverse residual stress is reduced.

The next three graphs show the residual stress both before without Side Heat, and after Side Heat is used.

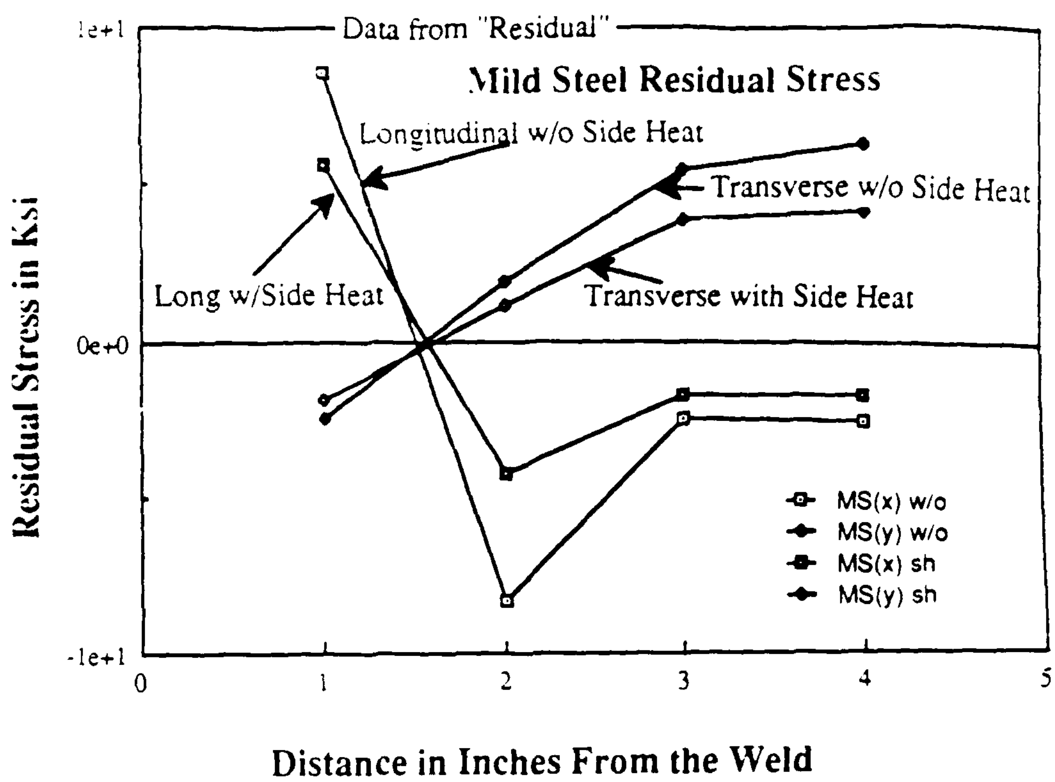
Data from "Residual"
Mild Steel Residual Stress
Longitudinal w/o Side Heat
Transverse w/o Side Heat
Long w/Side Heat
Transverse with Side Heat
MS(x) w/o
MS(y) w/o
MS(x) sh
MS(y) sh
1e+1
0e+0
-1e+1
0
1
2
3
4
5
Residual Stress in Ksi
Distance in Inches From the Weld

Figure 56

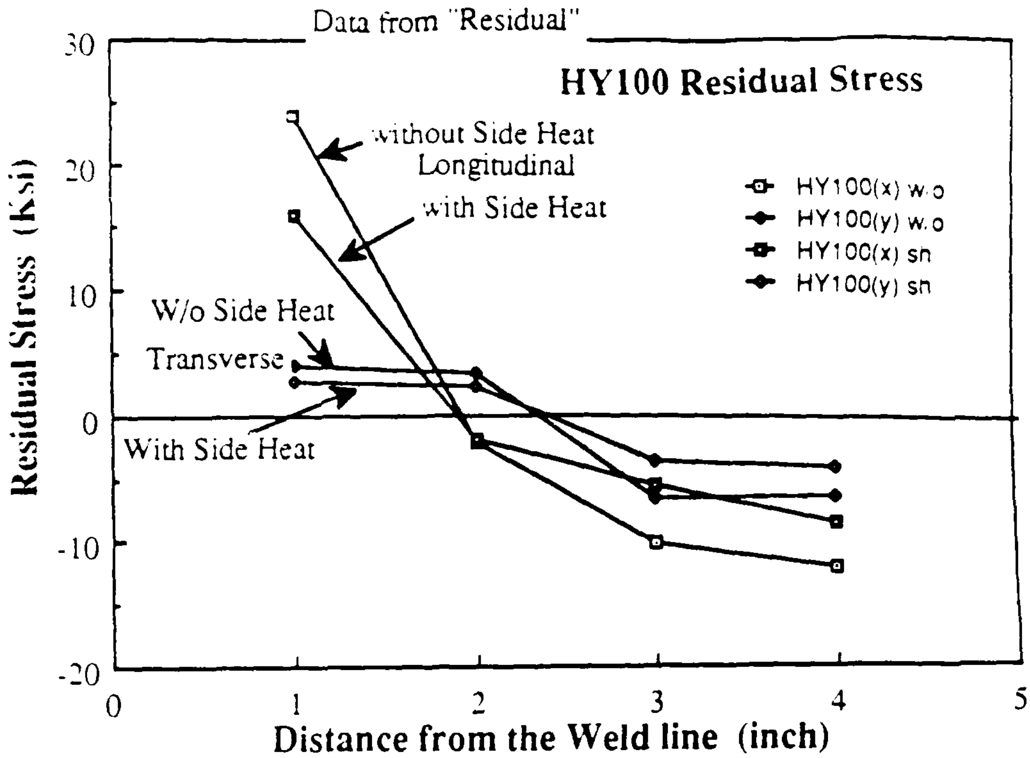
Data from "Residual"
HY100 Residual Stress
without Side Heat
Longitudinal
with Side Heat
W/o Side Heat
Transverse
With Side Heat
HY100(x) w.o
HY100(y) w.o
HY100(x) sn
HY100(y) sn
Residual Stress (Ksi)
30
20
10
0
-10
-20
0
1
2
3
4
5
Distance from the Weld line (inch)

Figure 57

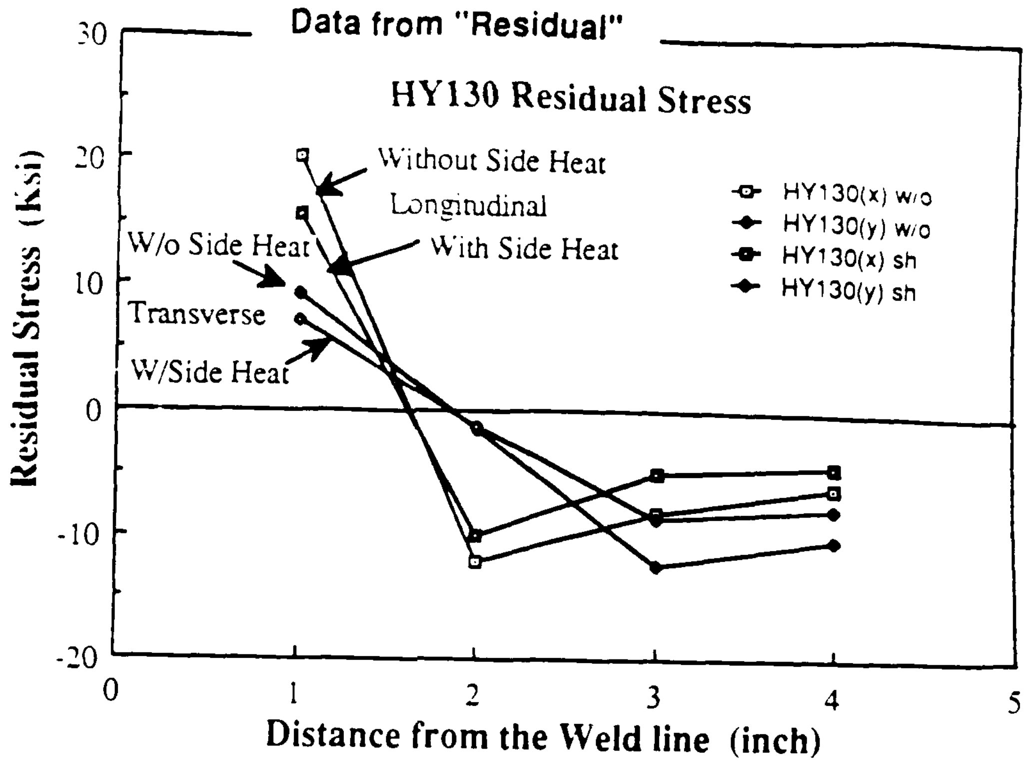

Figure 58

The next three graphs show the residual stress compare with each piece together.

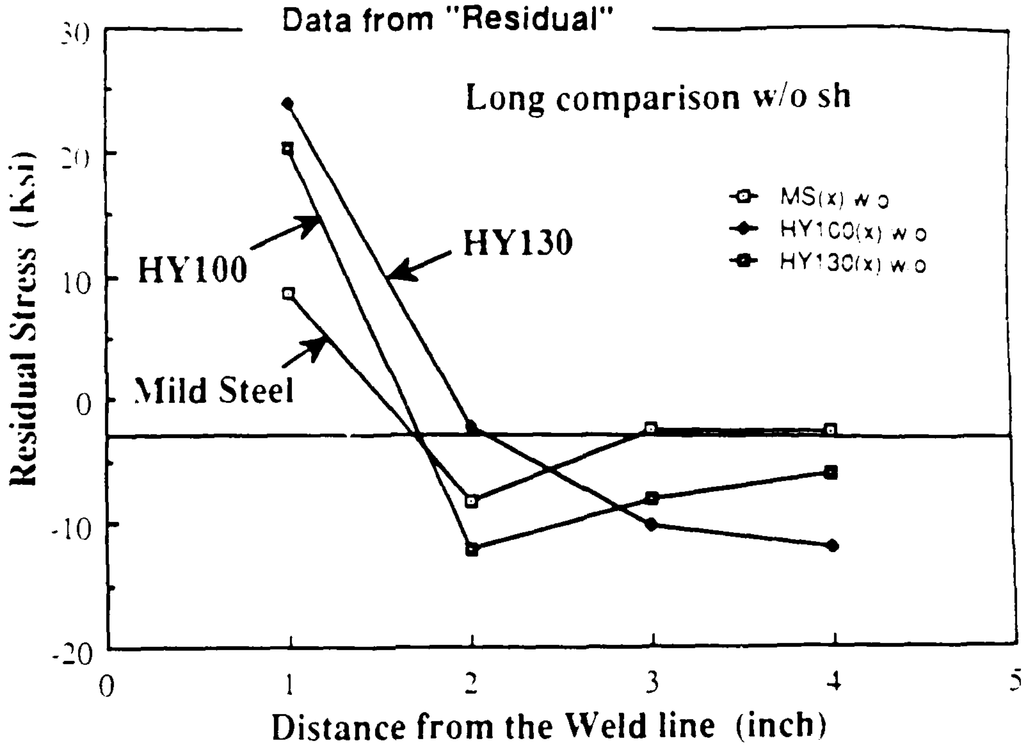

Figure 59

Longitudinally HY130 as expected had the highest value and Mild Steel the lowest.

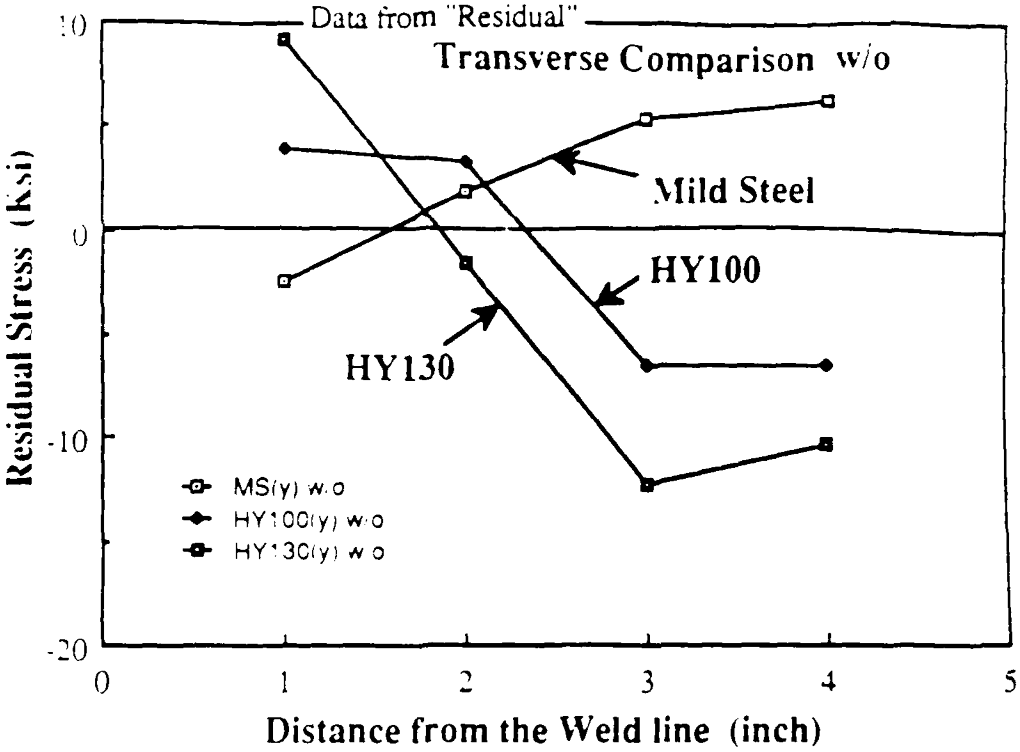
Data from "Residual"
Transverse Comparison w/o
Mild Steel
HY100
HY130
Residual Stress (Ksi)
10
0
-10
-20
MS(y) w/o
HY100(y) w/o
HY130(y) w/o
0
1
2
3
4
5
Distance from the Weld line (inch)

Figure 60

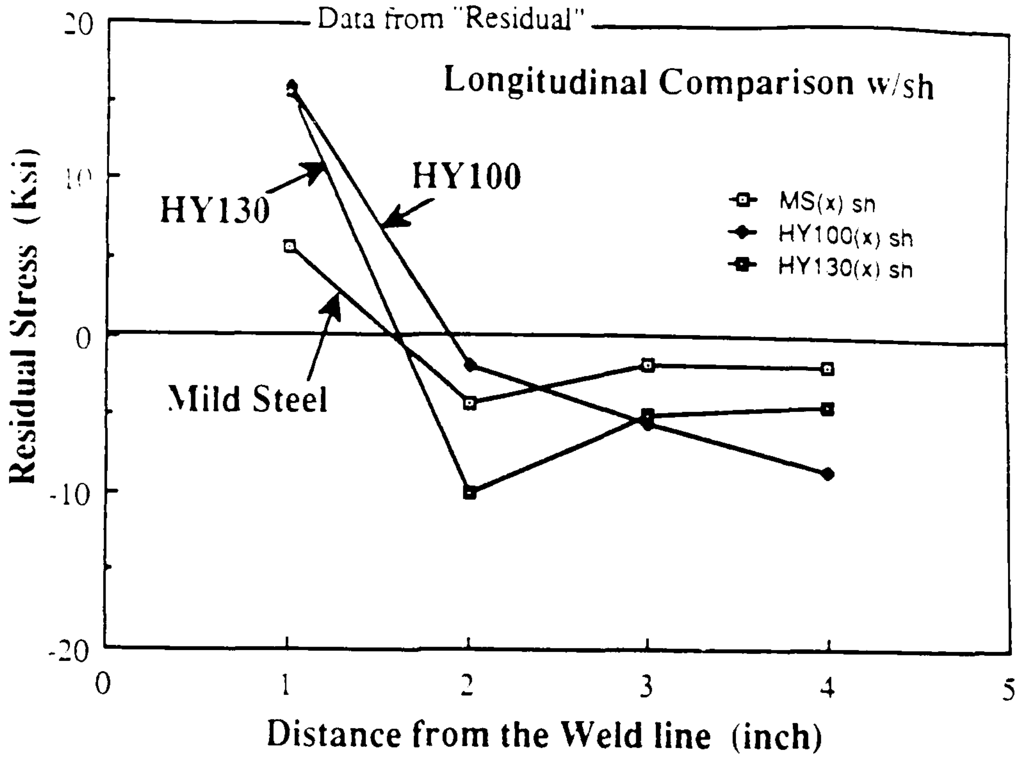

Figure 61

With Side Heat HY100 had the highest residual stress. This means that this technique works best with HY130.

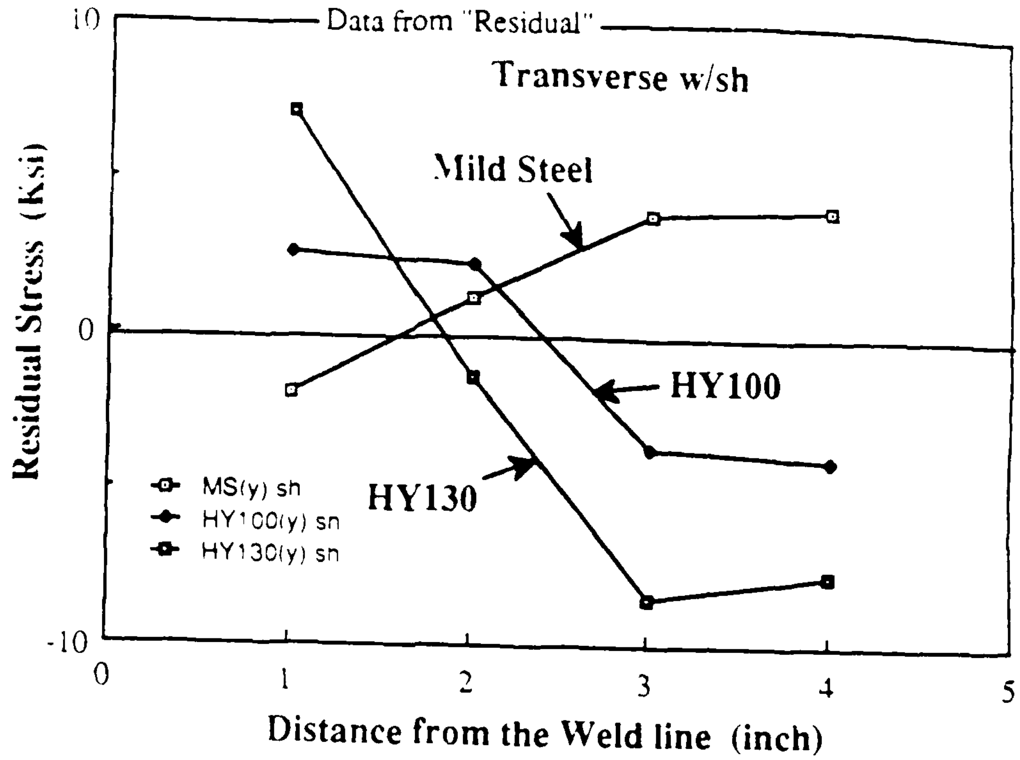

Figure 62

Transverse residual stresses were also reduced in all three steels but by a smaller amount than the longitudinal residual stress.

3.3.4: List of Equipment:

1 - Millennatic Automated Gas Metal Arc (GMA) Welding Machine.

2 - E70S weld sire reel (mounted on the Millermatic).

3 - HP3852A, Data Acquisition and Control System.

4 - HBM XY11 Strain Gages, Z-70 cement, and S-5 mounting kit.

5 - Omega Engineering Type K, Cromel-Alumel Thermocouples with quick disconnect OST plugs with type K compensation wire, and thermally conductive adhesive for mounting.

6 - PC6300 AT&T Personal Computer with Hardcard 20, 20MB hard disc and HP Data Magazine Control Board to run software.

7 - HP DC Power Supply (Reference for strain gage bridges).

8 - DVM.

9 - Simpson 260 (predominantly used for resistance continuity checks)

10 - Single wire shielded cable.

11 - Fabricated adjustable mounting for the side heat.

12 - Oxy-acetylene torch with hoses and cylinders.

13 - Helliarc Manual Welding Machine (for talk welding starter tabs).

3.4: Residual Stress Analysis in Ksi

		Measured Residual Stresses		
		W/o Side Heat	W/Side Heat	% Mag. Reduction
at 1" from weld:				
Mild Steel	Long.	8.57	5.632	34.28%
	Trans.	-2.46	-1.907	22.47%
HY100	Long.	23.99	15.99	33.35%
	Trans.	3.88	2.59	33.25%
HY130	Long.	20.35	15.65	23.10%
	Trans.	9.26	7.125	23.06%
at 2" from weld:				
Mild Steel	Long.	-8.34	-4.290	48.56%
	Trans.	1.18	1.154	38.62%
HY100	Long.	-2.23	-1.925	17.38%
	Trans.	3.323	2.274	31.57%
HY130	Long.	-12.06	-10.08	16.42%
	Trans.	-1.59	-1.427	10.25%
at 3" from weld:				
Mild Steel	Long.	-2.47	-1.764	28.58%
	Trans.	5.41	3.864	28.63%
HY100	Long.	-10.13	-5.552	45.19%
	Trans.	-6.54	-3.699	43.44%
HY130	Long.	-8.09	-4.924	39.17%
	Trans.	-12.27	-8.509	30.7%
at 4"from weld:				
Mild Steel	Long.	-2.56	4.115	33.48%
	Trans.	6.172	-8.452	36.91%
HY100	Long.	-11.97	-8.452	29.39%
	Trans.	-6.44	-4.063	36.91%
HY130	Long.	-5.95	-4.251	28.55%
	Trans.	-10.18	-7.730	24.07%

3.5: Conclusions:

1 - The temperature distributions obtained in these experiments were excellent and agreed well with analytical predictions on all three pieces of steel. HY100 consistently rose to the highest temperatures among the three steels tested with same welding condition.

2 - The Strain measurements also yielded distributions which agreed well with predicted values for all three steels.

3 - The strain longitudinal values measured were tensile near the weld 1" and did become compressive further away from the weld as anticipated.

4 - The distortion readings obtained during the experiments proved to be helpful in determining the overall metal movement from the thermal effects of both the welding arc and the side heating torch. With side heat, the distortion during welding was typically cut in half.

5 - The residual stresses measured were in line with predicted values for establishing a baseline in the first phase of this investigation. The first phase was without side heating for all three steels. In the third and final phase the residual stress measured using the side heating ranged from 17 - 39%. In all situations tested, the

side heating reduced the magnitude of the residual stress regardless of the type of steel.

6 - Positioning the side heat torch longitudinally ahead of arc 9" (30 sec.) or behind 9" (30 sec.), although some reduction in distortion and residual stress is evident, did not yield the best result. Side heating matched to the arc is longitude proved to be best.

7 - Side heating can be used as a method to not only reduce residual stress and distortion, but it can also be used to control the distortion during welding. This "in process control" can be accomplished by monitoring the metal movement and increasing or decreasing the side heat to control the attendant metal movement during welding.

Chapter 4:

4.0: Further Study

4.0.1: Use on Other Materials

The most significant feature of this investigation is the 50% reduction in distortion achieved during welding with the side heat. Since the distortion and metal movement are related to the residual stress, the residual stress was also generally by about 30%. The highly localized residual stress so commonly discussed when it applies to high strength steels was not examined during these experiments. The focus of this investigation was on arresting the distortion during welding and searching for a way to control this. There is little doubt that the side heating reduces the distortion significantly for all these steels: Mild Steel, HY100, and HY130. This is also no reason not to assume that this same technique will work on anything that can be welded and displays the same type of distortion response curve that is high tensile near the weld and compressive further away from the weld. This applies to all other types of welded material. The equipment set-up as is, would require some small adjustments to accommodate other materials. This technique may not work as well with those precipitation hardened materials like HSLA steels as it has in this investigation. But even applying this technique to a precipitation hardened material may work well enough with some small degradation of material characteristics. For example, sacrificing a small amount of nil ductility and fracture toughness may be tolerable when the potential to eliminate the distortion of HSLA steel is desired. There is some HSLA100 1/2" steel plate in the lab that could be tested in future experiments.

4.1: In Process Control:

The side heat needs to be controlled and some method for monitoring the metal movement is necessary. One method is to run a series of tests to obtain optimum side heat positioning and heat input and by knowing what the temperature should be at a certain point(s), then sliding thermocouples can be used to control the side heat to maintain the temperature at certain known points constant during welding. This method is cheap and uses temperature as the control as opposed to the strain which is more closely related to the distortion. Rolling strain gages are available and can easily be adapted to the Millermatic GMA weld machine. This method is surely the cheapest, but it may also be inadequate for large distortion in magnitude or very rapid changes.

A more direct approach is to measure the metal movement by distortion gage reading, strain or a combination. Rolling or moving strain transducers do seem to be non-existent but movement dial gages can be affixed to welding machine just like the side heat to monitor the metal movement during welding. An optical or laser measuring device would probably be the best for this situation.

The welding lab used in this study has side heating torches which are not remotely adjustible. A device to sense the heat input to the metal, or output of the torch if the heat input cannot be measured, that can be throttled up and down is needed. In the current set-up, if the dial gages go negative, then increase the heat of the torch until it reaches zero, or nearly so, and vice versa, if the dial gage goes positive decrease the heat of th secondary source.

Realistically, the side heat should be used to arrest the movement of the metal during welding therefore, some distortion will have to be tolerated. If the torch heat is increased so the distortion reads zero, it will probably cause the material to have much higher tensile strain when it cools down. In short, a side heating technique would be excellent for in process control of distortion and residual stress.

4.2: Impact on Industrial Use

Side heating is independent of the type of welding process used or type of metal being welded. Therefore, it can be used throughout the industry where welding is common.

For example, in shipyards where long weldments are common when welding hull plates together, side heat could be used to solve some of the mismatching that occurs when making very long welds. Metal separation from distortion at times renders very large plates useless. If the distortion could be controlled and reduced by this process a considerable dollar savings could result. 10 - 20% of the plates when joining a ship together generally became a problem during construction. Very often joint mismatches are patched over and sometimes the plate replaced. Even using Mild Steel at $1/lb, a 6 x 6 foot square plate weights 752 lbs and cost$ 752.00. HY100 and HY130 cost approximately three times and four times the Mild Steel respectively. To save a single plate form being rendered useless equates to over $3000.00 if using HY130. This does not include the cost of patching, weld wires weld machine, or the welder's time.

Even effectively reducing the 10% waste in the structural expense that occurs could mean significant savings into the millions of dollars in fabrication costs involved in very large projects, like building aircraft carriers.

Summary

The test results of this investigation validate the hypothesis that a secondary heat source can be used effectively to counter the thermal effects of arc welding, and reduce the attendant residual stress up to 39% and distortion up to 50% in the high strength steels of HY100 and HY130. The tests proved to be just as effective on Mild Steel. In fact, the graphs using the side heating and the analysis suggest this technique can be applied to any welded material to achieve similar results.

The focus of this investigation was on HY100 and HY130. There is little doubt that the distortion during welding, which is directly responsible for the plate's separation, is reduced and thereby allowing for these high strength steels to be more "weldable". In addition with the residual stresses reduced and the rate metal movement slowed, the tendency for these high strength steels to crack is reduced as well.

The theory of using opposing thermal forces is proven with this investigation. So far as metal movement as a result of welding is concerned, the tests conducted in this investigation have shown that this movement can be modified and adjusted, which means that it can be controlled in process.

Although the test pieces were not examined on a microscopic scale where the evidence of highly localized residual stress may exist, these experiments have shown that it is likely that even those localized high residual stress in the HAZ must also be somewhat relieved. It is likely that high measured residual stress, rapid or large amounts of metal movements for distortion are also associated with highly localized residual stress in the HAZ.

This simple side heating technique should be considered in similar situations where there is a cracking problem primarily due to residual stress in other types of material. For example, Aluminum alloys, Titanium alloys, and other steels which are susceptible to retaining high residual stresses as a result of welding.

References

1) Masubuchi, K., "Analysis of Welded Structures - Residual Stresses Distortion and Their Consequences", Pergamon Press, 1980.

2) Cook, N.H., "Mechanics and Materials for Design", McGraw-Hill, 1984.

3) Phillips, A.L., editor, "Current Welding Practices", American Welding Society, 1964.

4) Boulton, N.S. and H.E. Lance-Martin, "Residual Stresses in Arc Welded Plates", Proceedings of the Institution of mechanical Engineering, 1936.

5) Rosenthal, D. and R. Schmerber, "Thermal Study of Arc Welding", Welding Journal 17 (4), Supplement 208, 1938.

6) Rykalin, N.N., "Calculation of the Heat Process in Welding", printed in the USSR, 1960.

7) Hildebrand, F.B., "Advanced Calculus for Applications", Prentice Hall, 1976.

8) Carlsberg, J., "Review and Assessment of Linear Elastic Analysis Techniques for Surface Cracks in Structural Details With Residual Stresses", DTNRDC - 84/1070, March 1985.

9) Meitzener, C.F., "Stress Relief Cracking in Steel Weldments", Welding Research Council Bulletin 149, April 1970.

10) Masubuchi, K., "Control of Distortion and shrinkage During Welding", Welding Research Council Bulletin 149, April 1970.

11) Masubuchi, K. and D.C. Martin, "Investigation of Residual Stresses by Use of Hydrogen Cracking", Part I and Part II, Welding Journal, Vol. 40, No. 12, Research Supplement, 1966.

12) Kihara, H. and Ikeda Y., "Brittle Fracture Strength of the Welded Joint", Welding Journal, Vol. 49, Research Supplement, 1970.

13) DeGarmo, et. al., "The Effect of Weld Length Upon Residual Stresses of Unrestrained Butt Welds", Welding Journal, Vol. 25 (8), Research Supplement, 1946.

14) General Dynamics Corporation, "Welder's Handbook for Welding HY80, HY100, and HY130", 1975.

15) Hoffman, K., "The Strain Gauge, a Universal Tool of the Experimental Stress Analysis", HBM vd. 73004e, printed in West. Germany, 1988.

16) National Bureau of Standards, Circular #561, "Table for Thermocouples, Type K, Ni - Cr vs. NiAl (Cromel-Alumel) Thermocouples".

17) OMEGA Complete Temperature Measurement handbook and Encyclopedia, Vol. 26 OMEGA ENGINEERING CO. CATALOGUE, 1989.

18) ARMY TRAINING MANUAL, TM 9-2852, 110-111, p. 94 - 110.

Appendix 1
EXPERIMENT SYNOPOSIS

Experiment #1: Mild Steel 5.5" x 18" Bead on Edge

Set-up:

This experiment was conducted on a piece of Mild Steel with dimensions of 12 inches long, 5.5 inches wide, and .5 inches thick. Three longitudinal strain gages[22] were mounted at 1.25 inches, 3 inches, and 4.75 inches from the weld respectively. The connecting wire to the strain gages from the terminal block was not shielded cable, but the cable from the terminal block to the test equipment was shielded. The strain gages were connected to channels 0, 1, and 2, respectively of the HP3852A Data Acquisition Machine. The HP3852A was connected to the AT&T 6300 Personal Computer with a HP Language Processor board for communicating with the HP3852A and a Hardcard 20, 20MB hard disk installed. The cable from the terminal block was shielded cable. The initial welding conditions and settings for the Millermatic Gas Metal Arc (GMA) automatic welding machine was:

[22] HBM XY11 type strain gages, see appendix 3 for specifications and details.

Material	Mild Steel
Wire	E70S
Wire Diameter	.045 inches
Transfer Type	Spray
Gas Flow Rose	30 CFH of Ar 98% / 2% O_2 Shield Gas

Millermatic Settings:

1. Pre-flow Time	1 second
2. Run in	20 seconds
3. Spot Time	3 seconds
4. Spot/continuous	continuous
5. Time range	high (2.5 - 5 sec)
6. Burnback Time	.85 seconds
7. Post flow Time	2 seconds
DC volts	25 volts
Wire Feed Speed	400ipm
Carriage control:	
1. Auto/man	manual
2. Weld speed	.66 setting
Actual speed	(385 in/sec calibrated)
Power Supply	25 volts/200 amps

The foregoing settings provided a weld heat input of 12.987 KJ/inches. "Tempo-lac" temperature lacquer was also painted on the plate to get a general idea of the heat on the surface of the plate for subsequent thermocouple mounting in follow experiments. Previous practice beads on old plate indicated excessive spatter might be a problem for the unshielded wire attached to the strain gages and fear of the weld bead falling off the edge of the plate prompted the use a small splash plate mounted on the test plate using thin sheet steel 1 inch wide. The splash plate was held on by pressure clips made of the same sheet steel.The weld speed setting on the welding machine was way out of alignment. The weld speed was calibrated using a stop watch and a ruler.

Purpose:

The purpose of this experiment was to:

1. Verify adequate welding conditions (heat input 13 KJ/inch).
2. Verify and test the welding equipment set-up.
3. Test the data acquisition machine HP 3852A and PC during actual welding.
4. Test the "Tempo-lac".
5. Verify the program written to manage taking data
6. Test the operation of the strain gages under actual welding conditions.
7. To see if the welding arc causes electro-magnetic interference (EMI) that disrupts data taking or operation of other electronic equipment in the area.

Results - Did Not Get A Good Bead On Edge:

The arc started only after the "weld on" switch was toggled and the initial piece of weld wire snapped off. The initial starting "arc blow " was excessive. Shortly after the arc started the weld wire slid off the edge and welded the spatter plate to the base metal blowing several holes in the splash plate. The splash plate severely buckled toward the welding arc and bent above the original weld line before the arc reached the end of the plate. The shield seemed to be attracting the arc. The "Tempo-lac" worked well. The strain gages seemed to function properly but the timing on the data acquisition program was not correct. No attempt was made to use the data for this test.

Conclusions:

If a spatter shield is utilized, it cannot be allowed to buckle and interfere with welding arc. A spatter shield cannot make metal to metal contact during welding because the welding arc electrically "sees" no difference between the spatter plate and the base plate on edge. The spatter plate needs to be electrically shielded from the plate. In addition, the spatter plate making metal to metal contact will also act as a fin and will dissipate heat after welding, and this will disturb the temperature data taken from the plate by thermocouples.

There is apparently a timing mismatch on the system clocks between the HP 3852A and the PC. The computer system clock appears to be running at a slower speed compared to the HP 3852A. This resulted in timing errors generated while running the test, however it did not affect the data being read. But this is a good argument for getting a personal computer that has a faster and more powerful CPU. The AT&T PC 6300 uses a 8086 CPU running at 4 MHZ, while the HP 3852A clock runs at 8 MHZ. A PC with an 80286CPU running at 8 MHZ or more should solve this problem and move the speed with which data can be gathered to almost exclusively the sampling speed of the HP 3852A as opposed to the current set up where this limit now includes how fast the data can be handled by the PC. The sampling time for the HP 3852A Data Acquisition Machine is about one to two seconds.

Experiment #2: Mild Steel 5.5" x 18" Bead on Edge

Set-up:

The set-up for this experiment was the same as the first experiment. The size of the test pieces was lengthened to 18 inches which will be the size of test pieces used in subsequent experiments to obtain valid temperature and strain characteristics from the welding arc. The spatter plate was thickened to 1/4 inch steel strip. This was then tack welded to the starter tabs with 0.5 inch clearance for mounting on the base plate. The spatter plate was painted with high temperature paint to insulate it from the base plate. The starter tabs were wedged against the ends of the plate using thin strips of sheet steel hammered in and ground down until smooth with the weld edge surface. The starter tabs were used to absorb the initial "arc blow" when starting and "end blow" when the weld bead is stopped. Only "Tempo-lac" was used to look at the temperature distribution. The red high temperature RTV compound was also used to see what happens to it when placed in a high temperature situation.

Purpose:

The purpose of this experiment was to solve the problems previously encountered in the first experiment specifically:

1. Test the thicker spatter plate insulated from the specimen.
2. See if the thicker start and end tabs are sufficient to allow the weld bead to stabilize before welding on the plate.

3. Ensure proper alignment of the welding machine with the edge of the plate.

Results: Excellent Bead on Edge:

The weld bead stayed on the edge without spillover. Significant start and end blow did occur, but the starter tabs allowed the welding arc to be stable before it touched the base plate. The arc remained stable as it traveled along the edge of the plate. In short, the welding arc and weld pool was stable, the entire length of the plate. The weld bead took about 47 seconds to complete and the heat input was still approximately 13 KJ/inch. The amperage fluctuates while welding easily plus or minus 10 amperes, so the average amperage was utilized to calculate the heat input. The high temperature red RTV compound burned and crumpled and seemed to provide no better insulation qualities than regular RTV compound so the clear RTV compound will be used in subsequent experiments

Conclusions:

If properly aligned so that the weld wire comes down straight and in the center of the edge of the plate, then it should yield adequate welding results without the need for any splash or spatter guard. Alignment is most important for attaining good bead on edge results. The start and end tabs are very necessary to have a stable bead on edge and eliminate "arc blow" problems. The spatter guard also interferes with the "tempo-lac" thermal lacquer being used and although the spatter guard is insulated from the base, there is still some material, paint, and high temperature RTV compound touching the plate close to the weld that has the potential to interfere with the data being taken.

Experiment #3: HY130 6" x 12" Bead on Edge

Set-up:

This was the first piece of high strength steel to be welded. Three longitudinal (one dimensional) Y11 strain gages and two K-type thermocouples were mounted along with a single dial gage at the bottom edge of the plate. "Tempo-lac" was also painted on the plate. The welding conditions and settings were changed to the following:

Carriage Control:

1.	Auto/man	manual
2.	Weld speed	.575 (.3 in/sec calibrated)
3.	Wire feed speed	375ipm

Slowing the weld travel speed was done to increase the weld heat input since:

$$\text{Heat Input}\left(\frac{KJ}{in}\right) = \frac{[\text{Voltage (V)}]\,[\text{Arc Current (A)}]}{\text{Weld Travel Speed}\left(\frac{in}{sec}\right) \times 1000}$$

The strain gages were connected to strain gage channels 0, 1, and 2 respectively and the thermocouples were connected to temperature channels 0, 1 of the HP 3852A. "Tempo-lac" was also painted on.

Purpose:

The purpose of this experiment:

1. Test how the HY130 welded with the welding conditions, settings, and weld wire mismatch.

2. Verify correct functioning of the corrected data acquisition program set up to run for an eight hour period.

3. Test the dial gage during welding.

4. Test the new welding conditions with higher heat input (20 KJ/in).

5. Verify bead on edge without any spatter plate but tack weld start and end tabs that are about 1 inch square and 0.5 inch thick.to the ends of the test plate where the welding arc starts and ends.

6. To check the distortion readings on the dial gage after welding.

7. To see if any problem arises from the weld wire mismatch E70S wire while welding on HY130.

Results: Excellent Bead on Edge Results

The Bead on Edge resulted without spillover, the start and end tabs again absorbed the beginning and ending "arc blow". The "tempo-lac" was not interfered with and the distances they melted on the plate were measured.

Temperature lacquer ("Tempo-lac") melted band measurements:

1400° F	(760° C)	1/8 in	(.13")
1200° F	(649° C)	3/16 in	(.19")
1000° F	(538° C)	1/4 in	(.25")
800° F	(427° C)	3/8 in	(.38")
600° F	(316° C)	1/2 in	(.5")
400° F	(204° C)	1 in	(1.0")
200° F	(93° C)	2 13/16 in	(2.81")

The Heat Affected Zone (HAZ) was quite visible, bands of discoloration on the shining base metal that extended roughly one half inch from the weld. The program worked gathering strain and temperature data over an eight hour period without problems. The distortion dial gage worked but only a small amount of distortion was detected. Actual heat input was 18.17 KJ/in, 25V and .3 in/sec travel speed set with an average of about 218 amps read during welding.

Conclusion:

This was the first experiment where everything worked according to plan. The small distortion readings were in part due to the smaller size of this test piece (only 12" long) compared with the established minimum size as 18 inches long. For subsequent experiments in attaining strain and temperature data no more changes were anticipated.

Series of Bead on Edge:

Experiments #4	Mild Steel	5.5" x 18"
Experiments #5	HY100	5.5" x 18"
Experiments #6	HY130	5.5" x 18"

Set-up:

The set up was the same as experiment #3, except:

4 XY11 strain gages mounted	1", 2", 3", and 4"
4 K type thermocouples mounted	.5", 1.5", 2.5", and 3.5"
3 dial ages at the bottom	4.5", 9", and 13.75"
Tempo Lacquer painted on	

Welding conditions all set for approximately 20 KJ/in heat input on all three pieces.

Purpose:

These experiments were the first full series of test conducted to gather temperature and strain data over an eight hour period. These test were to conclude the first phase of this project which was to establish temperature and strain profiles for comparison with predicted results, and then to subsequently cut the specimens to obtain the residual stresses to establish a baseline.

Results: Excellent Bead on Edge

The tests ran smoothly and the data was plotted. The temperature and the distortion data appeared smooth on all three pieces. The strain data fluctuated initially, and then appears to smooth out after the welding arc reaches the middle of the plate where the strain gages are mounted. In both longitudinal and transverse (x and y) directions, the strain data fluctuates a small amount for approximately 30 seconds. It takes 60 seconds for each bead on edge test piece to be completed. The distortion data for experiment 6 was considered not accurate since some of the "tempo-lac" melted onto the tip of the dial gage in the center and may have fouled the distortion reading. Therefore, experiment #7 was conducted to re-examine the distortion of a piece of HY130.

Experiment #7: HY130 5.5" x 12" Bead on Edge

Set-up:

Same as experiment #3, except the dial ages were positioned at the bottom and "tempo-lac" painted on.

Purpose:

With just the dial gages fitted, this test was to verify the distortion readings obtained in experiment #3.

Results:

The distortion readings were similar to those experiment #3. The readings were smaller than expected with about the same heat input, 19.16 KJ/in.

Conclusions:

The distortion readings were not accurate enough for comparison with the normal test piece length. The top of the plate did not go into tension and give good negative readings on the dial gage as expected. The plate is too short to get good distortion readings. A full 18" long plate must be used for comparing distortion and strain. Therefore, another piece of HY130 was prepared to complete the data for phase I.

Experiment #8: HY130 5.5" x 18" Bead on Edge

Set-up:

Same as experiment #7 - 3 dial gages fitted.

Purpose:

To verify the distortion data in experiment #6 and to read the distortion data during welding. The distortion during welding was not recorded in the previous full test series (experiments #4, #5, and #6)

Results:

Good results were achieved. The final distortion for HY130 is less than HY100 or Mild Steel. The distortion data collected appeared smooth. The data was collected and used for plotting HY130 distortion.

Conclusions:

At this juncture, it is apparent that the higher the strength, the less the steel distorts from the effects of welding.

Experiment #9: HY100 5.5" x 18" Bead on Edge

Set-up:

Same as experiment #8 - 3 dial gages fitted.

Purpose:

To read distortion data during welding and verify distortion readings in experiment #5.

Results:

Good smooth readings collected for plotting. Heat input 19.16 KJ/in, 25A, 230A, .3 in/sec weld travel speed.

Experiment #10: Mild Steel 5.5" x 18" Bead on Edge

Set-up:

Same as experiment #8 and #9.

Purpose:

To verify distortion results in experiment #4 and to include distortion reading during welding on the Mild Steel.

Results:

The distortion readings were not good. The dial gages were set initially lower than in previous tests and a problem with the welding equipment developed. The weld bead was not smooth and stable. The weld bead varied significantly in width when examined closely.

Experiment #11: Mild Steel 5.5" x 18" Bead on Edge

Set-up:

Repeat of experiment #10.

Purpose:

To repeat experiment #10 and get distortion readings during welding and verify distortion readings in experiment #4.

Results:

The first three attempts at welding burned up the welding tips on the machine. After careful trouble shooting and checking the entire set-up, it was determined that the ground reference for the wire feed had broken loose. After replacing the alligator clip and re-attaching the ground reference wire, the equipment worked fine.

The distortion readings on the Mild Steel appear smooth and were collected for plotting. Heat input was 19.16 KJ/in, 25V, 230A, .3 in/sec weld travel speed.

Experiment #12: Mild Steel 5.5" x 18" Bead on Edge with Side Heat

Set-up:

The weld machine was rigged with a holder for an oxy-acetylene torch for use as a side heater on the base plate test piece. The fabricated piece is adjustable for positioning of the flame. The welding set-up is the same as experiments #4 - #11. The side heat travel speed is .3 in/sec the same as the weld speed. The flame is positioned 4" from the weld laterally and 2 1/4" ahead of the arc longitudinally. The torch used is a balanced type that will burn any combination of acetylene and oxygen with acetylene from 2 to 80 percent by volume. The cylinders were set with 2 psi of acetylene and 7 psi of oxygen. on the pressure gages.

Purpose:

To test the side heading with the current welding set-up. Preliminary discussion concluded that side heating roughly matched longitudinally to the arc and displaced 4" from the weld should counter the effects of the heat from the welding arc. The point where the roughly 200° C reaches in the base plate using the "tempo-lac" is about an 1" (see experiment #3). Four inches laterally from the weld was selected since the flame represents a poor point source and is more representative of an area heating source when compared to the welding arc. The part of the flame touching the plate involves about 1" diameter circle when the flame is held 1" away from the plate. Application of side heating without the welding arc does cause the dial gage to initially read positive (meaning the bottom of the plate is in tension) and this is opposite to the normal negative (compressive) reading achieved when welding. Side heating does appear to reduce distortion significantly when positioned longitudinally about the same or slightly ahead of the welding arc. The 2 1/4" ahead equates to 7 seconds ahead of the arc in real time.

Results:

Using the "tempo-lac" indicated that slightly less than 200° C was achieved on the plate opposite the flame, while the surface facing the flame rose to about 600° C where the flame touched. Although this may seem excessive this arrangement seemed best to get a rough 200° C around the point desired throughout the base plate. Adjusting the flame to get a 200° C heat throughout the plate proved to be a difficult task. After several practice runs on a pieces of scrap steel, the flame that seemed to work best was a flame 1" away from the plate with a 1/2" cone and a 2" feather. The size of the flame outer envelope was ignored. This result appears to be excellent with the distortion being reduced significantly.

Conclusion:

The side heating does produce a dramatic reduction is distortion during welding. The final distortion appears to be reduced approximately fifty percent. This was, in part, a desired goal of this experimental investigation. The residual stress discussed later is also expected to be reduced substantially as well.

Series of Bead on Edge with Side Heat:

Experiment #13	Mild Steel	5.5" x 18"
#14	HY100	5.5" x 18"
#15	HY 1130	5.5" x 18"

<u>Set-up:</u>

This series of experiments was designed to utilize the side heating technique during welding to reduce distortion. The equipment set-up was the same as in previous experiments:

Wire	E70S
Wire Diameter	.045 in
Transfer Type	Spray DCRP
Gas Flow Rate	20 CFH of Argon 98%/2% oxygen
Millermatic Settings:	
1. Pre-flow time	1 sec
2. Run-in	20 sec
3. Spot time	3 sec
4. Spot/continuous	continuous
5. Time range	high (2.5 - 5 sec)
6. Burnback time	.05 sec
7. Postflow time	2 sec
DC Volts	25 Volts
Wire Feed Speed	375 ipm
Carriage Control	
1. Auto/man	Manual
2. Weld Speed	.575 (.3 in/sec)

Power Supply	25V/230A
(amperage is average read during welding)	
Heat Input	19.16 KJ/in
Side Heat:	

1. Acetylene (C_2H_2) — 3 psi
2. Oxygen (O_2) — 8 psi
3. Flame Adjustment — 1/2" cone, 2" feather position 1" from plate
4. Torch position longitudinal — matched to arc
5. Torch position transverse — 4" from arc

Three dial gages were fitted at the bottom of the test specimens to record the distortion. "Tempo-lac" was also painted on to keep rough checks on the accumulated temperature distribution. The side heating torch was adjusted to match the arc longitudinally and displaced 4" transverse from the weld.

Purpose:

The purpose of this series was to test the side heating technique using an oxy-acetylene torch matched horizontally with the weld arc for all three steels; Mild, HY100, and HY130.

Results:

Distortion readings appear smooth with a reduction in distortion both during welding and final distortion readings on the order of 50 percent except for the HY130 piece. The distortion reduction on HY130 was less than expected.

Conclusion:

The HY130 piece has a thick blue coating which must be providing insulation where the side heating is being applied. Hereafter, the thick blue coating must be removed completely where the secondary heat source is applied. The area where the side heating was not cleaned as thoroughly as the area being welded. The thick coating is on the HY130 material only. In an effort to ensure the most accurate results all test pieces will be thoroughly cleaned in the area where the side heat is used as well as the edge where the welding arc is applied.

Experiment #16: HY130 5.5" x 18" Bead on Edge with Side Heat

Set-up:

Same as experiment #15, this time the blue coating completely removed from back of plate where side heating is applied. "Tempo-lac" painted on front and back.

Purpose:

Distortion readings with the coating removed is now on the order of a 50 percent reduction as expected.

Conclusions:

Previously meticulous cleaning was done only in the area being welded. It is now apparent that if a secondary heat source is introduced, it too, requires the surface area to be clean.

Experiment #17: Mild Steel 5.5" x 18" Side Heat Only

#18 HY100 5.5" x 18"

#19 HY130 5.5" x 18"

Set-up:

Just side heat was set-up in this series of experiments to isolate the effect of the side heat without the welding arc. Side heat was set as follows:

Acetylene (C_2H_2)	3 psi
Oxygen (O_2)	8 psi
Torch Speed	.3 in/sec
Flame Adjustment	1/2" cone, 2" feather positioned 1" from the plate 4" vertically down from the weld as before (experiment #12)

Three dial gages were fitted at the bottom and "tempo-lac" used to monitor temperature.

Purpose:

The purpose of this series is to isolate the effects of the side heat on the plate without the welding arc. To study the metal movement and distortion on all three types of steel.

Results:

The distortion readings are smooth and were plotted. The dial gage readings do move opposite to the readings during welding and reinforce the idea that side heat counters the thermal effect from the welding arc. The final distortion reading using just side heat varied between ± .0002 inches some time after the metal cooled.

Conclusions:

Side heating as positioned in this series of experiments does cause metal movement and distortion opposite to welding. If the side heating is set so it does not cause a Heat Affected Zone (HAZ) to develop, then the material should recover elasticity from the thermal expansion. Thus the final distortion is negligible with the current side heating set-up and affirms the assumption that raising the temperature of the plate to approximately 200° C has negligible effects on distortion after cooling. These plates were deemed fit for use as follow on test welding specimens.

Series of Bead on Edge with Side Heat 9" Ahead:

Experiments #20: Mild Steel

#21 HY100

#22 HY130

Set-up:

This series of tests was conducted with the welding torch positioned longitudinally 9 inches ahead of the welding arc (30 seconds in time). The welding set-up is the same as experiments #13, #14, and #16. These pieces are the same as #17, #18, and #19 (where side heat only was tested). Three dial gages and "tempo-lac" used as before.

Results:

The results were smooth and plotted. The plate initially yielded positive readings as expected from the side heat. When the welding arc's thermal effects took over the gage readings went negative and eventually back to positive as expected. The distortion during welding is slightly less than the experiments without side heating at all (#8, #9, and #11). The final distortion is less than the experiments with the side heat very close to, or matching the welding arc longitudinally (12 - 15).

Conclusions:

When the torch for side heat is positioned ahead of the arc, the metal movement from the side heat pre-positions before the arc arrives but does not directly counter the thermal effect of the arc. In this situation, the metal movement expansion from the side heat is just about finished when the arc arrives and its thermal effect overpowers the side heating effects. Therefore, placing the side heat well ahead of the arc does reduce distortion but does not give the best results. This does however, slow the rate of distortion during welding significantly. As expected, the final distortion readings were lowest with HY130.

Series of Bead on Edge with Side Heat 9" Behind:

Experiments #23 Mild Steel

#24 HY100

#25 HY130

Set-up:

Side heat was set-up following the arc by 9 inches (30 seconds behind). The welding set-up is the same as experiments #13, #14, and #16. Three dial gages and "tempo-lac" used as before.

Results:

This was interesting. The distortion readings went negative as expected from the thermal effects of the arc as expected and then began to go in the positive direction before the side heat arrived. The side heat provides an initial positive reading so this undoubtedly accelerated the distortion in the positive direction. The side heat did not appear to make the final distortion worse than without side heat, but did not help either. Side heat 30 seconds behind had little effect on the final distortion.

Conclusion:

Applying side heating after the arc does not improve the distortion and has the potential to cause the distortion to be worse than not using it at all. This is the classic closing the gate after the horse has already escaped. Applying side heating after the weld arc has passed yields undesirable results. Optimal placement of side heating is to either match the side heat longitudinally with the arc or slightly ahead. Very little difference was noted when wide heat was 2 1/4" (7 seconds) ahead and longitudinally matched in final distortion (experiments 12 and 13-16).

Bead on Edge with Side Heating Longitudinally Matched to Arc:

Experiment	#26	HY130	5.5" x 18"
	#27	HY100	5.5" x 18"
	#28	Mild Steel	5.5" x 18"

<u>Set-up:</u>

Final series to determine residual stresses while using side heating.

Experimental set-up:

Type of Wire	E70S
Wire Diameter	.045 in
Transfer type	Spray
Gas flow Rate	20 CFH 98% Argon/2% Oxygen
Millermatic CS-4	(GMA automatic welding machine)
1. Pre-flow time	1 sec
2. Run-in	2 sec
3. Spot Time	3 sec
4. Spot/Continuous	Continuous
5. Time Range	high (2.5 - 5 sec)
6. Burn Back Time	.05 sec
7.Post-flow Time	2 sec
DC volts	25 volts
Wire Feed Speed	375 ipm
Carriage Control:	
1. Auto/Man	Manual
2. Weld Speed	.575 (.3 in/sec calibrated)

Power Supply:	25V/230A
(Amperage is average reading during welding)	
Arc Heat Input	19.16KJ/in
Side Heating:	
1. Acetylene (C_2H_2)	3 psi
2. Oxygen (O_2)	8 psi
3. Flame Position Longitude	match to arc
4. Flame Position Vertical	4" transverse from arc
5. Flame Adjustment	Torch 1" away from plate
	1/2" cone, 2" feather
Side Heating:	
6. Torch Travel Speed	.3 in/sec (same as arc)

These test pieces have the following equipment attached to the plate:

4 K type Thermocouples	.5, 1.5, 2.5, 3.5 in vertically
4 XY11 Strain Gages	1, 2, 3, 4 in vertically
3 Dial Gages	4.25, 9, 13.5 in from left
	4.5, 9, 13.75 from the right

The thermocouples and strain gages are attached using single conductor shielded cables attached to the HP 3852A. The thermocouples are connected to temperature channels 0, 1, 2, and 3 on the thermocouple module in the HP3852A. The strain gages are attached to channels 0 - 7 on the strain gage module. The even channels are longitudinal strain, the odd channels transverse strain. Three dial gages are fitted at the bottom of the plate. "Tempo-lac" is also painted on.

Purpose:

This series of experiments is the last set of experiments conducted after determining the optimum side heat positioning. The prime reason for this series is to get the residual stress with the side heat applied. An accompanying temperature profile and distortion distribution for final analysis and plotting was desired.

Results:

The results were excellent. A good weld bead occurred. Temperature, strain and distortion data appeared smooth for plotting after eight hours. Initial strain readings were taken after welding, and the plates cooled. The plates were cut and final strain readings compared to ascertain the residual stress in all three specimens. The stress relaxation cutting was accomplished very slowly with metal saws. The plates were cooled while cutting to keep from developing a HAZ.

Conclusions:

Previous experiments with side heating have confirmed that optimal positioning of the side heat during welding either longitudinally matched or slightly ahead of th arc. If it more desirable to control or slow the rate of distortion, the slightly ahead position seems to be best. To get the best results on final distortion, the optimum placement is to longitudinally match the torch with the arc during welding. The torch should also have the same travel speed, so it stays longitudinally matched. This is ideal for automatic welding processes, but it can also be done manually with a rough match between the weld arc and side heat torch.

There is little doubt that the distortion in all cases is reduced by roughly one half. This reduction is most significant in that it is accomplished during welding. Since the distortion during welding is also directly related to residual stresses in the material due to welding, these also have to be significantly reduced. After plotting, it was found that 1 inch from the weld, the most important value from this study, the residual stress was reduced longitudinally 34% for mild steel, 33% for HY100, 23% for HY130, and transverse residual stresses was reduced by 22% for mild steel, 33% for HY100, and 23% for HY130.

Appendix 2
Tabulated Data Tables

This set of tables contains the temperature data read during phase 1 which involves experiments #4, 5, and 6 at 0.5", 1.5", 2.5", and 3.5" from the weld line:

Data Table	Title	Readings
1	Temp MS #4	Mild Steel experiment #4
2	Temp HY100 #5	HY100 experiment #5
3	Temp HY130 #6	HY130 experiment #6
4	Max Temp Data	Maximum temperature recorded on mild steel HY100 and HY130

[illegible] Graph Data — Temp MS #4 — Sun. Jun 4, 1989 [illegible] 28 AM

	Time #4	At 0.5 in.	At 1.5 in.	At 2.5 in.	At 3.5 in.
1	0	31.74	31.94	31.96	32.00
2	5	31.74	31.94	31.98	32.00
3	10	31.36	31.94	31.92	32.03
4	20	41.19	31.96	31.90	32.02
5	22	100.48	32.02	31.88	31.96
6	24	144.52	32.47	31.86	31.91
7	26	186.62	34.44	31.87	31.97
8	28	223.27	38.81	31.86	31.87
9	30	247.01	45.24	31.81	31.87
10	32	265.08	53.67	31.77	31.89
11	34	277.75	63.06	31.79	31.88
12	36	287.38	72.32	31.74	31.84
13	38	293.98	80.76	31.73	31.84
14	40	298.60	89.21	31.75	31.84
15	42	301.42	97.51	31.72	31.82
16	44	302.80	105.13	31.92	31.80
17	46	302.76	111.97	32.14	31.76
18	48	301.48	119.01	32.60	31.78
19	50	299.58	124.10	33.12	31.75
20	52	296.81	128.73	33.88	31.66
21	54	293.55	133.07	34.85	31.80
22	56	289.77	136.95	36.03	31.85
23	58	286.13	140.61	37.31	31.89
24	61	279.82	145.78	39.70	32.19
25	70	262.10	154.63	47.84	33.58
26	80	245.30	158.67	56.52	36.05
27	91	229.36	159.89	65.82	39.83
28	100	217.60	159.11	72.70	43.60
29	109	208.11	157.56	78.06	47.21
30	119	198.70	155.32	82.96	51.12
31	132	186.55	151.33	88.50	56.64
32	142	179.47	148.57	91.20	59.99
33	152	173.20	145.80	93.33	63.01
34	162	167.52	143.04	94.93	65.76
35	172	162.28	140.32	96.19	68.30
36	182	157.55	137.72	97.11	70.54
37	192	153.19	135.23	97.79	72.58
38	206	147.38	131.67	98.45	75.31
39	216	143.87	129.44	98.69	76.90
40	226	140.58	127.33	98.86	78.35
41	236	137.50	125.39	98.92	79.69
42	246	134.68	123.48	98.93	80.88
43	271	128.13	119.00	98.63	83.42
44	291	123.70	115.81	98.26	85.04
45	311	119.76	113.00	97.80	86.33
46	331	116.25	110.41	97.24	87.32
47	351	113.13	108.04	96.65	88.11
48	371	110.33	106.02	96.06	88.70
49	391	107.81	104.08	95.45	89.11
50	411	105.54	102.38	94.81	89.39
51	431	103.52	100.77	94.24	89.58
52	471	95.63	94.37	91.08	88.99
53	531	92.20	91.54	89.29	88.10
54	591	89.29	89.95	87.45	86.79

Cricket Graph Data — Temp MS #4 — Sun, Jun 4, 1989 [illegible]:28 AM

	Time #4	At 0.5 in.	At 1.5 in.	At 2.5 in.	At 3.5 in.
55	728	82.06	82.38	81.76	81.82
56	926	76.70	77.12	76.68	76.84
57	1123	72.19	72.61	72.20	72.26
58	1613	62.60	62.87	62.50	62.47
59	2396	51.81	52.04	51.82	51.75
60	3584	42.73	43.00	42.89	42.88

Cricket Graph Data Temp HY100 #5 Sun, Jun 4, 1989 11:29 AM

	Time #5	At 0.5 in.	At 1.5 in.	At 2.5 in.	At 3.5 in.
1	0	29.61	29.54	29.51	29.55
2	10	29.71	29.59	29.50	29.66
3	20	29.47	29.49	29.40	29.54
4	30	29.63	29.39	29.26	29.34
5	32	30.11	29.36	29.25	29.31
6	34	34.65	29.35	29.17	29.27
7	35	99.69	29.32	29.16	29.25
8	37	191.08	29.30	29.23	29.22
9	39	254.46	29.42	29.33	29.20
10	41	291.68	29.84	29.60	29.20
11	43	314.69	31.25	30.04	29.19
12	45	325.99	34.19	30.74	29.26
13	47	332.25	38.10	31.56	29.29
14	49	337.02	43.31	32.56	29.40
15	51	339.26	49.46	33.83	29.51
16	52	339.68	56.81	35.35	29.76
17	53	339.48	63.81	36.98	30.08
18	55	339.04	70.80	38.74	30.40
19	57	337.89	76.84	40.36	30.74
20	59	336.47	82.96	42.07	31.18
21	61	334.57	89.49	44.17	31.74
22	63	332.49	95.18	46.02	32.27
23	66	328.30	103.45	49.21	33.29
24	72	318.85	116.38	55.63	35.72
25	80	306.77	130.16	63.43	39.30
26	88	293.74	140.57	70.60	43.21
27	93	285.74	145.23	74.60	45.65
28	98	277.72	148.74	78.38	48.19
29	104	268.12	152.02	82.75	51.34
30	111	258.34	154.47	86.94	54.69
31	121	245.63	156.34	92.05	59.24
32	126	239.91	156.81	94.18	61.34
33	136	229.36	156.94	97.83	65.17
34	145	219.89	156.26	100.70	68.62
35	160	207.53	153.83	103.93	73.01
36	175	196.87	151.27	106.05	76.66
37	190	187.56	148.41	107.41	79.58
38	209	176.79	144.37	108.28	82.63
39	229	167.59	140.33	108.40	84.90
40	254	157.71	135.30	107.90	86.96
41	294	144.86	127.89	106.28	89.02
42	314	139.44	124.49	105.28	89.63
43	374	126.11	115.64	102.04	90.42
44	434	116.11	108.51	98.87	90.29
45	514	106.12	101.08	95.11	89.34
46	614	97.33	94.12	90.94	87.43
47	754	88.80	87.00	85.93	84.15
48	1001	78.89	78.01	78.44	77.85
49	1443	67.59	67.03	67.80	67.75
50	2031	57.31	56.89	57.50	57.63
51	3497	44.00	43.80	44.00	44.20
52	6096	35.73	35.60	35.71	35.82

Cricket Graph Data | Temp HY130 #6 | Sun, Jun 4, 1989 11:30 AM

	Time #6	At 0.5 in.	At 1.5 in.	At 2.5 in.	At 3.5 in.
1	0	31.62	31.64	31.43	31.49
2	10	31.57	31.60	31.44	31.44
3	19	31.62	31.52	31.27	31.44
4	27	69.58	31.43	31.06	31.35
5	29	137.48	31.34	30.95	31.28
6	31	185.18	31.62	31.08	31.34
7	33	223.67	32.00	31.01	31.31
8	35	256.70	33.36	30.94	31.32
9	36	285.83	36.02	30.87	31.21
10	38	300.00	39.98	30.81	31.25
11	40	308.29	45.33	30.90	31.19
12	42	312.49	51.08	30.74	31.19
13	44	314.52	57.36	30.72	31.16
14	46	314.77	63.63	30.62	31.17
15	48	314.50	69.75	30.59	31.14
16	50	313.86	76.00	30.69	31.10
17	52	312.87	82.16	30.69	31.08
18	58	308.05	99.53	31.17	31.03
19	61	303.77	108.90	31.90	30.98
20	66	298.72	118.25	33.35	30.99
21	75	287.55	131.79	37.91	31.15
22	80	278.80	138.18	41.69	31.55
23	86	269.59	144.31	45.91	32.16
24	94	258.53	149.35	51.37	33.30
25	101	248.29	152.83	56.63	34.77
26	113	234.10	155.47	64.13	37.56
27	123	223.70	156.07	69.59	40.16
28	133	214.41	155.72	74.27	42.88
29	148	202.20	154.04	80.05	47.03
30	163	191.70	151.56	84.50	51.00
31	178	182.57	148.65	87.85	54.66
32	197	172.24	144.54	90.95	59.00
33	217	163.51	140.37	92.89	62.68
34	237	155.91	136.29	94.05	65.83
35	277	144.68	129.48	94.82	70.25
36	317	134.24	122.67	94.52	73.95
37	377	122.06	113.98	92.99	77.53
38	437	112.66	106.94	91.01	79.53
39	517	103.19	99.64	88.29	80.63
40	617	94.62	92.71	85.02	80.43
41	756	86.16	85.56	80.73	78.50
42	1003	76.51	76.86	74.08	73.45
43	1348	67.63	68.35	66.46	66.33
44	2536	56.86	57.44	56.16	56.13
45	3514	46.10	46.56	45.69	45.73
46	4490	39.46	39.77	39.21	39.29

[illegible]cket Graph Data Max Temp Data Sun, Jun 4, 1989 [illegible] AM

	Distance, in	Mild Steel	HY-100	HY-130
1	0.5	302.80	339.68	314.77
2	1.5	159.89	156.94	156.07
3	2.5	98.93	108.40	94.82
4	3.5	83.58	90.42	80.63

Strain data tables record the microstrain longitudinally at 1", 2", 3", and 4" and transversely at 1.25", 2.25", 3.25", and 4.25". Tables 5, 6, and 7 are strain gage temperature compensated (appendix 4 contains the strain gage temperature compensation curve for XY11 strain gages):

Data Table	Title	Readings
5	Strain (y) MS #4 w/Tcomp	Transverse strain recorded on mild steel experiment #4
6	Strain (x) MS #4 w/Tcomp	Longitudinal strain recorded on mild steel experiment #4
7	Strain (y) HY100 #5 w/Tcomp	Transverse strain on HY100 experiment #5
8	Strain (x) HY100 #5 w/Tcomp	Longitudinal strain on HY100 experiment #5
9	Strain (y) HY130 #6 w/Tcomp	Transverse strain on HY130 experiment #6
10	Strain (x) HY130 #6 w/Tcomp	Longitudinal strain on HY130 experiment #6

Strain data tables without temperature compensation (actual microstrain readings):

Data Table	Title	Readings
11	Strain (y) MS #4 w/o Tcomp	Transverse strain on mild steel experiment #4
12	Strain (x) MS #4 w/o Tcomp	Longitudinal strain recorded on mild steel experiment #4
13	Strain (y) HY100 #5 w/o Tcomp	Transverse strain on HY100 experiment #5
14	Strain (x) HY100 #5 w/o Tcomp	Longitudinal strain on HY100 experiment #5
15	Strain (y) HY130 #6 w/o Tcomp	Transverse strain on HY130 experiment #6
16	Strain (x) HY130 #6 w/o Tcomp	Longitudinal strain on HY130 experiment #6

[illegible] Graph Data   Strain [illegible] MS #4 w Tcomp   Sun Jun 4, 1989 [illegible]

	Time #4	At 1.00 in	At 2.00 in	At 3.00 in	At 4.00 in
1	0	1.40	1.13	2.58	8.40
2	6	3.01	2.81	1.75	2.60
3	8	5.72	0.47	0.62	1.94
4	12	1.43	9.26	5.56	6.71
5	23	50.26	119.18	82.84	2.09
6	25	165.80	153.00	91.17	-5.37
7	27	213.97	181.57	101.15	2.81
8	28	368.33	233.58	116.65	-18.56
9	30	524.21	327.72	135.81	-22.49
10	32	567.52	435.38	165.35	-19.83
11	34	520.17	468.45	192.58	-21.65
12	36	567.84	514.31	219.71	-27.03
13	38	701.19	538.84	231.13	-8.53
14	40	840.26	531.88	264.59	-13.31
15	42	1069.44	520.53	280.92	11.84
16	44	1301.48	560.01	342.35	30.26
17	46	1425.05	543.16	325.64	28.34
18	48	1319.01	508.19	338.00	48.08
19	50	1282.39	512.37	341.65	45.32
20	52	1288.95	412.25	358.31	65.05
21	54	1332.47	352.84	362.45	67.83
22	56	1374.14	291.30	376.19	96.78
23	58	1436.17	229.13	376.63	104.14
24	60	1469.61	185.40	370.60	111.75
25	63	1474.52	113.64	368.06	125.63
26	72	1434.62	-57.67	351.79	156.24
27	82	1411.33	-166.63	333.34	173.60
28	93	1365.10	-287.90	262.40	185.77
29	102	1308.51	-285.95	232.65	188.46
30	111	1253.07	-284.24	205.50	184.96
31	121	1191.38	-289.09	183.05	171.35
32	135	1087.31	-295.24	175.90	163.43
33	145	1026.44	-293.49	163.53	155.10
34	155	964.04	-298.83	153.03	146.95
35	165	904.77	-301.96	152.22	146.93
36	175	851.00	-303.78	145.04	140.49
37	185	797.84	-303.72	149.75	154.22
38	195	752.72	-303.41	144.79	149.47
39	209	690.23	-301.47	142.73	147.43
40	219	652.17	-299.99	145.80	144.72
41	229	616.78	-298.27	142.64	143.56
42	239	583.38	-296.70	139.08	142.22
43	249	551.97	-294.87	135.99	141.73
44	274	480.65	-289.35	129.50	142.74
45	294	432.21	-285.06	131.97	162.40
46	314	389.14	-277.35	130.93	166.18
47	334	350.66	-274.43	127.02	167.38
48	354	316.01	-271.34	123.15	168.57
49	374	270.13	-271.89	116.43	169.29
50	394	242.35	-269.19	122.47	185.97
51	414	218.47	-266.94	119.34	186.61
52	434	196.44	-265.23	116.24	187.32
53	534	111.33	-265.86	106.09	187.67
54	594	64.14	-264.51	100.08	205.20

[illegible] Data Strain [illegible] MS #4 w Tcomp Sun Jun 4, 1989 [illegible] PM

	Time #4	At 1.00 in	At 2.00 in	At 3.00 in	At 4.00 in
55	605	32.38	-263.25	94.45	206.34
56	704	-18.71	-272.87	77.04	197.17
57	742	-58.11	-275.53	67.39	195.27
58	840	-129.07	-286.34	44.38	186.70
59	1137	-180.88	-286.68	34.63	189.22
60	1627	-308.36	-307.28	-6.16	172.15
61	2410	-441.04	-325.17	-44.67	158.66
62	3562	-539.51	-336.47	-72.83	151.54

	Strain, MS #4 w Comp				Sun Jun 4 1989 1:26 PM
	Time #4	At 1.25 in	At 2.25 in	At 3.25 in	At 4.25 in
1	0	6.33	6.12	6.39	4.92
2	6	4.40	4.05	6.57	3.44
3	8	9.88	1.03	1.92	2.92
4	12	0.98	-4.57	-6.93	-4.73
5	23	-43.04	-31.90	-53.30	-4.48
6	25	-50.50	-70.50	-47.90	1.58
7	27	103.79	-57.36	-38.60	9.33
8	28	92.82	-35.61	-26.04	18.79
9	30	36.60	-38.12	-14.93	27.41
10	32	22.80	-55.81	-11.38	31.85
11	34	63.51	-76.18	-13.86	33.54
12	36	153.63	-92.09	-15.48	38.32
13	38	252.37	-114.33	-12.52	36.50
14	40	335.49	-129.19	-32.27	37.43
15	42	413.95	-145.03	-39.32	28.32
16	44	486.34	-101.84	-52.33	19.59
17	46	584.10	-100.81	-62.64	6.82
18	48	648.03	-114.95	-71.25	13.42
19	50	779.05	-98.50	-78.80	7.79
20	52	904.17	-100.26	-82.68	2.55
21	54	982.56	-95.85	-84.76	-2.14
22	56	1098.79	-91.12	-61.31	-6.28
23	58	1197.38	-82.75	-79.89	-6.58
24	60	1225.74	-71.81	-76.05	-12.26
25	63	1295.01	-54.67	-67.34	-14.18
26	72	1362.82	2.57	-34.25	-24.11
27	82	1376.74	56.07	11.28	-28.43
28	93	1314.45	49.92	16.34	-25.31
29	102	1251.13	100.06	46.57	-20.44
30	111	1203.86	140.95	65.16	-18.50
31	121	1153.78	176.07	82.03	-22.75
32	135	1086.80	218.00	118.98	-16.25
33	145	1043.00	243.16	128.76	-14.34
34	155	1000.08	256.54	135.86	-13.64
35	165	957.91	267.25	148.87	-5.19
36	175	916.16	274.90	152.49	-4.84
37	185	877.33	280.00	164.79	12.09
38	195	842.54	284.08	166.66	12.73
39	209	796.15	289.47	171.41	12.69
40	219	769.32	291.49	179.11	13.44
41	229	745.18	296.03	178.95	13.77
42	239	723.12	296.46	178.97	14.74
43	249	703.08	297.45	178.87	15.35
44	274	658.30	299.80	177.04	17.19
45	294	628.47	301.72	183.00	36.40
46	314	602.59	306.25	185.00	37.68
47	334	580.05	307.05	184.10	38.84
48	354	560.03	308.33	183.47	40.44
49	374	527.84	305.79	179.41	41.79
50	394	512.22	306.28	186.84	57.42
51	414	498.68	307.26	186.12	58.22
52	434	485.79	307.58	185.66	59.25
53	534	435.96	302.34	183.79	57.84
54	594	408.41	302.71	181.82	74.68

	Time #4	At 1.25 in	At 2.25 in	At 3.25 in	At 4.25 in
55	605	392.16	303.03	180.17	74.92
56	704	359.56	292.65	168.15	64.58
57	742	337.94	289.65	163.63	61.69
58	940	295.60	278.08	149.74	50.54
59	1137	270.64	277.15	147.44	50.60
60	1627	200.02	255.11	121.68	29.71
61	2410	124.29	234.57	97.72	10.24
62	3562	75.01	221.84	82.32	-1.82

Cricket Graph Data Strain y: HY100 #5 w/Tcomp Sun, Jun 4, 1989 1:27 PM

	Time #5	At 1.25 in	At 2.25 in	At 3.25 in	At 4.25 in
1	0	4.78	3.32	-6.17	7.64
2	10	0.79	3.18	18.55	5.85
3	20	-39.64	-71.42	-52.72	-12.26
4	30	-15.00	-49.96	-2.58	33.77
5	32	-60.03	-26.17	2.09	67.68
6	34	-120.73	-43.99	20.95	57.33
7	35	-32.87	-51.60	-0.84	62.62
8	37	-41.24	-79.11	-68.74	75.32
9	39	-2.90	-135.09	18.73	63.51
10	41	54.20	-136.10	-39.25	59.97
11	43	67.50	-158.97	-46.66	54.08
12	45	221.97	-168.07	-62.85	53.42
13	47	320.00	-174.22	-69.44	49.80
14	49	397.32	-167.57	-74.92	46.89
15	51	495.25	-155.78	-122.77	64.98
16	53	577.85	-139.01	-59.44	52.61
17	55	687.99	-127.26	-88.59	48.05
18	57	809.86	-118.90	-90.38	42.59
19	59	914.58	-91.21	-91.27	25.36
20	61	1021.20	-77.12	-106.17	49.73
21	63	1108.14	-54.93	-100.66	33.23
22	65	1215.69	-36.96	-99.33	32.97
23	68	1323.22	-10.86	-95.39	30.03
24	74	1448.66	38.90	-81.82	22.81
25	82	1421.26	89.58	-59.56	14.29
26	90	1309.24	134.11	-37.07	7.37
27	95	1275.99	159.26	-15.30	9.87
28	100	1255.88	182.88	-3.69	8.46
29	106	1244.56	210.35	12.15	12.29
30	113	1297.06	237.30	25.21	14.60
31	123	1307.51	273.15	49.48	18.42
32	128	1317.00	287.93	57.69	21.20
33	138	1313.54	314.79	74.55	26.10
34	147	1302.48	335.54	84.21	32.36
35	162	1278.26	355.80	105.79	43.71
36	177	1240.86	364.50	120.95	51.24
37	192	1194.54	368.11	134.35	59.03
38	211	1122.90	366.03	147.27	64.26
39	231	1046.13	363.34	155.39	70.40
40	256	947.06	356.25	159.01	75.54
41	286	794.63	341.35	162.13	87.03
42	306	725.55	335.16	160.70	92.01
43	366	549.33	317.89	157.54	98.59
44	426	411.98	299.62	153.59	99.60
45	506	264.54	284.32	147.59	98.28
46	606	126.12	267.33	140.60	97.92
47	746	-10.71	249.55	134.55	94.53
48	993	-161.39	238.74	131.18	87.72
49	1435	-337.73	224.09	112.09	72.76
50	2023	-437.79	209.06	112.13	55.11
51	3489	-592.31	188.89	98.32	32.03
52	6024	-670.34	179.11	91.77	19.65
53					

Cricket Graph Data Strain(x) HY100 #5 w/Tcomp Sun, Jun 4, 1989 1:29 PM

	Time #5	At 1.00 in	At 2.00 in	At 3.00 in	At 4.00 in
1	0	-0.10	29.13	3.77	-1.22
2	10	-3.39	0.38	5.66	-3.83
3	20	-6.41	58.74	62.86	1.04
4	30	346.84	296.46	136.32	-49.37
5	32	530.99	372.73	166.62	-71.53
6	34	732.93	446.80	181.88	-78.96
7	35	858.53	529.73	222.76	-91.49
8	37	823.25	602.06	255.42	-85.63
9	39	780.56	674.57	292.70	-82.06
10	41	814.53	741.59	335.19	-75.58
11	43	884.44	780.94	371.99	-68.12
12	45	983.12	818.49	390.66	-65.14
13	47	1097.10	839.40	418.08	-55.12
14	49	1259.07	851.48	468.24	-48.20
15	51	1417.33	866.00	454.89	-39.82
16	53	1552.33	871.00	476.50	-32.21
17	55	1663.80	868.16	481.09	-21.39
18	57	1716.10	864.28	496.42	-16.04
19	59	1734.58	856.03	520.39	-8.67
20	61	1730.91	841.30	534.65	-0.95
21	63	1693.86	819.31	525.11	6.26
22	65	1650.12	801.18	527.74	13.85
23	68	1646.66	757.39	533.27	25.15
24	74	1567.89	666.40	537.91	48.64
25	82	1540.62	561.72	529.55	75.26
26	90	1533.12	474.08	504.31	96.65
27	95	1513.95	429.81	490.73	113.06
28	100	1490.62	391.93	464.53	123.66
29	106	1461.39	355.64	432.15	137.68
30	113	1435.42	326.93	393.46	148.06
31	123	1408.27	290.60	345.08	157.40
32	128	1389.10	272.61	319.93	160.87
33	138	1343.56	239.36	276.25	164.87
34	147	1296.31	209.11	233.87	166.37
35	162	1223.84	157.51	191.97	168.94
36	177	1151.12	141.09	156.72	166.26
37	192	1081.13	116.59	131.33	163.36
38	211	994.71	92.24	104.95	155.31
39	231	917.16	74.42	84.19	149.50
40	256	829.01	59.21	62.88	144.50
41	286	706.53	44.95	42.03	147.03
42	306	653.66	40.96	33.01	149.23
43	366	524.55	36.35	14.89	153.61
44	426	429.20	31.17	3.89	155.29
45	506	325.59	26.40	-7.75	154.55
46	606	227.38	21.96	-16.46	156.53
47	746	126.16	14.85	-22.71	155.09
48	993	18.39	14.16	-23.28	152.84
49	1435	-117.56	8.37	-23.92	145.68
50	2023	-255.18	1.80	-24.23	136.76
51	3489	-436.04	-6.43	-23.75	125.36
52	6024	-520.68	-10.90	-22.50	119.79
53					

[illegible] Graph Data   [illegible] MS #4 w/o T[illegible]   [illegible]

	Time#4 w/o	At 1.00 in	At 2.00 in	At 3.00 in	At 4.00 in
1	0	-.604	-3.13	.58	-10.39
2	6	1.01	19.81	-.25	.60
3	8	3.72	-1.54	-1.38	-.06
4	12	-.52	7.26	3.56	4.71
5	23	37.77	117.18	80.84	.09
6	25	83.33	150.56	89.17	-7.37
7	27	113.97	179.57	98.11	.81
8	28	268.34	231.57	114.66	-20.56
9	30	424.21	325.72	133.81	-24.49
10	32	467.52	433.37	163.35	-21.84
11	34	420.17	466.45	190.58	-23.65
12	36	467.84	512.31	217.71	-29.03
13	38	601.20	536.84	229.13	-10.53
14	40	740.26	529.19	262.59	-15.31
15	42	969.44	518.53	278.92	9.84
16	44	1201.48	495.01	340.35	.28
17	46	1325.45	460.66	323.64	26.34
18	48	1219.07	425.69	336.00	46.07
19	50	1182.39	412.37	339.65	43.32
20	52	1188.95	312.25	356.31	63.05
21	54	1232.47	252.84	360.45	65.83
22	56	1274.14	191.30	374.18	94.78
23	58	1336.17	129.13	300.63	102.14
24	60	1369.61	85.40	365.10	109.75
25	63	1374.52	13.64	362.56	120.63
26	72	1334.62	-157.67	339.29	154.24
27	82	1311.33	-266.63	303.34	171.60
28	93	1265.10	-321.44	256.33	179.58
29	102	1208.51	-333.08	220.15	179.46
30	111	1153.07	-342.24	193.00	175.96
31	121	1091.38	-354.09	170.56	169.35
32	135	987.31	-368.99	145.99	157.93
33	145	926.44	-375.99	133.53	145.60
34	155	864.04	-381.33	123.04	141.45
35	165	804.77	-384.46	114.72	134.43
36	175	751.00	-386.28	107.53	127.99
37	185	697.84	-386.22	102.25	124.22
38	195	652.72	-385.92	97.29	119.47
39	209	590.23	-383.97	91.73	117.43
40	219	552.16	-382.50	87.80	114.72
41	229	516.78	-380.77	84.64	113.56
42	239	483.38	-379.20	81.08	112.22
43	249	451.97	-377.37	77.99	111.73
44	274	380.65	-371.85	71.50	112.74
45	294	332.21	-367.56	66.97	114.90
46	314	289.14	-363.35	62.93	118.67
47	334	250.66	-360.47	59.02	119.88
48	354	216.01	-357.34	55.15	121.07
49	374	185.13	-354.39	51.43	121.79
50	394	157.35	-351.69	48.67	123.97
51	414	133.46	-349.44	45.54	124.61
52	434	111.44	-347.73	42.44	125.32
53	534	25.83	-341.36	30.59	128.67
54	594	-11.06	-339.71	24.88	130.00

Cricket Graph Data   Strain (y) MS #4 w/o Tcomp   Sun, Jun 4, 1989 1:35 PM

	Time#4 w/o	At 1.00 in	At 2.00 in	At 3.00 in	At 4.00 in
55	605	-42.82	-338.45	19.25	131.14
56	704	-83.71	-337.87	12.04	132.17
57	742	-120.11	-337.53	5.39	133.27
58	940	-130.07	-337.34	-6.62	135.70
59	1137	-231.87	-337.68	-16.37	138.22
60	1627	-338.36	-337.28	-36.16	142.75
61	2410	-453.54	-337.67	-57.17	146.16
62	3562	-545.01	-341.97	-78.33	146.04

	Time #4 w/o	At 1.25 in	At 2.25 in	At 3.25 in	At 4.25 in
1	0	4.33	4.12	4.39	2.92
2	6	2.40	2.05	-8.57	1.44
3	8	7.88	-.97	-.08	.92
4	12	[illegible]	-6.57	-8.93	-6.73
5	23	-60.54	-83.91	-55.29	-6.48
6	25	-63.00	-72.53	-49.88	-.42
7	27	3.78	-59.36	-40.60	7.33
8	28	[illegible]	-37.61	-28.04	16.80
9	30	-63.40	-40.12	-16.93	25.41
10	32	-77.19	-57.81	-13.38	29.85
11	34	-36.51	-78.18	-15.86	31.54
12	36	53.63	-94.09	-17.48	36.32
13	38	151.37	-116.33	-12.52	34.50
14	40	235.49	-131.19	-34.27	35.43
15	42	313.95	-147.03	-41.32	26.32
16	44	386.34	-166.48	-54.33	17.59
17	46	484.10	-183.31	-64.64	14.82
18	48	548.03	-197.45	-73.25	11.42
19	50	679.05	-198.50	-80.80	5.79
20	52	804.17	-200.26	-84.68	.55
21	54	882.56	-195.85	-86.76	-4.14
22	56	998.79	-191.12	-83.31	-8.28
23	58	1097.38	-182.75	-85.39	-8.58
24	60	1125.74	-171.81	-81.55	-14.26
25	63	1195.01	-154.67	-72.84	-18.04
26	72	1262.82	-97.43	-46.75	-26.11
27	82	1276.74	-43.93	-18.72	-30.43
28	93	1214.45	16.42	11.34	-30.82
29	102	1151.13	52.56	34.07	-29.44
30	111	1103.86	82.95	52.66	-27.50
31	121	1053.78	111.07	69.53	-24.75
32	135	986.80	144.25	88.98	-21.75
33	145	943.00	160.66	98.76	-19.84
34	155	900.08	174.04	105.86	-19.14
35	165	857.91	184.75	111.37	-17.69
36	175	816.16	192.40	114.99	-17.34
37	185	777.33	197.50	117.29	-17.91
38	195	742.54	201.58	119.16	-17.27
39	209	696.15	206.97	120.41	-17.31
40	219	669.32	208.99	121.11	-16.57
41	229	645.18	213.53	120.95	-16.23
42	239	623.12	213.96	120.97	-15.26
43	249	603.08	214.95	120.86	-14.65
44	274	558.30	217.30	119.04	-12.81
45	294	528.47	219.22	118.00	-11.10
46	314	502.59	220.25	117.00	-9.81
47	334	480.05	221.06	116.10	-8.66
48	354	460.03	222.33	115.47	-7.06
49	374	442.84	223.29	114.41	-5.71
50	394	427.22	223.78	113.04	-4.58
51	414	413.68	224.76	112.32	-3.78
52	434	400.79	225.08	111.86	-2.75
53	534	353.46	226.84	108.29	-1.16
54	594	333.21	227.51	106.61	-0.52

Cricket Graph Data | Strain @ MS #4 w/o Tcomp | Sun, Jun 4, 1989 1:35 PM

	Time #4 w/o	At 1.25 in	At 2.25 in	At 3.25 in	At 4.25 in
55	605	316.96	227.83	104.97	-0.28
56	704	294.56	227.65	103.15	-0.42
57	742	275.94	227.65	101.63	-0.31
58	940	244.60	227.08	98.74	-0.46
59	1137	219.64	227.15	96.44	-0.40
60	1627	170.02	225.11	91.68	-0.29
61	2410	111.79	222.07	85.22	-2.26
62	3562	69.51	216.34	76.82	-7.32

Pocket Graph Data Strain vs. HY100 #5 w/o Tcomp Sun, Jun 4 1989 1:37 PM

	Time #5 w/o	At 1.00 in	At 2.00 in	At 3.00 in	At 4.00 in
1	0	-2.09	-27.13	1.77	3.22
2	10	-5.39	-1.62	3.66	-5.83
3	20	-8.41	56.74	60.85	-0.95
4	30	344.84	294.46	134.32	-51.37
5	32	578.99	370.73	164.62	-73.53
6	34	730.93	444.80	181.88	-80.96
7	35	772.53	527.73	220.76	-93.49
8	37	759.64	600.06	253.42	-87.63
9	39	680.56	672.57	290.70	-84.06
10	41	714.53	735.92	333.19	-77.58
11	43	784.45	778.94	369.99	-70.12
12	45	883.12	814.49	388.66	-67.14
13	47	997.10	833.42	416.08	-57.11
14	49	1159.08	845.49	464.24	-50.20
15	51	1317.34	850.05	450.89	-41.82
16	53	1452.33	846.27	470.50	-34.20
17	55	1564.00	833.16	475.09	-23.39
18	57	1616.14	819.28	490.42	-18.04
19	59	1634.58	800.03	514.39	-10.67
20	61	1630.91	776.29	527.65	-2.95
21	63	1593.86	747.31	519.11	4.26
22	65	1550.12	722.18	517.74	10.85
23	68	1546.66	671.39	520.27	22.15
24	74	1467.89	569.39	515.91	45.64
25	82	1440.62	461.72	494.55	71.26
26	90	1433.12	374.08	459.31	92.65
27	95	1413.95	329.81	433.73	103.06
28	100	1390.62	291.93	404.53	111.66
29	106	1361.39	253.64	367.15	119.68
30	113	1335.42	226.93	326.46	126.06
31	123	1308.27	190.60	268.08	130.40
32	128	1289.00	172.61	240.94	130.87
33	138	1243.56	139.36	192.25	129.87
34	147	1196.31	109.11	150.87	126.37
35	162	1123.84	71.57	101.97	118.94
36	177	1051.12	41.09	64.72	110.26
37	192	981.13	16.59	36.33	101.36
38	211	894.71	-7.76	7.95	90.31
39	231	817.16	-25.58	-4.81	81.50
40	256	729.01	-40.79	-42.12	75.50
41	286	606.53	-55.05	-51.97	73.03
42	306	553.66	-59.04	-58.99	73.23
43	366	424.55	-63.65	-73.11	76.61
44	426	329.20	-63.83	-81.11	80.30
45	506	232.59	-61.61	-87.75	83.55
46	606	144.38	-58.04	-90.46	86.53
47	746	56.16	-53.15	-89.71	89.09
48	993	-41.62	-45.84	-83.28	93.84
49	1435	-160.56	-34.63	-66.92	102.68
50	2023	-280.18	-23.18	-49.23	111.76
51	3489	-443.04	-13.43	-30.75	118.36
52	6024	-526.68	-12.90	-24.50	117.79

Cricket Graph Data Strain x ...#5 w/o Tcomp Sun, Jun 4, 1989 1:37 PM

	Time #5 W/o	At 1.25 in	At 2.25 in	At 3.25 in	At 4.25 in
1	0	2.77	1.32	-8.17	5.64
2	10	-1.21	-5.18	16.55	3.85
3	20	-41.64	-73.41	-54.72	-14.25
4	30	-17.00	-51.96	-54.81	31.77
5	32	-62.03	-28.17	-45.81	31.77
6	34	-122.73	45.99	.09	65.68
7	35	-118.87	53.60	18.96	55.33
8	37	-141.24	-81.11	-2.83	60.62
9	39	-102.89	-137.09	-70.74	73.32
10	41	-45.80	-138.10	-16.17	61.51
11	43	-32.50	-160.96	-41.25	57.97
12	45	121.98	-172.07	-48.66	52.08
13	47	220.01	-176.22	-64.85	51.42
14	49	297.32	-173.57	-71.44	47.80
15	51	395.25	-171.78	-78.92	44.89
16	53	477.85	-164.01	-74.77	62.98
17	55	587.99	-162.26	-65.44	50.61
18	57	709.86	-163.89	-94.59	46.05
19	59	814.58	-147.21	-96.38	40.59
20	61	921.20	-142.13	-97.27	23.36
21	63	1008.14	-126.93	-113.17	47.73
22	65	1115.69	-115.96	-109.66	31.23
23	68	1223.22	-96.86	-109.33	29.97
24	74	1348.66	-58.10	-108.39	27.04
25	82	1321.26	-10.42	-103.82	19.81
26	90	1209.24	34.11	-94.56	10.29
27	95	1175.99	59.26	-82.07	3.37
28	100	1155.88	82.88	-72.90	-.02
29	106	1144.56	110.35	-63.59	-3.50
30	113	1197.06	137.30	-52.85	-5.71
31	123	1207.51	173.15	-41.78	-7.40
32	128	1217.00	187.93	-27.52	-8.58
33	138	1213.35	214.79	-21.31	-8.80
34	147	1202.48	235.54	-9.45	-8.90
35	162	1178.26	255.80	1.21	-7.64
36	177	1140.86	264.50	15.79	-6.28
37	192	1094.54	268.11	28.95	-4.76
38	211	1022.90	266.03	39.35	-2.97
39	231	946.13	263.35	50.27	-.74
40	256	847.06	256.25	58.39	2.40
41	286	694.63	241.35	64.00	6.54
42	306	625.55	235.16	68.13	13.03
43	366	449.33	217.89	68.70	16.01
44	426	311.98	204.62	69.54	21.59
45	506	171.54	196.32	68.59	24.60
46	606	43.12	187.33	67.59	27.28
47	746	-80.71	181.54	66.64	27.92
48	993	-221.39	178.74	67.55	28.53
49	1435	-380.73	181.09	71.18	28.72
50	2023	-462.79	184.06	79.29	29.76
51	3489	-599.31	181.88	87.13	30.11
52	6024	-672.34	177.11	91.32	25.03

[illegible] Graph Data [illegible] #6 w/o [illegible] Sun, Jun 4, 1989 [illegible]

	Time #6 w/o	At 1.00 in	At 2.00 in	At 3.00 in	At 4.00 in
1	0	11.45	-3.99	-7.69	13.24
2	10	28	-8.70	-2.94	33.97
3	19	113.67	45.65	46.30	47.13
4	27	200.78	243.40	105.25	43.26
5	29	268.13	281.20	106.39	33.05
6	31	432.84	339.67	113.86	13.78
7	33	724.47	423.97	124.73	3.49
8	35	738.08	516.96	168.85	-8.86
9	36	737.43	613.23	203.61	-17.64
10	38	725.00	690.58	251.56	-29.12
11	40	611.07	750.06	282.20	-12.95
12	42	669.08	813.45	312.68	-38.88
13	44	698.73	844.08	346.30	-41.63
14	46	781.91	873.14	357.23	-34.06
15	48	962.31	889.54	384.90	-30.14
16	50	1120.22	905.09	402.81	-24.08
17	52	1243.96	890.38	419.92	-13.06
18	53	1404.45	882.73	442.45	2.38
19	58	1619.86	848.54	453.30	24.06
20	61	1736.11	810.11	476.60	34.34
21	66	1756.57	744.93	491.23	45.57
22	75	1702.69	598.96	499.70	12.70
23	83	1645.09	512.74	491.55	27.97
24	91	1560.77	437.51	471.17	62.39
25	99	1488.64	365.89	445.09	92.14
26	106	1404.74	308.62	410.06	108.61
27	118	1136.54	245.15	353.41	123.28
28	128	1286.79	207.27	306.29	124.79
29	138	1225.22	176.83	262.40	128.53
30	153	1131.82	135.92	205.30	138.67
31	168	1044.61	100.90	161.54	145.93
32	183	967.05	72.36	127.84	204.57
33	202	881.15	43.21	94.77	208.57
34	222	814.81	21.28	70.02	152.01
35	242	764..22	5.73	51.63	142.21
36	277	699.92	-12.25	28.05	122.68
37	317	649.76	-21.56	10.67	106.85
38	377	601.23	-24.83	-4.85	89.14
39	437	568.85	-23.43	-14.33	74.16
40	517	542.25	-19.10	-20.13	44.26
41	617	521.87	-12.76	-27.35	34.31
42	756	505.60	-6.43	-31.11	25.76
43	1003	491.07	2.17	-30.34	17.84
44	1348	480.86	12.12	-24.24	22.04
45	1936	408.75	24.99	-13.95	38.36
46	2914	286.41	34.93	-5.18	54.93
47	3695	214.71	38.47	-3.12	66.64
48	5645	181.36	40.46	-2.63	47.39

Cricket Graph Data Strain vs. HY130 #6 w/o Thump Sun, Jun 4, 1989 1:35 PM

	Time #6 w/o	At 1.25 in	At 2.25 in	At 3.25 in	At 4.25 in
1	0	23.58	-2.29	7.34	-12.50
2	10	2.16	-46.87	-15.00	-4.00
3	19	-42.43	-60.25	-40.20	-21.38
4	27	-40.29	-149.13	-38.07	6.54
5	29	-55.89	-138.03	-21.21	24.67
6	31	-69.60	-31.42	38.00	34.95
7	33	-173.61	-34.19	-6.96	56.07
8	35	-301.52	-21.85	21.83	65.19
9	36	-413.25	-81.61	9.67	75.26
10	38	-484.30	-104.68	.50	68.11
11	40	-519.41	-134.62	-1.88	65.46
12	42	-532.70	-183.34	-40.26	64.28
13	44	-491.09	-187.41	-34.94	60.80
14	46	-424.48	-255.05	-55.81	56.97
15	48	-365.92	-201.58	-70.28	45.89
16	50	-310.58	-173.26	-68.51	51.62
17	52	-222.92	-200.85	-75.38	52.34
18	53	-108.35	-228.43	-81.94	43.18
19	58	-184.95	-188.87	-103.52	34.81
20	61	408.75	-175.68	-101.44	32.73
21	66	587.64	-144.78	-103.51	28.30
22	75	792.18	-93.08	-103.08	18.20
23	83	892.41	-59.85	-100.42	11.89
24	91	1022.55	-27.39	-93.63	5.81
25	99	1104.14	7.02	-83.32	.45
26	106	1108.35	35.50	-71.82	-2.99
27	118	1078.37	68.26	-54.30	-6.66
28	128	1033.13	88.73	-42.09	-7.63
29	138	991.05	105.97	31.27	-7.97
30	153	939.56	125.50	-17.92	-7.36
31	168	887.68	142.81	-8.02	-6.37
32	183	837.98	148.70	-.10	-5.62
33	202	783.86	152.24	6.78	-5.35
34	222	751.11	150.96	10.73	-5.77
35	242	731.80	146.25	13.23	-6.91
36	277	711.92	143.82	14.06	-8.45
37	317	698.42	130.59	13.45	-11.28
38	377	688.70	120.24	10.24	-13.99
39	437	684.87	111.62	7.66	-16.03
40	517	683.89	107.93	4.76	-17.85
41	617	685.53	101.82	2.83	-19.09
42	756	687.89	101.37	2.94	-18.97
43	1003	691.30	101.78	4.75	-17.13
44	1348	694.56	105.45	9.53	-13.27
45	1936	697.20	119.76	15.75	-8.34
46	2914	696.12	120.29	18.37	-5.86
47	3695	694.60	119.58	18.50	-6.09
48	5645	688.87	114.91	15.30	-9.39

Residual stress (in Ksi) contains residual stress data measured using the stress relaxation technique previously described. The first two columns show the value recorded for Mild Steel without side heat. Column one is the longitudinal residual stress at 1", 2", 3", and 4" from the weld line. Column two is the transverse residual stress at 1.25", 2.25", 3.25", and column 4 is the same for HY100 transverse. Column 5 is the same for HY130 longitudinal, and column 6 is the same for HY130 transverse. The same sequence is followed for the next six columns, except the side heating is applied from experiments #26, #27, and #28. The data analysis for chapter 4 shows the percentage of residual stress reduction achieved with the side heat from 17.38% to 39.17%.

Data Table	Title	Readings
17	Residual (3 pages)	Residual stress recorded in Ksi without side hat the first six columns (mild steel longitudinal and transverse, HY100, longitudinal HY130 longitudinal and transverse). The last six columns with side heat same sequence as before.
18	Residual (2 pages)	Before cutting and after cutting microstrain used to compute residual stress without side heat (#4 - #6).

[illegible] Graph Data Residual Sun, Jun 4 1989 [illegible] AM

	Distance in x	MS(x) w/o	MS(y) w/o	HY100(x) w/o	HY100(y) w/o
1	1	3 57	-2.46	23.99	3 88
2	2	-3 34	1 88	-2 23	3 323
3	3	2 47	5 41	-10 13	-6 54
4	4	-2 56	6 172	-11 97	-6 44

Cricket Graph Data   Residual   Sun, Jun 4, 1989 11:31 AM

	HY130(x) w/o	HY130(y) w/o	Distance in(y)	Side heating	MS(x) sn
1	20.35	9.26	1.25		5.632
2	-12.06	-11.59	2.25		-4.290
3	-8.09	-12.27	3.25		-1.764
4	-5.95	-10.18	4.25		-1.703

Cricket Graph Data | Residual | Sun Jun 4 1989 11:31 AM

	MS(y) sn	HY100(x) sn	HY100(y) sn	HY130(x) sn	HY130(y) sn
1	-1.907	15.99	2.59	15.65	7.125
2	1.154	-1.325	2.274	-10.08	-1.427
3	3.361	-5.552	-3.699	-4.921	-8.503
4	4.115	-8.452	-4.063	-4.251	-7.730

TABLE 18 RESIDUAL STRESS - BEFORE CUTTING

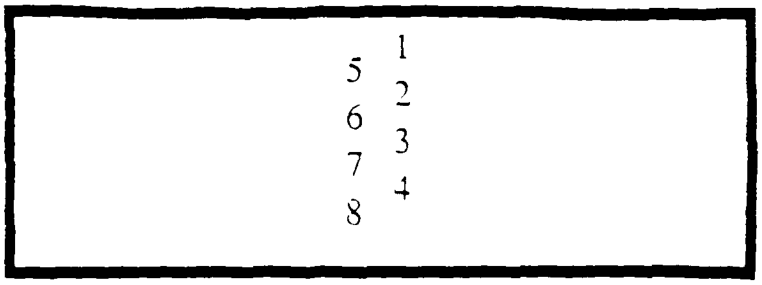

HY-130

1)	2.259e+02 μ	5)	4.479e+02 μ
2)	4.246e+02 μ	6)	4.700e+01 μ
3)	2.195e+02 μ	7)	3.622e+01 μ
4)	4.028e+02 μ	8)	2.358e+01 μ

HY-100

1)	5.843e+01 μ	5)	- 8.229e+01 μ
2)	2.106e+02 μ	6)	- 5.973e+02 μ
3)	3.240e+02 μ	7)	- 3.255e+02 μ
4)	4.570e+02 μ	8)	- 3.554e+02 μ

Mild Steel

1)	5.007e+02 μ	5)	2.827e+02 μ
2)	6.064e+02 μ	6)	- 3.532e+01 μ
3)	2.505e+02 μ	7)	6.549e+01 μ
4)	5.554e+02 μ	8)	- 1.206e+02 μ

TABLE 18 RESIDUAL STRESS - AFTER CUTTING

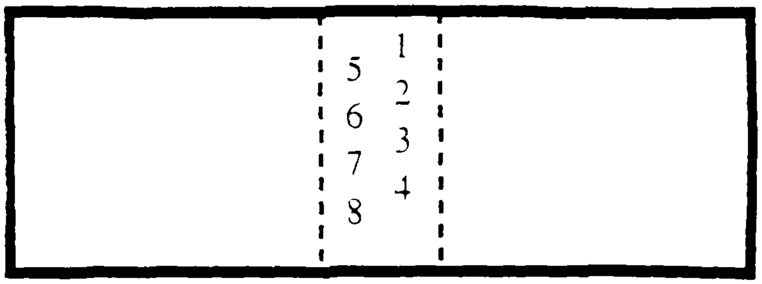

HY-130

1)	- 3.598e+02 μ	5)	3.427e+02 μ
2)	8.107e+02 μ	6)	- 2.056e+01 μ
3)	3.666e+02 μ	7)	3.642e+02 μ
4)	4.994e+02 μ	8)	3.033e+02 μ

HY-100

1)	- 8.192e+02 μ	5)	1.928e+02 μ
2)	3.182e+02 μ	6)	- 7.304e+02 μ
3)	5.963e+02 μ	7)	- 2.089e+02 μ
4)	7.915e+02 μ	8)	- 2.604e+02 μ

Mild Steel

1)	1.905e+02 μ	5)	4.505e+02 μ
2)	- 3.901e+02 μ	6)	- 1.573e+02 μ
3)	3.868e+02 μ	7)	1.394e+02 μ
4)	7.023e+02 μ	8)	- 3.519e+02 μ

Distortion data - these set of tables include large amount of distortion data gathered from experiments #8 through #28. The "Distortion Table contains 60 sequential columns as follows:

Data Table 19	Distortion Data	Strain Readings
	without side heating	HY130 column 1 - 4 HY100 column 5 - 8 Mild Steel column 9 - 12
	side heating longitudinally matched to arc	MS column 13 - 16 HY100 column 17 - 20 HY130 column 21 - 24
	side heating positioned 9" ahead of arc	MS column 25 - 28 HY100 column 29 - 32 HY130 column 33 - 36
	side heating positioned 9" longitudinally behind arc	MS column 36 - 40 HY100 column 41 - 44 HY130 column 45 - 58
	distortion data taken during the final series of experiments with side heat matched longitudinally to arc	MS column 49 - 52 HY100 column 53 - 56 HY130 column 57 - 60

Cricket Graph Data DISTORTION Table#1 Sun, Jun 4, 1989 11:41 AM

	Time130w/o	130w/o4.5"	130w/o9.00"	130w/o13.75"	Time100w/o
1	0	0	0	0	0
2	10	-.0050	-.0030	-.0050	9
3	24	-.0100	-.0080	-.0100	30
4	40	-.0140	-.0150	-.0140	42
5	50	-.0145	-.0170	-.0145	60
6	60	-.0150	-.0180	-.0150	69
7	88	-.0140	-.0175	-.0140	94
8	102	-.0130	-.0165	-.0130	106
9	110	-.0130	-.0160	-.0130	117
10	126	-.0120	-.0150	-.0120	133
11	138	-.0110	-.0140	-.0110	154
12	155	-.0100	-.0130	-.0100	179
13	172	-.0090	-.0115	-.0090	194
14	194	-.0080	-.0100	-.0080	215
15	209	-.0070	-.0090	-.0070	223
16	233	-.0060	-.0080	-.0060	234
17	254	-.0050	-.0070	-.0050	245
18	279	-.0040	-.0060	-.0040	269
19	308	-.0025	-.0050	-.0025	285
20	330	-.0020	-.0040	-.0020	297
21	350	-.0010	-.0035	-.0010	327
22	375	-.0005	-.0030	-.0005	366
23	395	-.0002	-.0025	-.0002	413
24	413	.0000	-.0020	.0000	467
25	446	.0010	.0000	.0010	519
26	491	.0015	.0005	.0015	602
27	520	.0020	.0010	.0020	695
28	609	.0030	.0020	.0030	778
29	642	.0030	.0020	.0030	964
30	762	.0035	.0030	.0035	1532
31	828	.0040	.0030	.0040	
32	937	.0040	.0032	.0040	
33	1281	.0040	.0040	.0040	
34					

Cricket Graph Data　　DISTORTION Table#1　　Sun, Jun 4, 1989 [illegible] AM

	100w/o 4.5"	100w/o 9.00"	100w/o 13.75"	TimeMSw/o	MSw/o 4.5"
1	0	0	0	0	0
2	-.0050	-.0040	-.0030	20	-.0060
3	-.0120	-.0100	-.0050	40	-.0090
4	-.0150	-.0160	-.0090	55	-.0100
5	-.0180	-.0200	-.0150	63	-.0100
6	-.0170	-.0190	-.0140	97	-.0070
7	-.0150	-.0170	-.0130	105	-.0060
8	-.0130	-.0140	-.0120	116	-.0050
9	-.0120	-.0130	-.0110	128	-.0030
10	-.0100	-.0110	-.0090	133	-.0020
11	-.0080	-.0090	-.0080	148	-.0010
12	-.0060	-.0070	-.0060	165	.0000
13	-.0050	-.0060	-.0050	171	.0005
14	-.0040	-.0050	-.0045	179	.0010
15	-.0030	-.0040	-.0040	183	.0020
16	-.0020	-.0040	-.0035	190	.0030
17	-.0015	-.0035	-.0030	210	.0045
18	.0000	-.0025	-.0020	227	.0050
19	.0000	-.0020	-.0018	244	.0065
20	.0010	-.0015	-.0010	252	.0070
21	.0020	.0000	.0000	275	.0080
22	.0030	.0010	.0010	305	.0090
23	.0040	.0020	.0020	333	.0100
24	.0050	.0030	.0025	342	.0105
25	.0058	.0040	.0030	391	.0115
26	.0062	.0050	.0040	447	.0123
27	.0070	.0053	.0042	488	.0130
28	.0072	.0057	.0050	531	.0131
29	.0078	.0060	.0050	636	.0132
30	.0080	.0070	.0050	720	.0135
31				1123	.0135
32				1300	.0135
33					
34					

Cricket Graph Data DISTORTION Table#1 Sun, Jun 4, 1989 11:4? AM

	MSw/o9.00"	MSw/o13.75"	TimeMSsh0"	MSsh0-4.5"	MSsh0-9.0"
1	0	0	0	0	0
2	-.0050	-.0010	20	-.0010	-.0020
3	-.0100	-.0050	40	-.0020	-.0040
4	-.0115	-.0080	50	-.0025	-.0050
5	-.0130	-.0090	63	-.0030	-.0055
6	-.0090	-.0080	97	-.0020	-.0050
7	-.0080	-.0060	103	-.0015	-.0040
8	-.0060	-.0050	124	-.0005	-.0025
9	-.0050	-.0040	130	.0000	-.0020
10	-.0040	-.0030	135	.0010	-.0010
11	-.0030	-.0020	151	.0020	.0000
12	-.0015	-.0015	172	.0030	.0015
13	-.0010	-.0010	189	.0040	.0030
14	.0000	.0000	220	.0055	.0045
15	.0010	.0000	230	.0060	.0050
16	.0020	.0010	245	.0070	.0060
17	.0030	.0020	272	.0080	.0070
18	.0040	.0025	303	.0085	.0080
19	.0050	.0030	326	.0090	.0090
20	.0060	.0040	359	.0100	.0100
21	.0070	.0050	411	.0103	.0105
22	.0080	.0060	443	.0110	.0110
23	.0095	.0065	564	.0115	.0120
24	.0100	.0070	624	.0120	.0125
25	.0110	.0080	900	.0120	.0125
26	.0120	.0085			
27	.0125	.0090			
28	.0130	.0095			
29	.0138	.0100			
30	.0140	.0105			
31	.0150	.0110			
32	.0150	.0110			
33					
34					

Cricket Graph Data DISTORTION Table#1 Sun, Jun 4, 1989 11:41 AM

	MSsh0-13.75"	Time100sh0"	100sh0-4.5"	100sh0-9.0"	100sh0-13.75"
1	0	0	0	0	0
2	-.0010	19	0	-.0010	0
3	-.0030	37	-.0040	-.0030	-.0020
4	-.0035	51	-.0060	-.0080	-.0050
5	-.0040	60	-.0070	-.0105	-.0080
6	-.0030	85	-.0080	-.0100	-.0090
7	-.0025	103	-.0060	-.0090	-.0080
8	-.0020	116	-.0050	-.0080	-.0070
9	-.0015	127	-.0045	-.0070	-.0060
10	-.0010	139	-.0040	-.0055	-.0050
11	.0000	164	-.0035	-.0050	-.0045
12	.0010	177	-.0030	-.0045	-.0040
13	.0020	197	-.0015	-.0035	-.0030
14	.0030	208	-.0010	-.0030	-.0025
15	.0035	226	.0000	-.0020	-.0020
16	.0040	251	.0010	-.0005	-.0010
17	.0050	278	.0015	.0000	.0000
18	.0060	299	.0020	.0010	.0005
19	.0065	350	.0035	.0030	.0020
20	.0070	399	.0040	.0040	.0030
21	.0070	467	.0050	.0050	.0035
22	.0080	584	.0060	.0060	.0040
23	.0090	840	.0065	.0070	.0050
24	.0090	1025	.0065	.0070	.0050
25	.0090				
26					
27					
28					
29					
30					
31					
32					
33					
34					

Cricket Graph Data DISTORTION Table#1 Sun, Jun 4, 1989 [illegible] AM

	Time130sn0"	130sn0-4.5"	130sn0-9.0"	130sn0-13.75"	TimeMS9+"
1	0	0	0	0	0
2	20	-.0030	-.0020	-.0010	13
3	30	-.0040	-.0040	-.0030	30
4	40	-.0050	-.0060	-.0050	43
5	60	-.0070	-.0100	-.0080	53
6	99	-.0060	-.0090	-.0075	67
7	110	-.0045	-.0080	-.0070	92
8	135	-.0040	-.0070	-.0060	101
9	155	-.0035	-.0060	-.0050	127
10	184	-.0025	-.0050	-.0040	145
11	205	-.0020	-.0040	-.0035	161
12	223	-.0015	-.0035	-.0030	178
13	246	-.0010	-.0030	-.0025	189
14	272	.0000	-.0020	-.0020	201
15	300	.0005	-.0010	-.0010	208
16	332	.0010	.0000	.0000	227
17	384	.0020	.0010	.0010	249
18	406	.0025	.0020	.0020	273
19	597	.0035	.0031	.0030	299
20	740	.0040	.0040	.0035	325
21	1107	.0045	.0050	.0040	341
22					371
23					395
24					464
25					564
26					716
27					1206
28					
29					
30					
31					
32					
33					
34					

Cricket Graph Data DISTORTION Table#1 Sun, Jun 4, 1989 11:41 AM

	MS9+4.5"	MS9+9.0"	MS9+13.75"	Time100-9+"	100-9+4.5"
1	0	0	0	0	0
2	.0040	0	0	16	.0010
3	.0070	.0070	.0040	30	.0040
4	.0050	.0060	.0060	44	.0020
5	.0020	.0030	.0030	60	-.0050
6	.0010	.0010	.0005	73	-.0100
7	-.0030	-.0050	-.0040	90	-.0095
8	-.0025	-.0040	-.0030	120	-.0090
9	-.0010	-.0020	-.0020	142	-.0085
10	.0000	-.0010	-.0010	159	-.0080
11	.0010	.0000	.0000	174	-.0070
12	.0025	.0010	.0010	192	-.0055
13	.0035	.0025	.0020	229	-.0045
14	.0040	.0030	.0025	257	-.0020
15	.0050	.0040	.0030	278	-.0015
16	.0060	.0050	.0040	309	.0000
17	.0070	.0065	.0050	351	.0010
18	.0080	.0080	.0060	420	.0020
19	.0085	.0090	.0070	477	.0030
20	.0092	.0100	.0072	577	.0035
21	.0100	.0105	.0080	635	.0040
22	.0102	.0110	.0085	789	.0040
23	.0110	.0120	.0090	900	.0040
24	.0115	.0130	.0100		
25	.0125	.0140	.0110		
26	.0130	.0145	.0110		
27	.0130	.0150	.0110		
28					
29					
30					
31					
32					
33					
34					

Cricket Graph Data DISTORTION Table#1 Sun, Jun 4, 1989 11:41 AM

	130-9+9.0"	130-9+13.75"	Time130-9+"	130-9+4.5"	130-9+9.0"
1	0	0	0	0	0
2	0	0	12	0020	0
3	0040	0010	30	.0050	.0030
4	0030	0020	41	0040	.0050
5	-.0040	-.0030	50	.0010	.0010
6	-.0090	-.0080	60	-.0050	-.0060
7	-.0150	-.0090	75	-.0080	-.0100
8	-.0130	-.0100	90	-.0120	-.0140
9	-.0110	-.0090	119	-.0100	-.0130
10	-.0100	-.0080	156	-.0090	-.0115
11	-.0090	-.0070	175	-.0080	-.0100
12	-.0065	-.0060	191	-.0070	-.0090
13	-.0050	-.0040	218	-.0060	-.0070
14	-.0030	-.0030	243	-.0040	-.0050
15	-.0020	-.0020	278	-.0030	-.0040
16	-.0005	-.0010	297	-.0020	-.0030
17	.0010	0000	325	-.0010	-.0020
18	.0025	0015	364	.0000	-.0005
19	0040	0020	374	.0005	.0000
20	.0050	0030	420	.0010	.0010
21	.0055	0035	472	.0018	.0020
22	0060	0040	531	.0025	0030
23	0060	0040	610	.0030	.0040
24			913	0040	.0050
25					
26					
27					
28					
29					
30					
31					
32					
33					
34					

	130-9-13.75"	TimeMS-9"	MS-9-4.5"	MS-9-9.0"	MS-9-13.75"
1	0	0	0	0	0
2	0	10	-.0020	-.0010	-.0005
3	.0020	20	-.0045	-.0035	-.0020
4	.0040	30	-.0100	-.0090	-.0050
5	.0020	40	-.0090	-.0110	-.0060
6	-.0030	50	-.0050	-.0080	-.0040
7	-.0050	60	-.0030	-.0040	-.0030
8	-.0100	72	.0000	.0000	-.0010
9	-.0090	82	.0010	.0010	.0010
10	-.0080	96	.0015	.0012	.0015
11	-.0070	114	.0020	.0020	.0020
12	-.0060	144	.0040	.0040	.0030
13	-.0050	157	.0045	.0050	.0040
14	-.0040	179	.0055	.0060	.0050
15	-.0030	196	.0060	.0070	.0055
16	-.0020	210	.0070	.0080	.0060
17	-.0010	232	.0080	.0090	.0070
18	.0000	267	.0085	.0100	.0080
19	.0000	292	.0090	.0110	.0085
20	.0010	317	.0100	.0120	.0090
21	.0018	376	.0110	.0130	.0100
22	.0025	440	.0110	.0140	.0105
23	.0030	493	.0110	.0145	.0110
24	.0040	589	.0110	.0150	.0110
25		890	.0120	.0150	.0115
26		900	.0120	.0150	.0115
27					
28					
29					
30					
31					
32					
33					
34					

	Time100-9-"	100-9-4.5"	100-9-9.0"	100-9-13.75"	Time130-9-"
1	0	0	0	0	0
2	10	-.0020	-.0010	-.0010	10
3	20	-.0060	-.0040	-.0030	20
4	30	-.0120	-.0120	-.0080	30
5	40	-.0150	-.0160	-.0100	40
6	50	-.0120	-.0140	-.0110	50
7	63	-.0080	-.0090	-.0080	60
8	76	-.0060	-.0080	-.0060	88
9	93	-.0050	-.0070	-.0050	120
10	120	-.0045	-.0065	-.0045	136
11	138	-.0040	-.0055	-.0040	145
12	157	-.0038	-.0050	-.0035	167
13	175	-.0035	-.0045	-.0030	198
14	185	-.0030	-.0040	-.0025	227
15	194	-.0020	-.0035	-.0020	252
16	242	-.0010	-.0020	-.0010	272
17	271	.0000	-.0010	.0000	313
18	311	.0010	.0000	.0010	360
19	371	.0020	.0010	.0015	413
20	426	.0030	.0020	.0020	495
21	620	.0040	.0030	.0030	631
22	814	.0045	.0040	.0035	823
23	995	.0050	.0040	.0040	971
24	1175	.0050	.0045	.0040	1165
25					
26					
27					

	130-9-4.5"	130-9-9.0"	130-9-13.75"	TimeMS#26	MS#26sh4.5"
1	0	0	0	0	0
2	-.0020	-.0010	-.0010	15	-.0015
3	-.0050	-.0050	-.0040	30	-.0020
4	-.0110	-.0120	-.0070	45	-.0030
5	-.0120	-.0150	-.0100	60	-.0040
6	-.0100	-.0140	-.0110	83	-.0035
7	-.0060	-.0100	-.0080	110	-.0025
8	-.0050	-.0090	-.0060	118	-.0020
9	-.0045	-.0080	-.0050	140	-.0010
10	-.0040	-.0070	-.0045	158	.0000
11	-.0030	-.0060	-.0040	176	.0010
12	-.0020	-.0050	-.0030	205	.0025
13	-.0010	-.0040	-.0020	230	.0035
14	.0000	-.0025	-.0010	260	.0045
15	.0015	-.0020	-.0005	304	.0055
16	.0025	-.0010	.0000	317	.0060
17	.0035	.0000	.0010	370	.0070
18	.0040	.0010	.0015	422	.0072
19	.0050	.0020	.0020	508	.0080
20	.0060	.0030	.0030	674	.0081
21	.0060	.0040	.0036	900	.0085
22	.0062	.0045	.0040	1122	.0085
23	.0062	.0050	.0040		
24	.0062	.0050	.0040		
25					
26					
27					

	MS#26sh9"	MS#26sh13.75	Time100#27	100#27sh4.5	100#27sh 9"
1	0	0	0	0	0
2	-.0010	-.0010	15	-.0003	-.0010
3	-.0020	-.0015	25	-.0010	-.0020
4	-.0030	-.0015	35	-.0020	-.0040
5	-.0060	-.0040	45	-.0040	-.0080
6	-.0050	-.0037	60	-.0050	-.0090
7	-.0040	-.0035	72	-.0065	-.0085
8	-.0035	-.0030	93	-.0055	-.0080
9	-.0020	-.0020	105	-.0050	-.0070
10	-.0010	-.0010	123	-.0040	-.0060
11	.0000	.0000	136	-.0035	-.0050
12	.0015	.0010	155	-.0030	-.0040
13	.0030	.0020	184	-.0015	-.0030
14	.0040	.0030	212	-.0005	-.0010
15	.0050	.0040	230	.0000	-.0003
16	.0060	.0045	249	.0005	.0000
17	.0070	.0050	300	.0020	.0020
18	.0080	.0060	363	.0030	.0030
19	.0088	.0065	426	.0040	.0040
20	.0091	.0068	500	.0050	.0050
21	.0095	.0070	607	.0055	.0060
22	.0100	.0070	688	.0055	.0065
23			865	.0060	.0070
24			1260	.0060	.0070
25					
26					
27					

	#27sn13.75"	Time130#28	130#28sn4.5	130#28sn9"	#28sn13.75
1	0	0	0	0	0
2	0	5	-.0010	-.0010	-.0010
3	-.0010	15	-.0020	-.0015	-.0015
4	-.0020	38	-.0040	-.0040	-.0020
5	-.0040	50	-.0050	-.0060	-.0030
6	-.0045	60	-.0080	-.0100	-.0050
7	-.0050	77	-.0075	-.0105	-.0060
8	-.0045	89	-.0070	-.0110	-.0070
9	-.0040	110	-.0060	-.0090	-.0060
10	-.0035	140	-.0050	-.0080	-.0050
11	-.0030	168	-.0035	-.0070	-.0040
12	-.0025	187	-.0030	-.0060	-.0035
13	-.0010	199	-.0025	-.0050	-.0030
14	.0000	222	-.0015	-.0040	-.0025
15	.0003	241	-.0010	-.0035	-.0020
16	.0010	274	.0000	-.0020	-.0010
17	.0020	332	.0010	-.0010	.0000
18	.0030	363	.0018	.0000	.0003
19	.0040	415	.0025	.0010	.0010
20	.0045	471	.0030	.0015	.0015
21	.0050	514	.0035	.0020	.0020
22	.0055	625	.0040	.0030	.0025
23	.0060	737	.0045	.0035	.0030
24	.0060	1009	.0050	.0040	.0035
25		1293	.0050	.0045	.0040
26		2220	.0050	.0050	.0040
27					

This table includes the distortion measured using side heat only (NO ARC WELD) to isolate the effects of the side heat torch.

Data Table 20

Strain Readings

SIDE HEAT ONLY {Mild Steel columns 1 - 4 | HY100 columns 5 - 8 | HY130 columns 9 - 12}

Cricket Graph Data SIDE HEAT ONLY Sun, Jun 4, 1989 12:38 PM

	TimeMS	MS at 4.5"	MS at 9.0"	MS at13.75"	TimeHY100
1	0	0	0	0	0
2	16	.0070	.0030	.0020	15
3	32	.0100	.0100	.0050	35
4	60	.0110	.0130	.0120	51
5	85	.0080	.0100	.0070	60
6	105	.0070	.0090	.0060	74
7	112	.0065	.0080	.0050	95
8	140	.0050	.0070	.0045	119
9	158	.0045	.0065	.0040	127
10	170	.0040	.0060	.0030	149
11	196	.0030	.0050	.0025	187
12	226	.0025	.0040	.0020	223
13	268	.0015	.0035	.0010	242
14	302	.0010	.0030	.0010	278
15	369	.0005	.0020	.0000	329
16	472	.0000	.0015	-.0003	462
17	692	.0000	.0010	-.0005	777
18	900	.0000	.0008	-.0005	858
19	900	.0000	.0008	-.0005	900

Cricket Graph Data SIDE HEAT ONLY Sun, Jun 4, 1989 12:38 PM

	HY100 at 4.5"	HY100 at 9.0"	HY100 13.75"	TimeHY130	HY130 at 4.5"
1	0	0000	0	0	0
2	0050	0020	.0010	17	.0030
3	0100	0080	0030	28	0050
4	0110	0130	0100	60	0080
5	0100	0120	.0090	97	.0060
6	0090	0110	0080	129	.0050
7	0080	0100	0070	146	.0045
8	0070	0090	.0065	168	.0040
9	.0065	0080	0060	212	.0030
10	.0060	0070	0050	285	.0020
11	0050	0060	0040	397	.0010
12	.0040	0050	0035	618	.0000
13	.0035	0045	.0030	910	.0000
14	.0030	0040	.0025		
15	.0020	.0030	0020		
16	.0010	.0020	.0010		
17	.0005	.0010	0000		
18	.0000	.0005	.0000		
19	.0000	.0005	.0000		

Cricket Graph Data SIDE HEAT ONLY Sun Jun 4 1989 10:36 PM

	HY130 at 9.0"	HY130 13.75"
1	0	0
2	0010	0005
3	0060	0020
4	0100	0080
5	0085	.0075
6	0070	0065
7	0065	0060
8	.0060	.0050
9	.0050	0040
10	.0035	.0030
11	.0020	.0020
12	.0010	.0010
13	.0002	0000
14		
15		
16		
17		
18		
19		

The last series of data are tables of temperature and strain collected during experiments #26 through #28. This series of data is similar to the data contained in a experiments #4 through #6, with the exception of having slightly elevated temperatures associated with side heating away from the weld. The only the residual stress data is plotted in this report from these experiments #26 through #28.

Data Table	Steel Type
21	MS Temperature
22	HY100 Temperature
23	HY130 Temperature

Strain	Steel Type
24	MS Transverse (y) w/Tcomp
25	Ms Longitudinal (x) w/Tcomp
26	HY100 Transverse (y) w/Tcomp
27	HY100 Longitudinal (x) w/Tcomp
28	HY130 Transverse (y) w/Tcomp
39	MS (y) Transverse w/o Tcomp
30	MS (x) Longitudinal w/o Tcomp
31	HY100 (y) Transverse w/o Tcomp
32	HY100 (x) Transverse w/o Tcomp
33	HY130 (y) Longitudinal w/o Tcomp
34	HY130 (x) Longitudinal w/o Tcomp

Cricket Graph Data Temp MS w sn #26 Sun Jun 4 1989 12 45 PM

	Time	At 0.5 in	At 1.5 in	At 2.5 in	At 3.25 in
1	0	30.51	30.34	30.52	29.13
2	5	30.51	30.58	30.00	29.32
3	13	30.28	30.49	30.58	36.86
4	15	30.19	30.35	30.52	40.90
5	17	30.29	30.20	30.36	46.35
6	19	30.25	30.44	30.35	54.99
7	21	30.38	30.31	30.24	68.31
8	23	30.42	30.49	30.44	82.18
9	24	30.44	30.50	31.05	89.81
10	26	30.12	30.89	31.02	95.67
11	32	30.59	31.60	35.90	102.36
12	36	40.35	32.20	39.86	103.46
13	38	92.17	32.73	42.22	103.41
14	40	133.58	33.65	45.67	103.29
15	42	163.90	35.77	50.72	102.80
16	44	183.33	38.43	55.10	102.75
17	46	205.73	41.50	59.55	102.43
18	47	224.15	44.72	62.25	102.07
19	49	239.15	48.22	65.04	101.82
20	51	252.62	53.08	66.87	101.50
21	53	262.76	57.96	68.64	101.29
22	55	270.30	62.97	70.22	100.93
23	57	276.47	68.41	71.97	100.76
24	59	280.69	73.95	73.69	100.67
25	61	284.04	79.60	76.08	100.60
26	63	285.93	85.31	76.82	100.66
27	64	286.92	89.73	78.15	100.68
28	66	287.33	94.14	79.54	100.74
29	67	287.34	98.50	80.97	100.84
30	69	286.91	102.92	82.58	101.01
31	74	284.10	113.01	87.07	101.57
32	80	278.03	124.24	93.45	102.70
33	88	268.78	133.42	100.82	104.48
34	96	259.02	141.67	108.16	106.49
35	104	249.42	148.78	114.68	108.62
36	116	236.25	156.23	122.68	111.63
37	126	226.61	159.88	127.74	113.87
38	136	217.59	162.06	131.76	115.89
39	146	209.73	163.12	134.74	117.60
40	166	196.07	163.02	138.62	120.38
41	186	185.01	161.28	140.62	122.40
42	205	175.86	158.76	141.31	123.87
43	230	166.60	155.15	140.99	125.08
44	256	158.92	151.55	140.04	125.82
45	316	145.67	143.67	136.44	126.15
46	376	136.48	137.02	132.37	125.35
47	456	127.66	129.99	127.26	123.25
48	556	119.78	122.97	120.99	119.78
49	666	114.01	117.00	115.39	115.98
50	864	104.79	107.16	105.20	108.10
51	1061	97.36	99.24	96.91	100.64
52	1356	87.60	89.04	86.43	90.82
53	1748	77.06	78.11	75.42	80.04
54	2042	70.57	71.39	68.97	73.40

Jacket Graph Data		Temp VS w sh #26		Sun, Jun 4, 1989 12:45 PM

	Time	At 0.5 in	At 1.5 in	At 2.5 in	At 3.25 in
55	2531	61.80	62.46	60.11	64.31
56	3372	51.89	52.46	50.37	53.83
57	4544	42.71	43.17	41.69	44.16
58	6164	36.08	36.42	35.57	37.13
59	8991	31.52	31.71	31.43	32.17

Cricket Graph Data   Temp HY100 w sn #27   Sun, Jun 4, 1989 12:46 PM

	Time	At 0.75 in	At 1.5 in	At 2.5 in	At 3.25 in
1	0	26.41	26.51	26.17	25.56
2	7	26.31	26.51	26.00	25.36
3	15	26.57	27.25	25.53	25.29
4	22	26.35	28.04	27.04	27.08
5	23	27.52	28.17	27.97	28.73
6	25	32.53	28.53	28.96	30.76
7	27	51.07	29.21	30.05	33.39
8	28	81.87	30.90	31.28	37.05
9	30	115.32	33.90	32.67	41.73
10	32	140.96	37.69	34.04	48.43
11	33	161.79	41.79	36.11	59.19
12	35	177.59	46.43	39.25	72.85
13	37	188.72	51.61	42.93	84.74
14	38	197.23	56.97	46.41	93.04
15	40	204.96	62.84	49.45	99.58
16	42	211.85	70.24	52.29	103.99
17	44	216.15	76.36	53.95	106.13
18	46	220.49	83.74	56.11	107.54
19	48	224.09	91.38	58.25	108.17
20	52	230.16	104.74	61.72	108.09
21	54	232.70	110.81	63.23	107.66
22	56	234.86	115.58	64.83	107.12
23	58	236.73	120.77	66.34	106.53
24	60	238.36	125.65	67.60	105.89
25	62	239.74	130.05	69.19	105.27
26	65	241.34	136.50	71.37	104.24
27	68	242.26	141.70	73.57	103.30
28	71	242.65	146.33	75.83	102.47
29	73	242.61	148.38	76.94	102.11
30	78	241.75	153.82	80.36	101.24
31	84	239.26	159.75	84.98	100.57
32	99	229.48	168.97	96.48	100.92
33	118	216.94	173.27	108.38	103.72
34	132	207.87	173.86	115.69	106.66
35	157	195.15	171.90	124.31	111.55
36	177	186.78	169.32	128.70	114.84
37	196	179.74	166.35	131.57	117.47
38	231	169.54	160.88	133.77	120.59
39	291	156.10	151.90	133.35	122.95
40	351	146.05	144.18	130.89	123.11
41	431	135.67	135.60	126.63	121.47
42	531	125.53	126.72	120.97	117.96
43	652	116.25	118.11	114.42	112.86
44	800	107.30	109.46	107.04	106.31
45	1047	95.93	98.16	96.45	96.25
46	1342	85.18	87.17	85.67	85.62
47	1636	76.45	78.17	76.87	76.84
48	2088	67.29	68.55	67.55	67.59
49	2773	55.66	56.54	55.90	55.94
50	3554	46.96	47.62	47.18	47.20
51	5310	36.90	37.23	37.07	37.14

Cricket Graph Data Temp HY130 w/sn #28 Sun, Jun 4, 1989 12:47 PM

	Time	At 0.5 in	At 1.5 in	At 2.5 in	At 3.25 in
1	0	22.81	22.32	24.07	22.17
2	7	23.01	22.63	24.04	22.02
3	17	23.43	23.60	24.86	22.36
4	22	23.92	23.89	26.62	24.22
5	23	27.60	24.06	27.67	25.48
6	25	64.95	24.15	28.71	27.35
7	26	124.91	24.44	29.84	29.67
8	28	170.65	25.23	30.66	32.26
9	29	213.69	27.09	31.70	35.11
10	31	240.63	30.24	32.62	38.48
11	33	265.24	34.36	34.44	43.77
12	35	281.26	39.84	36.91	52.61
13	37	292.28	46.75	41.48	64.61
14	39	299.18	54.15	46.05	75.00
15	41	303.71	62.27	49.27	81.97
16	43	306.32	69.66	51.79	85.86
17	45	307.95	77.92	53.29	88.12
18	47	308.81	87.83	55.04	89.40
19	49	308.84	96.00	56.33	90.11
20	51	308.22	102.72	57.41	90.57
21	53	306.92	108.77	58.86	90.87
22	55	305.08	114.17	59.82	91.03
23	57	303.08	119.28	60.83	91.06
24	60	299.02	127.57	62.47	91.05
25	69	289.41	143.20	67.84	90.58
26	77	279.59	152.68	73.19	89.75
27	84	269.32	161.10	78.91	89.57
28	92	259.26	166.31	84.63	90.00
29	100	249.46	169.87	90.38	90.98
30	110	238.67	172.11	96.79	92.68
31	120	229.08	173.10	102.56	94.73
32	135	216.62	172.83	109.86	98.09
33	145	209.52	171.99	113.88	100.27
34	165	197.54	169.39	119.83	104.17
35	184	187.78	166.27	124.34	107.40
36	204	179.64	162.95	127.05	109.89
37	233	169.74	158.07	128.73	112.49
38	289	155.85	149.73	129.14	115.25
39	349	144.79	141.97	127.45	115.93
40	409	136.21	135.36	124.86	115.40
41	489	127.17	127.93	120.93	113.60
42	569	118.41	120.32	115.84	110.45
43	748	108.17	110.85	108.38	104.84
44	946	98.47	101.38	99.82	97.41
45	1340	84.16	86.83	85.86	84.14
46	1634	75.90	78.34	77.51	76.04
47	2125	65.06	67.13	66.31	65.31
48	2710	55.63	57.24	56.45	55.87
49	3492	46.80	47.91	47.27	46.97
50	4858	37.23	37.87	37.39	37.37
51					

Cricket Graph Data Strainy: MS #26 w sh+Tcomp Sun, Jun 4, 1989 12:49 PM

	Time #26	At 1.00 in	At 2.00 in	At 3.00 in	At 4.00 in
1	0	4.75	-3.97	-1.96	21.84
2	5	-2.02	-13.16	-15.14	4.88
3	13	16.90	-17.23	28.64	-46.80
4	15	22.50	-52.04	9.22	-36.06
5	17	-16.59	-68.54	50.71	-13.85
6	19	-9.71	-84.84	60.50	-20.75
7	21	18.74	-35.68	71.28	19.81
8	23	75.14	-93.43	66.98	88.14
9	24	164.91	-59.94	112.87	100.55
10	26	261.57	-43.01	142.68	169.21
11	32	785.66	-94.89	237.84	372.14
12	36	768.34	-141.09	331.31	383.28
13	38	758.43	-164.53	338.66	249.31
14	40	739.60	-177.43	337.45	256.93
15	42	724.99	-184.01	434.77	312.30
16	44	717.69	-184.52	429.19	297.41
17	46	761.72	-170.57	444.77	300.78
18	47	944.13	-118.44	472.83	248.83
19	49	1260.05	-37.15	508.31	252.59
20	51	1567.16	46.92	494.33	234.22
21	53	1873.65	72.02	505.11	240.18
22	55	2045.21	110.71	507.31	205.42
23	57	2170.76	73.80	505.57	204.56
24	59	2252.56	-62.65	498.79	173.15
25	61	2290.35	-222.64	511.99	280.98
26	63	2350.80	-217.20	505.38	196.05
27	64	2385.35	-351.53	504.20	192.67
28	66	2403.27	-371.99	505.41	188.80
29	67	2423.40	-579.84	505.46	184.94
30	69	2429.33	-273.14	498.30	182.77
31	74	2374.17	-534.54	471.70	175.26
32	80	2337.64	-891.42	454.79	169.44
33	88	2295.59	-463.45	448.56	173.36
34	96	2253.85	-687.82	446.83	173.23
35	104	2213.21	-701.57	451.49	175.58
36	116	2142.35	-756.79	435.96	187.65
37	126	2087.27	-763.04	459.91	192.33
38	136	2032.63	-739.46	442.65	196.89
39	146	1979.71	-727.51	434.75	201.75
40	166	1882.43	-698.79	391.79	209.57
41	186	1792.11	-690.73	367.12	216.40
42	205	1713.54	-935.45	353.09	221.74
43	230	1627.74	-908.27	319.72	226.28
44	256	1548.34	-988.57	291.90	230.36
45	316	1398.46	-1006.31	253.12	234.66
46	376	1287.50	-1018.75	228.59	235.42
47	456	1177.28	-1033.21	215.05	233.10
48	556	1078.67	-1046.08	198.45	228.04
49	666	999.87	-1055.74	186.33	222.04
50	864	872.89	-1074.19	183.40	205.52
51	1061	765.80	-1091.87	180.09	188.19
52	1356	635.89	-1096.66	174.04	176.05
53	1748	488.22	-1100.23	160.15	156.18
54	2042	399.05	-1106.63	159.32	145.61

Cricket Graph Data Strain (µ) MS #26 w sh+Tcomp Sun, Jun 4, 1989 12:49 PM

	Time #26	At 1.00 in	At 2.00 in	At 3.00 in	At 4.00 in
55	2531	222.49	-1105.89	158.56	128.37
56	3372	108.62	-1123.65	158.45	110.03

Cricket Graph Data　　Strainixi MS #26 w/sh+Tcomp　　Sun, Jun 4, 1989 1:02 PM

	Time #26	At 1.25 in	At 2.25 in	At 3.25 in	At 4.25 in
1	0	-1.89	14.21	-8.11	-10.69
2	5	-5.66	28.65	-27.89	-6.08
3	13	-14.09	28.65	-35.21	21.58
4	15	-21.84	27.70	-59.74	66.05
5	17	-33.06	24.23	-48.07	-7.61
6	19	-68.21	107.50	-42.77	56.58
7	21	-84.84	87.33	0.52	23.66
8	23	-119.74	129.90	69.09	-13.31
9	24	-108.77	162.85	117.10	-338.34
10	26	-35.27	215.47	41.71	-160.10
11	32	-136.90	540.08	7.94	130.41
12	36	-121.40	620.30	43.63	173.87
13	38	13.69	647.56	-21.95	100.31
14	40	102.69	701.97	-28.25	139.07
15	42	171.35	683.67	35.77	265.93
16	44	248.56	677.70	22.18	403.93
17	46	314.41	723.46	14.28	247.10
18	47	383.36	761.13	19.22	378.10
19	49	455.53	684.61	23.08	197.05
20	51	528.74	762.25	32.23	332.96
21	53	645.23	698.67	-3.06	319.27
22	55	807.94	682.84	-11.22	339.07
23	57	960.80	688.61	-11.42	320.15
24	59	1046.16	659.39	-9.96	368.92
25	61	1081.36	532.67	-11.05	378.94
26	63	1099.65	587.54	-2.18	427.17
27	64	1114.52	568.54	0.04	438.18
28	66	1124.06	549.22	2.78	448.72
29	67	1120.78	529.13	6.22	458.92
30	69	1120.33	511.92	8.93	467.75
31	74	918.09	491.67	18.79	492.90
32	80	873.50	449.58	33.94	521.00
33	88	883.10	408.49	62.51	557.99
34	96	902.56	377.68	85.58	581.19
35	104	895.33	349.13	113.13	599.50
36	116	835.29	305.65	161.97	626.56
37	126	809.11	277.66	194.01	637.63
38	136	779.14	256.14	281.91	646.42
39	146	753.12	239.03	236.92	652.00
40	166	714.61	218.30	261.18	658.26
41	186	679.40	210.80	274.94	661.08
42	205	668.18	207.55	282.92	661.71
43	230	662.04	204.55	288.65	661.12
44	256	651.62	200.62	291.12	659.62
45	316	614.67	191.48	290.64	654.69
46	376	568.12	180.30	286.95	650.82
47	456	506.57	168.47	281.21	645.06
48	556	436.39	155.50	273.34	637.52
49	666	374.30	145.94	266.27	631.19
50	864	276.02	128.28	248.77	613.81
51	1061	191.19	111.99	231.23	596.94
52	1356	91.54	102.08	218.66	585.22
53	1748	-16.75	85.68	198.35	565.32
54	2042	-76.22	76.57	188.12	554.44

Cricket Graph Data   Strain(x), MS #26 w/sn-Tcomp   Sun, Jun 4, 1989 [illegible]:02 PM

	Time #26	At 1.25 in	At 2.25 in	At 3.25 in	At 4.25 in
55	2531	-63.79	61.57	170.93	536.93
56	3372	-50.74	46.58	152.09	517.78

Cricket Graph Data   Strain y, HY100 #27 w sn+Tcomp   Sun, Jun 4, 1989 1:02 PM

	Time #27	At 1.00 in	At 2.00 in	At 3.00 in	At 4.00 in
1	0	1.78	3.89	0.64	8.89
2	7	12.75	-5.00	68.63	16.10
3	15	-31.66	30.11	30.65	38.98
4	22	-36.29	93.97	70.49	26.53
5	23	-41.98	127.02	31.34	-29.40
6	25	59.01	157.61	-31.82	-218.56
7	27	117.13	199.90	-55.68	-399.60
8	28	227.02	218.04	-38.33	-261.35
9	30	375.81	292.72	74.59	-125.47
10	32	644.57	419.25	116.19	-23.91
11	33	796.57	532.14	190.41	66.13
12	35	865.06	627.15	234.81	125.05
13	37	858.61	705.26	263.08	175.79
14	38	807.45	785.12	328.08	216.07
15	40	749.35	845.20	356.06	246.57
16	42	725.77	891.22	327.43	279.86
17	44	721.61	920.48	388.68	317.11
18	46	773.67	941.67	472.67	336.24
19	48	980.84	950.22	462.78	336.72
20	52	1511.92	926.13	427.28	369.07
21	54	1654.59	909.76	493.74	380.06
22	56	1735.06	885.92	461.36	402.32
23	58	1915.76	863.33	461.71	414.80
24	60	1951.77	817.68	532.67	428.05
25	62	1979.35	797.82	506.50	438.38
26	65	2053.53	746.44	511.77	456.53
27	68	2100.41	698.98	513.23	473.04
28	71	2131.58	658.43	511.69	488.77
29	73	2059.25	637.56	510.44	495.59
30	78	1934.64	596.72	501.29	515.52
31	84	1881.03	537.75	482.04	537.59
32	99	1803.74	455.84	416.88	575.88
33	118	1732.83	389.68	361.62	597.48
34	132	1686.69	389.98	335.39	603.02
35	157	1606.91	480.09	285.50	603.80
36	177	1542.86	576.05	255.10	603.19
37	196	1482.19	643.75	227.64	596.78
38	231	1382.04	693.75	193.92	587.37
39	291	1208.73	694.02	161.12	576.60
40	351	1089.78	676.33	143.29	567.63
41	431	976.78	659.29	128.80	557.89
42	531	873.15	646.44	117.79	548.23
43	652	776.79	637.72	109.75	540.29
44	800	674.97	629.65	102.59	533.19
45	1047	525.93	613.62	87.99	517.15
46	1342	382.19	599.08	76.24	502.93
47	1636	264.51	586.55	65.81	489.36
48	2088	143.99	580.73	62.26	481.37
49	2773	-5.31	582.59	67.29	480.36
50	3554	-138.11	569.05	56.18	463.47
51	5310	-273.96	556.73	46.31	443.84

Cricket Graph Data Strain vs. HY100 #27 w/sh+Tcomp Sun, Jun 4, 1989 1:03 PM

	Time #27	At 1.25 in	At 2.25 in	At 3.25 in	At 4.25 in
1	0	-2.11	1.46	-1.04	1.72
2	7	-3.95	-22.95	7.07	-15.92
3	15	-5.41	-32.89	-64.00	-55.78
4	22	-49.84	-77.62	-44.40	-85.21
5	23	-81.84	-74.16	-12.29	-53.63
6	25	-34.54	-65.41	31.88	-46.18
7	27	-28.51	-29.38	50.12	14.06
8	28	88.67	-7.36	-30.10	77.79
9	30	65.94	-20.13	-99.04	172.72
10	32	58.21	-49.06	-123.36	247.88
11	33	-4.28	-69.17	-77.69	292.85
12	35	-42.35	-82.26	-54.68	317.32
13	37	-46.43	-128.90	-33.06	335.99
14	38	-32.91	-147.26	-34.73	326.90
15	40	54.51	-169.43	-8.35	323.86
16	42	47.76	-186.50	-16.32	337.40
17	44	88.27	-191.10	-23.28	319.30
18	46	107.40	-188.41	-34.61	309.49
19	48	131.34	-189.79	-11.36	302.49
20	52	251.16	-178.36	-25.03	285.96
21	54	339.24	-170.31	-14.01	261.29
22	56	555.89	-174.81	-23.80	308.52
23	58	626.87	-154.84	-12.98	247.62
24	60	636.67	-122.30	-13.67	245.32
25	62	524.31	-106.10	-13.26	239.65
26	65	309.70	-82.45	-12.49	229.72
27	68	326.89	-60.48	-10.67	220.05
28	71	339.39	-37.05	-8.90	211.81
29	73	346.20	-29.35	-7.52	207.73
30	78	183.39	13.95	-3.89	196.83
31	84	157.76	53.98	4.82	184.75
32	99	302.57	178.57	34.39	165.97
33	118	276.30	253.23	83.80	156.94
34	132	196.64	292.80	124.86	155.30
35	157	130.26	336.99	172.50	159.37
36	177	106.22	351.21	198.19	167.85
37	196	82.99	360.16	211.71	171.23
38	231	43.91	366.88	225.09	176.66
39	291	-40.71	388.97	230.72	182.39
40	351	-131.95	343.70	228.61	184.24
41	431	-242.08	323.55	221.89	184.75
42	531	-362.02	308.32	214.32	183.63
43	652	-484.45	297.84	207.68	182.64
44	800	-600.81	303.77	200.04	179.55
45	1047	-764.41	284.79	183.51	167.27
46	1342	-911.19	269.29	167.74	155.91
47	1636	-1027.31	256.69	154.32	144.91
48	2088	-1133.20	249.78	146.92	140.80
49	2773	-1253.59	251.48	146.99	145.90
50	3554	-1375.71	236.05	131.25	135.26
51	5310	-1484.73	223.71	116.45	127.65

Cricket Graph Data　　Strain y, HY130 #28 w sn+Tcomp　　Sun, Jun 4, 1989 1:04 PM

	Time #28	At 1.00 in	At 2.00 in	At 3.00 in	At 4.00 in
1	0	56.16	20.55	7.12	8.36
2	7	53.88	24.85	26.06	19.59
3	17	-12.59	21.24	48.26	51.20
4	22	2.33	109.82	69.98	47.51
5	23	41.74	145.04	80.34	11.15
6	25	163.31	194.70	64.18	-87.45
7	26	290.74	249.85	53.82	-322.72
8	28	404.73	262.28	32.84	-389.01
9	29	621.16	321.37	77.19	-263.29
10	31	321.17	383.06	170.04	-79.81
11	33	178.03	553.12	198.25	29.33
12	35	204.36	723.54	302.58	98.32
13	37	189.65	777.49	342.69	157.82
14	39	150.53	897.82	379.66	213.07
15	41	302.30	970.27	439.91	248.59
16	43	490.13	1022.68	467.89	279.54
17	45	639.05	1059.47	462.15	304.19
18	47	713.28	1105.49	518.06	271.40
19	49	852.49	1093.94	519.69	348.09
20	51	841.35	1107.20	485.78	377.00
21	53	775.94	1062.77	547.77	386.81
22	55	622.31	1054.09	553.15	400.18
23	57	492.83	1019.22	571.34	411.56
24	60	569.50	963.28	568.41	439.37
25	69	513.19	814.07	577.11	485.69
26	77	484.16	695.68	571.62	522.48
27	84	500.95	603.61	536.01	552.02
28	92	533.39	531.44	499.85	575.81
29	100	527.86	468.94	462.70	595.36
30	110	507.60	409.66	415.86	615.59
31	120	483.59	366.48	374.70	624.29
32	135	438.07	324.62	318.15	641.15
33	145	406.35	305.04	288.25	644.50
34	165	347.33	285.87	244.58	648.00
35	184	289.88	265.88	211.44	643.88
36	204	231.48	244.87	184.56	636.53
37	233	153.20	228.54	154.76	625.95
38	289	22.56	186.39	121.64	608.39
39	349	751.57	177.73	111.51	601.42
40	409	632.75	167.66	100.28	589.78
41	489	522.62	160.22	91.01	577.69
42	589	521.73	157.37	83.13	565.05
43	748	386.34	152.64	76.77	552.02
44	946	251.56	144.59	67.20	537.13
45	1340	147.78	138.66	61.50	522.79
46	1634	58.58	134.89	56.81	513.01
47	2125	-60.14	127.07	51.08	498.30
48	2710	-164.59	125.23	49.16	489.26
49	3492	-264.58	121.05	45.69	478.21
50	4858	-355.59	114.79	39.33	464.90
51	7198	-408.80	114.51	38.47	458.34

Cricket Graph Data Strain x HY130 #28 w sn+Tcomp Sun, Jun 4, 1989 1:05 PM

	Time #28	At 1.25 in	At 2.25 in	At 3.25 in	At 4.25 in
1	0	0.86	-15.25	17.35	-1.58
2	7	-5.67	-12.02	-17.46	-12.95
3	17	-20.84	-89.13	-77.15	-68.04
4	22	-174.45	-100.33	-64.78	-99.13
5	23	-117.09	-110.45	-47.40	-62.51
6	25	-102.10	-96.21	1.01	-47.91
7	26	17.57	-57.90	54.40	-17.50
8	28	80.55	-8.73	46.20	86.20
9	29	61.23	-94.73	35.93	188.95
10	31	14.20	-94.02	-36.49	276.27
11	33	-93.41	-76.27	-52.54	335.19
12	35	-87.92	-124.45	-76.36	375.20
13	37	-42.90	-169.21	-64.02	409.60
14	39	39.21	-157.76	-91.11	413.29
15	41	136.39	-244.35	-136.89	401.52
16	43	284.32	-218.59	-108.91	384.96
17	45	399.11	-233.48	-102.12	377.64
18	47	530.81	-220.86	-122.87	364.95
19	49	692.17	-198.49	-127.79	357.82
20	51	884.94	-248.38	-117.78	334.86
21	53	1004.26	-174.76	-162.24	321.79
22	55	1318.40	-253.02	-119.60	313.24
23	57	1464.36	-128.71	-129.48	303.28
24	60	1457.58	-152.61	-148.68	301.35
25	69	916.84	-96.71	-97.47	264.35
26	77	740.37	-44.93	-67.29	244.76
27	84	1063.97	6.05	-51.16	228.92
28	92	1348.06	70.08	-23.81	216.53
29	100	1387.86	121.24	9.04	207.06
30	110	1434.81	165.34	45.16	200.23
31	120	1458.95	196.47	77.19	190.12
32	135	1463.98	230.77	117.38	188.99
33	145	1448.34	246.84	142.03	185.84
34	165	1406.99	267.73	187.25	183.65
35	184.	1361.55	278.67	221.36	181.36
36	204	1306.47	283.77	244.34	178.92
37	233	1229.83	284.28	262.54	180.60
38	289	1106.24	272.58	273.79	188.13
39	349	997.88	268.10	283.12	205.92
40	409	906.79	257.55	279.44	212.31
41	489	805.34	246.16	273.93	217.33
42	589	709.29	238.46	266.55	218.73
43	748	586.12	228.77	257.26	218.36
44	946	468.94	217.55	244.02	211.31
45	1340	304.51	209.45	230.02	203.90
46	1634	207.15	204.35	219.83	197.14
47	2125	76.62	195.45	205.53	185.81
48	2710	-36.76	191.60	196.25	179.61
49	3492	-145.76	185.90	185.31	171.29
50	4858	-256.03	177.37	172.00	160.73
51	7198	-315.80	175.07	165.23	156.30

Cricket Graph Data　Strain (µ) MS #26 sn w/o Tcomp　Sun, Jun 4, 1989 1:06 PM

	Time#26 w/o	At 1.00 in	At 2.00in	At 3.00 in	At 4.00 in
1	0	4.50	-3.72	-2.21	21.59
2	5	-2.27	-13.41	-15.39	4.63
3	13	-17.15	16.98	28.39	-47.04
4	15	-22.75	-52.29	3.72	-41.56
5	17	-16.34	-68.79	38.21	-26.35
6	19	-9.96	-85.09	39.20	42.05
7	21	18.49	-95.93	27.29	-24.19
8	23	74.89	-93.68	1.98	23.14
9	24	164.66	-59.94	37.37	25.05
10	26	261.32	-43.26	60.18	86.71
11	32	785.41	-95.14	151.84	286.14
12	36	762.84	-141.34	245.37	297.28
13	38	683.43	-164.78	333.16	243.81
14	40	639.61	-177.68	224.95	244.43
15	42	624.99	-196.51	345.27	222.80
16	44	617.69	-204.02	343.19	211.41
17	46	661.72	-200.57	358.76	214.78
18	47	844.13	-148.44	386.83	162.38
19	49	1160.05	-74.15	422.31	166.60
20	51	1467.17	9.92	408.33	148.22
21	53	1773.66	35.02	419.11	154.18
22	55	1945.21	63.21	421.31	119.42
23	57	2070.46	263.05	419.57	118.56
24	59	2152.56	-110.15	412.79	87.15
25	61	2190.35	-277.14	425.90	194.97
26	63	2250.81	-264.70	419.98	110.05
27	64	2285.34	-396.03	418.20	106.67
28	66	2303.27	-419.49	419.41	102.80
29	67	2323.20	-627.34	419.46	98.94
30	69	2329.33	-320.64	412.29	96.77
31	74	2274.17	-610.04	385.70	89.26
32	80	2237.64	-973.92	368.79	83.87
33	88	2195.59	-549.45	355.56	80.36
34	96	2153.84	-780.82	353.83	80.23
35	104	2113.21	-801.56	358.49	92.58
36	116	2042.35	-856.79	335.96	87.65
37	126	1987.27	-863.04	359.91	92.33
38	136	1932.63	-839.45	342.65	96.89
39	146	1879.71	-827.50	334.75	101.75
40	166	1782.43	-798.78	291.79	109.57
41	186	1692.11	-790.37	267.12	116.40
42	205	1613.54	-1035.45	253.09	121.74
43	230	1527.74	-1082.73	219.72	126.27
44	256	1448.34	-1088.57	191.89	130.35
45	315	1298.46	-1106.32	153.12	134.66
46	326	1187.50	-1118.75	128.58	135.42
47	456	1077.28	-1133.20	115.05	133.10
48	556	978.67	-1146.08	98.45	128.04
49	666	899.87	-1155.75	86.33	122.04
50	864	779.89	-1167.19	197.26	112.52
51	1061	683.30	-1174.47	119.99	105.69
52	1356	560.39	-1172.16	98.54	100.55
53	1748	430.22	-1158.23	102.15	98.18
54	2042	351.55	-1154.13	124.83	98.11

Cricket Graph Data Strain y, MS #26 sn w/o Tcomp Sun, Jun 4, 1989 [illegible] PM

	Time#26 w/o	At 1.00 in	At 2.00in	At 3.00 in	At 4.00 in
55	2531	192.50	-1135.89	223.65	98.37
56	3322	96.12	-1136.16	324.75	97.53
57	4544	-4.68	-1133.43	502.34	93.79
58	6164	-68.90	-1134.21		88.53
59	8991	-116.74	-1131.97		81.65

Pocket Graph Data Strain x MS #26 sn w/o Tcomp Sun Jun 4, 1989 [illegible] PM

	Time#26 w/o	At 1.25 in	At 2.25 in	At 3.25 in	At 4.25 in
1	0	-1.64	1.40	-8.36	-10.94
2	5	-5.91	28	-2.81	-6.34
3	13	-14.34	28.40	-35.46	21.33
4	15	-22.09	27.45	-65.24	60.55
5	17	-33.31	23.98	-60.57	-20.11
6	19	-68.46	107.25	-64.07	35.28
7	21	-85.09	87.08	-43.48	-20.34
8	23	-119.99	129.65	4.09	-78.31
9	24	-109.02	162.60	41.60	-413.80
10	26	-35.52	215.22	-40.79	-242.60
11	32	-137.15	539.83	-78.06	44.41
12	36	-126.90	620.05	-42.37	87.87
13	38	-61.81	641.31	-27.45	94.81
14	40	2.69	701.72	-40.75	126.57
15	42	71.35	671.17	-53.73	175.93
16	44	148.56	658.20	-63.82	317.93
17	46	214.41	693.46	-71.72	161.10
18	47	283.36	731.13	-66.78	292.10
19	49	355.53	647.61	-62.92	111.05
20	51	428.74	725.25	-53.77	246.96
21	53	545.23	661.68	-82.94	233.27
22	55	707.93	635.34	-97.22	253.07
23	57	860.80	641.11	-97.42	234.15
24	59	946.16	611.89	-95.96	282.92
25	61	981.36	478.17	-97.05	292.95
26	63	999.65	540.04	-88.18	341.17
27	64	1014.52	521.04	-85.36	352.18
28	66	1024.06	501.72	-83.22	362.72
29	67	1020.77	481.63	-79.78	372.92
30	69	1020.33	464.42	-77.07	381.75
31	74	818.09	416.17	-67.21	406.90
32	80	773.50	366.98	-52.06	435.00
33	88	783.10	322.49	-30.48	464.99
34	96	802.56	284.68	-7.42	488.19
35	104	795.33	249.13	20.13	506.50
36	116	735.29	205.64	61.96	526.56
37	126	701.11	171.66	94.01	537.64
38	136	679.14	156.14	118.92	546.42
39	146	653.12	139.03	136.92	551.99
40	166	614.61	118.29	161.18	558.26
41	186	579.40	110.80	174.94	561.08
42	205	568.18	107.55	182.92	561.71
43	230	562.03	104.55	188.65	561.12
44	256	551.61	100.62	191.12	559.62
45	315	514.67	91.48	190.64	554.69
46	326	468.11	80.30	186.95	550.82
47	456	406.57	68.47	181.21	545.06
48	556	336.39	55.49	173.34	537.52
49	666	274.30	45.94	166.27	531.19
50	864	183.02	35.28	155.77	520.80
51	1061	108.69	29.48	148.72	514.44
52	1356	16.04	26.57	143.16	509.73
53	1748	-74.25	27.69	140.35	507.32
54	2042	-123.72	29.07	140.62	506.94

Cricket Graph Data   Strain (MS #26 sh w/o Tcomp   Sun Jun 4 1989

	Time#26 w/o	At 1.25 in	At 2.25 in	At 3.25 in	At 4.25 in
55	2531	-33.79	31.57	140.93	506.93
56	3322	-63.24	34.08	139.59	505.29
57	4544	-88.02	33.78	135.61	501.51
58	6164	-94.94	30.78	130.00	495.85
59	8931	-71.00	25.54	123.02	488.06

Cricket Graph Data   Strain(y): HY100#27 sn w/oTcomp   Sun Jun 4 1989 1:09 PM

	Time#27 w/o	At 1.00 in	At 2.00 in	At 3.00 in	At 4.00 in
1	0	1.53	.36	.39	8.64
2	7	12.51	-5.26	68.38	15.85
3	15	-31.91	29.86	30.40	38.73
4	22	-36.54	93.72	70.25	26.28
5	23	-42.23	126.77	31.09	-29.65
6	25	58.76	157.36	-32.07	-218.81
7	27	104.63	199.65	-55.93	-39.98
8	28	169.02	217.79	-38.58	-261.59
9	30	334.56	292.47	69.09	-130.97
10	32	544.57	413.75	110.69	-29.41
11	33	696.57	526.64	160.41	36.13
12	35	765.05	614.69	187.31	77.55
13	37	758.61	699.76	198.08	110.79
14	38	707.45	772.62	252.58	140.57
15	40	649.35	833.69	273.56	164.07
16	42	625.77	873.42	282.63	192.06
17	44	621.61	900.97	295.68	224.11
18	46	673.67	911.67	379.67	243.23
19	48	880.84	920.23	369.78	243.72
20	52	1411.92	896.13	334.28	276.07
21	54	1554.59	879.86	400.74	287.06
22	56	1635.09	850.62	368.36	309.31
23	58	1815.76	828.03	368.71	321.80
24	60	1851.74	782.38	439.67	335.05
25	62	1879.35	750.31	413.50	345.38
26	65	1950.53	698.94	418.77	363.53
27	68	2000.42	651.48	420.23	380.00
28	71	2031.58	607.43	418.69	395.77
29	73	1959.25	586.56	417.44	402.59
30	78	1834.64	531.72	408.29	422.52
31	84	1781.03	472.74	389.04	444.60
32	99	1703.74	362.84	323.88	482.88
33	118	1632.83	296.68	268.62	504.48
34	132	1586.69	290.00	242.29	510.02
35	157	1506.91	380.09	190.50	508.80
36	177	1442.86	476.05	155.10	503.19
37	196	1382.19	543.75	127.56	496.78
38	231	1282.04	593.75	93.92	487.37
39	291	1108.73	594.02	61.11	476.60
40	351	988.78	576.33	43.29	467.63
41	431	876.68	559.29	28.80	457.89
42	531	773.16	546.44	17.79	448.23
43	652	676.79	537.72	9.75	440.29
44	800	577.97	532.65	5.59	436.18
45	1047	442.43	531.12	5.48	434.65
46	1342	317.19	534.08	11.24	437.93
47	1636	217.02	539.05	18.31	441.86
48	2088	108.62	545.07	26.96	446.07
49	2773	-35.31	552.59	37.29	450.36
50	3554	-150.61	556.55	43.68	450.97
51	5310	-274.21	556.48	46.09	443.59
52	6479	-313.13	555.17	45.07	438.37
53	8039	-331.53	553.70	44.11	434.92

Cricket Graph Data Strain (x), HY100#27 sn w oTcomp Sun, Jun 4, 1989 1:09 PM

	Time#27 w o	At 1.25 in	At 2.25 in	At 3.25 in	At 4.25 in
1	0	-2.37	1.21	-12.94	14.75
2	7	-4.20	-23.20	6.82	-1.62
3	15	-5.66	-33.14	-64.25	-56.03
4	22	-50.09	-77.87	-44.65	-85.46
5	23	-81.73	-74.41	-12.54	-53.88
6	25	-84.79	-65.66	32.13	-46.43
7	27	-41.01	-29.63	49.87	13.81
8	28	30.67	-7.61	-30.35	7.75
9	30	24.69	-20.39	-104.54	167.22
10	32	-41.79	-54.56	-128.86	242.38
11	33	-104.28	-74.67	-107.69	262.85
12	35	-142.35	-94.76	-102.18	269.82
13	37	-146.44	-139.40	-98.06	270.98
14	38	-132.91	-159.76	-110.23	251.39
15	40	-45.49	-181.93	-90.85	241.36
16	42	-52.24	-204.30	-104.12	249.60
17	44	-11.73	-210.60	-116.28	226.30
18	46	7.40	-218.41	-58.39	216.19
19	48	31.34	-219.79	-104.36	209.59
20	52	151.16	-208.36	-118.03	192.96
21	54	239.24	-200.31	-106.01	168.29
22	56	455.88	-210.11	-116.80	215.52
23	58	526.87	-190.14	-105.99	154.62
24	60	536.67	-157.60	-106.67	152.32
25	62	424.31	-153.59	-106.26	146.65
26	65	209.70	-129.94	-105.50	136.71
27	68	226.89	-107.98	-103.67	127.05
28	71	239.39	-88.05	-101.90	118.81
29	73	246.20	-80.34	-100.52	114.73
30	78	83.39	-51.05	-96.88	103.83
31	84	57.76	-11.02	-88.18	91.75
32	99	202.57	85.58	-58.60	73.00
33	118	176.30	160.24	-92.00	63.94
34	132	96.64	192.80	31.86	62.30
35	157	30.25	236.99	77.50	64.37
36	177	6.22	251.21	98.09	67.95
37	196	-17.01	260.61	111.71	71.23
38	231	-56.09	266.88	125.09	76.66
39	291	-140.71	288.97	130.72	82.39
40	351	-231.95	243.70	128.61	84.24
41	431	-342.09	223.55	121.89	84.75
42	531	-462.02	208.32	114.32	83.63
43	652	-584.45	197.84	107.68	82.64
44	800	-700.81	206.78	103.04	82.55
45	1047	-846.91	202.29	101.01	84.76
46	1342	-976.19	204.29	102.74	90.91
47	1636	-1074.81	209.19	106.82	97.41
48	2088	-1168.60	214.48	111.62	105.50
49	2773	-1283.59	221.48	116.99	115.91
50	3554	-1388.21	224.35	118.75	122.76
51	5310	-1484.95	223.46	116.21	127.40
52	6479	-1507.77	221.49	113.67	127.61
53	8039	-1522.36	219.60	112.04	127.00

Cricket Graph Data Strain(y) HY130 #28 sn w/oTcomp Sun, Jun 4, 1989 [illegible] PM

	Time#28 w/o	At 1.00 in	At 2.00 in	At 3.00 in	At 4.00 in
1	0	54.16	18.55	5.12	6.36
2	7	51.87	22.85	24.06	17.59
3	17	-14.59	29.24	50.26	49.20
4	22	83	107.81	50.26	47.51
5	23	43.74	145.04	82.34	11.15
6	25	126.21	194.70	66.18	85.45
7	26	190.74	249.85	55.82	-330.72
8	28	304.73	262.28	34.84	-391.01
9	29	521.16	323.37	75.19	-265.29
10	31	-221.17	381.06	168.04	-83.81
11	33	-78.03	551.12	196.25	22.32
12	35	-104.36	723.54	300.58	80.32
13	37	-89.65	767.50	335.69	122.82
14	39	50.53	876.82	370.66	158.07
15	41	202.30	938.27	423.91	186.59
16	43	390.13	977.68	449.88	209.54
17	45	539.05	1001.47	442.15	233.19
18	47	613.28	1035.49	497.06	197.40
19	49	752.49	1014.94	496.69	273.09
20	51	741.35	1017.19	462.78	302.00
21	53	675.94	967.77	520.77	311.81
22	55	522.32	959.09	526.15	325.18
23	57	392.83	919.93	541.34	336.56
24	60	469.50	863.28	538.41	364.37
25	61	413.19	714.07	536.11	410.70
26	77	384.16	595.67	513.62	448.47
27	84	400.59	503.61	478.01	478.02
28	92	433.39	431.44	434.85	501.81
29	100	427.86	368.94	387.70	520.36
30	110	407.59	309.66	332.86	536.59
31	120	383.59	266.47	284.70	547.29
32	135	338.07	224.62	223.15	555.15
33	145	306.35	205.04	191.25	556.50
34	165	247.33	185.87	144.58	554.99
35	184	189.88	165.87	111.44	548.98
36	204	131.48	144.87	84.56	541.52
37	233	53.20	118.54	54.76	528.95
38	289	-77.44	86.39	21.64	509.39
39	349	651.57	77.73	11.51	502.42
40	409	532.75	67.66	28	490.78
41	489	422.62	60.22	-8.99	479.69
42	589	421.73	57.37	-14.87	470.05
43	748	291.24	55.64	-18.63	460.02
44	946	166.56	58.59	-17.80	454.13
45	1340	78.78	68.66	-8.50	453.79
46	1634	3.58	76.89	-.19	456.01
47	2125	-98.16	89.07	13.08	460.30
48	2710	-189.59	100.23	24.16	464.26
49	3492	-277.58	108.04	32.68	465.21
50	4858	-357.59	112.80	37.33	462.89
51	7198	-410.80	112.51	36.47	456.34

Cricket Graph Data Strain (%) HY130 #28 sn w/oTcomp Sun, Jun 4, 1989 1:12 PM

	Time#28 w/o	At 1.25 in	At 2.25 in	At 3.25 in	At 4.25 in
1	0	-11.14	1.73	15.35	-3.57
2	7	-17.67	-14.02	-19.47	-14.95
3	17	-22.34	-91.13	-79.15	-70.04
4	22	-76.46	-102.33	-62.78	-99.13
5	23	-115.10	-110.45	-45.40	-62.51
6	25	-139.10	-96.21	3.01	-45.91
7	26	-82.43	-57.90	56.40	-15.50
8	28	-19.45	-8.73	48.20	84.20
9	29	-38.77	-92.73	33.93	186.95
10	31	-85.80	-96.02	-38.50	272.27
11	33	-193.41	-78.27	-54.54	328.19
12	35	-187.92	-124.45	-78.36	357.20
13	37	-143.00	-179.21	-71.02	374.60
14	39	-60.79	-178.76	-100.11	358.28
15	41	36.39	-276.35	-152.89	339.52
16	43	184.32	-263.58	-126.91	314.96
17	45	299.11	-291.47	-122.12	306.64
18	47	430.81	-290.86	-143.87	290.95
19	49	592.17	-277.49	-150.79	282.82
20	51	784.44	-338.38	-140.78	259.86
21	53	994.26	-269.76	-189.23	246.79
22	55	1218.40	-348.02	-146.60	238.23
23	57	1364.36	-228.71	-159.48	228.28
24	60	1378.57	-252.61	-178.69	226.35
25	61	816.85	-196.71	-138.48	189.34
26	77	640.37	-144.93	-125.29	170.76
27	84	963.97	-93.95	-109.16	154.92
28	92	1248.06	-29.92	-88.81	142.53
29	100	1287.86	21.24	-65.96	132.06
30	110	1334.81	65.34	-37.84	121.23
31	120	1358.95	96.47	-12.81	113.12
32	135	1363.98	130.77	22.38	102.99
33	145	1348.34	146.84	45.03	97.85
34	165	1307.00	167.73	87.25	90.65
35	184	1261.55	178.67	121.36	86.36
36	204	1206.47	183.77	144.34	83.92
37	233	1129.83	184.28	162.54	83.60
38	289	1006.24	172.58	173.79	89.13
39	349	897.88	168.09	183.62	106.92
40	409	806.79	157.55	179.44	113.30
41	489	705.33	146.16	173.93	119.33
42	589	609.29	138.46	168.55	123.73
43	748	491.12	131.77	162.26	126.36
44	946	383.94	131.55	159.02	128.31
45	1340	235.51	139.45	160.02	134.89
46	1634	152.15	146.35	162.83	140.14
47	2125	38.61	157.45	167.53	147.81
48	2710	-61.76	166.60	171.25	154.61
49	3492	-158.76	173.00	172.31	158.29
50	4858	-258.03	175.37	169.98	158.73
51	7198	-317.80	173.07	163.23	154.30

Appendix 3
Strain Gages

Strain gages are devices fitted to material that actually measure the movement of the material in either expansion or contraction. Since their output is an analog representation of the actual materiel movement conversion is not necessary.

The type of strain gage selected for this investigation was the XY 11 produced by Hottinger Baldwin Messtechnik, Company (HBM). This strain gage was recommended for use on steel.Although the XY11 only measures surface strain, it was considered adequate for this experimental investigation since the thickness of all the test plates was one half inch. A special residual stress type of strain gage was considered but it was not cost effective. A Z -70 quick drying room temperature curing cement was used for mounting the strain gages.

Strain Gage Functioning[23]

A strain gage delivers strain (ε) as an output signal proportional to the input. It function basically is the strain effect on electrical conductors first discovered by Wheatstone in 1943 and researched by Thompson in 1856.

[23] Hoffman, K., "The Strain Gauge, A Universal Tool of the Equipmental Stress Analysis", HBM vd. 73004e, printed in West Germany, 1989.

If stressed resistance (R) changes with a ratio $\frac{\Delta R}{R_0}$. If mechanically stressed length changes by $\varepsilon = \frac{\Delta L}{L_0}$. The change in resistance depend on both the geometry change and conductivity (ρ) described by:

$$\frac{\Delta R}{R_0} = \varepsilon\left[(1 + 2_\mu) + \left(\frac{d\rho}{d\varepsilon} \cdot \frac{1}{\rho}\right)\right]$$

Geometry Texture (Conductivity)

Recall that resistance (R) for any conductor is a function of conductivity (ρ), length (L), and area cross - section: $R = \frac{\rho L}{A}$. Material with stable resistance characteristics are preferred for strain gages. Constanton, A Ni- Cu alloy is one of the best known materials for a linear relationship between strain and resistance change: $\frac{\Delta R}{R_0} = \varepsilon \cdot k$ $\quad$ k = gage factor.

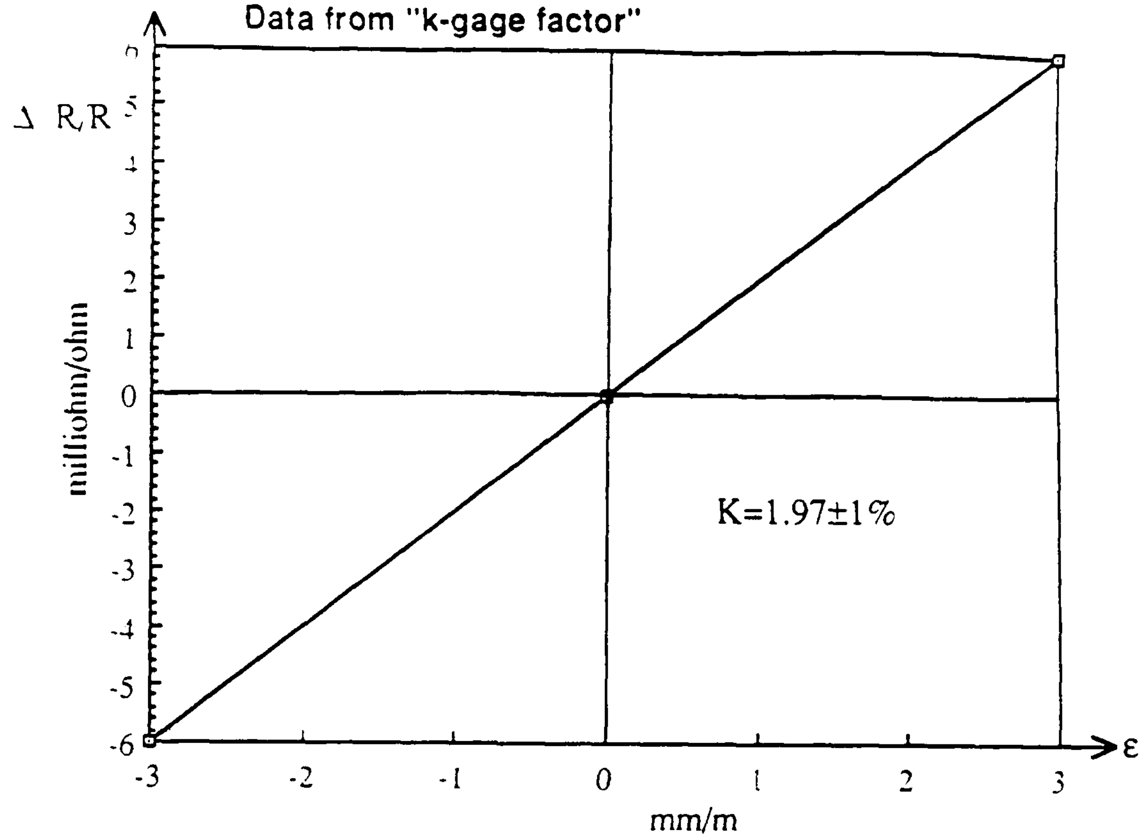

The strain is the measured value $\varepsilon = \frac{\frac{\Delta R}{R}}{k}$. For use in the welding process a temperature compensation chart is also used to correct the measured strain value and eliminate the temperature effects on the strain age itself.

Temperature Compensation Graph for the XY 11:

$$\varepsilon_{READ} - \varepsilon_{COMPENSATION\ VALUE} = \varepsilon_{ACTUAL}$$

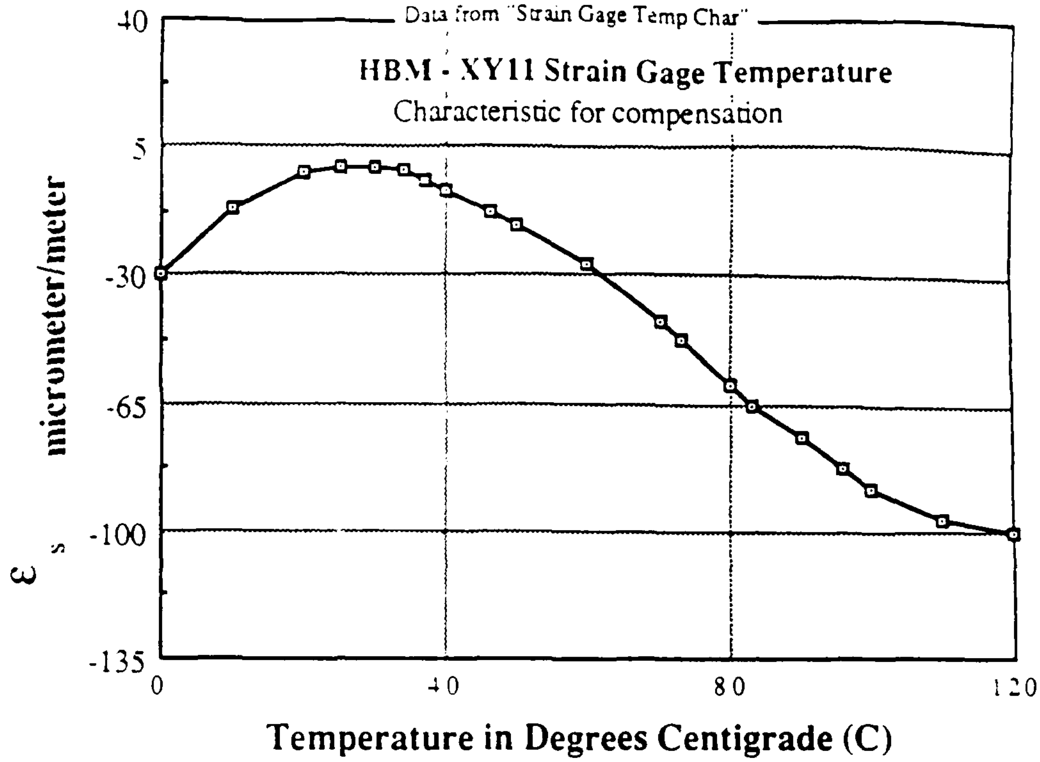

Adjust the strain reading by this chart. For example, if the strain reading was 1000 at 120°C, then the actual compensated reading is 1120.

HBM 3/350 XY 11	Specifications
Resistance	350Ω ± .35%
Gage Factor (k)	1.97 ± 1%
Temperature Coefficient of Gage Factor	$\frac{95\ \text{ppm}}{1^\circ\text{K}}$
Temperature Compensated For Steel	$\alpha = \frac{11\ \text{ppm}}{1^\circ\text{K}}$

Part number	213.18 - 2204
Foil Lot	A258/25
Lot Number	EV(55998700.2)

HBM - XY11 Strain Gage

2 Dimensional

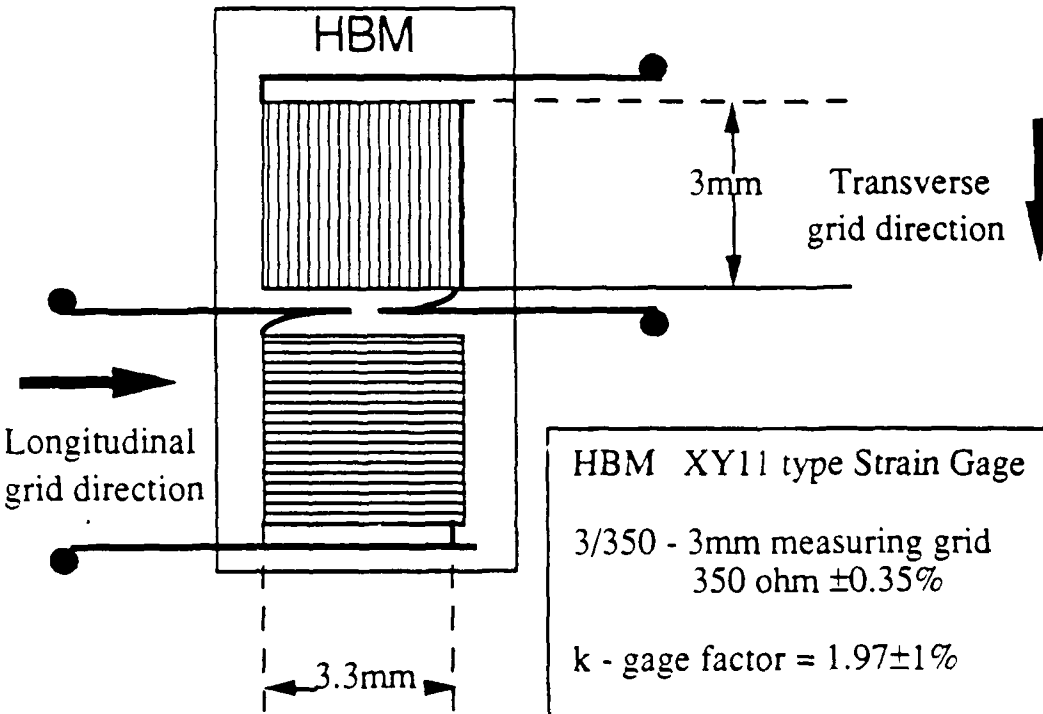

HBM XY11 type Strain Gage

3/350 - 3mm measuring grid
350 ohm ±0.35%

k - gage factor = 1.97±1%

α = 11ppm/°K or 6.1ppm/°F
Temperature Compensation
for Steels

Temperature Coefficient
=95ppm/°K

The above XY11 strain gage is specifically calibrated for use on steel.

Recommended Adhesives:

Z70: Room temperature curing single component cement. This adhesive requires a smooth surface and not more than 120°C ambient temperature for a one minute curing time (works like super glue!)

X60: Room temperature cure, F - 24 hours, maximum ambient temperature 80°C.

EP250: High temperature curing two component, maximum ambient temperature 250 degrees C.

EP 310: High temperature cure, two component, 310°C maximum ambient temperature.

In this investigation, Z70 was used to mount strain gages.

$$XY\ 11 \quad \alpha = 11 \times \frac{10^{-6}}{^{\circ}K} \quad \frac{3}{350} = 3\text{mm grid and } 350\Omega$$

All strain gages were mounted so the longitudinal strain was on top hence the strain gage orientation on the test plates is shown below.:

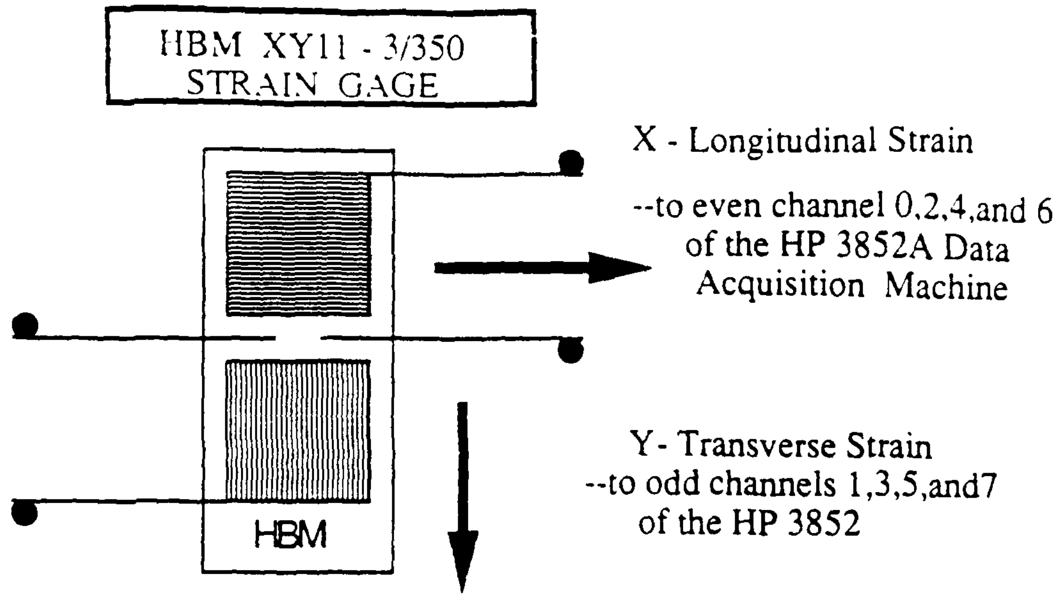

In experiment #3 before any full series of tests was started, Y11 strain gages were mounted on the test piece. The Y11 strain gage has the same specifications as the XY11, except the Y11 is a one dimensional strain gage as shown in the following figure:

HBM - Y11 STRAIN GAGE
One Dimension

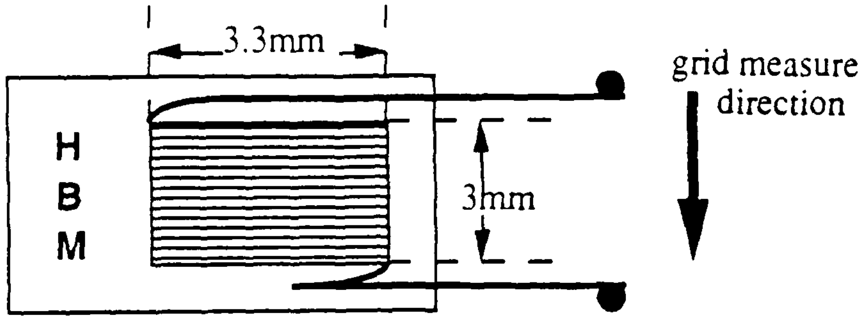

HBM - Y11 Strain Gage

3/350 - 3mm measureing grid
350 ohm ±0.35%
k-gage factor = 1.97±1%
α = 11ppm/°K or 6.1ppm/°F
TemperatureCompensation
for Steels

In experiment #3 the Y11 strain gages were all mounted to measure longitudinal strain.This was the only test that Y11 type strain gages were used. A block diagram of the test set up follows in figure :

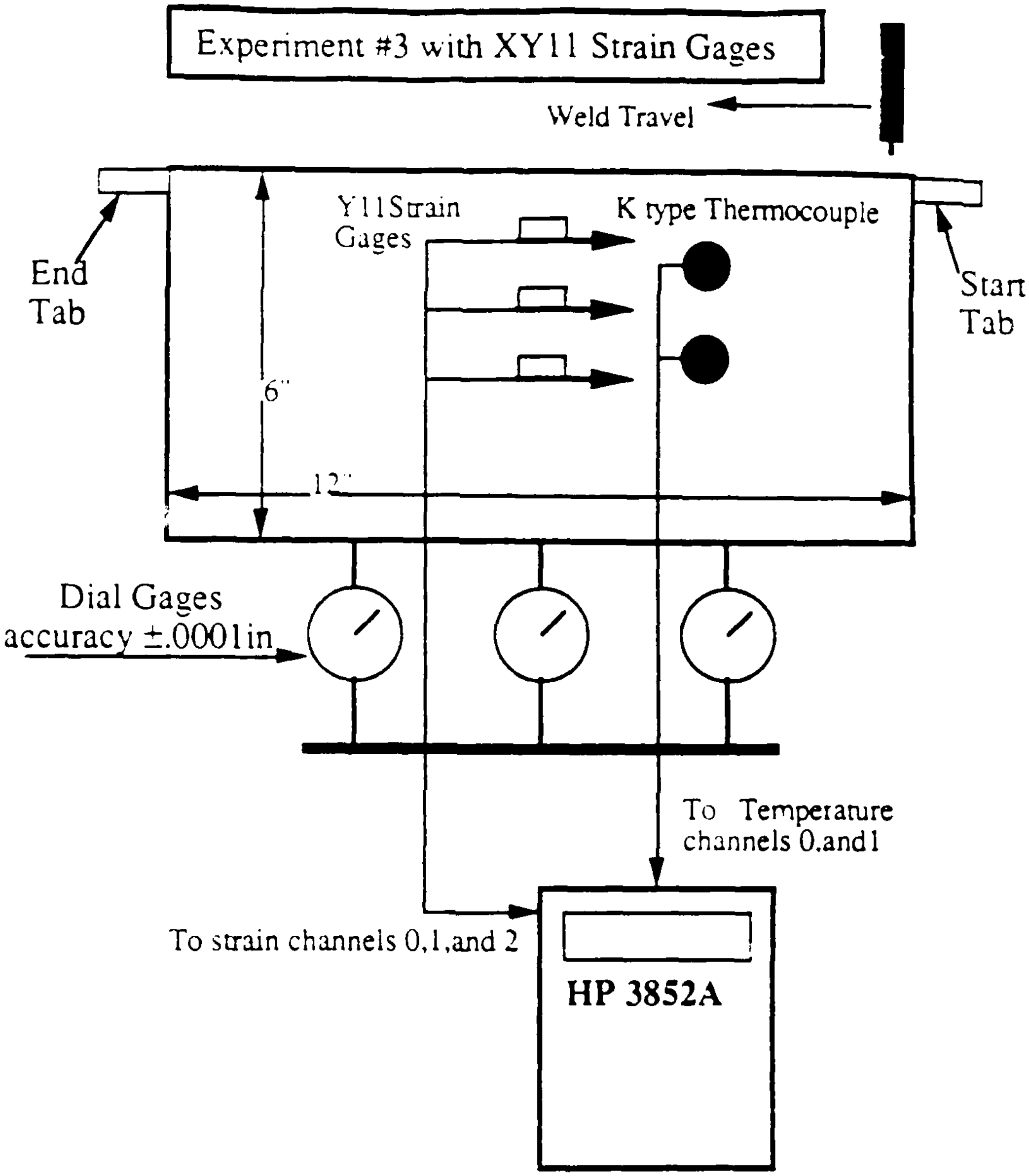

The combination of very sensitive strain gages and the Data Acquisition Machine proved to be relatively easy to use. Reliable test results were obtained throughout this investigation even though experiment #3 data was not used because the plate was too short in length.

Appendix 4

Thermocouples[24]

When dissimilar metals are joined there is a potential difference at the joint. Thomas Seebeck discovered this in 1821 and this is called the "Seebeck effect":

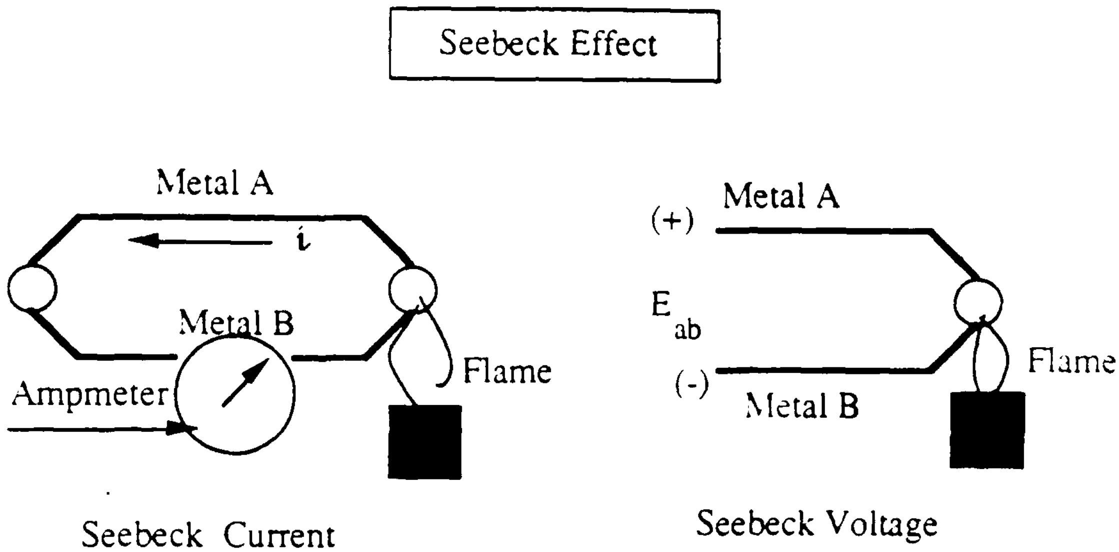

Figure 15

for small changes in temperature, the seebeck voltage is linearly proportional to the temperature:

$$\Delta e_{AB} = \alpha \Delta T.$$

To convert voltage to temperature a conversion table is used provided by the National Bureau of Standards called thermocouple tables[24] with 0°C as the reference junction.

[24] Excerpts from OMEGA Complete Temperature Measurement Handbook and Encyclopedia, 16.26, OMEGA Engineering Co., ©1989.

[24] NBS Circular #561, Type K, Ni - Cr vs. Ni - Al (Cromel - Alumel).

The seebeck voltage vs. temperature for different types of thermocouples can be also described by an expanded Taylor polynomial:

$$T = a_0 + a_1 x + a_2 x^2 + \ldots + a_n x^n$$

where T = temperature

x = thermocouple voltage

a = coefficient unique to each thermocouple type

n = maximum order of polynomial

The following figure displays the thermocouple characteristic curves for different types:

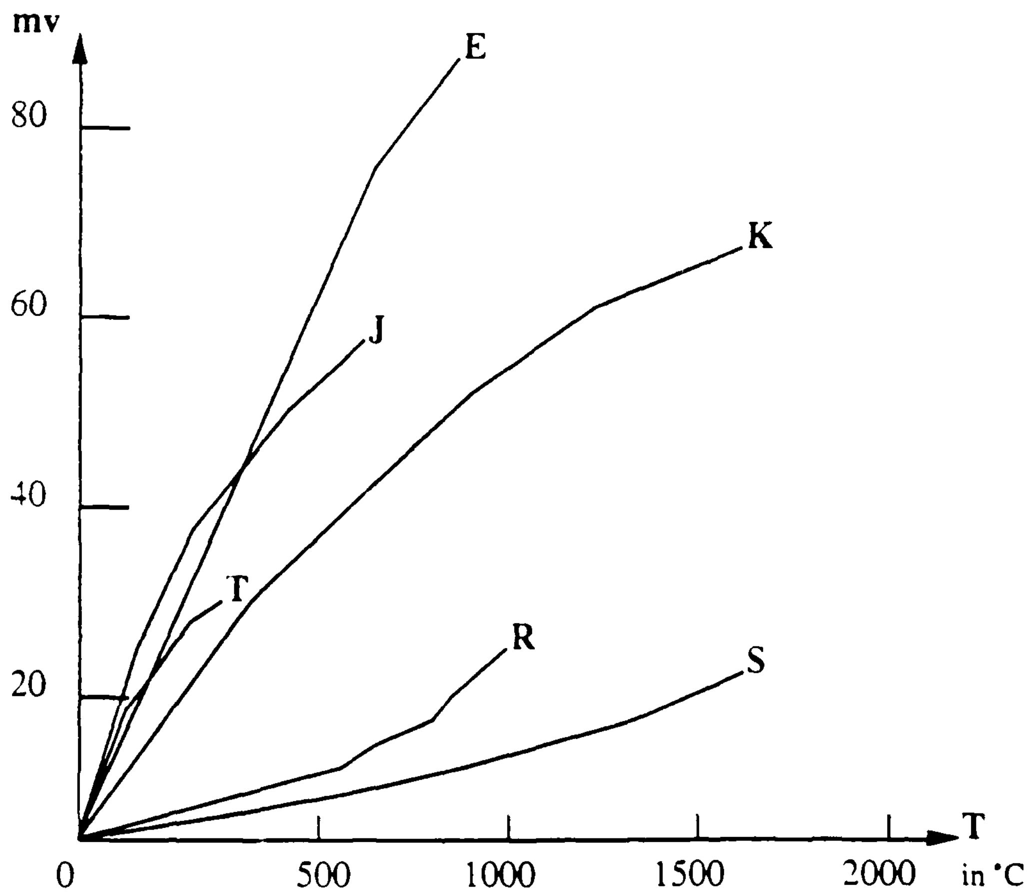

Thermocouple Response Curve

Figure 17

Type	Thermocouple Junction Material	Temp. Range	Polynomial Order
E	N_i (.10) C_r (+) vs. constantan(-)	-100 to 1000 ± .5	9
J	F_e (+) vs. constantan (-)	0 to 760 ± .1	5
K	N_i (.10) C_r (+) vs. N_i (.05) Al - S_i (-)	0 to 137° ± .7	8
R	P_l (.13) R_h (+) vs. P_l (-)	0 to 1000 ± .5	8
S	P_l (.10) R_h (+) vs. P_l (-)	0 to 1750 ± 1	9
T	C_u (+) vs. constantan (-)	-160 to 400 ± .5	7

The type selected for this investigation was type K which require a digital voltmeter sensitivity (DVM) of .4μv to detect a 0.1°C change. The seebeck coefficient is $\frac{40\mu v}{°C}$.

The NBS 8th order polynomial coefficient for K type are:

$a_0 = 0.226584602$

$a_1 = 24152.10900$

$a_2 = 67233.4248$

$a_3 = 2210340.682$

$a_4 = -860963914.9$

$a_5 = 4.83506E + 10$

$a_6 = -1.18452E + 12$

$a_7 = 1.38690E + 13$

$a_8 = -6.33708E + 13$

The HP3852A satisfies the sensitivity requirement with the integrating DVM and when K type thermocouple in selected, the NBS polynomial coefficients are selected internally for conversion. The solution of the polynomial determines the actual temperature which is displayed. The themocouples used in this investigation were purchased from Omega Engineering, Inc. A typical set-up is displayed in the following figure (not drawn to scale).

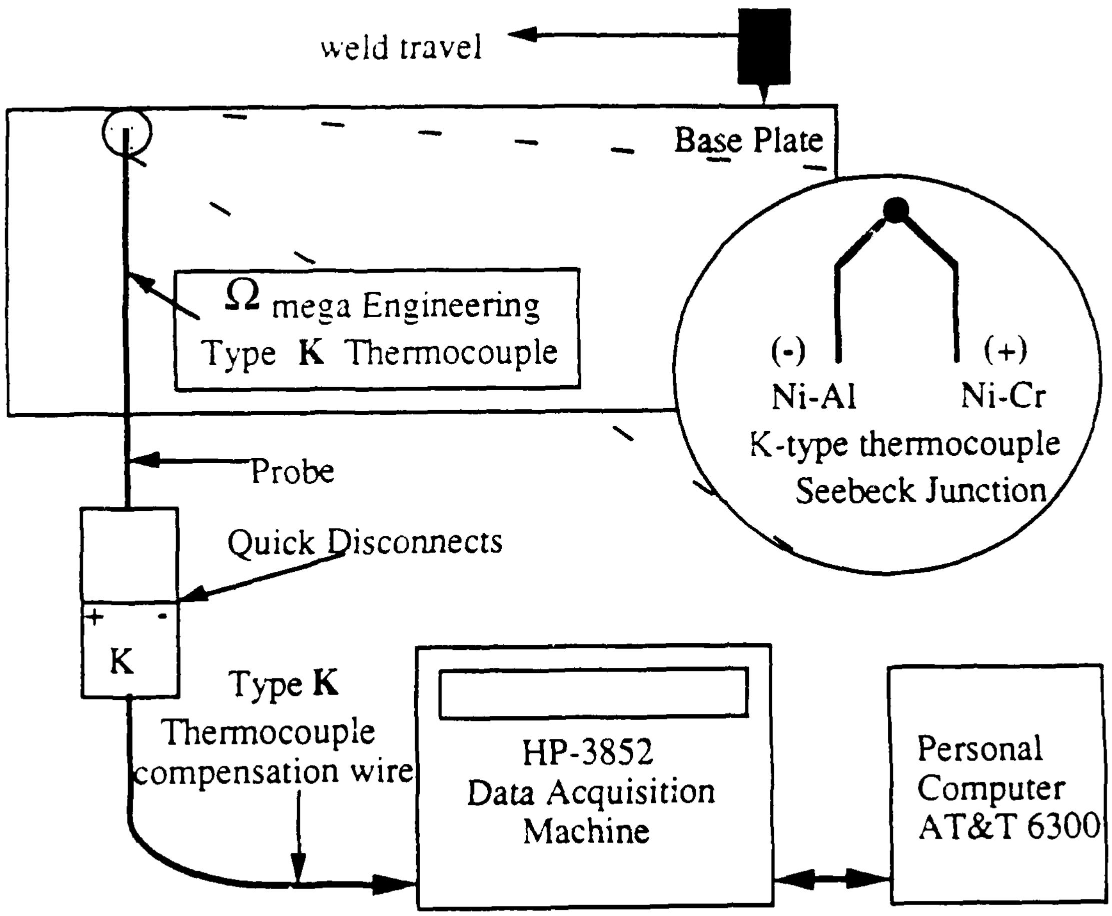

Thermocouple Type K and Experimental Connection

Figure 16

Other Temperature Transducers:

Temperature Transducers and their measured values

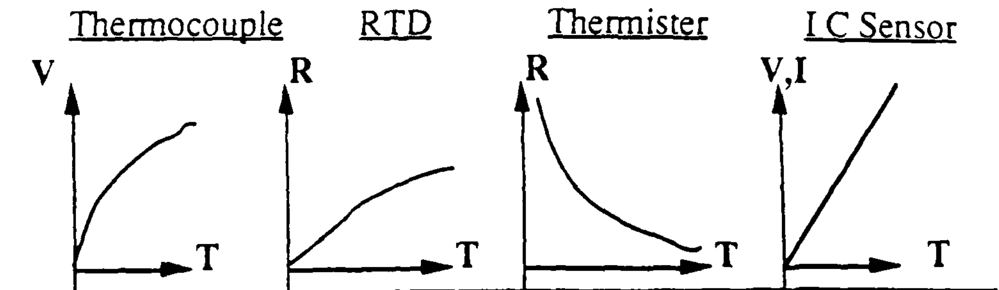

Measured Value	Voltage	Resistance	Resistance	Voltage or Current

Figure 21

Temperature Transducer Symbols

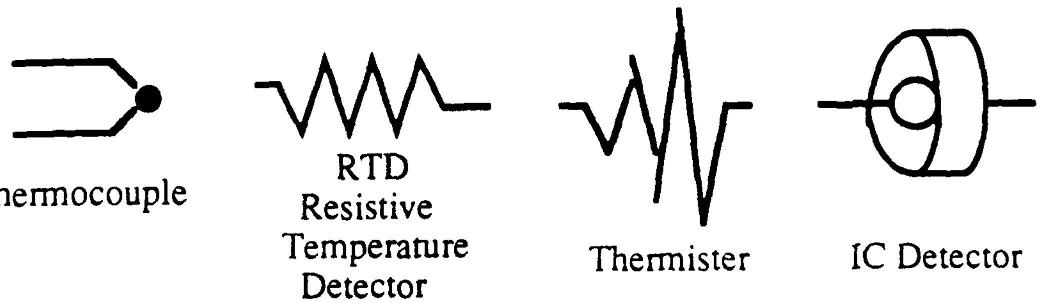

Figure 20

Advantages:

Self powered Simple	Most stable Most accurate	High output Fast	Most linear Highest output
Rugged	More linear than thermocouples	2-wire ohm measurement	Inexpensive
Variety wide T range			

Disadvantages:

Nonlinear	Expensive	Nonlinear	T < 200°C
Low voltage	Current source req.	Limited range	Power req.
Reference req.	Small ΔR	Current source	Slow
Least stable	Low /R/	Fragile	Self-heat
Least sensitive	Self-heating	Self-heating	Low variety

In looking at temperature transducers for a welding environment, a K type thermocouple seems best primarily because of its wide temperature range, simplicity, and ruggedness.

For this investigation standard, Omega Engineering type OST probe termination thermocouples with a standard 12" length, and 1/8" diameter probe was ordered. Thermocouples type K compensation wire was used to connect to the thermocouple to the HP3852A data acquisition machine.

Appendix 5
Oxy-acetylene Welding Equipment

The equipment used as the side heating torch in these experiments consisted of a cylinder of oxygen (O_2), cylinder of acetylene (C_2H_2) a regulator on each cylinder, a torch without a cutting attachment and the appropriate red (acetylene) and green (oxygen) twin hoses.

The laboratory has two sets of hoses and two torches but only one was used in this experimental investigation. An oxidizing flame produces a temperature of approximately 6300°F, a neutral flame 5850°F and a carburizing flame about 5700°F[26].

The flame utilized in these experiments was adjusted so that an oxidized flame with a 0.5 inch cone and a 2 inch feather was used. The flame outer envelope was ignored in the adjustment. Care was taken to ensure the tip of the cone in the flame did not touch the plate to keep from developing another undesirable Heat Affected Zone (HAZ) and the attendant brittleness, loss of fracture toughness, and microstructure composition changes that occur with the development of Heat Affected Zones in steel.

Trying to determine accurately the amount of heat input using a torch is a very difficult task. After conducting several tests using scrap pieces of

26 Army Training Manual TM. 9-2852, "Oxy-Acetylene Welding: Equipment Procedure and Technique", 110 - 111, CH - 5, p. 93 - 110.

steel painted with temperature lacquer, it was decided the a good set up was achieved when the edges of the 400°F "tempo-lac" strip began to melt on the side of the plate opposite the flame. The side facing the direct flame

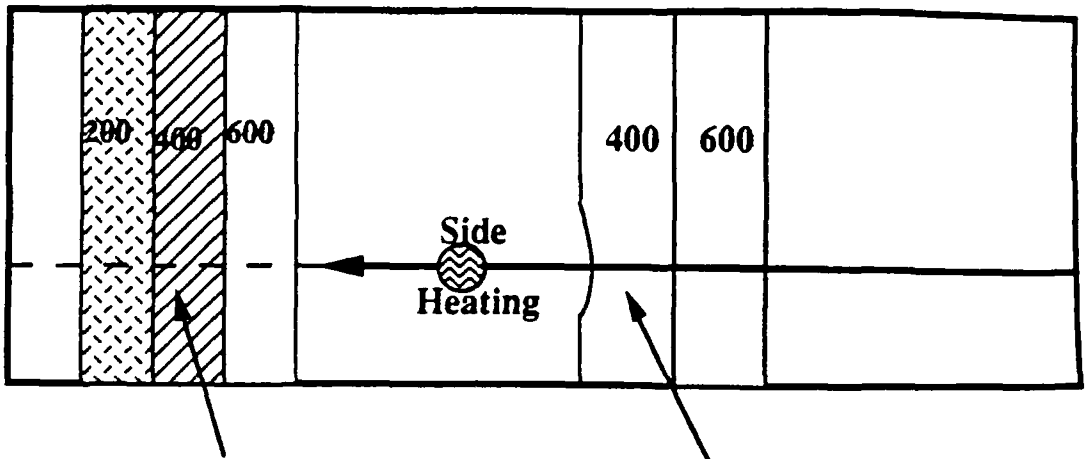

Normal "Tempo-Lacquer" painted on test piece

Using Side Heating Torch:
The 200(C) band melts away,
400(C) band is just beginning to melt
600(C) is not affected

Effects of Side Heating by changes in the Temperature Lacquer

The side facing the direct flame burned off the temperature lacquer in the region where the flame was spreading on the surface. All the "tempo-lac" bands burned off about an inch wide where the flame touched the plate. The torch was positioned one inch away form the surface of the plate.

The "tempo-lac" worked well, thermocouples confirmed that the torch did not exceed 200°C on the side opposite the flame, but the surface where the flame was reached as high as 600°F (315.6°C°).

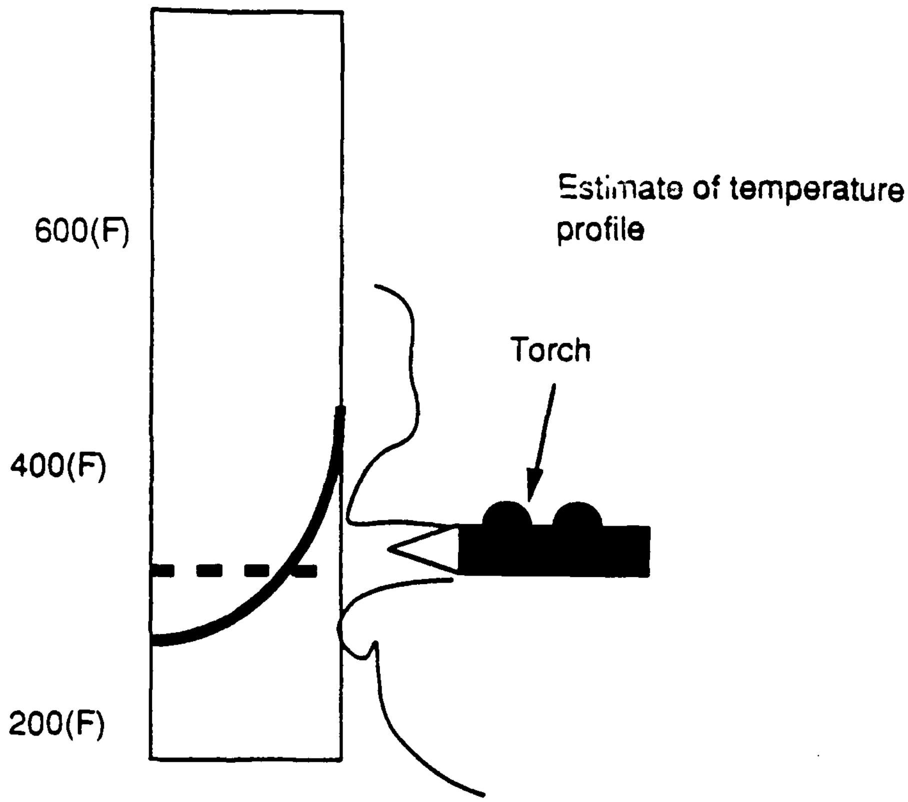

This is an estimate of what the temperature distribution looks like from the side heat. When the torch passes the temperature settles rapidly to just under 400°F (204°C). The surface where the flame touches the plate does not appear to develop a heat affected zone by visual inspection despite the high temperature. The discolored bands that extend about a half inch into the plate clearly visible when arc welding were not present so long as the tip of the cone in the flame does not touch the plate.

Experience from conducting several experiments has shown that the material discolors, developing a series of thin bands extending a half inch into the plate from the weld line when a heat affected zone develops. Although a microscope was not used to confirm this, after cutting several pieces of metal with metal saws the metal cutting equipment does reveal the presence of a hardened edge or area which is brittle and confirms the presence of a heat affected zone at the discolored edge. The hardened (HAZ) edge proved to be more difficult to cut and frequently dulled saw blades rendering them useless, especially when cutting HY130.

Experiment photograph Appendix 6[27]

[27] This section can be removed without loss of continuity.

1. EXPERIMENT #1: Splash plate buckled and arc blew holes in it.

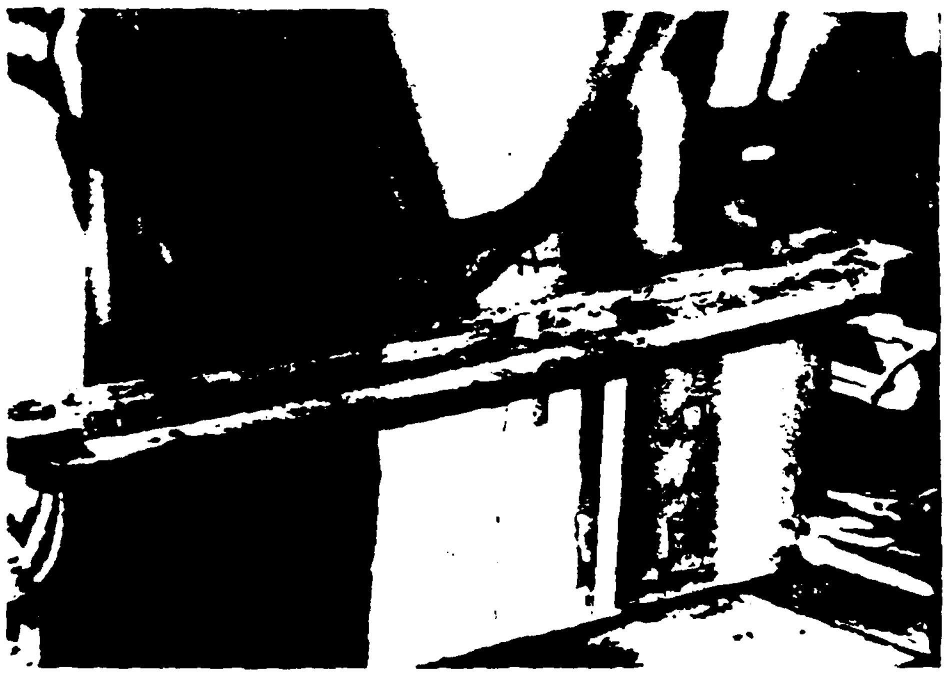

2. EXPERIMENT #2: Good bead, no spillover.

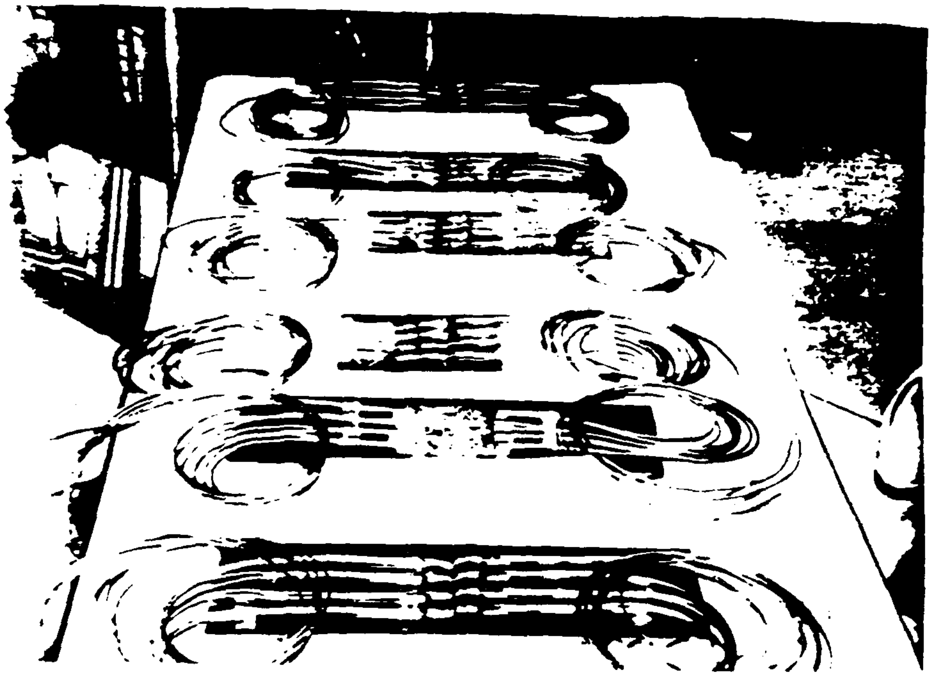

3. Prepared Specimens ready for welding (4) XY Strain Gages mounted with shielded cable.

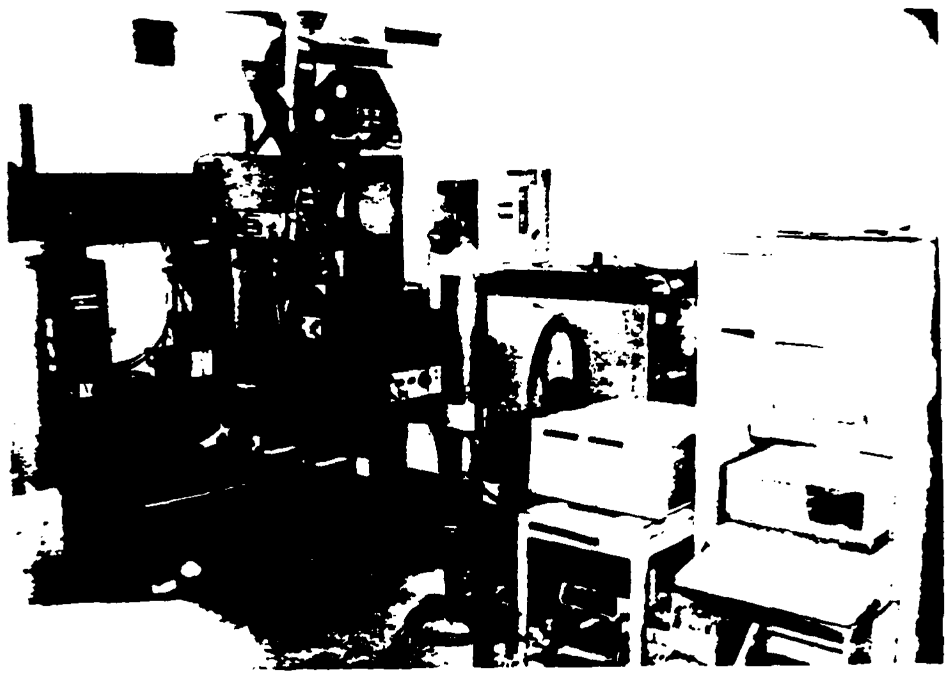

4. LAB SET-UP: (from left to right), Test Bench with EXPERIMENT #2 on it; Millermatic GMA weld machine; table with shield cables; terminal block on table; HP3852A Data Acquisition and Control System; and PC, AT&T 6300.

5. EXPERIMENT #3: Bead on Edge.

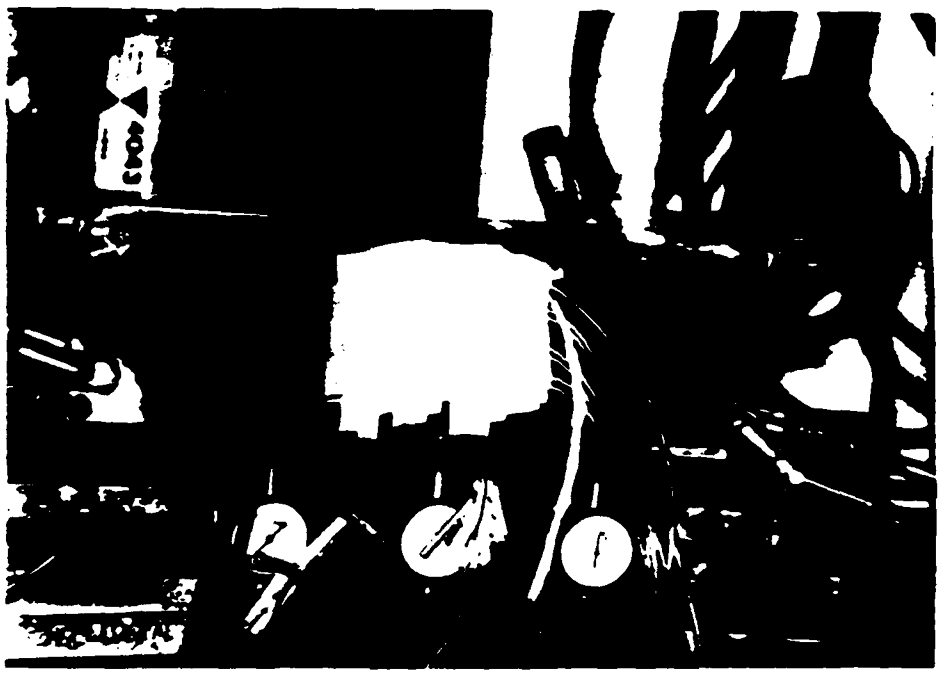

6. EXPERIMENT #4: Full test piece after welding with (4) XY Strain Gages, (4) Thermocouples, and (3) Dial Gages at the bottom of a piece of Mild Steel.

7. "Tempo-Lac" in EXPERMENT #4: Mild Steel.

8. "Tempo-Lac" in EXPERMENT #5: HY100.

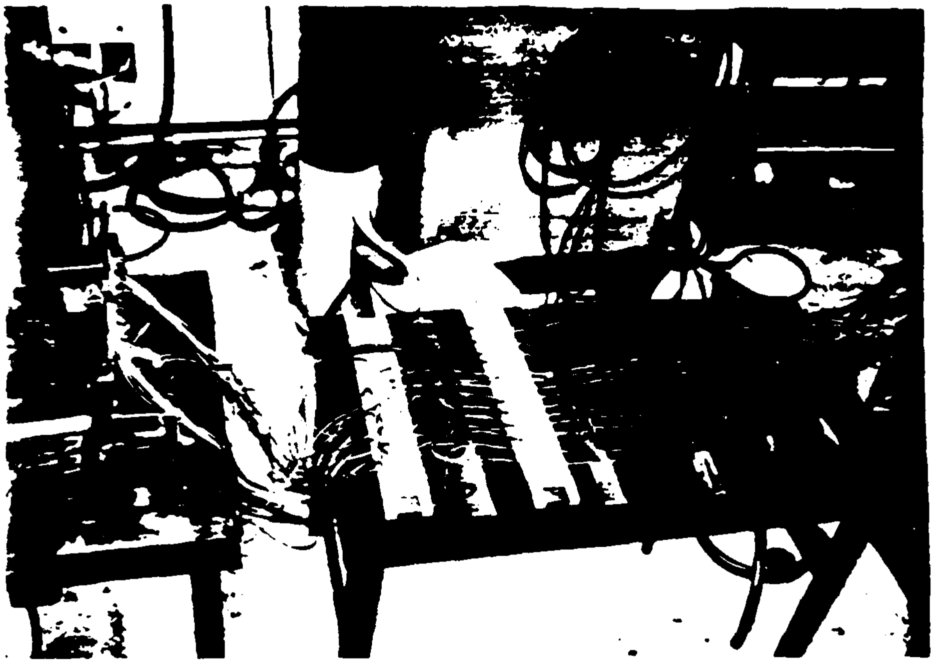

9. Terminal Block: Cable connections from the test piece to the equipment.

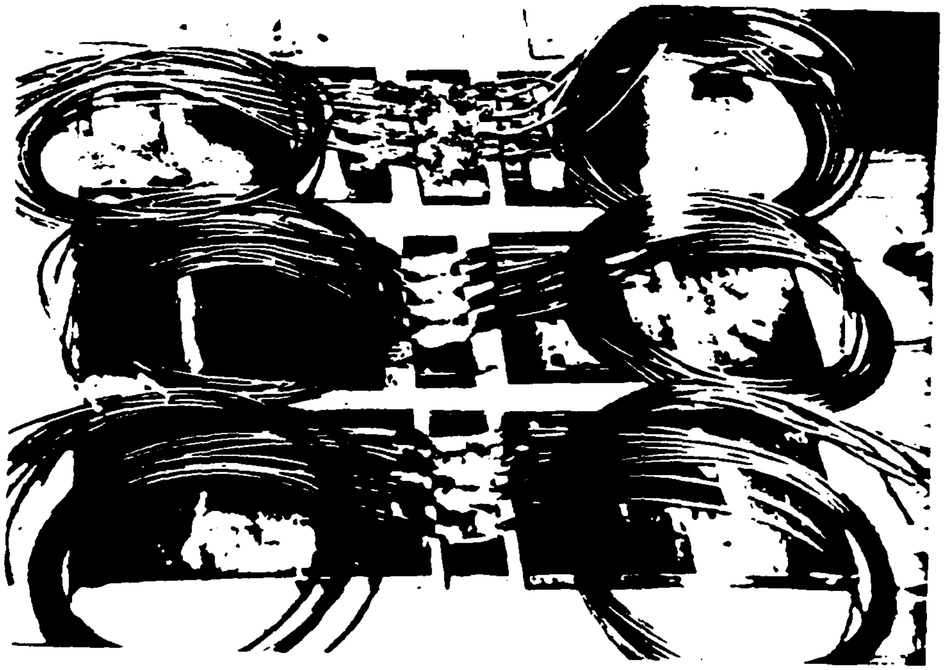

10. EXPERMENT #4 - #6: Stress Relieved pieces.

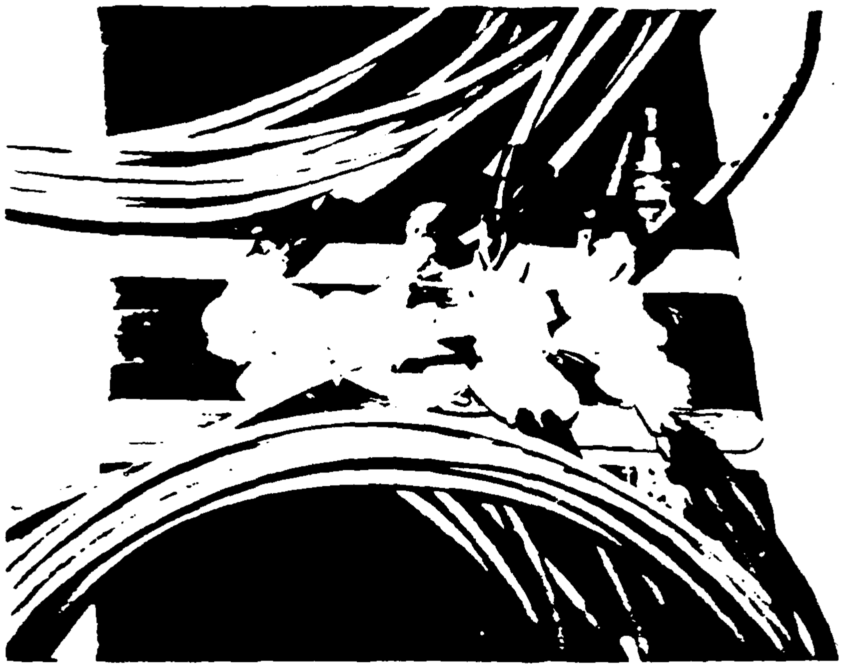

11. Close up of Stress Relieved Mild Steel piece from EXPERMENT #4: Mild Steel.

12. Stress Relieved piece from EXPERMENT #5: HY100.

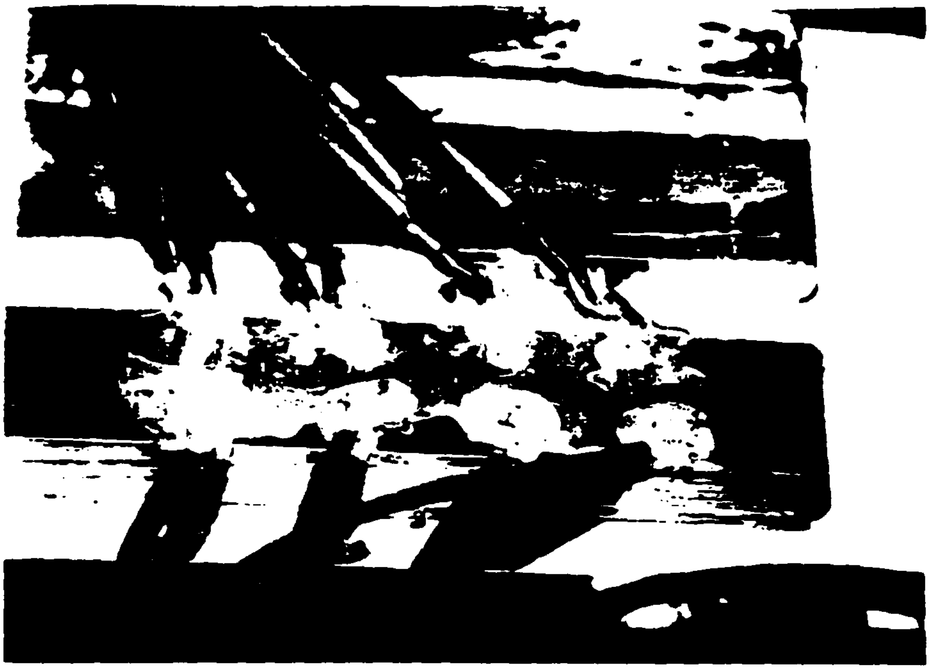

13. Close up Stress Relieved from EXPERMENT #6 HY130.

14. Side Heat set-up (9" ahead).

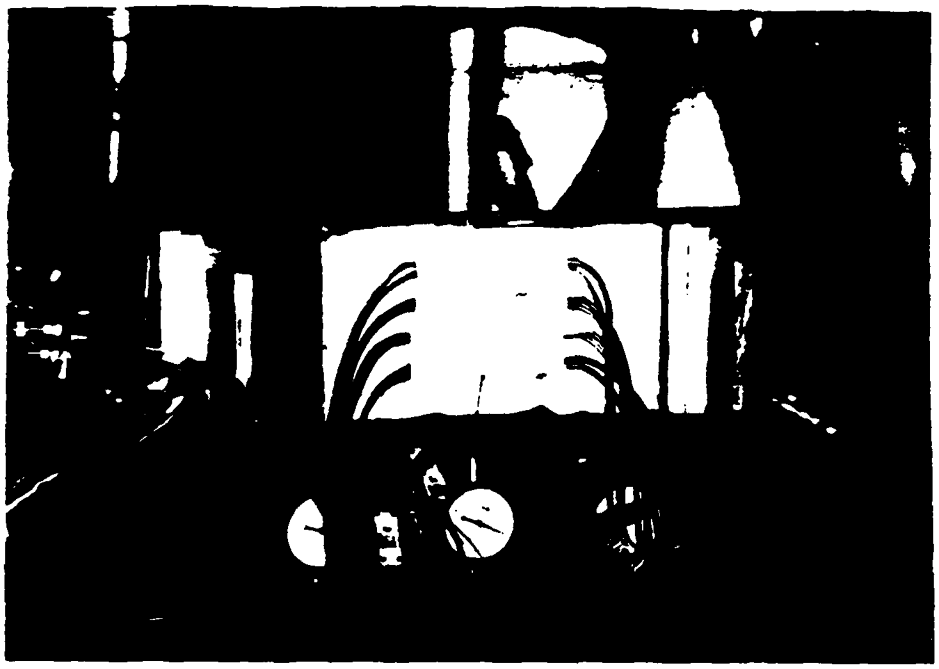

15. Final test piece after weld, EXPERIMENT #28: HY130: (4) XY Strain Gages; (4) Thermocouples; and (3) Dial Gages with Side Heat.

16. Stress Relieved pieces form EXPERIMENT #26, #27, and #28.